Het effect van pH-gevoelige superabsorberende polymeren
voor het zelfdichten en -helen van scheuren in beton

Effect of pH-Responsive Superabsorbent Polymers
on the Self-Sealing and Self-Healing of Cracks in Concrete

Arn Mignon

Promotoren: prof. dr. ir. N. De Belie, prof. dr. S. Van Vlierberghe
Proefschrift ingediend tot het behalen van de graad van
Doctor in de ingenieurswetenschappen

Vakgroep Bouwkundige Constructies
Voorzitter: prof. dr. ir. L. Taerwe
Faculteit Ingenieurswetenschappen en Architectuur

Vakgroep Organische en Macromoleculaire Chemie
Voorzitter: prof. dr. J. Martins
Faculteit Wetenschappen

UNIVERSITEIT
GENT

Academiejaar 2016 - 2017

ISBN 978-90-8578-956-7
NUR 955, 914
Wettelijk depot: D/2016/10.500/88

Supervisors:

Prof. dr. ir. Nele De Belie
Ghent University, Department of Structural Engineering

Prof. dr. Sandra Van Vlierberghe
Ghent University, Department of Organic and Macromolecular Chemistry

Research institutes

Magnel Laboratory for Concrete Research
Department of Structural Engineering
Faculty of Engineering and Architecture

Polymer Chemistry and Biomaterials Group
Department of Organic and Macromolecular Chemistry
Faculty of Sciences

Ghent University

Additional members of the examination committee

Prof. dr. ir. Luc Taerwe (chairman)
Ghent University, Department of Structural Engineering

Prof. dr. ir. Wim Van Paepegem (secretary)
Ghent University, Department of Materials Science and Engineering

Prof. dr. ing. Kim Van Tittelboom
Ghent University, Department of Structural Engineering

Prof. dr. Peter Dubruel
Ghent University, Department of Organic and Macromolecular Chemistry

Col. Prof. dr. Peter Lodewyckx
Royal Military Academy, Department of Chemistry

Prof. dr. ir. Viktor Mechtcherine
Technical University of Dresden, Department of Building Materials

Research funding

A. Mignon would like to thank the FWO (Research Foundation Flanders) for project funding.

Dankwoord

Vooreerst zou ik mijn dankwoord willen richten tot de twee mensen die het mij mogelijk gemaakt hebben om dit doctoraat uit te voeren en tot een goed einde te brengen. Dit zijn mijn beide promotoren. Professor Nele De Belie en professor Sandra Van Vlierberghe.

Professor De Belie heeft me welkom geheten in de wereld van de bouwkunde en hoewel ik na 4 jaar nog geen expert ben op dat vlak, heb ik toch enorm veel geleerd van haar. Ik bedank haar ook voor de vele input die ze me gegeven heeft gedurende die periode en uiteraard ook voor het ter beschikking stellen van alle toestellen en technieken in het labo.

Professor Sandra Van Vlierberghe wil ik ook bedanken. Zij heeft me altijd geholpen als ik even vastzat met het onderzoek en als ik even een motivatie speech nodig had om er weer tegenaan te vliegen. Haar wil ik evenzeer bedanken voor al de tijd die ze gestoken heeft in het lezen, verbeteren en suggesties geven. Ze heeft geholpen mijn kennis in de chemie extensief uit te breiden. Ik heb aan beide promotoren een enorme steun gehad waarvoor nogmaals mijn oprechte dank.

Het onderzoek werd vooral uitgevoerd in Laboratorium Magnel voor Betononderzoek en Laboratorium voor Polymeerchemie en Biomaterialen. Daarom wil ik naast professor De Belie ook professor Peter Dubruel bedanken voor de mogelijkheid om in zijn labo te mogen werken en gebruik te mogen maken van de brede waaier aan analysetechnieken.

Het technische en administratief personeel wil ik bedanken in beide labo's voor de hulp bij de proeven en het regelen van dienstreizen en andere financiële aspecten. Een speciaal dankwoord hiervoor gaat naar Veerle Boterberg die altijd klaarstond om haar kennis omtrent alle technieken in het chemische labo te delen en waar ik voor zelfs het kleinste probleem bij haar terecht kon.

Ook zou ik graag Didier Snoeck willen bedanken. Hij heeft me sterk begeleid doorheen de jaren van mijn doctoraat en me veel technieken bijgeleerd in het bouwkundig labo. Omdat onze beide onderwerpen dicht bij elkaar aansloten, hebben we er een mooie samenwerking van kunnen maken.

De thesis studenten en bachelorproef studenten (Niels Collyns, Charlotte Colman, Dries Devisscher, Kenny D'Halluin, Annelore Podevyn, Gilles Trenson, Jolien Vermeulen en Laurens Van Daele) zou ik willen bedanken voor hun harde inzet en mooie resultaten die ze behaald hebben tijdens hun scriptie.

Anderzijds wil ik Elke Van De Walle en professor Matthieu De Beule bedanken om mij te begeleiden tijdens mijn masterproef. Het is dankzij hen dat ik de microbe van het onderzoek te pakken heb gekregen en de beslissing genomen heb om dit doctoraat te starten.

Additionally I would like to thank the people who I worked together with, aside from my own research: Laurence De Meyst, Joanna Lewandowska-£añcucka, Joren Sweeck and Jianyun Wang.

I would also like to thank Col. professor Peter Lodewyckx and Leticia Velasco from the Royal Military Academy for our nice collaboration on this FWO project.

Ik heb de kans gehad om een aantal interessante congressen mee te maken op een aantal erg interessante locaties en zou al de collega's/vrienden die meegeholpen hebben om tijdens deze conferenties het aangename aan het nuttige te koppelen willen bedanken.

Naast het doctoraat moet er ook nog wat tijd zijn voor ontspanning, daarom wil ik mijn vaste loopbuddy's (Jasper, Lara, Maxime en Sandra) bedanken om me er niet telkens af te lopen en naast de mentale inspanningen ook te helpen de fysieke inspanningen te onderhouden.

Tradities moeten onderhouden worden en Carcassonne en Kolonisten van Catan waren zulke rituelen onder de middagpauze waar we even onze gedachten mee konden verzetten onder andere dankzij Birgit, Geert-Jan, Jasper, Karolina, Lara, Liesbeth, Maxime, Nele en Tom.

A special thanks to all my colleagues from both the PBM group as well as the Magnel lab of which some have really become good friends. I never got bored of coming to work thanks to the pleasant atmosphere in both groups.

Dankzij mijn vrienden heb ik ook naast het doctoraat een prachtige tijd beleefd. Zonder hen zou ik deze 4 jaar niet doorgeraakt zijn. Hierbij denk ik speciaal aan zowel de vrienden van de 'bende van Giesbaargen' als ook die van 'ons reisgenootschap'. Ook zou ik mijn medemuzikanten willen bedanken voor de leuke repetities en concerten.

Ik wil ook mijn familie bedanken en dan vooral in het bijzonder mijn ouders die me deze kans gegeven hebben om enerzijds verder te studeren en uiteindelijk dit einddoel te bereiken. Zij stonden ook altijd klaar om te helpen in of tijdens de moeilijke momenten die een doctoraatstudent nu eenmaal moet doorstaan (of verdroegen mijn gezaag als het eens tegenstak).

Arn Mignon

Table of contents

Abbreviations and symbols

AA	acrylic acid
AcOH	acetic acid
agaMOD	methacrylated agarose
Al	aluminum
algMOD	methacrylated alginate
AM	acrylamide
AMPS	2-acrylamido-2-methylpropanesulfonic acid
ANOVA	analysis of variance
APS	ammonium persulfate
ATR-IR	attenuated total reflectance infrared
$BaSO_4$	barium sulfate
BDDA	1,4-butanediol diacrylate
Ca^{2+}	calcium ion
C_3A	tricalcium aluminate
CaAlg	calcium alginate
$CaCl_2$	calcium chloride
$CaCO_3$	calcium carbonate
C_4AF	tetracalcium aluminoferrite
CaO	calcium oxide
$Ca(OH)_2$	calcium hydroxide
carMOD	methacrylated κ-carrageenan
$CaSO_4$	calcium sulfate
CF	cement filtrate
chiMOD	methacrylated chitosan
CO_2	carbon dioxide
CO_3^{2-}	carbonates
C_2S	dicalcium silicate
C_3S	tricalcium silicate
CSH	calcium silicate hydrate
DCl	deuterium chloride
DDA	degree of deacetylation [%]
d-DMSO	dimethyl sulfoxide-d6
DM	degree of methacrylation [%]
DMAEMA	2-(dimethylamino)ethyl methacrylate
DMAP	4-dimethylaminopyridine
DMAPMA	dimethylaminopropyl methacrylamide
DMF	dimethylformamide
DMSO	dimethylsulfoxide
D_2O	deuterium oxide

DS	degree of substitution [%]
DVS	dynamic vapor sorption
EDS	energy-dispersive spectroscopy
FT-IR	fourier transform infrared
G-block	α-L-guluronate
HCl	hydrochloric acid
HCO_3^-	bicarbonates
HEMA	hydroxyethyl methacrylate
HNO_3	nitric acid
H_2O_2	hydrogen peroxide
HPAEC	high-performance anion-exchange chromatography
HPSEC	high-performance size exclusion chromatography
HR-MAS ^{1}H-NMR	high-resolution magic angle spinning proton nuclear magnetic resonance
ICP-MS	inductively coupled plasma mass spectroscopy
ICP-OES	inductively coupled plasma optical emission spectroscopy
K^+	potassium cation
LCST	lower critical solution temperature
LWA	lightweight aggregates
MAA	methacrylic acid
MAAH	methacrylic anhydride
MALS	multi-angle light scattering detector
M-block	β-D-mannuronate
MBA	N,N'-methylene bisacrylamide
MC	multiple cracking [%]
Mg^{2+}	magnesium cation
MS	mass spectroscopy
Mw	weight-average molecular weight
MWNT	multiwalled carbon-nanotube
N_2	nitrogen gas
Na^+	sodium cation
NaAlg	sodium alginate
NaOH	sodium hydroxide
NH_3	ammonia
NIPAAm	N-isopropylacrylamide
PEVA	poly(ethylene-co-(vinyl acetate))
PMC	polymer modified concrete
PNIPAAm	poly(N-isopropyl acrylamide)
PVA	poly(vinylalcohol)
PVC	poly(vinylchloride)
RH	relative humidity [%]
SAP	superabsorbent polymer
SAP A	copolymer of acrylamide and sodium acrylate
SAP B	copolymer of acrylamide and sodium acrylate

SEI	secondary electron imaging
SEM-EDS	scanning electron microscopy energy-dispersive spectroscopy
Si	silicium
SO_3.Py	sulfur trioxide pyridine complex
SPSS	statistical package for the social sciences
TEMED	N,N,N',N'- tetramethylethylene-diamine
TGA	thermogravimetric analysis
W/C	water to cement ratio
σ_{fc}	first-cracking strength [MPa]
σ_p	peak strength [MPa]

Samenvatting

Beton is het meest gebruikte door de mens gemaakt materiaal. Desondanks heeft het een lage treksterkte wat kan leiden tot scheurvorming. Dit bedreigt de duurzaamheid van beton en kan leiden tot corrosie van de wapening, doordat schadelijke stoffen, opgelost in vloeistoffen of gassen, kunnen binnendringen. Inspectie, onderhoud en herstel van constructies worden op die manier onvermijdelijk en restauratiekosten kunnen oplopen tot ongeveer de helft van het jaarlijks constructiebudget, terwijl herstel soms zelfs onmogelijk wordt als scheuren gevormd worden ter hoogte van onbereikbare plaatsen. Een interne, actieve behandeling zou economisch voordeliger zijn dan een externe, passieve behandeling. Daarom werd in dit doctoraats-onderzoek het gebruik van superabsorberende polymeren (SAPs) geëvalueerd. Deze SAPs kunnen tot enkele honderden malen hun eigen gewicht in water opnemen en vasthouden. Door dit uitgesproken zwelgedrag kunnen deze SAPs uitzetten en scheuren in beton dichten (i.e. zelfdichting). Daarenboven kunnen zij dit water afgeven aan ongehydrateerde cementdeeltjes om op deze manier een herwinning in waterdichtheid en sterkte te bekomen (i.e. zelfheling).

Het hoofddoel van dit doctoraatsonderzoek was om de meest geschikte SAP te identificeren voor bovenstaande toepassing. De SAP moet enerzijds een sterke zwellingscapaciteit vertonen wanneer water in een scheur dringt teneinde de scheuren volledig te kunnen dichten, maar anderzijds moet deze een lage zwellingsgraad vertonen wanneer de SAP toegevoegd wordt aan mortel, om het effect op de buig- en druksterkte te minimaliseren (liefst verwaarloosbaar klein). Mocht de SAP sterk zwellen tijdens het inmengen in mortel, zou die het opgenomen water vrijstellen tijdens het bindings- en verhardingsproces en aanleiding geven tot macroporiën die de sterkte negatief beïnvloeden. Om dit probleem aan te pakken kunnen pH-gevoelige SAPs een sterk voordeel bieden, aangezien de pH van water dat in een scheur binnendringt neutraal is of licht alkalisch wordt, terwijl de pH van verse mortel sterk alkalisch is. Drie types van pH-gevoelige SAPs kunnen onderscheiden worden. De aanwezigheid van zure groepen leidt tot een toename van de zwelling met stijgende pH. Deze zure functionaliteiten worden gedeprotoneerd boven hun pKa en beginnen elkaar af te stoten, waardoor een meer volumineuze structuur bekomen wordt en een sterkere mogelijkheid tot zwelling. Andere SAPs bezitten amine groepen, welke worden geprotoneerd beneden hun pKa, opnieuw resulterend in elkaar afstotende ladingen en dus een toename in zwelling met afname in pH, wat het gewenste gedrag is voor hun toepassing in zelfhelend beton. Het laatste type SAP bezit geen van de vorige functionaliteiten en bezit daarentegen functionele groepen die niet pH-gevoelig zijn in het te onderzoeken pH-gebied, zoals alcoholen of amides. Daarenboven zou de geselecteerde SAP niet mogen degraderen wanneer hij blootgesteld wordt aan de omringende omstandigheden. Als aan deze vereisten voldaan is, zou de SAP bovendien de scheuren in mortel moeten kunnen opvullen en dichten en mogelijks leiden tot een sterkteherwinning door zelfheling.

Het uitgevoerde werk kan opgesplitst worden in twee luiken, die focussen op synthetische en semi-synthetische SAPs. In het eerste hoofdstuk worden SAPs met N,N'-methyleen bisacrylamide (MBA) als synthetische vernetter bestudeerd. In eerste instantie wordt MBA gecombineerd met

acrylzuur (AA) (bezit zuren groepen), wat als monomeer reeds uitgebreid gebruikt wordt voor de ontwikkeling van SAPs op industriële schaal. De ladingen van AA trekken kationen aan die aanwezig zijn in de gebruikte oplossingen om zwelgedrag na te gaan: enerzijds van natrium hydroxide (NaOH) dat werd toegevoegd om alkalische waterige oplossingen te bekomen en anderzijds de mono- en multivalente kationen in cement filtraat. Dit leidt tot een afname in zwelling door een afschermend effect van het tegenion op de poly-anion keten. Acrylamide (AM) is een hydrofiel monomeer dat niet geladen is in het onderzochte pH-bereik (pKa van acrylamide is 17 en het onderzochte pH-bereik is gelegen tussen pH 1 en 13). AM is daarom niet beïnvloed door de aanwezigheid van deze kationen in de gebruikte oplossingen. Het was dus nuttig om een copolymeer van AA en AM te testen. Omdat water dat een scheur binnendringt een lagere pH heeft (neutraal tot licht alkalisch na contact met mortel) dan het mengwater in mortel (pH rond 13) was het interessant om het potentieel van een pH-gevoelige SAP te onderzoeken die meer zwelling vertoont in neutrale dan bij sterk alkalische condities. Dit werd gerealiseerd door MBA te vernetten met 2-(dimethylamino)ethyl methacrylaat (DMAEMA) (cfr. bevat amine groepen).

In een tweede deel van dit doctoraatsproefschrift werden polysachariden geïntroduceerd, waaronder alginaat teneinde semi-synthetische SAPs te creëren. Deze bio-gebaseerde polymeren vertonen sterke zwellingseigenschappen, waardoor ze interessant waren om te onderzoeken als alternatieve SAP. Eerst werd het potentieel van natrium- en calciumalginaat (NaAlg en CaAlg respectievelijk) onderzocht. Bovenop de aanwezige elektrostatische interacties, werd een sterker covalent netwerk beoogd door het modificeren van alginaat met methacrylzuuranhydride teneinde methacrylaat-functionaliteiten in te voeren (algMOD). AlgMOD werd vervolgens gecombineerd met carbonzuren (AA) en sulfonzuren (i.e. 2-acrylamido-2-methylpropaan sulfonzuur (AMPS)) om het effect op de zwelling en mortelsterkte te onderzoeken. Uit deze studie bleek dat algMOD in combinatie met AA leidde tot de beste resultaten met een verwaarloosbare afname in morteldruksterkte. Daarom werd de combinatie van algMOD en AA vergeleken met algMOD in combinatie met zowel AA als AM. Dit maakt een vergelijking mogelijk tussen de semi-synthetische en synthetische SAPs gebaseerd op AA en AA/AM. Daarnaast werd ook het effect van een variatie in de modificatiegraad van algMOD onderzocht met betrekking tot zwelling, mortelsterkte en zelfheling. Tot slot werden pH-gevoelige basische monomeren (DMAEMA en dimethylaminopropyl methacrylamide (DMAPMA)) die amine functies bezitten, gecombineerd met verschillende gemethacryleerde polysachariden (namelijk gemodificeerd alginaat (algMOD), agarose (agaMOD) en chitosan (chiMOD)). Het gebruik van alginaat kan, vooral in alkalische waterige en cementfiltraat oplossingen, leiden tot een sterk afschermend effect door de aanwezigheid van (multivalente) kationen wat resulteerde in een afname van de zwelling. Het was daarom interessant om het effect van polysachariden die geen carboxylaat functionaliteiten bevatten (bv. agarose, dat enkel alcoholen bezit) of die een tegengestelde pH-gevoeligheid vertonen in alkalische condities (bv. chitosan, wat amine groepen bevat) te bestuderen. In een laatste deel werd het potentieel van gesulfateerde polymeren onderzocht waaronder gesulfateerd algMOD, gemethacryleerd κ-carrageenan (carMOD) en algMOD gecombineerd met AMPS. Een techniek beschreven in de literatuur werd gebruikt om algMOD te sulfateren, maar die sulfatatie leidde tot een dusdanige afname in de substitutiegraad (DS) dat geen vernetting meer mogelijk was. In toekomstig

onderzoek zou de sulfatatie van alginaat idealiter dienen te gebeuren voor de methacrylatie. Een ander polysacharide met sulfaatgroepen, κ-carrageenan, werd ook succesvol gemethacryleerd en vervolgens vernet met behulp van fotopolymerisatie. Helaas degradeerde dit materiaal in een cementfiltraat oplossing, waardoor het niet bruikbaar is voor de beoogde toepassing. Het carMOD systeem kan echter leiden tot eventueel verbeterde polymeernetwerken voor biomedische toepassingen waaronder afgifte van geneesmiddelen of wondbehandeling.

Een diepgaande karakterisering werd uitgevoerd op de ontwikkelde SAPs. Eerst werd de chemische structuur nader toegelicht aan de hand van '*attenuated total reflectance*' infrarood (ATR-IR) spectroscopie, gevolgd door het meten van de efficiëntie van vernetting door '*high-resolution magic angle spinning proton nuclear magnetic resonance*' (HR-MAS 1H-NMR) spectroscopie. Voor alle materialen werden de monomeren correct ingebouwd en bevatten de structuren slechts een verwaarloosbare hoeveelheid dubbele bindingen na vernetting.

Omdat niet alle constructies blootgesteld worden aan indringing van water (bv. regen), was het ook belangrijk om te bepalen hoeveel vocht een SAP kan vasthouden bij een variërende relatieve vochtigheid. Dit werd onderzocht door dynamische vochtopname (DVS) experimenten. Voor deze data is het van belang te kijken naar de opname bij 60% relatieve vochtigheid (RV), wat relevant is voor toepassing in landen met een lage jaarlijks gemiddelde RV zoals New York of Athene, alsook een RV van 90% welke dicht bij de gemiddelde RV van Brussel ligt, die 83% bedraagt. Een RV van 95% kan nuttig zijn in regenachtige condities. Alle synthetische SAPs vertoonden een lage vochtopname gaande tot 46% van het droog gewicht van de SAP bij 95% RV. De meeste van de semi-synthetische SAPs hadden een sterkere opname van waterdamp, vooral bij 95% RV. Alginaat gecombineerd met AMPS nam dan 110% op, chiMOD met DMAPMA zelfs 122%. Maar vooral CaAlg had een extreem sterke opname, tot meer dan twee maal zijn eigen gewicht bij een RV van 95%. Dit is hoger dan wat werd bekomen voor commerciële systemen bij 95% RV (tot 129%).

Omdat de SAP moet zwellen om de scheuren te dichten en de pH van water die indringt in de scheur verschillend is van die van verse mortel, werd de zwellingsgraad bepaald in waterige oplossingen met een variërende pH alsook in cementfiltraat. De SAPs vertoonden een variërende pH-afhankelijke zwelling, waardoor ze onderling moeilijk te vergelijken zijn. Idealiter dienen SAPs met een gelijkaardig pH-responsief gedrag vergeleken te worden. Voor de SAPs die zure groepen bezitten, hadden de synthetische SAPs met AA en AM sterke zwellingseigenschappen gaande tot 456 g_{water}/g_{SAP} bij pH 12. Voor de semi-synthetische SAPs leidden de SAPs bestaande uit algMOD met een lage DS gecombineerd met AA en gecopolymeriseerd met AA en AM tot extreem hoge zwellingsgraden (tot 630 g_{water}/g_{SAP} en 371 g_{water}/g_{SAP} respectievelijk bij pH 12). AlgMOD gecombineerd met AMPS leidde tot de sterkste zwelling bij neutrale pH (195 g_{water}/g_{SAP}). De SAPs die amines bezitten, hadden over het algemeen een lagere zwellingscapaciteit. De synthetische SAPs met DMAEMA met een lage graad van vernetting vertoonden een zwelling van 68 g_{water}/g_{SAP} bij pH 3, wat vergelijkbaar is met de zwelling van semi-synthetische SAPs gebaseerd op chiMOD met DMAPMA (75 g_{water}/g_{SAP}) en werden alleen overtroffen door agaMOD gecombineerd met DMAEMA (111 g_{water}/g_{SAP} bij pH 3).

Vervolgens werd ATR-IR spectroscopie gebruikt om te onderzoeken of de SAP vatbaar is voor hydrolyse. De meeste SAPs vertoonden enkel hydrolyse in waterige oplossingen bij extreem alkalische condities (pH ≥ 12). Dit was minder zichtbaar bij cementfiltraat. Dit kan verklaard worden door een interne afschermende werking door de aanwezigheid van opgeloste kationen in cementfiltraat die kan leiden tot een uitgestelde pH-geïnduceerde hydrolyse. Voor sommige SAPs, zoals de synthetische SAPs met DMAEMA, was er zelfs geen hydrolyse waarneembaar in alle oplossingen.

Na SAP karakterisering werden de SAPs in een standaard mortelmengsel ingemengd om de buig- en druksterkte van mortel te bepalen na toevoegen van 0.5 of 1 m% SAP ten opzichte van het gewicht aan cement. Extra water werd toegevoegd om de wateropname door de SAPs te compenseren en mengsels te maken met een zelfde verwerkbaarheid (vloeimaat van 210 mm) als het referentiemateriaal met een water-cement verhouding van 0.50. Vorig onderzoek uitgevoerd binnen Labo magnel heeft aangetoond dat het toevoegen van SAPs aan mortel geen invloed heeft op de bindingstijd, hoewel dit nog niet bevestigd is voor de SAPs ontwikkeld in huidig PhD. Voorgaande studies hebben aangetoond dat het toevoegen van een hoge hoeveelheid SAP kan leiden tot een ernstige daling van de sterkte en het was deel van dit onderzoek om dit effect zoveel mogelijk te limiteren. De DMAEMA-gebaseerde SAPs met een hoge hoeveelheid vernetter leidden bij de synthetische SAPs tot de kleinste afname in druksterkte van mortel (i.e. een afname van 19% bij toevoegen van 1 m% SAP). Vooral alginaat-gebaseerde SAPs (met AA) induceerden een minimale afname in druksterkte, met de beste resultaten voor algMOD met een hoge DS gecombineerd met AA (tot 7% afname bij additie van 1 m% SAP). Anderzijds resulteerden algMOD gecombineerd met AMPS en AA/AM copolymeren met de synthetische vernetter beiden in een enorme afname van de sterkte.

Tenslotte werd voor de meest performante SAPs de dichtingsgraad van scheuren (zelfdichting) en herstel van de waterdichtheid en sterkte (zelfheling) onderzocht door een waterpermeabiliteitstest of via een vierpuntsbuigproef. Met de permeabiliteitstest is het mogelijk om de dichting en de opvulling van scheuren via microscopie te bepalen. De mate van sterkteherwinning kan niet opgemeten worden. Deze test werd uitgevoerd uitgaande van synthetische SAPs met AA en AM. Toevoegen van 1 m% SAP aan de mortelmengsels induceerde een sterke zelfdichtingscapaciteit, met permeabiliteitswaarden die de waarden van ongescheurde proefstukken naderden en veel beter waren dan bij referentiemonsters die geen SAPs bevatten.

Voor de vierpuntsbuigproef kan via microscopie de kinetiek bepaald worden waarmee de scheuren zich vullen, alsook de helingsgraad via berekening van de sterkteherwinning. Het is anderzijds niet mogelijk om de zelfdichting van scheuren te meten via waterpermeabiliteit. Deze techniek werd uitgevoerd op een aantal semi-synthetische SAPs. Alginaat, zowel met een hoge als een lage DS, gecombineerd met AA werd getest en vertoonde sterkteherwinning tot 63% (voor scheuren tot 65 µm) wat vergelijkbaar is met andere zelfhelingssystemen zoals tubulaire capsules die een mengeling van poly(urethaan) en bacteriën bevatten als helingsmechanisme en niet erg significant verschillend van het gebruik van commerciële SAPs. Voor algMOD met AA en AM werd een herwinning in sterkte van 57% voor scheuren tot 55 µm waargenomen, wat wel

significant lager was dan bij de beste commerciële systemen. De semi-synthetische SAPs van agaMOD en chiMOD met DMAPMA resulteerden in zelfhelingscapaciteiten van 67% en 65% respectievelijk voor scheuren tot 40 µm, wat dicht in de buurt komt van de commerciële systemen.

Daarnaast werd de kosteneffectiviteit van de voorgestelde strategieën onderzocht door rekening te houden met de extra kost geassocieerd met het gebruik van deze SAPs in beton. Alle synthetische SAPs en de meeste semi-synthetische SAPs (behalve NaAlg en agaMOD en chiMOD met DMAPMA) zijn erg kosteneffectief vergeleken met andere zelfhelingsmechanismen zoals autonome heling met polymeren ingebed in capsules, bacteriële heling met adsorptie van bacteriën op diatomeeënaarde of het gebruik van commerciële SAPs met of zonder toevoeging van microvezels.

In conclusie, de meest performante gesynthetiseerde SAPs zijn algMOD met een hoge en lage DS, gecombineerd met AA. Ze vertoonden een gelijkaardig zelfhelend effect vergeleken met commerciële SAPs, maar induceerden slechts een minimaal effect op de druksterkte van mortel. Een andere veelbelovende SAP is algMOD met een hoge DS gecombineerd met AA en AM. In toekomstig werk zou het interessant zijn om de synthetische SAPs op basis van DMAEMA te optimaliseren, aangezien deze slechts een licht verschillende zwellingsgraad tegenover de semi-synthetische DMAPMA SAPs vertoonden (waarbij deze laatste veelbelovende zelfhelende eigenschappen hadden) en minder effect induceerden op de mortelsterkte. Toekomstig onderzoek kan aantonen of deze synthetische SAPs eventueel nog betere zelfhelende eigenschappen kunnen vertonen. Als de kost van chitosan en agarose kan afnemen, zouden deze gemethacryleerde polysachariden in combinatie met DMAPMA ook sterke kandidaten zijn.

Abstract

Concrete is the most used man-made material. However, it has a low tensile strength, which leads to the formation of cracks. This endangers the durability of concrete and can lead to corrosion of the reinforcement, since a pathway for harmful particles dissolved in fluids and gases is generated. Manual inspection, maintenance and repair of structures becomes unavoidable and the restoration costs can increase up to approximately half the annual construction budget, while repair activities can even become impossible if cracks are formed in inaccessible places. Instead of an external, passive treatment, an internal, active treatment would be economically more interesting. Therefore, the use of superabsorbent polymers (SAPs) was introduced in the present PhD manuscript. These cross-linked polymer networks can absorb and retain aqueous solutions up to several hundred times their own weight. By swelling extensively, these SAPs can expand and block the cracks in concrete (i.e. self-sealing). In addition, they can deliver this water to unhydrated cement to induce a regain in water-tightness and strength (i.e. self-healing).

The main goal of the current PhD research was to identify the most appropriate SAP for the above-mentioned purposes. It should have a strong swelling capacity when water enters the cracks on the one hand to completely be able to block the cracks, but a low swelling capacity upon incorporation in mortar to induce a minimal effect on the flexural and compressive strength (preferably negligible). If it would swell strongly during the mixing of mortar, they would start to release their water during the hardening process for internal curing and leave behind macro pores, which negatively influences the strength. To meet this problem, pH-responsive SAPs could offer benefits as the pH of infiltrating water in cracks is neutral or becomes slightly alkaline and the pH of fresh mortar is highly alkaline. There are three types of pH-responsiveness. The presence of acid functionalities leads to an increase of the swelling with an increasing pH. These acid moieties become deprotonated above their pKa value and will start to repel each other, leading to a more open SAP structure and more possibility to swell. Other SAPs contain amine moieties. These become protonated below their pKa value, again leading to repelling charges and thus finally an increase in swelling with a decreasing pH, which is the envisaged behavior for application in self-healing concrete. The final type of SAPs contain neither of the previously mentioned functionalities and instead have moieties which are not pH-responsive in the investigated pH-range, such as alcohols or amides. Additionally, the SAP should not degrade when exposed to these highly alkaline conditions. On top of these requirements, the SAPs should be able to fill and seal cracks in mortar and lead to possible strength regain.

The performed work could be subdivided into two parts focusing on synthetic and semi-synthetic SAPs. In the first chapter, SAPs containing N,N'-methylene bisacrylamide (MBA) as a synthetic cross-linker have been studied. MBA was first combined with acrylic acid (AA) (containing acid moieties), which has been used extensively as monomer for SAP development on industrial scale. The charges in acrylic acid attract cations in the swelling media due to addition of NaOH for alkaline aqueous solutions and the presence of mono- and multivalent

cations in cement filtrate solution. This leads to a decreased swelling due to a screening effect of the counter ion on the poly-anion chain. Acrylamide (AM) is a hydrophilic monomer, not charged within the investigated pH-range (pKa acrylamide is 17 and the investigated pH range is between pH 1 and 13). AM is not influenced by the presence of these cations in the solutions. It was thus useful to test copolymers of AA and AM. As water entering a crack has a lower pH (neutral to slightly alkaline) than the mixing water of mortar (pH around 13) it was interesting to investigate the potential of a pH-responsive SAP, exhibiting more swelling in neutral compared to extreme alkaline conditions. This was developed by cross-linking MBA with 2-(dimethylamino)ethyl methacrylate (DMAEMA) (containing amine moieties).

In a second part of this manuscript polysaccharides were introduced, including alginate, to create semi-synthetic SAPs. These bio-based polymers show excellent swelling properties, rendering them interesting to investigate as alternative SAP constituent. First, the potential of sodium and calcium alginate (NaAlg and CaAlg respectively) has been examined. Subsequently, in addition to electrostatic interactions, a stronger, covalent network was targeted by modifying alginate with methacrylic anhydride to incorporate methacrylate moieties (algMOD). AlgMOD was subsequently combined with carboxylic (AA) and sulfonic acids (i.e. 2-acrylamido-2-methylpropanesulfonic acid (AMPS)) to assess their effect on the swelling capacity and mortar strength. Out of this study, algMOD combined with AA performed best with a negligible effect on the compressive mortar strength. As such, the combination of algMOD and AA was compared to algMOD copolymerized with AA and AM. This made a comparison between the semi-synthetic and synthetic SAPs based on AA and AA/AM possible. Additionally, the effect of varying the degree of modification (DS) of algMOD on the swelling capacity, mortar strength and self-healing capacity was assessed. Finally, pH-responsive monomers (DMAEMA and dimethylaminopropyl methacrylamide (DMAPMA)) containing amine moieties were combined with several methacrylated polysaccharides (i.e. algMOD, agaMOD versus chiMOD). The use of alginate could, especially in alkaline aqueous and cement filtrate (CF) solutions, lead to a strong screening effect due to the presence of (multivalent) cations which had its effect on the swelling capacity. It is therefore interesting to investigate the effect of polysaccharides which do not possess carboxylates in a pH-range relevant for concrete (e.g. agarose, containing only alcohols) or which show an opposite pH-sensitivity in alkaline conditions (e.g. chitosan, containing amines). In a final subchapter, the potential of sulfated polymers was evaluated including sulfated algMOD, methacrylated κ-carrageenan (carMOD) and algMOD combined with AMPS. A technique described in literature was used to sulfate methacrylated alginate, but unfortunately, sulfation led to a decrease in the DS, even to the point that no cross-linking could occur anymore. Future research should ideally involve sulfation of alginate in a first step, followed by performing the methacrylation of sulfated alginate. Another sulfate-containing polysaccharide, κ-carrageenan, was successfully methacrylated and subsequently cross-linked through photo-polymerization. Unfortunately, as it degraded in cement filtrate solution, it is not suited for the envisaged application. However, this carMOD system could lead to potentially improved polymer networks for biomedical applications including drug delivery and wound treatment.

A profound characterization has been performed on all developed SAPs. First, the chemical structure has been elucidated by attenuated total reflectance infrared (ATR-IR) spectroscopy

followed by measuring the cross-linking efficiency by high-resolution magic angle spinning proton nuclear magnetic resonance (HR-MAS ^{1}H-NMR) spectroscopy. For all materials, the monomers were correctly built-in and only a negligible amount of double bonds were remaining after cross-linking.

As not all structures are exposed to ingress of external water (e.g. rain), it was also important to explore the amount of moisture the SAP can retain with a varying relative humidity, which has been investigated by dynamic vapor sorption measurements. When comparing the moisture sorption data, particularly the values for a relative humidity (RH) of 60% are of relevance for application in countries with a low annual average RH such as New York or Athens, while a RH of 90% is close to for example the annual RH in Brussels being 83% and a RH of 95% could be useful in rainy weather conditions. All synthetic SAPs showed a limited moisture uptake capacity going up to a maximum of 46% the original weight of the SAP at a RH of 95%. Most of the semi-synthetic SAPs had a stronger moisture uptake, especially at 95%RH. Alginate combined with AMPS took up to 110%, modified chitosan with DMAPMA 122%. But especially CaAlg led to an extreme moisture uptake capacity, rising over two times its own weight at a relative humidity of 95%. This is higher than what was found for commercial systems at 95% RH (up to 129%).

As the SAP needs to swell to block the crack and the pH of water entering the crack is different from the one in fresh mortar, the swelling capacity has been identified in aqueous solutions of varying pH as well as in cement filtrate solutions. The SAPs show varying pH dependent swelling, meaning it is difficult to compare between SAPs. It is best to compare SAPs which show a similar pH-responsiveness. For the SAPs containing acid moieties, the synthetic SAPs with AA and AM have strong swelling capacities going up to 456 g_{water}/g_{SAP} at pH 12. For the semi-synthetic SAPs, those composed of algMOD with a low DS combined with AA and copolymerized with AA and AM led to extremely strong swelling capacities (up to 630 g_{water}/g_{SAP} and 371 g_{water}/g_{SAP} respectively at pH 12). AlgMOD combined with AMPS led overall to the strongest swelling at neutral pH (195 g_{water}/g_{SAP}). The SAPs containing amine moieties generally have a lower swelling capacity. The synthetic SAP based on DMAEMA with a low amount of cross-linker led to 68 g_{water}/g_{SAP} at pH 3, which is comparable to the swelling of the semi-synthetic SAP based on chiMOD combined with DMAPMA (75 g_{water}/g_{SAP}) and is only outperformed by agaMOD combined with DMAEMA (111 g_{water}/g_{SAP} at pH 3).

Next, ATR-IR spectroscopy has been applied to investigate whether or not the SAPs were prone to hydrolysis. Most SAPs showed only hydrolysis in aqueous solutions at extremely alkaline conditions (pH ≥ 12). However, the latter was observed less strongly in cement filtrate. It could be anticipated that an internal shielding effect occurred due to the presence of dissolved cations in cement filtrate which could lead to a delayed pH-induced hydrolysis. Interestingly, for some SAPs, such as synthetic SAPs based on DMAEMA, no hydrolysis was observed in any solution.

After SAP characterization, the SAPs were incorporated in a standard mortar mixture to explore the bending and compressive strength of mortar after incorporation of 0.5 and 1 m% SAP with respect to the binder weight. Additional water was added to compensate for the presence of the SAPs and to create mixtures exhibiting a similar workability as the reference material with a water-to-cement ratio of 0.50. Previous research performed in the research group has indicated

that addition of SAPs to mortar did not influence the setting properties, although this has not been confirmed for the current developed SAPs. It has been observed in previous studies that the addition of high amounts of SAP could lead to a severe decrease of the strength and it was part of the current research to try to limit this effect to the greatest extent possible. The DMAEMA-based SAP with a high amount of cross-linker led to the highest remaining compressive mortar strength for synthetic SAPs with only a decrease up to 19% with addition of 1 m% SAP. Especially alginate-based SAPs (with AA) led to smaller decreases in compressive strength, with the best results for algMOD with a high DS combined with AA (up to 7% decrease for addition of 1 m% SAP). On the other hand, algMOD combined with AMPS and AA/AM copolymers with the synthetic cross-linker led both to severe strength decreases.

Finally, for the best performing SAPs, the degree of crack blocking (self-sealing) and regain of water-tightness and strength (self-healing) has either been investigated by a water permeability test or a four-point-bending test on mortar samples. With the water permeability test it is possible to measure the sealing of cracks and the crack filling through microscopy. It is not possible to measure the strength regain though. This test was performed on synthetic SAPs with AA and AM. The introduction of 1 m% SAP to the mortar mixtures induced a strong self-sealing capacity, leading to water permeability values close to the values of uncracked samples and much stronger sealing capacities than for the reference sample which did not contain any SAP.

With the four-point-bending test, the filling kinetics can be measured via microscopy and the healing ratio can be determined through strength regain. It is, however, not possible to measure the sealing of the cracks through water permeability. This has been performed on a range of semi-synthetic SAPs. Alginate with both a high and low DS, combined with AA was tested and showed strong healing capacities (compared to the healing efficiency of 40% for the reference), with the mortar containing SAP of high DS reaching strength regains up to 63% (for cracks going up to 65 µm) which is comparable to other self-healing systems such as tubular capsules containing a mixture of poly(urethane) and bacteria as healing agent and not very significantly different from commercial SAPs. The results for algMOD with a high DS combined with AA and AM also indicated a strong regain in first-cracking strength σ_{fc} (up to 57% for cracks going up to 55 µm), albeit significantly lower compared to the best commercial SAPs. Interestingly, pH-responsive semi-synthetic SAPs composed of agaMOD and chiMOD combined with DMAPMA resulted in a self-healing capacity up to 67% and 65% respectively for cracks up to 40 µm, which comes close to the strength regain values upon addition of 1 m% of the best performing commercial SAP.

Furthermore, the cost effectiveness of the proposed strategy has been screened by taking into account the additional concrete cost associated with the use of SAPs. All synthetic and most of the semi-synthetic SAPs (except for NaAlg and agaMOD and chiMOD combined with DMAPMA) are very cost-effective compared with any other self-healing mechanism such as the use of autonomous polymeric healing by capsules, bacterial healing through encapsulation in diatomaceous earth, or the use of commercial SAPs with or without additional microfibers.

In conclusion, the best performing synthesized SAPs include algMOD with both a high and low DS, combined with AA. They showed a similar self-healing effect, and interestingly induced a

much more limited effect on the compressive mortar strength compared to the commercially available SAPs. Another promising SAP is algMOD with a high DS combined with AA and AM. It would, however, in future work be interesting to revisit and optimize the synthetic SAPs based on DMAEMA, as they showed only a slightly lower swelling capacity than the semi-synthetic DMAPMA SAPs (which showed promising self-healing properties) and induced less effect on the mortar strength. Future work will indicate whether these synthetic SAPs can reach perhaps even higher self-healing capacities. In case the cost of chitosan and agarose could be decreased, these modified polysaccharides combined with DMAPMA would also be equally promising self-healing candidates.

I. Introduction

Aim and outline

The main aim of the current PhD thesis was the identification of the best superabsorbent polymer (SAP) for the intended application, namely sealing and healing of cracks in concrete. The SAP should exhibit a sufficiently high swelling capacity to let the SAPs block the crack (self-sealing), while its effect on the flexural and compressive strength upon incorporation in mortar should be limited (preferably negligible). It should also aid in forming healing products by releasing this water to the surrounding matrix (self-healing). Additionally, SAPs shouldn't degrade when exposed to highly alkaline conditions as fresh mortar is characterized by an alkaline pH around 13. However, when cracks occur and water infiltrates, the pH will be decreased depending on the surrounding conditions. It is therefore also useful to consider the effect of pH-responsive SAPs. Finally, the SAPs should be cost-effective to make them economically viable.

Chapter I provides a literature overview of the problems associated with concrete durability together with potential solutions, mainly focusing on crack formation and healing of cracks through the use of healing agents. A particular focus will be put on the possibilities which superabsorbent polymers offer as well as their plethora of application fields. The difference between natural and synthetic SAPs will be highlighted in detail and the usefulness of stimuli-responsive SAPs will be described. Finally, the application of SAPs in concrete and future challenges that still need to be overcome will complete the introduction. In a second chapter, materials and methods are discussed in detail. In the third chapter (§III.1 – III.4), synthetic SAPs will be investigated. As acrylic acid (AA) has already been used often in the field of superabsorbent polymers, §III.1 will elucidate a SAP synthesized by combining AA with N,N'-methylene bisacrylamide (MBA) as cross-linker. After an in-depth characterization, the results showed that despite a limited swelling at neutral pH, incorporation of the required amount of these SAPs (i.e. 1 m% with respect to the added amount of cement) into mortar leads to a significant reduction of the compressive strength of mortar. Additionally, these polymers were prone to alkali-induced hydrolysis. Therefore, other options were screened and in §III.2, acrylamide (AM) will be introduced and a copolymer of AA and AM will be synthesized, again with the same synthetic cross-linker. AM is added to the system to increase the swelling potential at a neutral pH. To limit the effect on the mortar strength, in §III.3 a pH-responsive monomer, 2-(dimethylamino)ethyl methacrylate (DMAEMA), will be introduced, again combined with MBA. In a final subchapter (§III.4) a comparative study will be performed for all these SAPs with respect to their moisture uptake capacity, swelling potential and their effect on the mortar strength. Finally, their actual cost will be estimated to assess their cost-effectiveness to become introduced in concrete.

In the fourth chapter (§IV.1 – IV.6), polysaccharides will be introduced to create semi-synthetic SAPs. §IV.1 will explore the potential of sodium alginate and calcium alginate. As alginate seems to be indeed very promising towards the envisaged application, the incorporation of covalent linkages to create stronger SAPs will be targeted subsequently (§IV.2) by the methacrylation of alginate followed by combining it with both a carboxylic acid monomer (AA) and a sulfonic acid

(2-acrylamido-2-methylpropanesulfonic acid (AMPS)). Characterization of these polymers and the assessment of their effect on the mortar strength showed that alginate combined with AA seems to be the most promising. In §IV.3, the latter material will be further tested for its self-sealing and -healing potential. AM will then also be added as second monomer, to create a semi-synthetic SAP comparable to the SAPs developed in §III.2 to evaluate the performance of synthetic versus semi-synthetic SAPs containing similar monomers. Additionally, the degree of substitution of alginate will be changed to investigate the effect of the network density on the swelling and mortar strength. In a subsequent chapter (§IV.4), the pH-responsiveness of SAPs will again be introduced by using both DMAEMA from §III.3 as well as dimethylaminopropyl methacrylamide (DMAPMA) and combining them with methacrylated alginate, agarose and chitosan to create both pH-sensitivity associated with the built-in monomers as well as the polysaccharide backbone. It is useful to compare the potential of these SAPs with the synthetic SAPs produced in §III.3. Again, for these materials an in-depth characterization will be performed and the best performing SAPs will be selected to assess their self-sealing and -healing towards cracks. As algMOD combined with AMPS showed a strong swelling potential (§III.2), it is useful to investigate the potential of polysaccharides containing sulfated moieties. As such, in a next subchapter (§IV.5), different types of sulfated SAPs will be compared. On the one hand, methacrylated alginate will be sulfated. In addition, the sulfated polysaccharide κ-carrageenan will also be introduced and methacrylated. These above-mentioned materials will be compared to methacrylated alginate combined with AMPS (§IV.2). Finally, in §IV.6, a similar comparative study is performed as in §III.4 to identify the most promising semi-synthetic SAPs as well as the best performing material developed throughout the current PhD manuscript. Finally, a general conclusion will be given together with future perspectives relevant in the context of the envisaged application.

I.1. Concrete: its problems and possible solutions

I.1.1. The chemistry of concrete

Concrete is the most used man-made material with a world-wide production of in-between 35 and 53 billion tonnes in 2014 (estimated on the cement production, equivalent to 8-12% of the concrete production [1, 2]). As such, it has become indispensable in our modern society. This extensive use can be explained by its high compressive strength, durability, relatively low cost and possibility to shape it in any form and texture. As it is often combined with reinforcing steel, concrete finds its applications in floors and walls of buildings, in the infrastructure of bridges, roads, dams to even power plants but also in art applications in for example statues. It is a material with a huge life span, as a lot of the buildings from Roman times can still be found standing today.

Concrete is derived from the Latin word 'concretus', meaning 'to grow together'. The difference between mortar and concrete lies in the used materials. Mortar is a combination of cement, water and fine aggregates such as natural sand. Concrete consists of these same ingredients with additionally coarse aggregates like gravel. It hardens through a chemical process over a period of days. Its final strength is commonly determined at 28 days. Cement is created by burning limestone and clay with a small amount of gypsum at temperatures up to 1450 °C for gray cement or up to 1550 °C for white cement [3, 4]. The calcium carbonate ($CaCO_3$) in the limestone reacts in this process with the silicates in clay to form calcium silicates.

Table I.1: Chemical composition of Portland cement [5, 6].

Cement Compound	Cement Chemistry Abbreviation	Chemical Formula
Tricalcium silicate	C_3S	Ca_3SiO_5 or $(CaO)_3.SiO_2$
Dicalcium silicate	C_2S	Ca_2SiO_4 or $(CaO)_2.SiO_2$
Tricalcium aluminate	C_3A	$Ca_3Al_2O_6$ or $(CaO)_3.Al_2O_3$
Tetracalcium aluminoferrite	C_4AF	$Ca_4Al_2Fe_2O_{10}$ or $(CaO)_4.Al_2O_3.Fe_2O_3$
Gypsum	-	$CaSO_4.(H_2O)_2$

After the mixing of cement with water, these compounds undergo hydration and the following reactions take place with the silicates [3]:

$2\ (CaO)_3.SiO_2 + 6\ H_2O \rightarrow (CaO)_3.(SiO_2)_2.(H_2O)_3 + 3\ Ca(OH)_2$

$2\ (CaO)_2.SiO_2 + 4\ H_2O \rightarrow (CaO)_3.(SiO_2)_2.(H_2O)_3 + Ca(OH)_2$

$(CaO)_3.Al_2O_3 + 6\ H_2O \rightarrow (CaO)_3.Al_2O_3.(H_2O)_6$

$(CaO)_4.Al_2O_3.Fe_2O_3 + 2\ Ca(OH)_2 + 10\ H_2O \rightarrow (CaO)_3.Al_2O_3.(H_2O)_6 + (CaO)_3.Fe_2O_3.(H_2O)_6$

At first, an amorphous layer of calcium silicate hydrate (CSH) is quickly formed around the calcium silicates, which slows down the cement hydration. Part of the C_3S and C_2S (cfr. Table I.1 for chemical composition) hydrolyses to form calcium and hydroxide ions which raises the pH over 13 [7]. As a result, the reaction slows down but continues to produce these ions until the solution becomes saturated and calcium hydroxide ($Ca(OH)_2$) crystallizes which again increases the reaction rate. However, the CSH also crystallizes and forms a thick paste that hinders the diffusion of water. This again slows down the reaction [4, 6]. The water to cement ratio (W/C) is a determining factor for the strength of concrete. An inadequate W/C can result in unreacted cement particles and a low workability due to a high viscosity [8]. However, if the W/C is too high, an excess of water may not be consumed by the silicates which can cause a segregation in concrete, resulting in pore formation which impairs the compressive and bending strength of concrete.

I.1.2. Disadvantages accompanying concrete

The popularity of concrete comes with a number of disadvantages. It brings an enormous ecological footprint. Additionally, approximately 5 to 7% of all CO_2 emission is traced back to the cement industry [9, 10]. To give an idea, for every ton of cement produced, approximately 1 ton of CO_2 is emitted due to the burning of limestone during which $CaCO_3$ is converted into calcium oxide (CaO) by releasing CO_2. On top of this, the production of concrete is very water-consuming which poses a significant problem in dry countries [11]. In the end, the disposal of concrete is also important as it contributes to a large part of solid waste in industrialized nations. To address these issues, several solutions are possible: use of supplementary cementitious materials such as fly ash and silica fume to reduce the needed amount of Portland cement [1, 11], use of recycled materials [1, 11], reuse of wash water [11, 12] and improve the durability and material properties of concrete [9].

I.1.3. Durability of concrete and possible issues occurring

Durability has been a major aspect in civil engineering, especially in the last 20 to 30 years. It may be defined as the ability of concrete to endure chemical attacks, weathering action and abrasion while maintaining the desired engineering properties [13]. Concrete deteriorates over time due to various time-dependent phenomena such as shrinkage, freeze/thaw cycles, aggressive agents and alkali-silica reaction… The criteria for safety and cost-effectiveness need to be fulfilled at all times, if they are not, maintenance, repair or even demolition will become necessary.

For these reasons, a life cycle cost gives a better indication of the needed cost than just the initial cost of construction. Furthermore, due to the long design service life (minimum of 50 years for normal structures and 100 years for bridges and other civil engineering structures,

according to NBN EN 1990), the production and disposal phase could be considered far less significant than the in-use phase. The major concern for concrete durability is keeping the cost minimal while still having a high performance [14, 15]. Improving the durability and lifetime of the concrete mixture can postpone or possibly eliminate these measures. Durability of concrete and life cycle cost are however not easy to assess, as the conditions where the concrete is exposed to and the concrete properties depend on the needed application. In structures such as tunnels or highways, the concrete is in continuous service, meaning that regular inspection and maintenance of these structures will be difficult and very expensive [14, 16, 17].

Concrete has a low tensile strength despite a high compressive strength [18]. This needs to be compensated by an additional reinforcement to bear the tensile stresses introduced by external loads, imposed deformations and expansive reactions [19, 20]. Subsequently, cracking can occur and the crack width will need to be limited. This is depending on the relevant exposure class and load. These crack width limitations can be found in Table 7.1N in NBN EN 1992-1-1. The presence of cracks endangers the durability of concrete and can lead to corrosion of the reinforcement, since a pathway for harmful particles dissolved in fluids and gases is generated [21]. These cracks can have several causes.

Early-age cracking can be caused by drying and self-desiccation shrinkage. Fresh concrete shrinks upon drying during the curing process due to loss of water after casting. Additionally, concrete expands when heated (caused by the cement hydration) or when wetted and contracts again upon cooling or drying, which can lead to a differential thermal stress [20]. This tendency to contract or expand thus results in the potential crack formation. By curing, the evaporation of water should be prevented and the degree of cement hydration maximized [22].

High performance concrete has a low water-to-cement (W/C) ratio (< 0.4) and will have an insufficient amount of mixing water for complete hydration. First the capillary water is consumed, followed by a reaction of the cement with the more strongly bound gel water [23]. The microstructure rapidly densifies in the first few days, impeding the penetration of external curing water. This leads to reaction products which take up a smaller volume than the initial reactants and a lack of external water to fill up the resulting voids. This problem of insufficient mixing water causes self-desiccation of the cementitious matrix and hence shrinkage and crack formation [22, 24-26].

Autogenous shrinkage is the dimensional change of cement paste, mortar, or concrete caused by chemical shrinkage. At the time the internal relative humidity is below a certain given threshold (when extra water is no longer available), self-dessication of the paste can occur. This leads to a uniform reduction of the volume. It is not due to thermal causes, stress caused by external loads or restraints or due to loss of moisture to the environment [27]. Autogenous shrinkage can on the other hand also have a positive effect. It can cancel out thermal expansion during the hardening and ensure a favourable clamping pressure on fibers or aggregates embedded in the concrete. Nevertheless, cracking will still occur as early-age shrinkage develops when the cement

paste not reached sufficient strength. Needless to say, this is a negative influence on the mechanical properties and durability of the concrete structure [24].

Mitigating the early-age cracking can be done by reducing the overall cementitious content. By optimizing the aggregate gradation across the matrix, the cement paste required to surround the aggregates can be minimized. This is an autogenous strategy. Other examples are the use of saturated and fine lightweight aggregates, acting as internal water reservoirs for internal curing [22, 24, 28]. Difficulties can occur here concerning the rheological consistency, especially a reduction of the concrete strength and elastic modulus. It is particularly helpful in mitigating autogenous shrinkage of concrete mixtures with a low W/C. Another example is using a passive internal restraint system due to non-shrinking aggregates, resulting in a reduced shrinkage in the case of an increased aggregate volume [22]. In the case of high performance concrete, this can lead to local stresses and thus cracking as the stiffness of the paste comes close to that of the aggregates. A last autogenous strategy is the use of expansive cements which are either produced via the formation of ettringite or the hydration of free lime (CaO) or periclase (MgO). However, in this case, the expansion is very difficult to control as it depends on the distribution of the expansive components in the cement powder [29].

Another way to mitigate the early-age cracking is using a non-autogenous strategy by a free ingress of water during the first days of hardening, which leads to a delayed shrinkage and possible prevention of cracking. External restraints can play an important part in crack formation [30]. Flexible formwork is sometimes more useful in case of geometry restraints and reinforcement can cause the growth of more uniformly spaced cracks instead of a few large ones. Another non-autogenous strategy includes the use of thermal expansion to reduce autogenous shrinkage [31]. This is unfortunately very unpredictable as the weather conditions cannot be controlled.

I.1.4. Solving the crack issues in concrete

As a result of this cracking, many concrete structures worldwide suffer from severe deterioration. Inspection, maintenance and repair will therefore become unavoidable and the restoration costs can increase up to approximately half the annual construction budget [32, 33]. If cracks are formed in inaccessible places, manual repair even becomes impossible [34].

For crack repair, a variety of external techniques are available including manual repair with epoxy [35], polyurethane [19, 36], coating the concrete surface by electro-deposition of chemical compounds [37], impregnation, replacement of contaminated concrete and steel bars and coatings, etc [38, 39]. These solutions are expensive, time-consuming and in some cases, visually unattractive. Throughout the last decades, great advances have arisen in concrete repair technology. As such, instead of an external, passive and expensive treatment, an internal and active mitigation treatment can offer a superior solution. Self-healing materials have the ability to reverse the damage development once or multiple times and aid in expanding the lifetime and reliability of the concrete (i.e. the so-called ‘damage management concept’ introduced by

Van der Zwaag) [40]. This is an enormous advantage for crack repair. Cracks would be able to seal and heal automatically, similar to broken bones and damaged skin or tissue that is able to regenerate.

Concrete as such already shows a sort of self-healing (i.e. autogenous healing) [41, 42]. This effect has been noticed already in 1836 by the French Academy of Science. The healing is believed to be the result of a combination of multiple mechanisms as can be seen in Figure I.1. Of these four causes, the primary mechanism with the highest self-healing capacity remains a matter of debate. In general, for very young concrete, self-healing can be attributed to further hydration due to the considerable amount of unhydrated cementitious materials. At a later age and in contact with water and CO_2, $Ca(OH)_2$ is formed and scattered along the crack edges. Subsequently, free calcium ions (Ca^{2+}) react with bicarbonates (HCO_3^-) or carbonates (CO_3^{2-}) and the formation of $CaCO_3$ becomes the dominant mechanism, whereby the crack is filled with a white crystalline substance [16, 41, 43, 44].

$$H_2O + CO_2 \rightleftarrows H_2CO_3 \rightleftarrows H^+ + HCO_3^- \rightleftarrows 2H^+ + CO_3^{2-}$$

$$Ca^{2+} + CO_3^{2-} \rightleftarrows CaCO_3 \qquad (pH > 8)$$

$$Ca^{2+} + HCO_3^- \rightleftarrows CaCO_3 + H^+ \qquad (7.5 < pH < 8)$$

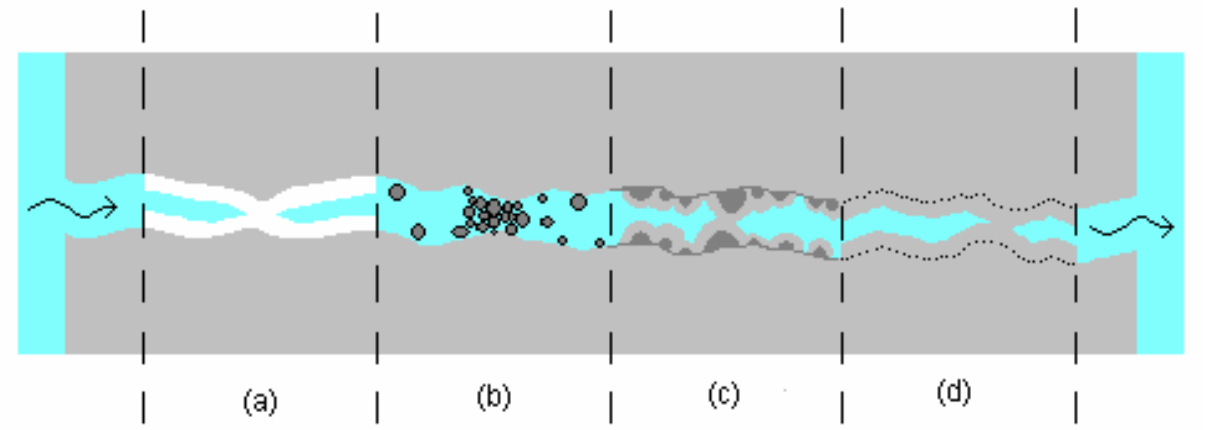

Figure I.1: Different mechanisms of autogenous healing: (a) the deposition of $CaCO_3$ or $Ca(OH)_2$ crystals, (b) filling of the crack by pollutants in the water and loose concrete particles from spalling, (c) formation of new silicates by hydration of unreacted cement particles near the edge of the fracture and (d) expansive reaction of the hydrated cementitious matrix [45].

As water enters the crack, unhydrated cement particles, which are still present in the concrete matrix, will be hydrated and new calcium silicate hydrate (C-S-H) will form together with the deposition of calcium carbonate for blocking the crack [46]. This will aid in healing small cracks completely up to 30-50 µm and partially up to 150 µm [44, 47] in cementitious materials. The width of crack closure depends on the surrounding conditions and composition [48]. However, autogenous healing will not be sufficient for full crack repair in case of larger cracks and is very difficult to control [49]. As nowadays much finer cement particles are available, a reduction in

amount of unreacted particles can be noticed, which limits the potential of ongoing hydration [50]. In the case of high strength concrete, due to a lower W/C ratio, there still is a high amount of unhydrated cement particles. To get self-healing in these materials further hydration of the grains is needed, in the case external water is available [43]. Additionally, the growth rate of $CaCO_3$ crystals is not influenced by the hardness of water or the concrete mixture (cement and aggregate type) [41].

It is possible to increase the effect of autogenous healing. This can be done by three different measures: limitation of the crack width, supply of certain chemical ions and the presence of moist environmental conditions, as seen in Figure I.2.

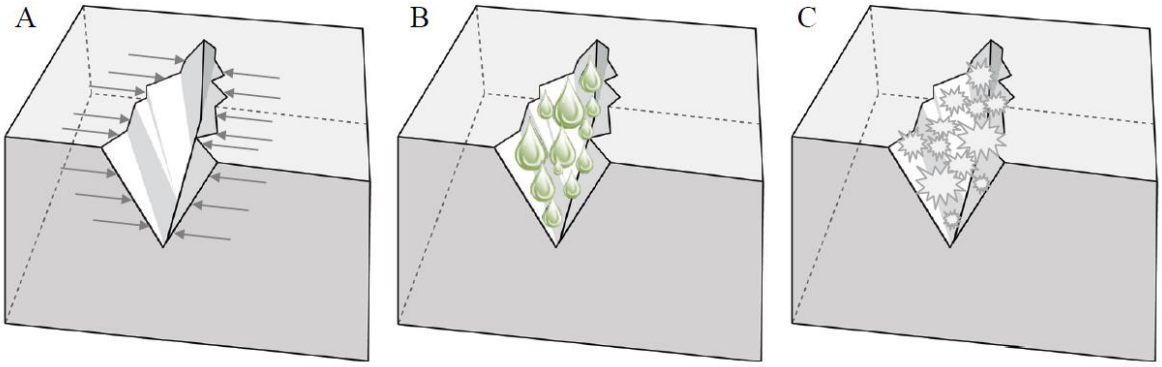

Figure I.2: Improved autogenous healing approaches: (A) crack width limitation, (B) moist environmental conditions and (C) improved hydration and crystallization [49].

Limitation of the crack width

As anticipated, a larger crack is more difficult to be sealed and self-healing will have less effect [44]. The upper limit of crack width for crack healing possibility depends on different test conditions used e.g. mortar or concrete mixture, mix proportions, cement type, relative humidity, etc. [42]. According to [44], the crack width must be lower than 150 µm and 50 µm to experience respectively partially and fully self-healed cracks. Exerting mechanical pressure on the crack to create contact between both faces improves the self-healing capacity when enough humidity is present [50-52].

The first use of fibers as reinforcement for constructions can be found in ancient civilizations such as the Egyptians, Sumerians and Babylonians who used straw and horse hair to reinforce their clay bricks. Looking more recently, other types of fibers are being used in concrete applications such as natural, glass, carbon, metal and synthetic fibers [43]. Engineered cementitious composites have also been developed that restrict crack widths to below 60 µm by mixing polyethylene or poly(vinyl alcohol) fibers in the matrix which causes multiple small cracks instead of a single larger crack [53, 54]. Their advantage over normal steel reinforcement bars, is their uniform distribution in the matrix. They can give more control over the crack propagation and width. Instead of a few large unhealable cracks, multiple smaller cracks will be introduced [22]. Fibers also have a few shortcomings. Their length is limited as it reduces the workability of the material. Additionally, distributing them uniformly is quite a challenge.

Another crack width reduction technique is the use of memory shape alloys. Upon crack formation, the alloys will introduce a contraction force to maintain their original, shorter shape. The main advantage is that even larger cracks can initiate self-healing and there is a strong regain of the mechanical properties. On the other hand, it will lead to a huge additional cost and heat is needed to initiate the shrinkage mechanism, which makes this technique only useful on a fundamental view [14, 16].

Improving hydration by additives

Self-healing of cracks is initiated by Ca^{2+}, CO_2 and unhydrated particles. Fly ash could be a stimulus for autogenous healing. It is a pozzolan, which is a partly siliceous and partly aluminous material that does not contribute to the structure of the concrete but will react with $Ca(OH)_2$ and water to form cementitious materials. A high percentage remains unhydrated even after 28 days. During crack formation, the water infiltrates and hydrates the fly ash to let a CSH gel deposit in the crack [55]. In portland cement, ettringite crystals can be formed by a reaction of C_3A with $CaSO_4$ [56]. The addition of expansive additives such as crystalline admixtures or calcium-sulfo-aluminate-based agents in the fresh mixture of concrete increases the ettringite formation and results in self-healing upon water infiltration in cracks [53] as can also be seen in Figure I.3. On the other hand, if the ettringite formation is delayed, care must be taken regarding increased tensile stress and micro-crack growth as the chemicals expand upon crystallization [57]. This expansive reaction is hard to control. A solution to this could be by encapsulating the additives to avoid possible crack formation [49, 58, 59]. Another disadvantage is their limitation in amount, reducing the self-healing capacity after some time [50].

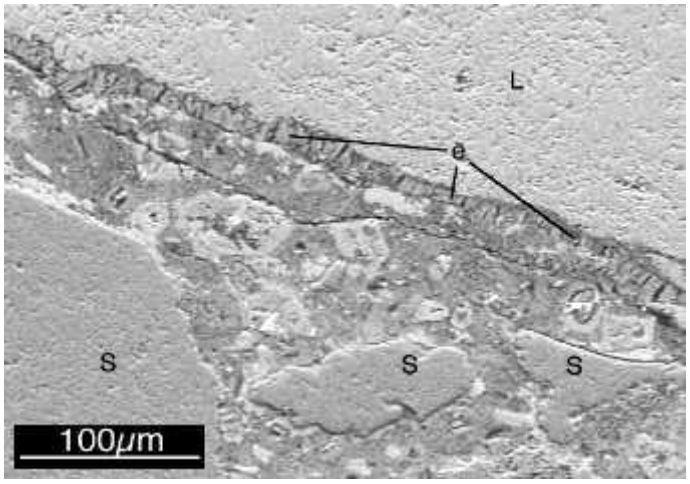

Figure I.3: Scanning electron microscope image of ettringite formation: ettringite (e) is surrounded by coarse limestone aggregate (L) and fine silica sand aggregate (S) [60].

Conditions with a moist environment

To have a strong self-healing capacity, a humid environment is needed. An attempt was made by encapsulating water in paraffin. However, the majority of the water leached out during the first days, making the method not viable so far [61]. To improve the contact with water, additional

particles could also be incorporated such as lightweight aggregates (LWA) or superabsorbent polymers (SAPs).

LWA particles can reduce the autogenous shrinkage as they can act as internal water reservoirs and help provide internal curing [62, 63]. A major disadvantage, especially with coarse LWA particles, is a decrease in the consistency and strength of the concrete matrix. Additionally, these aggregates replace normal aggregates which would have a higher strength [26, 62].

SAPs are cross-linked materials with an extreme high water uptake capacity of up to several hundred times their own weight [26, 34, 64-66]. The SAPs can retain this water and by inserting them in mortar or concrete, use it for water entrainment to reduce self-desiccation shrinkage during the hardening [49, 67]. They give a similar effect as the LWA particles as they gradually discharge absorbed water and provide internal curing. They are not only useful for internal curing, but can be applied also for crack-sealing and -healing. The amount of additional SAP is limited to keep the possible strength reduction under control. SAPs and its possible applications in concrete will be discussed further in §I.2.

I.1.5. Autonomous crack healing by healing agents

To enhance the autonomous healing capacity of concrete, a variation of different healing additives are possible. Upon crack formation, these additives undergo or aid in the chemical process to close and heal the crack.

I.1.5.1. Healing agents inside the concrete matrix

Epoxy can react with the alkaline environment of concrete to form a hard bead with a soft, unreacted liquid core. When cracks begin to form the beads break, releasing the liquid epoxy, which then hardens and blocks the entrance of the crack [68, 69]. Polymer modified concrete (PMC) can be used for increased strength or autonomous healing. It is made by using an organic polymer as additive. An example used already for its self-healing capacity is poly(ethylene-co-(vinyl acetate)) (PEVA). A huge disadvantage is that heating up to 150°C is needed to enable the healing effect. The particles will then melt, flow into the crevice and solidify upon cooling [70].
Another approach is the use of $CaCO_3$-producing bacteria. These spores are mixed in with nutrients such as calcium lactate and can remain dormant for over two centuries before becoming active through water ingress. Then a multiplication step occurs. These bacteria also excrete CO_2 which reacts with $Ca(OH)_2$ from the matrix to form additional $CaCO_3$ precipitation and sealing the crack [71]. Care must be taken by using bacteria in concrete. Nutrients and water are necessary for it to work and a high amount of nutrients can have a detrimental effect on the setting time and strength characteristics of concrete. Especially cracks smaller than 1 mm in diameter can possibly be healed by using bacteria [72]. The densification of the matrix during the hardening of concrete will cause a collapse of the bacteria if the pores become smaller than the size of the bacterial spores [73, 74]. The pH inside concrete is extremely alkaline (around 13). Combined with the dry condition after hardening, this makes it for the bacteria a very harsh environment to survive [73]. Solutions for these problems have been tried already by protecting

them with a coating of modified alginate (algMOD) [74], silica gel [19], expanded clay [73], ceramic material [75], geopolymer [76] or glass [77]. These encapsulated bacteria are protected from water and the alkaline environment and can still work to heal cracks.

I.1.5.2. Healing agents inside capsules

Another technique for the self-healing application focuses on the use of capsules containing a liquid healing agent. The idea is that the capsules break when cracking occurs and the healing agent is released followed by a chemical reaction causing hardening of the liquid to seal and fill the crack with the newly formed product [49]. The capsules are cylindrical or spherical and made from a variety of materials such as gelatin, glass, poly(propylene), wax, silica, urea formaldehyde, ceramics etc [32, 49, 78-84]. There are four types of healing agents applied in these capsules, as can be seen in Figure I.4.

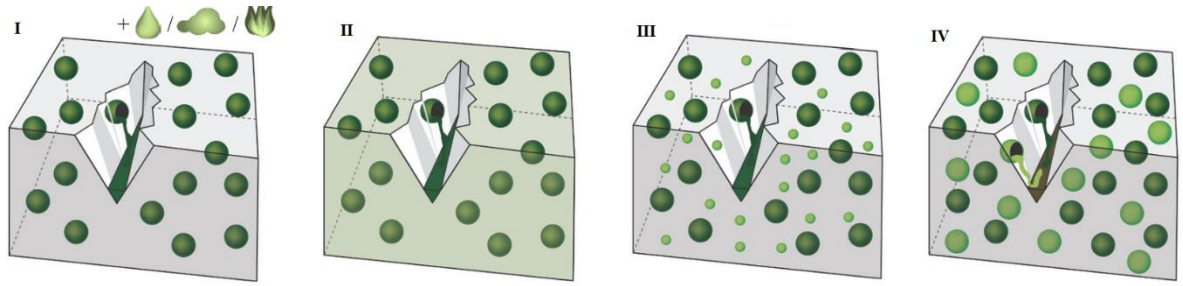

Figure I.4: The four categories of healing agents in capsules for self-healing: reaction with (I) moisture, air or due to heating, (II) with the cementitious matrix, (III) with a second component added to the matrix, (IV) with a second component introduced in additional capsules [49].

The first category contains healing agents reacting spontaneously upon exposure to air, moisture or due to heating. Some examples include tung oil and cyanoacrylate which harden when in contact with air. $Ca(OH)_2$ will react with CO_2 from the air to form $CaCO_3$. A few examples which require heating to enable reaction include methyl methacrylate and epoxy [32, 78, 79].

The second type are healing agents reacting when in contact with a component of the cementitious matrix. The bacteria mentioned earlier in section 1.5.1. can also be introduced in capsules for protection against the alkaline conditions inside the concrete matrix [80]. Another example is sodium silicate which, when the capsule breaks, reacts with the $Ca(OH)_2$ present in concrete to form CSH which deposits on the crack surface [81].

In the third category, the healing agents don't react with the matrix itself, but with a second additive incorporated in, but inert to the matrix. The combination of epoxy in capsules and a hardener in the matrix is a good example here. Upon crack formation, the epoxy is released, comes in contact with the hardener and reacts and blocks the gap [82].

The last type is a multi-capsule system where two or more components of the healing agents are separated in different capsules. During crack initiation, both components are released and undergo the chemical reaction in the matrix, expand and harden to block the crack. A combination of methyl methacrylate and triethylborane as an initiator is a good example [84].

Also, a two-component epoxy system resulted in healing at room temperature. However, a stronger healing was obtained by heating at 120°C [83].

There are a few disadvantages of using capsules. Capsules tend to rupture already during the concrete mixing. As they are also not uniformly spread over the matrix, only a limited amount will actually break and release their healing agents. Using capsules with a lower strength than the strength of the matrix may cause a widespread reduction of the concrete strength [85]. As concrete is expected to last for a long time, the limited amount of available healing agents and its longevity are also a major issue [16, 86].

I.1.5.3. Healing agents inside vascular tubes

A third technique is the use of vascular tubes to seclude healing agents. They run through the matrix and are connected with the outside of the structure. The healing agents can be administered manually [16, 87] or by means of gravitational force and a reservoir at a higher level in a single or multiple component system as seen in Figure I.5. As cracks appear, tubes will break and let the healing agent flow resulting in a similar healing effect as with capsules. The tubes can be refilled from the external side and prolong the healing effect. Due to the cracking, parts of the tube will be cut off and become unavailable again for further healing. As such, repetition is not indefinitely. Glass tubes can be used [86], which can break during casting or can consist of a hole structure filled with epoxy and supplied by a syringe. To avoid an undesired strength reduction, it is better to fill the holes with porous concrete [87]. Again, as discussed with the capsules, the healing agents can be single or multiple component systems. In the latter case, each tube contains one component. The type of agents used are similar as with the capsular approach [49, 88]. Additives showing a delayed hydration, crystallization or chemical reaction are consumed during the healing process. This means that only one or a few repairs can be done at the same location of the matrix. Other problems relate to the prematurely fracture or, in the case of a multiple component system, the breakage of only one tube and thus a failure of the self-healing [16, 50]. They are also quite costly, compared to the price of concrete itself, difficult to cast and a large amount of tubes can have a severe effect on the concrete strength [16].

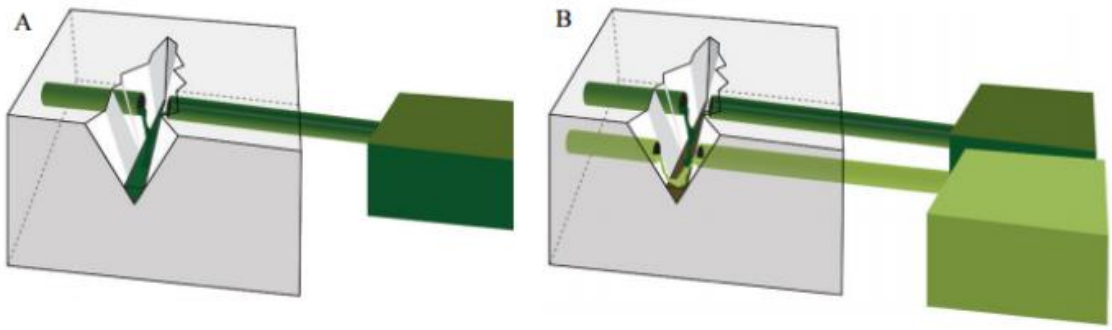

Figure I.5: (A) One channel vascular system vs. (B) multiple channel vascular system, connected to a reservoir [49].

As described above in section 1.4, the use of SAPs could be extremely useful to create a moist environment and help to self-heal the cracks. It is thus not unnecessary that these should be looked into in more detail.

I.2. Superabsorbent polymers

Superabsorbent polymer materials (SAPs) are cross-linked hydrogel networks consisting of water-soluble polymers. SAPs are generally composed of ionic monomers and possess a low cross-linking density, resulting in a large fluid uptake capacity. Interestingly, these super-absorbent networks can absorb and retain aqueous solutions up to several hundred times their own weight [89-93] as displayed in Figure I.6 and retain it even under pressure [89, 92]. A clear distinction exists between hydrogels and SAPs. Hydrogels are macromolecular networks composed of hydrophilic polymer chains characterized by a high cross-linking density and a limited absorption capacity. Conversely, SAPs are generally composed of ionic monomers and possess a lower cross-linking degree, which results in a larger fluid uptake capacity compared to conventional hydrogels [93].

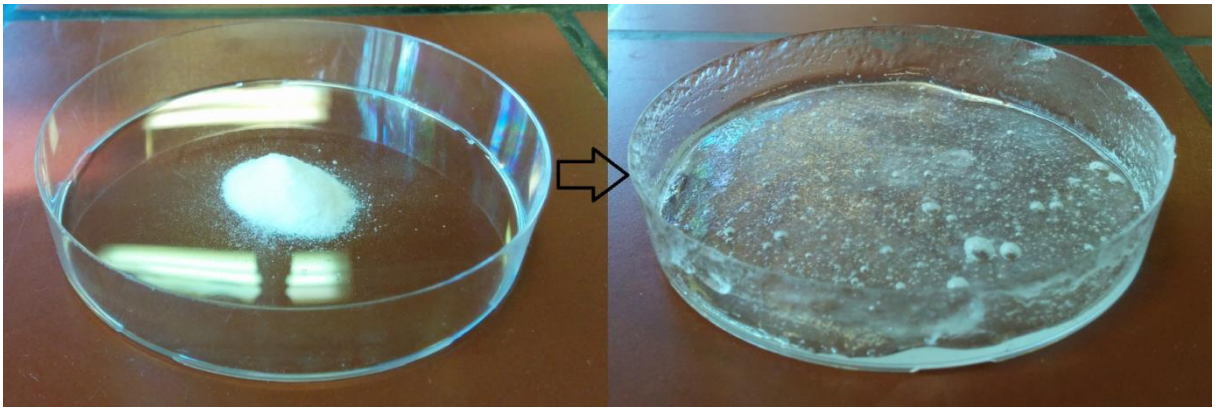

Figure I.6: Dry SAP powder and swollen SAP.

I.2.1. What is the ideal SAP

There is no such thing as the ideal SAP. It would need to fulfill a number of requirements including: a high absorption capacity; desired rate of absorption tuned towards the application; high absorbency under load; a large gel fraction after reaction; low cost price; excellent durability and stability upon swelling or storage; non-toxicity and re-wetting capability (i.e. the ability to completely release the absorbed liquid as a function of time or to maintain it as long as possible) [94, 95]. The goal is not to meet all these requirements, but to optimize those parameters that are useful for the desired application.

I.2.2. Factors determining the absorption capacity of a SAP

One of the most important characteristics a SAP needs to have is a large absorption capacity, which is the water absorbed by the SAP relative to the mass of the gel sample. This is determined by several factors. The osmotic pressure forces water into the polymer due to a higher ionic concentration inside the polymer compared to the surrounding solution because of the presence of charged groups on the ionic starting monomers. The combination of these charged groups and additional polar moieties in the SAP (hydroxyl, carbonyl or amine functionality) attract water and induce hydrogen bonding. The amount of polar or ionic groups is directly proportional to the swelling capacity. Introducing a SAP in a solution with a lower ion concentration will lead to a higher swelling capacity [96].

The elasticity on the other hand depends on the cross-linking density. A denser network results in a stiffer and more inelastic material, which leads to a lower absorption capacity. On the other hand, an insufficient amount of cross-linking can result in a material which partially dissolves when introduced in an aqueous solution. Raising the temperature reduces the time required to reach equilibrium swelling. However, a higher temperature can often result in a reduced or increased swelling, depending if the SAP offers a thermo-responsive behavior [97], this will be discussed further in the section regarding stimuli-responsive SAPs.

As mentioned earlier, SAPs are often composed of ionic parts. These ionic charges result from an acid-base equilibrium. As such, changing the pH of the aqueous environment could lead to (de)protonation of acidic or basic groups. An acidic (basic) monomer will be mainly protonated below (above) its pKa, leading to a neutral polymer, reduced hydrophilicity and thus less swelling. When the pH is higher (lower) than the pKa, the groups become charged and result in an increased swelling due to an increased affinity for water. Additionally, the repulsion of the charges lead to an increased free volume, where water can accumulate. Exerting a mechanical force on a swollen SAP will press some of the water out. The swelling capacity during application of such a force is called the absorbency under load. Due to a higher surface to volume ratio, small particles swell faster than larger particles.

I.2.3. Possible applications for superabsorbent polymers

Over the last 20 years, SAP research has had a growing tendency. This can be noticed as the amount of published research articles containing ‘hydrogel’ or ‘superabsorbent polymer’ increases gradually, see Figure I.7. SAPs nowadays find their entry in a plethora of applications including diapers and sanitary napkins [98, 99] and biomedical purposes (e.g. drug release, disposable lenses, tissue engineering and wound healing) [99-105]. Furthermore, another beneficiary is the agricultural sector, where e.g. soil conditioners, nutrient carriers and water reservoirs to conserve water in dry areas are provided by SAPs [98, 106-110]. It is also used for water purification [111] and as a water-blocking tape, composed of a non-woven textile covered with a SAP and a binder. In this latter example, the tape enfolds for example power transmission cables and retains water that seeps through the plastic casing around the cable [98, 112]. A final

application which has got a lot of attention lately is the use of SAPs in mortar and concrete and especially for the self-sealing and self-healing of cracks [34, 47, 64, 113-116]. An overview of the different biomedical and non-biomedical applications regarding SAPs are listed in Figure I.8.

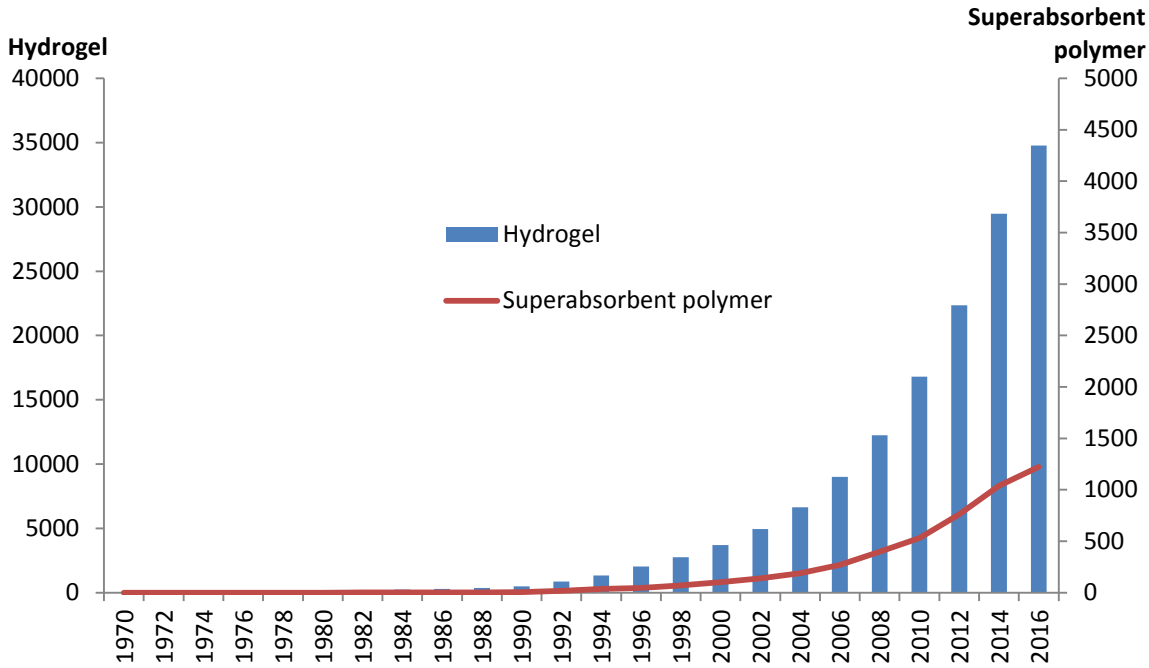

Figure I.7: Number of publications over the years containing the words 'hydrogel' or 'superabsorbent polymer' according to Web Of Science.

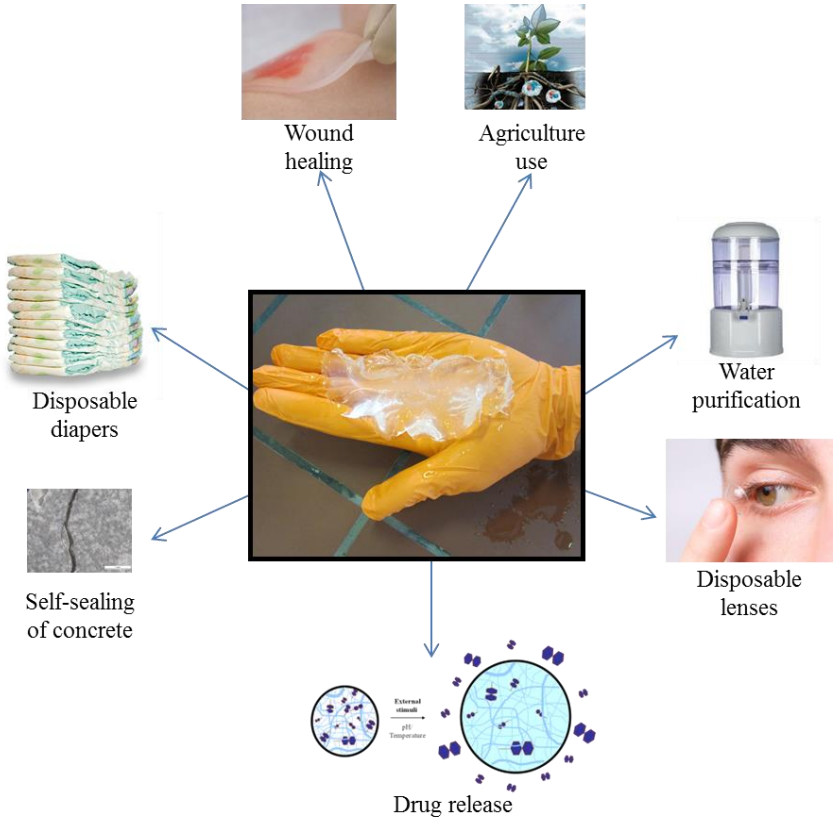

Figure I.8: Different biomedical and non-biomedical applications for SAPs.

I.2.4. Classification of the polymers

Depending on the properties needed, the SAPs are divided in different classifications.

Classification regarding the morphology

SAPs can have a different morphological appearance, depending on the intended application. This can vary from fibers [117], emulsions [118], powders [64, 119], granules [120, 121] or even membranes [89, 122]. The original shape of the SAP may not be haltered by water uptake, meaning the SAP should have enough strength to avoid any physical degradation of the structure, even under pressure [95].

Classification regarding the type of used raw material

The distinction made here is regarding the main building block of the SAP which can be either synthetic, natural or a combination of both (semi-synthetic [123]). Synthetic SAPs are petrochemical based, while natural SAPs are based on polypeptides or polysaccharides. In the case of semi-synthetic SAPs, natural and synthetic polymers are combined to create a type of SAPs with specific characteristics for certain applications [95, 124]. This classification will be discussed further in § I.2.6.

Classification based on the gelation mechanism

There can be either a physical or chemical cross-linking, which will give a different bonding between the chains of the polymer. Physical bonds such as hydrogen bonds or molecular entanglement are weak compared to chemical covalent bonding as these can also be reversed by applying a force or due to modified physical conditions. Chemical cross-linking leads to strong and stable covalent bonds.

Classification based on the type of electrical charges present

In this classification, there are four different categories depending on the presence of electrical charges along the polymer backbone and/or side chains [89]: (1) non-ionic—polymers with no charge; (2) ionic—SAPS with either anionic or cationic moieties; (3) ampholytic—both acidic as well as basic functionalities are present; (4) zwitter-ionic—SAPs containing both anionic and cationic groups, with a net charge of zero.

I.2.5. Polymerization techniques to produce SAPs

The majority of SAPs are produced by a free radical polymerization technique. Most often it is done by combining a vinyl group with a divinyl-based cross-linker in the presence of an initiator to form free radicals which propagate chain growth and create a polymer network. The free radical polymerization can be performed in bulk, solution, suspension or emulsion [94, 95] as seen in Figure I.9.

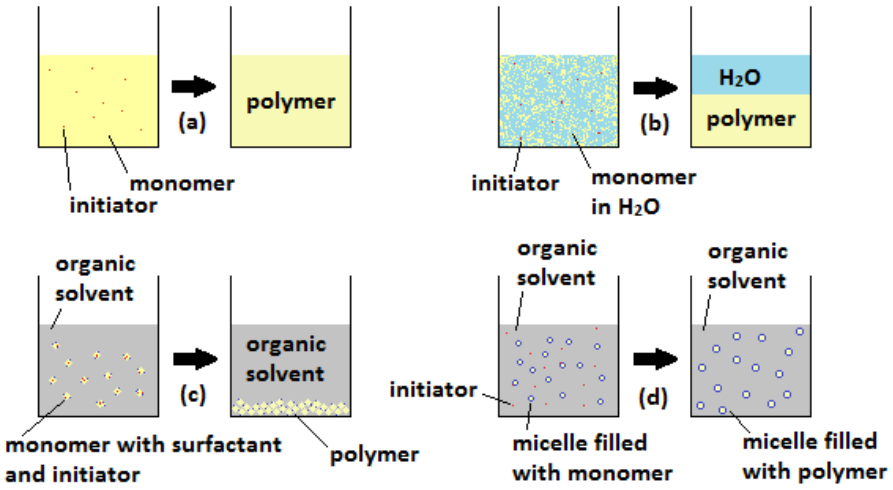

Figure I.9: Different types of free radical polymerization for synthesis of SAPs: (a) bulk, (b) solution, (c) inverse-suspension and (d) inverse-emulsion polymerization [125].

During bulk polymerization, only monomers and a monomer-soluble initiator are needed, which makes this technique the most straightforward. Due to a high monomer concentration, a high degree of polymerization and a high polymerization rate are obtained. When the reaction continues, the viscosity increases, till a solid gel is formed. A severe problem for this type of reaction is a significant heat generation. Another problem forms the monomer, which can only be liquid, as no solvent is present enabling the dissolution of the initiator.

The difference between bulk and solution polymerization is the presence of a solvent in the latter case. Due to the mobility of the monomers in this solvent, a higher polymerization degree can be obtained during gel formation. On top of that, the solvent can be used as a heat sink. The amount of solvent is important for the reaction. When it is higher than the uptake capacity of the SAP, a phase separation will occur. If not enough solvent is added, the product will resemble what is obtained in a bulk polymerization. Of course, the largest issue with this polymerization lies in the removal of the solvent.

In the case of inverse suspension or dispersion polymerization, both the initiator and the monomers are dispersed in a continuous water-in-oil, hydrophobic phase by using a mechanical stirrer in the presence of a surfactant. The monomers now form small droplets which will act as sort of separate reactors. The viscosity of the monomer, stirring speed and type of dispersant will determine the particle size and shape. The final product is a powder or bead which is easy to work with. A problem, however, forms the removal of both the solvent and surfactant, which can be quite difficult.

Inverse emulsion polymerization is similar as suspension polymerization with a significantly higher amount of surfactant even above the critical micelle concentration. This means that the micelles are filled with monomer solution. A control of the location of polymerization can be done by using an initiator only soluble in the continuous phase. This leads to polymerization at the edge of the micelles. The micelles expand during the polymerization process. Spherical

particles with a final diameter from 50 – 300 nm are expected. The same problem occurs here as with inverse suspension. The solvent and surfactant still need to be removed [126].

I.2.6. Natural versus synthetic SAPs

Next to the classification based on the composition (ionic, non-ionic, ampholytic or zwitter-ionic) or type of cross-linking (covalent vs. non-covalent) or physical appearance, the most important division is between synthetic, semi-natural or semi-synthetic and natural SAPs [95]. Synthetic SAPs are synthetized from petrochemically-based monomers such as acrylates or acrylamides. Typical monomers include acrylic acid (AA), methacrylic acid (MAA), acrylamide (AM), 2-(dimethylamino)ethyl methacrylate (DMAEMA), dimethylaminopropyl methacrylamide (DMAPMA), 2-acrylamido-2-methylpropane sulfonic acid (AMPS) etc. They can be synthesized into a cross-linked (co)polymer network with a synthetic cross-linker such as N,N'-methylenebisacrylamide (MBA). Semi-synthetic or semi-natural SAPs can be synthesized by addition of a synthetic part onto a natural polymeric backbone by graft polymerization [92, 127-129]. Natural SAPs are based on polysaccharides or polypeptides. Polysaccharides can be retrieved from biosynthesis in plants and animals. These days, polysaccharides produced by microbes such as bacterial hyaluronan, gellan or xanthan are investigated [130]. The natural biopolymers used for SAPs are alginate [130-133], chitosan [130, 134], agar [135], carrageenan [136], dextrin [137], cellulose [108, 138], starch [138], gellan gum [130, 139] and proteins [95]. They show a growing trend regarding the focus as biodegradable, easily available, biocompatible, non-toxic and sustainable materials. In addition, due to the increasing cost and finite nature of crude oil [129, 140], natural polymers form a more cheap alternative, as renewable organic substances. Water-soluble polysaccharides possess functional groups such as alcohols, carboxylic acids or amines which can be easily used for derivatizations like grafting or cross-linking in order to form a gel. As such, a short subsection, dealing with the origin, composition and application fields of both synthetic and natural materials is not redundant. This script will cover both synthetic and semi-natural SAPs. The most often used natural polymers will be discussed further, those are alginate, chitosan, agarose and κ-carrageenan.

I.2.6.1. The composition, origin and use of synthetic SAPs

The largest volume of SAPs have a synthetic or petrochemical origin. The most often used monomers are acrylic acid (AA), its salts and acrylamide (AM), but also polyesters and other acidic and basic monomers such as N-isopropylacrylamide, 2-(dimethylamino)ethyl methacrylate (DMAEMA) and dimethylaminopropyl methacrylamide (DMAPMA) have been used [141, 142]. Acrylic acid is a colorless liquid with a vinegar odor. It has the ability to convert into its dimer. The level of this dimer must be minimized to limit yield reduction, loss of solublility, residual monomers etc. To avoid this problem, manufacturers often do moisture exclusion, just-in-time delivery and temperature controlled storage [95, 143]. The most often used technique to prepare acrylic-based synthetic SAPs is by a free-radical polymerization of the vinyl monomers with a multifunctional cross-linker [95, 143]. Initiation is most often performed chemically by free-radical azo or peroxide thermal dissociative species or by a redox system [144]. A solution polymerization of AA with or without its salts in an aqueous solution together with a water-

soluble cross-linker such as N,N'-methylene bisacrylamide is a straight forward process which often leads to a gel-like elastic product. Problems arising this method are the lack of reaction control, the particle size distribution and difficulty to handle a rubbery/solid reaction product. It is a less expensive and fast technique, so often the choice of manufacturers [89]. In industrial production, the inhibitor is also not usually removed due to technical reasons [145]. Another polymerization technique to make these type of SAPs is the inverse-suspension polymerization. It is a highly flexible and versatile technique. A water-soluble initiator is used and gives a better efficiency than an oil-soluble type. When the initiator dissolves in the used dispersed aqueous phase, each particle contains the reactive species and behaves like a micro-batch polymerization reactor [146]. The inverse-suspension polymerization technique has been used widely for poly(acrylamide)-based SAPs due to its easy removal and management of the residual, hazardous acrylamide monomer from the polymer [147, 148].

The synthetic SAPs can be used in a lot of biomedical applications going from coatings for catheters [149], contact lenses [150], burn dressings [151], drug delivery systems [152, 153], electrophoresis gels [154] and many more [155]. It can also be used in non-biomedical applications such as diapers [156], as a water purification system, as water beads for plants [157] or as matrix for electronics [158].

I.2.6.2. The composition, origin and use of natural SAPs based on alginate

Sodium alginate is a water-soluble unbranched anionic polysaccharide extracted from the cell walls of brown algae (phaeophyceae) [131, 159]. The quality and amount of alginate depends on the type and age of the algae and applied extraction method [130, 132]. It is a linear copolymer composed of β-D-mannuronate (M, pKa of 3.38) and α-L-guluronate (G, pKa of 3.65), covalently linked in varying sequences and blocks and is commercially available as a sodium salt (NaAlg) [160, 161]. G-blocks are stiffer than M- or alternating GM-blocks because they are linked via axial positions, instead of the equatorial links that are found in M-blocks. The exact composition of the alginate chains varies with the source, harvest location, season and part of the seaweed used. These factors also influence the gelling capacity and strength of the produced alginate. Typical molecular weights range between 50 and 100 000 kDa. Alginate contains carboxylic acid groups which become negatively charged in aqueous solutions with a pH above the pKa values of the monosaccharide units. The overall alginate production is estimated to be roughly 40000 tonnes per year [130]. The structure of alginate is composed of two saccharide building blocks of M and G as is shown in Figure I.10a.

The two types of processing methods to manufacture alginates are the 'acid precipitation method' and 'calcium precipitation method' [162]. The polymer is typically extracted using 0.1 - 0.2 M mineral acid (e.g. HCl). The insoluble alginic acid is then converted into soluble NaAlg through an aqueous alkali solution such as sodium hydroxide. The extract is filtered to remove undesired solid material. Subsequently, the NaAlg can be obtained by evaporation. A different method is to add calcium chloride or an acid to precipitate calcium alginate or alginic acid respectively [163]. Aqueous alginate solutions exhibit shear thinning and the viscosity depends on the polymer concentration, its molecular weight and the polymer composition [164].

Interestingly, when NaAlg is combined with multivalent cations such as calcium (Ca^{2+}, originating from salts such as calcium chloride, $CaCl_2$), a physically cross-linked network between alginate chains is formed as the carboxylate groups become coordinated by the cations, which becomes insoluble in water. The anionic groups will attract water into the structure, leading to a SAP behavior. Helical chains are formed in the presence of calcium ions and arrange in the so-called 'egg-box' model, as seen in Figure I.10b [165]. Another way for gel formation is by forming intermolecular hydrogen bonds by lowering the pH of the alginate solution below the pKa of both uronic acid groups. These gels are however more brittle compared to the ionic calcium alginate gels [166].

Alginate is often used in biomedical applications (controlled drug release, cell encapsulation, dental impression, wound dressing) [167-170] and bioplastic areas (packaging, textiles, paper) [171, 172]. It is also used in the food industry as a stabilizer or emulsifier as well as a gelling agent [130, 132, 173, 174]. When modified with propylene glycol, it can be used to bind edibles under acidic conditions.

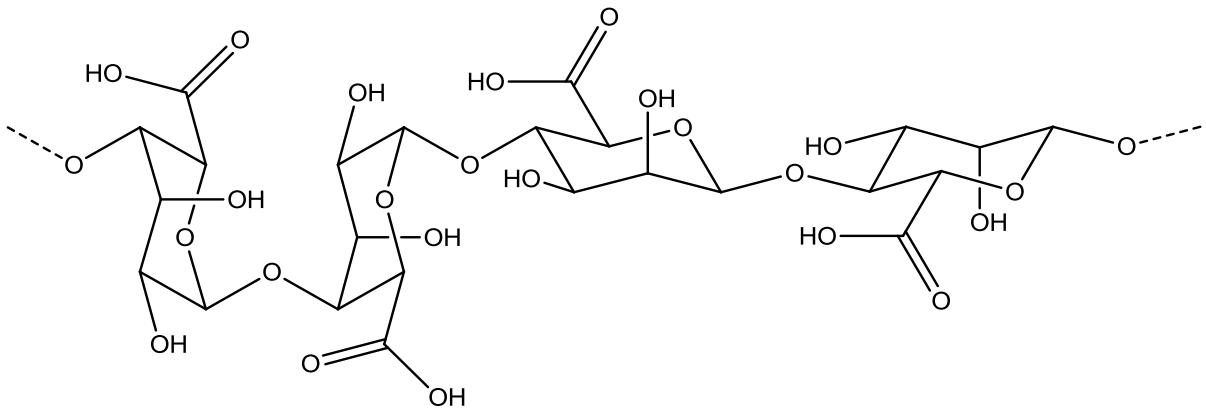

(a)

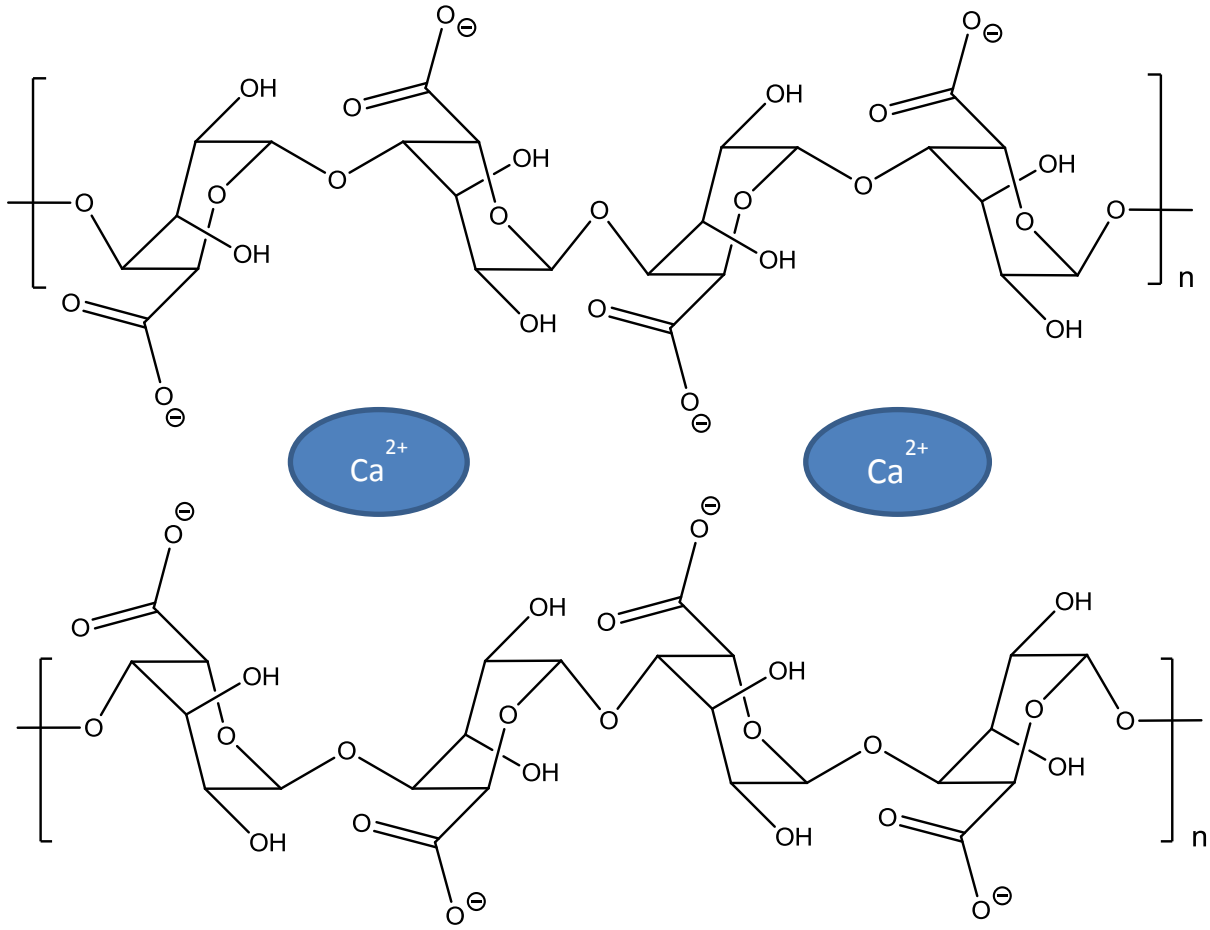

(b)

Figure I.10: Chemical structure of a typical alginate strain composed of the building blocks β-D-mannuronate (M) and α-L-guluronate (G) (a). Helical chains coordinating around calcium ions illustrate the 'egg-box' model *(b).*

I.2.6.3. Natural SAPs based on chitosan

Chitosan is another linear polysaccharide made from glucosamine building blocks. Glucosamine is a so-called amino sugar as it has the same structure as glucose with the hydroxyl moiety at the C_2-position replaced by an amine. Chitosan is made from chitin, extracted from the exoskeletons of invertebrate's such as crabs and shrimps. It can also be found in the cell walls of fungi, by partial deacetylation in an alkaline environment of N-acetylamino groups or by enzymatic hydrolysis in the presence of a chitin deacetylase. Since complete deacetylation is difficult to achieve, commercial sources always report the degree of deacetylation (DDA). Chitin with a DDA higher than 50% is considered chitosan. Chitin is impossible to dissolve in most solvents. Chitosan, on the other hand, has a pK_a value for the conjugate acid of 6.0 which results in a protonation in acidic environments and increases the solubility in acidic aqueous media [134, 175, 176]. The structures of both chitin and chitosan can be seen in Figure I.11.

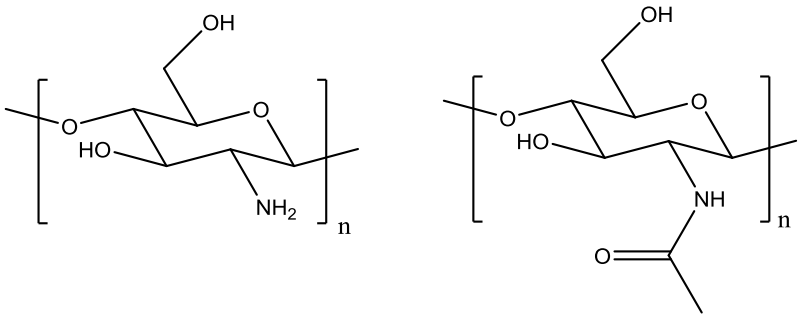

Figure I.11: Structures of chitosan and chitin.

Chitosan has many uses in the biomedical sector as tissue engineering material, wound dressing, hair treatment and drug delivery. It also knows applications in the depollution of waste water and agricultural sector as a seed treatment and biopesticide against fungal infections and in winemaking as a preservative as they are considered biocompatible and non-toxic [176-180].

I.2.6.4. Natural SAPs based on agarose

Agar is extracted from red algae (rhodophyta) and was initially discovered in the 17th century in Japan and used for its gelling properties [130, 181]. Agar is made of two components: agarose and agaropectin. Agarose is made up of β-D-galactopyranose and 3,6-anhydro-L-galactopyranose. It contains only hydroxyl functional groups as can be seen in Figure I.12. Agaropectin on the other hand consists of the same building blocks as agarose, but additionally contains anionic groups such as sulfate or pyruvate. Agarose dissolves in water only at temperatures higher than 85°C. Due to cooperative hydrogen bonds, a gel is formed by double helices at lower temperatures. Due to the slow organization of these double helices, physical agarose gels exhibit a syneresis behavior at which water is extruded from the gel over time. Agarose gels are used for gel electrophoresis of large pieces of DNA, RNA, plasmids and chromosomes and in the food industry as a vegetarian gelatin substitute. They are also used in the pharmaceutical sector as sustained release devices, for the production of intricate casts used in dentistry and for dye making [181, 182].

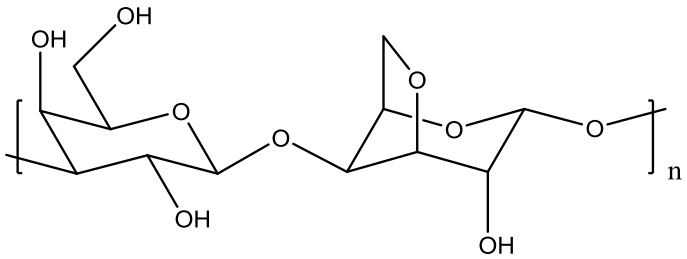

Figure I.12: Agarose, composed of the agarobiose disaccharide.

I.2.6.5. Natural SAPs based on carrageenan

Carrageenan is also refined from the cell walls of red algae (rhodophyta). To extract it, an alcohol precipitation method is used. This is a versatile method for every type of seaweed, but comes with a major investment. A second technique is 'gel press technology'. Due to its lower cost, it

has started to completely replace the first method. However, with this latter technique, only κ-carrageenan is produced, which is visualized in Figure I.13. Carrageenan is composed of repeating units of β-D-galactopyranose and α-D-galactopyranose [183]. It is especially used in pharmaceutical and food industry as emulsifiers, stabilizers or thickeners [136, 184].

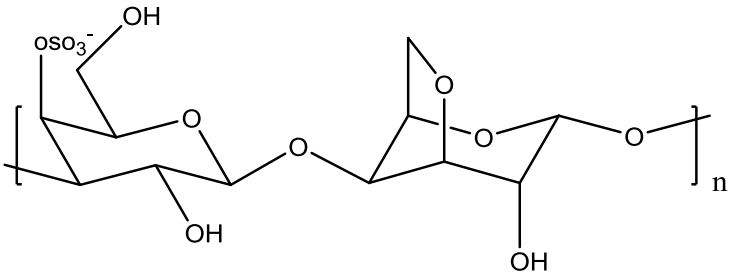

Figure I.13: κ-carrageenan composed of β-D-galactopyranose and α-D-galactopyranose.

I.2.6.6. Derivatives of polysaccharides

Derivatives of alginate

As polysaccharides have a strong potential for a variety of applications, it is often the case that they are being modified. The hydroxyl groups of alginate can be modified by acetylation to increase the swelling potential of calcium gels [185], by phosphorylation which increases the resistance towards degradation [186] and by sulfation to provide blood-compatibility and anticoagulant activity [187]. Its interaction with a cellular environment could be enhanced by introduction of cell signaling molecules [188, 189]. To induce hydrophobic or amphiphilic characteristics, hydrophobic moieties can be attached to the hydrophilic alginate backbone [190-193].

Graft polymerization can be used as an alternative method to change some characteristics of an alginate gel. Characteristics such as hydrophobicity and steric bulkiness can be introduced to prevent too rapid dissolution and erosion for drug release applications. A great deal of polymers have already been grafted onto alginate such as poly(acrylonitrile), poly(methyl acrylate), poly(methyl methacrylate), polyamides and itaconic acid [194-198]. Poly(N-isopropyl acrylamide) (PNIPAAm) has been grafted onto alginate using the carboxylic acid moieties by activating the acid with a carbodiimide followed by a reaction with the amino group of PNIPAAm to introduce an amide bond connected to alginate [199]. Additional cross-linking with Ca^{2+} created a thermo-responsive polymer as the lower critical solution temperature (LCST) behavior of PNIPAAm will decrease the swelling capacity at temperatures higher than the critical temperature as can be seen in Figure I.14.

Instead of physical cross-linking with a limited stability, covalent cross-linking methods have been introduced. Calcium alginate beads with epichlorohydrin in a NaOH-solution leads to alginate chain links between the hydroxyl groups [200, 201]. Glutaraldehyde can also be used for the formation of acetal groups by using the hydroxyls functionalities [194]. Another technique for covalent cross-linked alginate polymers is by activating the acid moiety with subsequent reaction by a diamine to create amide-linked chains [195]. These techniques have led to a great

amount of applications such as beads for ion exchange chromatography to separate optical isomers of water-soluble α-amino acids and encapsulation and controlled drug release [163].

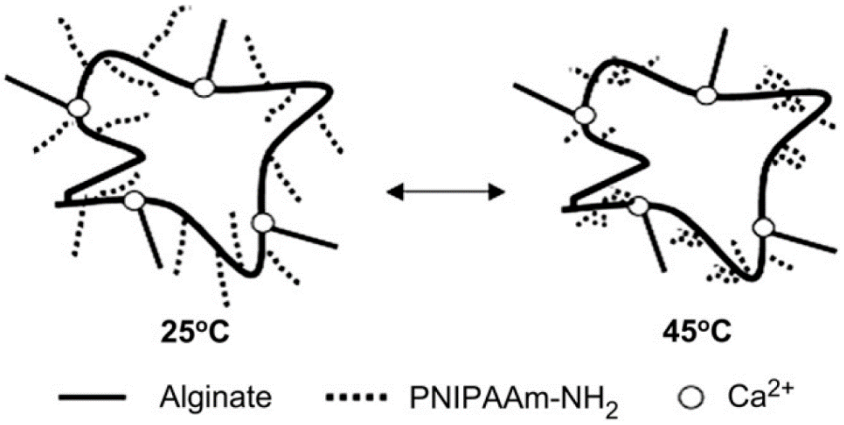

Figure I.14: Temperature-sensitive behavior of PNIPAAm-g-alginate hydrogels [163]. At temperatures above the LCST of PNIPAAm, it will collapse and result in a reduced swelling.

Derivatives of agarose

The main difference between agarose and alginate lies in the presence of the carboxylic acid moieties in alginate. Therefore, only the derivatizations on the hydroxyl groups described above can also be used for agarose. Additionally, an important derivatization of agarose is possible by using 1,3-dibromo-2-propanol to produce covalently cross-linked beads. These can be introduced in separation technology [202]. Further functionalization is often performed depending on the intended need. Agarose beads were epoxidized with epichlorohydrin followed by a reaction with ethylene diamine or cysteine to create a support for enzyme immobilization [203]. Other researchers covalently cross-linked either alginate or chitosan with agarose using carbonyldiimidazole to study the effect of charges on neural tissue scaffolds [204].

Derivatives of chitosan

Amine moieties are more reactive than the hydroxyl groups in agarose or alginate. Derivatizations described in literature thus often take place at this functionality although some modifications show hydroxyl selectivity. N- or O-carboxymethylation, phosphorylation and alkylation are some of the derivatizations on chitosan [205-208]. Chitosan can react with oxalic acid to deliver a hydrogel that is physically cross-linked via an ammonium-carboxylate complex which can adsorb copper(II) [209]. A thermo-responsive hydroxybutyl chitosan can be created by reaction with 1,2-epoxybutane [210, 211].

Derivatives of carrageenan

There are a series of chemical modifications to modulate physicochemical properties of carrageenan. For splitting the ι-carrageenan chain, the Smith periodate degradation could be used [212]. K-carrageenan containing hydroxyalkyl groups has been synthesized to create a gel with a decreased syneresis and thus a wider industrial possibility [213]. An association of

κ-carrageenan with $CaCl_2$ changes the swelling capacity of the gel [214]. Another often used type of modification for these polysaccharides is an alkalization. Different types of carrageenans can undergo a cyclization when using a concentrated sodium hydroxide solution at an increased temperature. This increases gelling properties, such as its strength [215-217]. By using an alkaline hydrolysis or microwave irradiation, carrageenan gels could be 'cross-linked' with poly(acrylamide) [218], acrylic acid [219], methyl methacrylate [220] or a copolymerization with acrylic acid and 2-acrylamido-2-methylpropane-sulfonic acid [221].

These hydrogels are especially very promising for industrial immobilization of enzymes [222]. By precipitating calcium phosphate into a κ-carrageenan matrix, porous nanocomponsites could be prepared useful for bone tissue engineering [223]. Other derivatizations performed are acetylation, oversulphatation and phosphorylation of κ-carrageenan [224]. These modifications can enhance the antioxidant activity of carrageenans [225]. Synthetic κ-seleno-carrageenans may inhibit the proliferation of breast cancer cells [226]. An *O*-maleoyl derivative of κ-carrageenan could be manifested by reaction of tetrabutylammonium salt of the anionic carrageenan fragments with maleic anhydride, 4-dimethylaminopyridine and tributylamine under homogeneous conditions in *N*,*N*-dimethylformamide [227]. As can be seen, the derivatization of carrageenan is very versatile [184].

Methacrylation of polysaccharides

Methacrylic anhydride (MAAH) can be used to enable simultaneous grafting on and cross-linking of the polysaccharides. Reaction of the hydroxyl groups on alginate with the anhydride will result in methacrylated alginate as displayed in Figure I.15. This newly introduced double bond on the backbone can be used in a free radical polymerization in the presence of a whole range of monomers such as acrylic acid, acrylamide etc [228-230].

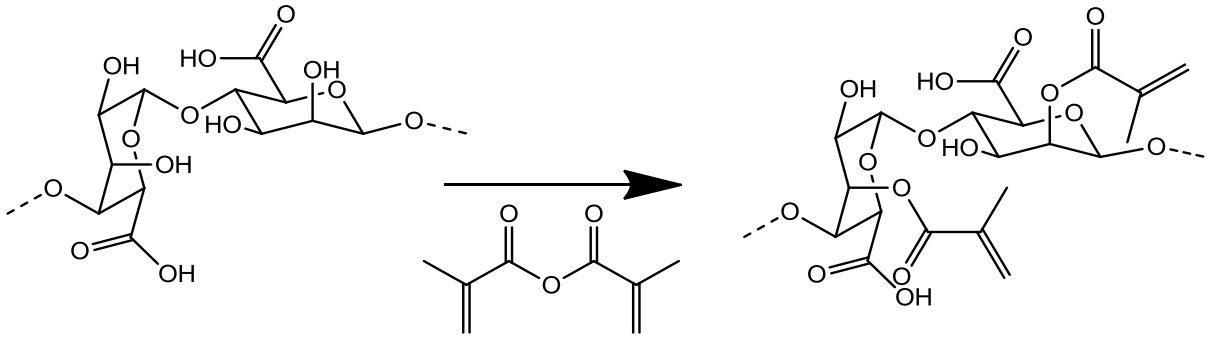

Figure I.15: Methacrylation of alginate. Activated double bonds are incorporated in the alginate backbone to serve as a functional handle for a free radical polymerization.

I.2.7. Stimuli-responsive superabsorbent polymers

Some SAPs undergo large physical and chemical changes upon small environmental variations [231]. These so-called 'smart' polymers [232] have the ability to sense environmental stimuli [233] including changes in pH [233-236], temperature [233, 237-239], light [240, 241], pressure [242] etc. Some applications, including drug release, illustrate an extensive use of pH-sensitive,

'smart' SAPs [233, 243]. The aim is to create a system which releases bioactive components in a manner that precisely matches physiological needs at the correct time and/or appropriate site. To achieve this, the system needs to 'sense' a signal caused by disease or injury and respond accordingly [233]. Some of the 'smart' hydrogel systems will be discussed here.

I.2.7.1. Smart SAPs with thermo-responsive behavior

The most used type of 'smart' hydrogel is a temperature-responsive hydrogel [238, 239]. These polymers are characterized by hydrophobic groups and a lower critical solution temperature (LCST) below which the polymer will remain in solution. Some synthetic examples include poly(N-isopropyl acrylamide), poly(2-oxazoline) and poly(N,N-diethyl acrylamide) [233, 244] as seen in Figure I.16. Chitosan is also thermo-responsive and is used for neural tissue engineering and skin regeneration [245, 246]. At a temperature below the LCST, the hydrophilic segments interact with water and the polymer starts to absorb the surrounding water. When the temperature increases the gel starts to shrink and forces the absorbed liquid out, as now the hydrophobic interactions increase. This decrease in swelling with an increase in temperature is called a negative temperature sensitivity. An interpenetrating network of poly(acrylic acid) and poly(acrylamide) shows an increased swelling with an increase in the temperature and is thus a positive temperature sensitive polymer [247].

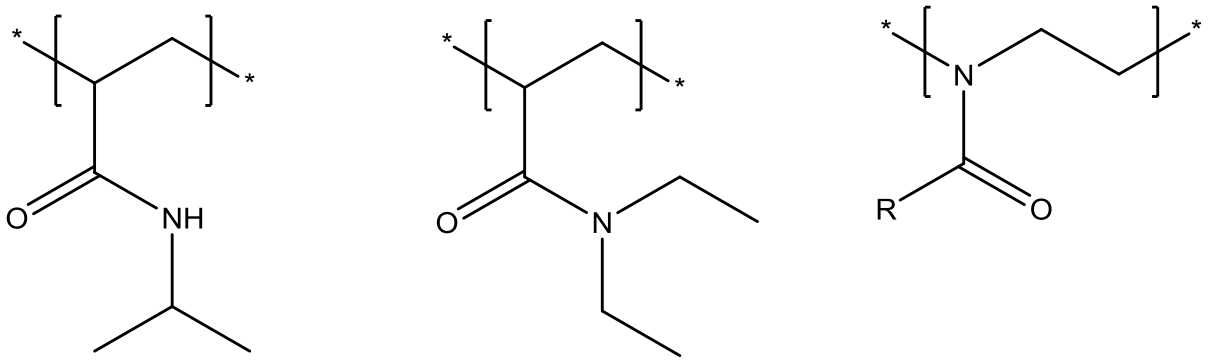

Figure I.16: Chemical structure of some commonly utilized synthetic temperature sensitive polymers. From left to right: PNIPAAm, poly(N,N-diethyl acrylamide) and poly(2-oxazoline).

I.2.7.2. Smart photo- and electro-sensitive SAPs

Light-sensitive hydrogels are very interesting as they might have a huge impact on the properties of the polymer and on the solubility of the polymer to which the respective group is attached. The stimulus can be delivered directly with high accuracy. An example of a UV-responsive hydrogel is a network containing leucocyanide moieties [241]. A dissociation of the molecule into a cyano anion and triphenyl methyl cation occurs upon irradiation. This leads to an increased water affinity and electrostatic repulsion of the ionic groups and thus an increased swelling capacity. An opposite effect can occur when using a VIS-sensitive chromophore, such as chlorophyllin sodium copper salt and incorporate it in a temperature sensitive hydrogel such as poly(N-isopropyl acrylamide), the swelling ratio will now decrease by illumination [248]. As the

chromophore absorbs the light, it disperses the energy as heat due to radiation-less transitions, heating the hydrogel and thus due to the negative temperature sensitivity of PNIPAAm leads to a decreased swelling.

Electro-responsive hydrogels are similar as pH-responsive hydrogels as in both case the sensitivity is related to the present ionic groups. An electrical or chemical potential can be created as ionic groups are attracted by oppositely charged electrodes. Depending on the charges of the ions and the electrodes, this can lead to either an increased or a reduced swelling degree [233, 249].

I.2.7.3. Smart pH-sensitive SAPs

Due to the formation of ions at specific pH-values, the reactive groups in the polymer networks of pH-sensitive hydrogels (e.g. carboxylic acid, sulfonic acid or amine groups) either repel or attract one another. This changing behavior thus depends on the acidity or basicity of the aqueous environment. Electrostatic repulsions between charged conjugates of acidic or basic moieties leads to additional ionization. This means that the pK_a of a polymer is more spread out over a pH-range instead of a single value for the individual monomer. As a result, the water uptake capacity increases or decreases respectively. Identical charges repel one another and create more free volume where a higher amount of water can be absorbed and the swelling capacity thus increases. Acid moieties will be negatively charged above its pK_a, basic moieties below its pK_a as can be seen in Figure I.17. These type of 'smart' SAPs are especially very interesting for drug delivery [233, 243].

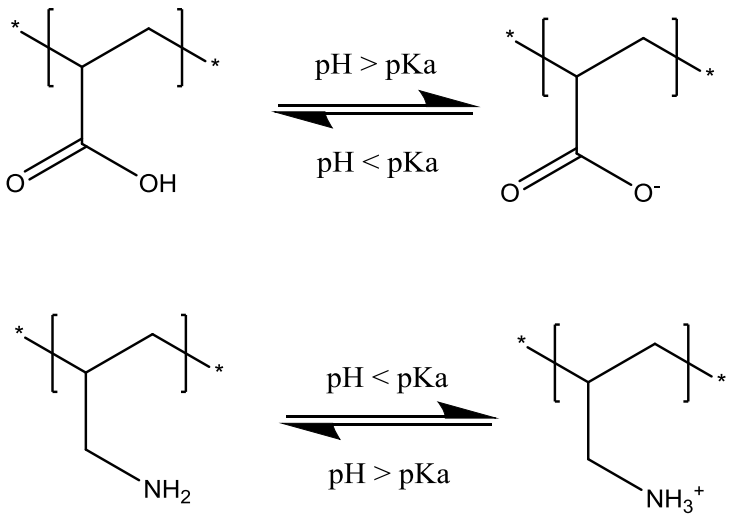

Figure I.17: pH-responsive behavior of a carboxylic acid and amine respectively.

Especially these type of responsive SAPs could be extremely interesting in the intended application as admixture in mortar or concrete for the self-sealing and self-healing of cracks as will be explained subsequently.

I.2.8. Applications of SAPs in concrete

On top of the mentioned fields of SAPs in biomedical, hygienic, agricultural and other applications, it can also be added to cementitious materials. They can be deployed for reduction of autogenous shrinkage, increasing freeze/thaw resistance and inducing self-sealing and -healing of cracks.

During the mixing process, these SAPs will take up a part of the initial mixing water, which later on can be released inside the matrix during the hardening process and lead to internal curing and as such an autogenous shrinkage reduction [22, 49, 67, 113, 250-257]. They result in a similar effect as the LWA particles as they gradually discharge absorbed water and provide internal curing. However, it needs to be taken into account that only cracking due to restrained self-dessication should be prevented to ascertain the cost and benefit of water entrainment. SAP percentages lower than 0.3 m% compared to the added amount of cement are often used. A higher percentage of SAP could otherwise lead to changes in rheological properties and these effects cannot be neglected [67, 258].

The principle of autogenous shrinkage mitigation is shown in Figure I.18. The figures follow the theory of Powers [259]. In Figure I.18a, a system with a high water-to-cement ratio is shown. Here, a lot of capillary water is available to realize complete hydration. In a system with a low water-to-cement ratio (Figure I.18b, lower than 0.42 [254, 259]), the amount of capillary water is completely consumed. The hydration continues with part of the bound gel water, but is limited. In case an additional source of water is provided (Figure I.18c), no gel water is used and overall, the volume does not change and no autogenous shrinkage is found if the system adequately and ideally provides the water for internal curing.

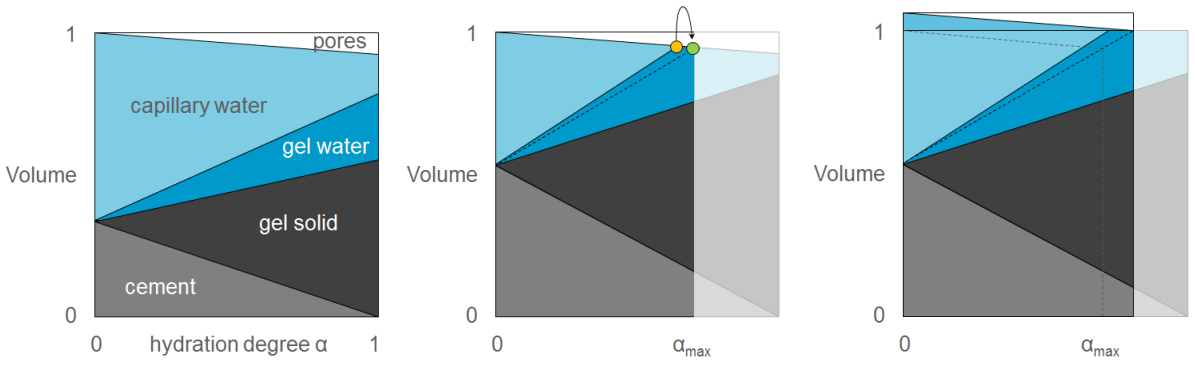

(a) (b) (c)

Figure I.18: Principle of autogenous shrinkage in a system with a high water-to-cement ratio (a) and a low water-to-cement ratio without (b) and with internal curing (c) [260].

As the available water influences the microstructural development and hardening, the water kinetics in samples with SAPs is a key parameter in the microstructural properties and moisture transport processes. Hydration of a mixture determines the microstructural development. Pastes

with SAPs show less capillary porosity at later ages if additional water is used (compared to in case no additional water is used) [256]. The water released from the SAPs results in continued hydration, thus decreasing the micro-porosity at later ages [256], except from the macro-pores created by the SAPs. An X-ray tomography study [261] showed a reduction of the amount of smaller capillary pores. This is due to two effects: filling of the existing pores with hydration products due to internal curing and reduction of the initial micro-cracks in the interior of a cementitious matrix, as autogenous shrinkage is partially reduced. Mercury intrusion porosimetry (MIP) [252, 262] showed a higher total porosity due to macro-pore formation in specimens with SAPs and additional water. If no additional water was added, the total porosity was lower for mixtures with SAPs [262]. MIP does not directly measure the macro-pores (> 50 nm), since the range is narrow (working range of MIP; 0.1 nm < pore size < 100 µm), but macro-pores do show up in the total porosity. The macro-pores are hereby accessed only through smaller capillary pores, so that the volume is assigned to these narrower radii. Mixtures with the same effective water-to-cement ratio (ratio of the mixing water not held by the SAPs over the cement content), show the same capillary porosity [263]. These researchers also found a lower water permeability for mixtures with SAPs and additional water (24 g water/g SAP). The microstructure in between SAPs is denser due to internal curing and the macro-pores do not interconnect. Therefore, the permeability is lower than of reference samples and this was also shown by neutron radiography [264].

There are several important factors to take into consideration to receive perfect mitigation of autogenous shrinkage. First, the cementitious mixture is an influencing factor. It has been shown that autogenous shrinkage can be mitigated in systems with Portland cement, silica fume [255] and in systems containing blast-furnace slag [23, 265, 266] or fly ash [23]. Second, the superabsorbent polymer is another factor of influence [260]. There are different shapes of SAPs, ranging from spherical and irregular to fiber types. They all show a different surface area available to transfer water towards the cementitious matrix for internal curing. Furthermore, the polymeric properties of the SAPs are important. They influence the osmotic pressure responsible for swelling but also for desorption. If the SAP is releasing the water too fast (before final setting), then it would increase the total water-to-cement ratio. If it is too slow, it will keep its water and will not provide it to the cementitious matrix for internal curing. It is therefore of utmost importance to use specific types of superabsorbent polymers which can ideally provide water at the right times. If not, the autogenous shrinkage may not be reduced or counteracted and the overall properties at later ages may be completely different.

Microstructural properties directly affect the strength characteristics of the cementitious material. But, in literature, the influences of SAPs are ambiguous. They can lead to an increase and/or a decrease in mechanical properties. It all depends among other on the used type of SAP, the addition of water to counteract the loss in workability and the mixing procedure.

Several authors mention that the flexural and compressive strength decreases when SAPs and additional water are added [34, 252, 253, 255, 256, 267-269]. In these studies additional water was added until the same flow/slump was reached as a compensation for the loss of workability due to the water uptake of SAPs compared to reference mixtures, unless stated differently. The

lower the water-to-cement ratio, the more the strength of the composite is influenced by the addition of SAPs [256]. This effect is more pronounced at early ages due to the higher total porosity at early ages [252, 270]. Internal curing leads to further hydration and the effect of SAPs on strength-loss is thus reduced at later ages. Theoretically, even a complete hydration due to internal curing is possible [259]. In Powers' model, however, complete hydration in saturated systems is only possible in systems above a certain water-to-cement ratio (0.42 [254, 259]) and this complete hydration is not possible for cementitious materials with a very low water-to-cement ratio. This is because one gram of cement chemically binds 0.23 g water and will bind 0.19 g of gel water [254]. The sum of both is 0.42 g. If this total amount of water is not available, total hydration is not possible unless water is provided from the surroundings during hardening.

Further hydration thus improves the mechanical properties but is mostly counteracted by the strength-loss caused by the macro-pores created by the SAPs [271]. SAPs thus have both a positive and a negative effect on the mechanical properties. A decrease in strength is observed at earlier testing ages (< 7 days) while sometimes increases are obtained at later ages [250], especially in systems with supplementary cementitious materials where the internal curing reservoirs are available for the longer term pozzolanic reactions. Also, the water-to-cement ratio has to be taken into account. At a value of 0.35 for example, the increased degree of hydration may counteract the strength loss due to macro-pore formation [272]. At higher water-to-cement ratios, this is not the case.

The structure of a cementitious material is affected by the water-to-cement ratio. As SAPs take up the mixing water, the water-to-cement ratio appears lower, resulting in a closely-packed matrix and subsequent hydration due to the release of that water. Samples without SAPs do not have access to this free water. Therefore, water penetration in samples with and without SAPs is different.

According to different authors, there is a link between freeze/thaw resistivity and internal curing. As the SAPs will release their water during the hardening, they will leave behind air-filled pores. During freeze/thaw cycles, these voids can protect the concrete on a similar way as by using air entrainment [22, 113, 273]. With SAPs, the dimensions of the voids are fixed to the swollen state of the SAP during mixing, in contrast to regular air entrainment. Addition does not necessarily affect the compressive strength and seems to be promising independent from local raw materials and production processes [274]. There is a considerable improvement in the material performance with the use of SAP in terms of decreasing mass loss due to scaling after the given number of freeze-thaw cycles [274]. The dynamic elastic Young's modulus decreased less after tests without deicing salt. This demonstrates that increasing freeze-thaw resistance by use of SAP is a promising approach. Another advantage is avoiding air void fusions during vibrations as these polymer particles are very stable in fresh concrete [275]. From a more practical point of view, concrete with air entrainment is less stable when it needs to be transported. When using SAPs, the properties are fixed and the concrete can easily be transported. Also, as the macro-pore size is fixed, one can engineer the material in the ideal way, also taking the ideal spacing factor into account. The appropriate size-designed pore systems could improve the durability in terms of freeze/thaw resistance.

As these SAPs create pores in the concrete matrix, they can also be used for self-sealing and self-healing purposes [34, 47, 49, 64, 116, 276, 277]. First, there is a distinction between self-sealing due to blockage and self-healing due to further hydration. This is important to know as a possible temporal self-sealing effect may not lead to a regain in mechanical properties. Due to the swelling of the SAPs, there is an immediate sealing, but not permanent. Together with the promoted autogenous healing, there will be a permanent sealing in time, when the healing products are formed. Due to the presence of these voids, cracks will propagate through these weakened sections and ensure the SAP to be at the intended location. Water entering the cracks will fill the voids and let the SAP swell, expand and block the further ingress of any harmful particle as schematically described in Figure I.18 [278]. When the crack is ideally sealed from further ingress, less deteriorating mechanisms may occur. The ingress of water for example could induce steel corrosion, frost attack, chemical attack and internal expansion, endangering the durability of a structure. The sealing of a crack can be monitored by means of studying the (water) permeability. Lee et al. [278-280] investigated the incorporation of SAPs in concrete in order to obtain self-sealing properties. When liquids enter a crack, SAP particles along the crack faces will swell and block the crack. This is reflected in a decrease of water permeability through a crack. When a water head is imposed, the SAPs are able to withstand water movement, as studied and visualized by means of neutron radiography [264]. Song et al. [281] synthesized a superabsorbent resin in situ to repair concrete leakage, but this was rather a manual repair than an intrinsic sealing mechanism. The amounts of SAP needed for self-sealing and -healing are often higher (up to 1 m% versus cement weight, similar as for promoted autogenous healing) compared to the amount needed for internal curing (typically 0.3-0.6 m%).

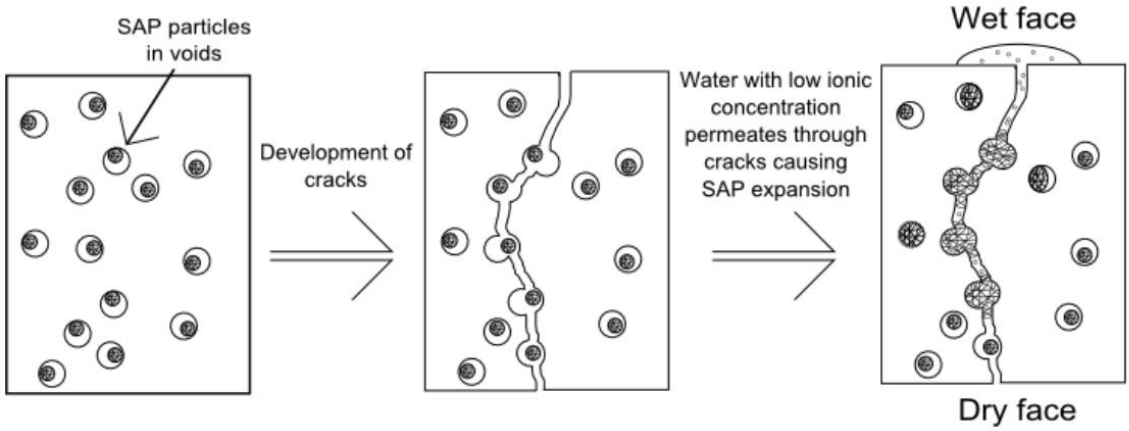

Figure I.18: Schematic display of self-sealing of cracks in concrete by using SAPs [278].

SAP-particles are very useful for autogenous healing as they absorb water during wet periods and slowly release it during dry periods. When liquids enter a crack, SAP particles along the crack faces will swell and block the crack. Also, as the SAPs swell, they will initially seal a crack from intruding fluids, thus increasing the durability [278, 279]. By absorbing fluids from the surrounding environment, water is available for healing [282]. This is beneficial as water will also be available during dry periods as well. This is preferential for $CaCO_3$ crystallization after dissolution of CO_2 from air in the water released from the SAPs. Formation of new cracks was noticed upon reloading the samples containing SAPs and regain of mechanical properties was shown. The regain was higher compared to reference specimens without SAPs. Even second

reloading of healed samples leads to partial additional regain in mechanical properties [283]. Again, this regain is higher compared to the reference. The healing products were visualized by means of X-ray computed microtomography [284]. The extent of autogenous healing in a cementitious material depends on the crack depth. Only near the crack mouth (0 up to 800–1000 µm) the crack is closed by calcium carbonate formation in case of wet/dry cycles [284, 285]. In combination with superabsorbent polymers, the extent of healing was more substantial.

For mixtures containing superabsorbent polymers there was even partial healing in the interior of the crack when stored at a relative humidity of 60% or more than 90%. Energy-dispersive spectroscopy combined with microscopic analysis showed that the healing products were mainly calcium carbonate. The cementitious material with superabsorbent polymers is thus an excellent material to use in future building applications as the healing capacity is improved.

I.2.9. Challenges to overcome by using SAPs in concrete

SAPs take up mixing water when added to mortar or concrete. If no additional water is provided, the workability and the W/C factor of the mixture will be reduced and the needed strength cannot be guaranteed anymore [275]. For example, 0.4 w% SAP relative to the cement weight with an absorption capacity of 15 g/g can lower the effective W/C by 0.06 [67]. By the swelling capacity of the SAP in a cement filtrate solution, an idea can be made to the right needed amount of supplementary water to eliminate the influence on the workability and obtain a similar W/C factor as the reference by aiming for a same slump/flow [277]. This needed amount depends on the polymer elasticity, osmotic pressure in the mix and polymer affinity for the mixing water and is more restricted in a concrete mixture than in the cement filtrate solution. This limits the expansion of the SAPs [278].

SAPs can be introduced in different ways. Most researchers dry mix the polymers prior to water addition. This ensures a homogenous distribution of the SAPs. Other researchers pre-saturate or pre-soak the SAPs prior to mixing [286, 287]. Depending on the targeted application, this can be useful. However, such pre-saturation will lead to clusters of SAPs, and a non-homogenous mixture. This is unwanted as the overall properties may differ and less control is achieved. It is important to always take the effective water-to-cement ratio into account. One should make a verification when the matrix is hardened, i.e. by calculating the size of the actual macro-pores and to back calculate the true absorption of mixing water [269, 288].

Different SAPs react differently. They all may influence the cementitious properties in their own intrinsic way. This can have desired and unwanted influences. One needs to be very careful when using/buying specific SAPs as the targeted effect may not be attained. The effect of the SAPs can serve one purpose but not the other. There are thus different applications for which a specific SAP may be more useful compared to another.

The SAPs take up additional water when mixed in and release it again due to a lower relative humidity during the cement hydration process. This hereby promotes internal curing and helps to maintain the internal relative humidity of the matrix [23]. By releasing this water, they leave behind macro pores which negatively influences the strength [289]. Despite this decrease in

strength, a decrease in the micro-porosity can be noticed due to further hydration. The latter also causes a reduction in autogenous shrinkage as well as in micro-cracks [269]. It all depends on the added amount of SAP, and thus the intended application whether the effect of further hydration and internal curing leading to a strength increase on the one hand is more profound than the pore formation and strength loss on the other hand [290, 291]. It is thus of the utmost importance to limit SAP swelling in fresh concrete, but not at the expense of further hydration. As a solution, the use of pH-responsive SAPs, which will swell when needed, can become extremely useful [34, 64].

I.2.10. Conclusions

Concrete is the most used man-made material worldwide. Despite its many advantages, it also has a few main issues, such as cracking. To autogenously heal those cracks, the crack width should be limited, there should be moist environmental conditions present and an improved hydration by using additives. To enhance the autogenous healing capacity of concrete, a variation of different healing additives are possible. Upon crack formation, these additives provide or aid in the chemical process to close and heal the crack. The main healing method used further in this PhD manuscript is the use of superabsorbent polymers. They have been used already for internal curing, freeze/thaw resistance and self-sealing and self-healing of cracks. This latter application is the intended one for this manuscript. These materials can absorb up to several hundred times their own weight making it possible to completely block cracks in concrete. Additionally, when releasing that absorbed water again to the surrounding matrix, it can aid in the self-healing of cracks. Both synthetic and semi-synthetic SAPs have their advantages and disadvantages and will be introduced throughout this manuscript. Interestingly, pH-responsive SAPs have the effect that they can swell differently while varying the pH. In fresh mortar, with a high pH, they should swell less, to reduce the strength loss accompanied with macro pores formed. When cracks occur, the water entering has a more neutral to slightly alkaline pH and the swelling should be stronger to be able to block the crack. There are still some challenges accompanying the use of SAPs in concrete and they will be discussed during this work.

I.2.11. References

[1] World Business Council for Sustainable Development WBCSD. *The Cement Sustainability. Initiative - Recycling Concrete*. 2009.
[2] CEMBUREAU - The European Cement Association . Key Facts and Figures [Online; accessed 31 March 2016]. http://www.cembureau.be/about-cement/key-facts-figures.
[3] Taerwe L. *Betontechnologie*. 2006.
[4] Thomas J, Jennings H. The Science of Concrete. http://iti.northwestern.edu/cement/index.html. 2008.
[5] Velez K, Maximilien S, Damidot D, Fantozzi G, Sorrentino F. Determination by nanoindentation of elastic modulus and hardness of pure constituents of Portland cement clinker. Cement and Concrete Research. 2001;31(4):555-61.
[6] Lewis J. Concrete: A material for the new stone age. http://matse1.matse.illinois.edu/concrete/concrete.html. 1995.
[7] Van Eijk RJ, Brouwers HJH. Prediction of hydroxyl concentrations in cement pore water using a numerical cement hydration model. Cement and Concrete Research. 2000;30(11):1801-6.
[8] Wittmann FH, Roelfstra PE, Mihashi H, Huang Y-Y, Zhang X-H, Nomura N. Influence of age of loading, water-cement ratio and rate of loading on fracture energy of concrete. Mat Struct. 1987;20(2):103-10.
[9] Van Breugel K. Is there a market for self-healing cement-based materials. Proceedings of the first international conference on self-healing materials 2007.
[10] Mahasenan N, Smith S, Humphreys K, Kaya Y. The cement industry and global climate change: current and potential future cement industry CO2 emissions. Greenhouse Gas Control Technologies-6th International Conference: Elsevier; 2003. p. 995-1000.
[11] Meyer C. The greening of the concrete industry. Cement and Concrete Composites. 2009;31(8):601-5.
[12] Asadollahfardi G, Asadi M, Jafari H, Moradi A, Asadollahfardi R. Experimental and statistical studies of using wash water from ready-mix concrete trucks and a batching plant in the production of fresh concrete. Construction and Building Materials. 2015;98:305-14.
[13] Aggoune S, Imache R, Khadraoui A, Mezghiche M. Evaluation of e-government information systems agility in the perspective of sustainability. Electronic Government and the Information Systems Perspective: Springer; 2011. p. 315-29.
[14] Mihashi H, Nishiwaki T. Development of engineered self-healing and self-repairing concrete-state-of-the-art report. Journal of Advanced Concrete Technology. 2012;10(5):170-84.
[15] Ferrara L, Krelani V, Carsana M. A "fracture testing" based approach to assess crack healing of concrete with and without crystalline admixtures. Construction and Building Materials. 2014;68:535-51.
[16] Wu M, Johannesson B, Geiker M. A review: Self-healing in cementitious materials and engineered cementitious composite as a self-healing material. Construction and Building Materials. 2012;28(1):571-83.
[17] Stewart MG, Rosowsky DV. Time-dependent reliability of deteriorating reinforced concrete bridge decks. Structural Safety. 1998;20(1):91-109.
[18] Arıoglu N, Girgin ZC, Arıoglu E. Evaluation of ratio between splitting tensile strength and compressive strength for concretes up to 120 MPa and its application in strength criterion. ACI Materials Journal. 2006;103(1):18-24.
[19] Van Tittelboom K, De Belie N, De Muynck W, Verstraete W. Use of bacteria to repair cracks in concrete. Cement and Concrete Research. 2010;40(1):157-66.
[20] Sellevold EJ, Bjøntegaard Ø. Coefficient of thermal expansion of cement paste and concrete: Mechanisms of moisture interaction. Mat Struct. 2006;39(9):809-15.
[21] Wang K, Jansen DC, Shah SP, Karr AF. Permeability study of cracked concrete. Cement and Concrete Research. 1997;27(3):381-93.

[22] Bentz DP, Jensen OM. Mitigation strategies for autogenous shrinkage cracking. Cement and Concrete Composites. 2004;26(6):677-85.
[23] Snoeck D, Jensen OM, De Belie N. The influence of superabsorbent polymers on the autogenous shrinkage properties of cement pastes with supplementary cementitious materials. Cement and Concrete Research. 2015;74:59-67.
[24] Weber S, Reinhardt HW. A new generation of high performance concrete: concrete with autogenous curing. Advanced Cement Based Materials. 1997;6(2):59-68.
[25] Shen D, Jiang J, Shen J, Yao P, Jiang G. Influence of curing temperature on autogenous shrinkage and cracking resistance of high-performance concrete at an early age. Construction and Building Materials. 2016;103:67-76.
[26] Jensen OM, Hansen PF. Water-entrained cement-based materials: I. Principles and theoretical background. Cement and Concrete Research. 2001;31(4):647-54.
[27] Tazawa E-i, Miyazawa S. Influence of cement and admixture on autogenous shrinkage of cement paste. Cement and Concrete Research. 1995;25(2):281-7.
[28] Reynolds D, Browning J, Darwin D. Lightweight aggregates as an internal curing agent for low-cracking high-performance concrete Masters Abstracts International 2009.
[29] Ribeiro MSS. Expansive cement blend for use in shrinkage-compensating mortars. Mat Struct. 1998;31(6):400-4.
[30] Koerner RM, Koerner GR. Geotextiles used as flexible forms. Geotextiles and geomembranes. 1996;14(5):301-11.
[31] Swayze MA. Early concrete volume changes and their control. Journal Proceedings 1942. p. 425-40.
[32] Cailleux E, Pollet V. Investigations on the development of self-healing properties in protective coatings for concrete and repair mortars. 2nd international conference on self healing materials, Chicago, USA 2009.
[33] Joseph C, Jefferson AD, Cantoni MB. Issues relating to the autonomic healing of cementitious materials. Proceedings of the 1st International Conference on Self-Healing Materials, Noordwijk, the Netherlands Springer; 2007.
[34] Mignon A, Snoeck D, Schaubroeck D, Luickx N, Dubruel P, Van Vlierberghe S, et al. pH-responsive superabsorbent polymers: A pathway to self-healing of mortar. Reactive and Functional Polymers. 2015;93(0):68-76.
[35] Sanjay P, Kshitij CS, Yusuke S, Toshihiro O, Ryosuke K, Yoshikazu A. Feasibility of externally activated self-repairing concrete with epoxy injection network and Cu-Al-Mn superelastic alloy reinforcing bars. Smart Materials and Structures. 2014;23(10):105027.
[36] Bang SS, Galinat JK, Ramakrishnan V. Calcite precipitation induced by polyurethane-immobilized Bacillus pasteurii. Enzyme and Microbial Technology. 2001;28(4–5):404-9.
[37] Ryu JS. An experimental study on the repair of concrete crack by electrochemical technique. Mat Struct. 2001;34(7):433-7.
[38] Allen RTL, Edwards SC, Shaw DN. Repair of concrete structures: CRC Press; 1992.
[39] Broomfield JP. Corrosion of steel in concrete: understanding, investigation and repair: CRC Press; 2002.
[40] Hager MD, Greil P, Leyens C, van der Zwaag S, Schubert US. Self-Healing Materials. Advanced Materials. 2010;22(47):5424-30.
[41] Edvardsen C. Water Permeability and Autogenous Healing of Cracks in Concrete. Materials Journal. 1999;96(4):448-54.
[42] Neville A. Autogenous Healing - A Concrete Miracle? Concrete International. 2002;24(11):76-82.
[43] Snoeck D, De Belie N. From straw in bricks to modern use of microfibers in cementitious composites for improved autogenous healing–A review. Construction and Building Materials. 2015;95:774-87.
[44] Yang Y, Lepech MD, Yang E-H, Li VC. Autogenous healing of engineered cementitious composites under wet–dry cycles. Cement and Concrete Research. 2009;39(5):382-90.
[45] Ter Heide N. Crack healing in hydrating concrete. Delft University of Technology, Delft. 2005.

[46] Achal V, Mukherjee A, Basu PC, Reddy MS. Lactose mother liquor as an alternative nutrient source for microbial concrete production by Sporosarcina pasteurii. Journal of industrial microbiology & biotechnology. 2009;36(3):433-8.
[47] Snoeck D, Van Tittelboom K, De Belie N, Steuperaert S, Dubruel P. The use of superabsorbent polymers as a crack sealing and crack healing mechanism in cementitious materials. Concrete Repair, Rehabilitation and Retrofitting III: 3rd International Conference on Concrete Repair, Rehabilitation and Retrofitting, ICCRRR-3, 3-5 September 2012, Cape Town, South Africa: CRC Press; 2012. p. 58.
[48] Van Tittelboom K, De Belie N. Autogenous healing of cracks in cementitious materials with varying mix compositions. 2nd International conference on Self-Healing Materials (ICSHM 2009)2009.
[49] Van Tittelboom K, De Belie N. Self-healing in cementitious materials—A review. Materials. 2013;6(6):2182-217.
[50] Van Tittelboom K. Self-Healing Concrete through Incorporation of Encapsulated Bacteria-or Polymer-Based Healing Agents. PhD thesis Ghent University; 2012.
[51] ter Heide N, Schlangen E. Self-healing of early age cracks in concrete. First international conference on self healing materials Springer, Dordrecht2007.
[52] Schlangen E, Ter Heide N, Van Breugel K. Crack healing of early age cracks in concrete. Measuring, Monitoring and Modeling Concrete Properties: Springer; 2006. p. 273-84.
[53] Li VC. On engineered cementitious composites (ECC). Journal of Advanced Concrete Technology. 2003;1(3):215-30.
[54] Snoeck D, De Belie N. Mechanical and self-healing properties of cementitious composites reinforced with flax and cottonised flax, and compared with polyvinyl alcohol fibres. biosystems engineering. 2012;111(4):325-35.
[55] Termkhajornkit P, Nawa T, Yamashiro Y, Saito T. Self-healing ability of fly ash–cement systems. Cement and Concrete Composites. 2009;31(3):195-203.
[56] Huang H, Ye G, Damidot D. Effect of blast furnace slag on self-healing of microcracks in cementitious materials. Cement and Concrete Research. 2014;60:68-82.
[57] Diamond S. Delayed ettringite formation—processes and problems. Cement and Concrete Composites. 1996;18(3):205-15.
[58] Sisomphon K, Copuroglu O, Koenders EAB. Self-healing of surface cracks in mortars with expansive additive and crystalline additive. Cement and Concrete Composites. 2012;34(4):566-74.
[59] Sisomphon K, Copuroglu O, Koenders EAB. Effect of exposure conditions on self healing behavior of strain hardening cementitious composites incorporating various cementitious materials. Construction and Building Materials. 2013;42:217-24.
[60] Concrete by SEM. http://www.whd.co.uk/Concrete/concretebysem.html 2016.
[61] Janssen D. Water encapsulation to initiate self-healing in cementitious materials: Master Thesis, Delft University of Technology, Delft, The Netherlands; 2011.
[62] Akcay B, Tasdemir MA. Effects of lightweight aggregates on autogenous deformation in concrete. Measuring, Monitoring and Modeling Concrete Properties: Springer; 2006. p. 163-70.
[63] Bentz DP, Snyder KA. Protected paste volume in concrete: extension to internal curing using saturated lightweight fine aggregate. Cement and Concrete Research. 1999;29(11):1863-7.
[64] Mignon A, Graulus G-J, Snoeck D, Martins J, De Belie N, Dubruel P, et al. pH-sensitive superabsorbent polymers: a potential candidate material for self-healing concrete. J Mater Sci. 2014;50(2):970-9.
[65] Snoeck D, Van Tittelboom K, Steuperaert S, Dubruel P, De Belie N. Self-healing cementitious materials by the combination of microfibres and superabsorbent polymers. Journal of Intelligent Material Systems and Structures. 2014;25(1):13-24.
[66] Snoeck D, Dubruel P, De Belie N. How to seal and heal cracks in cementitious materials by using superabsorbent polymers. Application of Superabsorbent Polymers and Other New Admixtures in Concrete Construction: RILEM Publications; 2014. p. 375-84.
[67] Jensen OM, Hansen PF. Water-entrained cement-based materials: II. Experimental observations. Cement and Concrete Research. 2002;32(6):973-8.

[68] Katsuhata T, Ohama Y, Demura K. Investigation of microcracks self-repair function of polymer-modified mortars using epoxy resins without hardeners. Honolulu: Tagungsunterlagen, X ICPIC. 2001.
[69] Ohama Y. Recent progress in concrete-polymer composites. Advanced Cement Based Materials. 1997;5(2):31-40.
[70] Zuo X, Li H. The crack self-healing properties of cement-based material with EVA heat-melt adhesive. Journal of Wuhan University of Technology-Mater Sci Ed. 2011;26(4):774-9.
[71] Wiktor V, Jonkers HM. Quantification of crack-healing in novel bacteria-based self-healing concrete. Cement and Concrete Composites. 2011;33(7):763-70.
[72] Jonkers HM, Thijssen A, Muyzer G, Copuroglu O, Schlangen E. Application of bacteria as self-healing agent for the development of sustainable concrete. Ecological engineering. 2010;36(2):230-5.
[73] Erşan YÇ, Da Silva FB, Boon N, Verstraete W, De Belie N. Screening of bacteria and concrete compatible protection materials. Construction and Building Materials. 2015;88:196-203.
[74] Wang J, Mignon A, Snoeck D, Wiktor V, Boon N, De Belie N. Application of modified-alginate encapsulated carbonate producing bacteria in concrete: a promising strategy for crack self-healing. Frontiers in Microbiology. 2015;6.
[75] Van Tittelboom K, De Belie N, Van Loo D, Jacobs P. Self-healing efficiency of cementitious materials containing tubular capsules filled with healing agent. Cement and Concrete Composites. 2011;33(4):497-505.
[76] De Koster SAL, Mors RM, Nugteren HW, Jonkers HM, Meesters GMH, Van Ommen JR. Geopolymer coating of bacteria-containing granules for use in self-healing concrete. Procedia Engineering. 2015;102:475-84.
[77] Li VC, Lim YM, Chan Y-W. Feasibility study of a passive smart self-healing cementitious composite. Composites Part B: Engineering. 1998;29(6):819-27.
[78] Dry CM. Three designs for the internal release of sealants, adhesives, and waterproofing chemicals into concrete to reduce permeability. Cement and Concrete Research. 2000;30(12):1969-77.
[79] Joseph C, Jefferson AD, Isaacs B, Lark RJ, Gardner DR. Experimental investigation of adhesive-based self-healing of cementitious materials. Magazine of concrete Research. 2010;62(11):831-43.
[80] Jonkers HM. Bacteria-based self-healing concrete. Heron, 56 (1/2). 2011.
[81] Huang H, Ye G. Application of sodium silicate solution as self-healing agent in cementitious materials. International RILEM conference on advances in construction materials through science and engineering: RILEM Publications SARL; 2011. p. 530-6.
[82] Yin T, Rong MZ, Zhang MQ. Self-Healing Epoxy Composites–Part I: Curing Kinetics and Heat-Resistant Performance. Advanced Materials Research: Trans Tech Publ; 2013. p. 383-6.
[83] Xing F, Ni Z, Han N, Dong B, Du X, Huang Z, et al. Self-healing mechanism of a novel cementitious composite using microcapsules. Proceedings of the International Conference on Durability of Concrete Structures, Hangzhou, China 2008.
[84] Yang M, Zhu X, Ren G, Men X, Guo F, Li P, et al. Tribological Behaviors of Polyurethane Composite Coatings Filled with Ionic Liquid Core/Silica Gel Shell Microcapsules. Tribology Letters. 2015;58(1):1-9.
[85] Huang H, Ye G. A review on self-healing in reinforced concrete structures in view of serving conditions. 3rd International Conference on Service Life Design for Infrastructure, Zhuhai, China, 15-17 Oktober 20142014.
[86] Huang H, Ye G, Shui Z. Feasibility of self-healing in cementitious materials–By using capsules or a vascular system? Construction and Building Materials. 2014;63:108-18.
[87] Sangadji S, Schlangen E. Self Healing of Concrete Structures-Novel approach using porous network concrete. Journal of Advanced Concrete Technology. 2012;10(5):185-94.
[88] Mihashi H, Kaneko Y, Nishiwaki T, Otsuka K. Fundamental Study on Development of Intelligent Concrete Characterized by Self-Healing Capability for Strength. Concrete Research and Technology. 2000;11(2):21-8.
[89] Zohuriaan-Mehr MJ, Omidian H, Doroudiani S, Kabiri K. Advances in non-hygienic applications of superabsorbent hydrogel materials. J Mater Sci. 2010;45(21):5711-35.

[90] Kim D, Park K. Swelling and mechanical properties of superporous hydrogels of poly(acrylamide-co-acrylic acid)/polyethylenimine interpenetrating polymer networks. Polymer. 2004;45(1):189-96.
[91] Abd Alla SG, Sen M, El-Naggar AWM. Swelling and mechanical properties of superabsorbent hydrogels based on Tara gum/acrylic acid synthesized by gamma radiation. Carbohydrate Polymers. 2012;89(2):478-85.
[92] Yu Y, Liu L, Kong Y, Zhang E, Liu Y. Synthesis and properties of N-maleyl chitosan-cross-linked poly (acrylic acid-co-acrylamide) superabsorbents. Journal of Polymers and the Environment. 2011;19(4):926-34.
[93] Buchholz FL, Graham AT. Modern superabsorbent polymer technology. John! Wiley & Sons, Inc, 605 Third Ave, New York, NY 10016, USA, 1998 279. 1998.
[94] Ahmed EM. Hydrogel: preparation, characterization, and applications. Journal of advanced research. 2013.
[95] Mohammad J. Zohuriaan-Mehr KK. Superabsorbent Polymer Materials: A Review. Iranian Polymer Journal. 2008;17((6)):451-77.
[96] Horkay F, Tasaki I, Basser PJ. Osmotic swelling of polyacrylate hydrogels in physiological salt solutions. Biomacromolecules. 2000;1(1):84-90.
[97] Rosa F, Casquilho M. Effect of synthesis parameters and of temperature of swelling on water absorption by a superabsorbent polymer. Fuel Processing Technology. 2012;103:174-7.
[98] Buchholz FL. Superabsorbent Polymers: An Idea Whose Time Has Come. Journal of Chemical Education. 1996;73(6):512-5.
[99] Caló E, Khutoryanskiy VV. Biomedical applications of hydrogels: A review of patents and commercial products. European Polymer Journal. 2015;65:252-67.
[100] Silva D, Fernandes AC, Nunes TG, Colaço R, Serro AP. The effect of albumin and cholesterol on the biotribological behavior of hydrogels for contact lenses. Acta biomaterialia. 2015;26:184-94.
[101] Kim DW, Kim KS, Seo YG, Lee B-J, Park YJ, Youn YS, et al. Novel sodium fusidate-loaded film-forming hydrogel with easy application and excellent wound healing. International Journal of Pharmaceutics. 2015;495(1):67-74.
[102] Sadeghi M, Hosseinzadeh H. Synthesis of Starch—Poly(Sodium Acrylate-co-Acrylamide) Superabsorbent Hydrogel with Salt and pH-Responsiveness Properties as a Drug Delivery System. Journal of Bioactive and Compatible Polymers. 2008;23(4):381-404.
[103] Pourjavadi A, Barzegar S. Synthesis and Evaluation of pH and Thermosensitive Pectin-Based Superabsorbent Hydrogel for Oral Drug Delivery Systems. Starch - Stärke. 2009;61(3-4):161-72.
[104] Torres-Lugo M, Peppas NA. Molecular Design and in Vitro Studies of Novel pH-Sensitive Hydrogels for the Oral Delivery of Calcitonin. Macromolecules. 1999;32(20):6646-51.
[105] Cheung S-w, Cho P, Chan B, Choy C, Ng V. A comparative study of biweekly disposable contact lenses: silicone hydrogel versus hydrogel. Clinical and Experimental Optometry. 2007;90(2):124-31.
[106] Guilherme MR, Aouada FA, Fajardo AR, Martins AF, Paulino AT, Davi MFT, et al. Superabsorbent hydrogels based on polysaccharides for application in agriculture as soil conditioner and nutrient carrier: A review. European Polymer Journal. 2015;72:365-85.
[107] Vundavalli R, Vundavalli S, Nakka M, Rao DS. Biodegradable Nano-Hydrogels in Agricultural Farming-Alternative Source For Water Resources. Procedia Materials Science. 2015;10:548-54.
[108] Demitri C, Scalera F, Madaghiele M, Sannino A, Maffezzoli A. Potential of cellulose-based superabsorbent hydrogels as water reservoir in agriculture. International Journal of Polymer Science. 2013;2013.
[109] Woodhouse J, Johnson MS. Effect of superabsorbent polymers on survival and growth of crop seedlings. Agricultural Water Management. 1991;20(1):63-70.
[110] Mo C, Shu-quan Z, Hua-Min L, Zhan-bin H, Shu-qin L. Synthesis of poly(acrylic acid)/sodium humate superabsorbent composite for agricultural use. Journal of Applied Polymer Science. 2006;102(6):5137-43.
[111] Davies LC, Novais JM, Martins-Dias S. Detoxification of olive mill wastewater using superabsorbent polymers. Environ Technol. 2004;25(1):89-100.

[112] Sheu JJ. Cables such as optical fiber cables including superabsorbent polymeric materials which are temperature and salt tolerant. Google Patents; 1992.
[113] Craeye B, Geirnaert M, Schutter GD. Super absorbing polymers as an internal curing agent for mitigation of early-age cracking of high-performance concrete bridge decks. Construction and Building Materials. 2011;25(1):1-13.
[114] Wang J, Snoeck D, Van Vlierberghe S, Verstraete W, De Belie N. Application of hydrogel encapsulated carbonate precipitating bacteria for approaching a realistic self-healing in concrete. Construction and Building Materials. 2014;68(0):110-9.
[115] Viktor Mechtcherine LD, Joachim Schulze. Internal curing by super absorbent polymers (SAP) – effects on material properties of self-compacting fibre-reinforced high performance concrete. In: O. M. Jensen PL, K. Kovler, editor.: RILEM Publications SARL; 2006. p. 87 - 96.
[116] Mignon A, Snoeck D, D'Halluin K, Balcaen L, Vanhaecke F, Dubruel P, et al. Alginate biopolymers: Counteracting the impact of superabsorbent polymers on mortar strength. Construction and Building Materials. 2016;110:169-74.
[117] Hansen MR, Young Sr RH. Superabsorbent polymer fibers. Google Patents; 1996.
[118] Lim D-W, Song K-G, Yoon K-J, Ko S-W. Synthesis of acrylic acid-based superabsorbent interpenetrated with sodium PVA sulfate using inverse-emulsion polymerization. European Polymer Journal. 2002;38(3):579-86.
[119] Brueggemann H, Dahmen K, Lehwald D, Theilmann R. Water-swellable superabsorbent polymer and water-soluble polymer, as a matrix of sheet-like design wherein the superabsorbent component is integrated or fixed. Google Patents; 2000.
[120] Gross JR, Baer SC, Leptick S, Erspamer JP. Absorbent structures with integral layer of superabsorbent polymer particles. Google Patents; 2002.
[121] Mudiyanselage TK, Neckers DC. Highly absorbing superabsorbent polymer. Journal of Polymer Science Part A: Polymer Chemistry. 2008;46(4):1357-64.
[122] Fang YE, Cheng Q, Lu XB. Kinetics of in vitro drug release from chitosan/gelatin hybrid membranes. Journal of Applied Polymer Science. 1998;68(11):1751-8.
[123] Dash M, Chiellini F, Ottenbrite RM, Chiellini E. Chitosan—A versatile semi-synthetic polymer in biomedical applications. Progress in polymer science. 2011;36(8):981-1014.
[124] Laftah WA, Hashim S, Ibrahim AN. Polymer hydrogels: A review. Polymer-Plastics Technology and Engineering. 2011;50(14):1475-86.
[125] Devisscher D. Bio-based pH-Sensitive Superabsorbent Polymers for Self-Sealing and -Healing Mortar. Thesis. UGent2014-2015.
[126] Odian G. Principles of polymerization: John Wiley & Sons; 2004.
[127] Mahdavinia GR, Pourjavadi A, Hosseinzadeh H, Zohuriaan MJ. Modified chitosan 4. Superabsorbent hydrogels from poly(acrylic acid-co-acrylamide) grafted chitosan with salt- and pH-responsiveness properties. European Polymer Journal. 2004;40(7):1399-407.
[128] Zhang J, Wang Q, Wang A. Synthesis and characterization of chitosan-g-poly (acrylic acid)/attapulgite superabsorbent composites. Carbohydrate Polymers. 2007;68(2):367-74.
[129] Hua S, Wang A. Synthesis, characterization and swelling behaviors of sodium alginate-g-poly (acrylic acid)/sodium humate superabsorbent. Carbohydrate Polymers. 2009;75(1):79-84.
[130] Rinaudo M. Main properties and current applications of some polysaccharides as biomaterials. Polymer International. 2008;57(3):397-430.
[131] Percival E. The polysaccharides of green, red and brown seaweeds: their basic structure, biosynthesis and function. British Phycological Journal. 1979;14(2):103-17.
[132] Rinaudo M. Biomaterials based on a natural polysaccharide: alginate. TIP Revista especializada en ciencias químico-biológicas. 2014;17:92-6.
[133] Kim YJ, Yoon KJ, Ko SW. Preparation and properties of alginate superabsorbent filament fibers crosslinked with glutaraldehyde. Journal of Applied Polymer Science. 2000;78(10):1797-804.
[134] Dutkiewicz JK. Superabsorbent materials from shellfish waste—a review. Journal of Biomedical Materials Research. 2002;63(3):373-81.

[135] Pourjavadi A, Farhadpour B, Seidi F. Synthesis and investigation of swelling behavior of new agar based superabsorbent hydrogel as a candidate for agrochemical delivery. Journal of polymer research. 2009;16(6):655-65.
[136] Mihaila SM, Gaharwar AK, Reis RL, Marques AP, Gomes ME, Khademhosseini A. Photocrosslinkable Kappa-Carrageenan Hydrogels for Tissue Engineering Applications. Advanced healthcare materials. 2013;2(6):895-907.
[137] Ding X, Li L, Liu Ps, Zhang J, Zhou Nl, Lu S, et al. The preparation and properties of dextrin-graft-acrylic acid/montmorillonite superabsorbent nanocomposite. Polymer Composites. 2009;30(7):976-81.
[138] Nnadi F, Brave C. Environmentally friendly superabsorbent polymers for water conservation in agricultural lands. Journal of Soil Science and Environmental Management. 2011;2(7):206-11.
[139] Coutinho DF, Sant SV, Shin H, Oliveira JT, Gomes ME, Neves NM, et al. Modified Gellan Gum hydrogels with tunable physical and mechanical properties. Biomaterials. 2010;31(29):7494-502.
[140] Wu L-Q, Embree HD, Balgley BM, Smith PJ, Payne GF. Utilizing renewable resources to create functional polymers: chitosan-based associative thickener. Environmental science & technology. 2002;36(15):3446-54.
[141] Yin X, Hoffman AS, Stayton PS. Poly(N-isopropylacrylamide-co-propylacrylic acid) Copolymers That Respond Sharply to Temperature and pH. Biomacromolecules. 2006;7(5):1381-5.
[142] Liu Y-Y, Shao Y-H, Lü J. Preparation, properties and controlled release behaviors of pH-induced thermosensitive amphiphilic gels. Biomaterials. 2006;27(21):4016-24.
[143] Ahmed EM. Hydrogel: Preparation, characterization, and applications: A review. Journal of advanced research. 2015;6(2):105-21.
[144] Don T-M, Huang M-L, Chiu A-C, Kuo K-H, Chiu W-Y, Chiu L-H. Preparation of thermo-responsive acrylic hydrogels useful for the application in transdermal drug delivery systems. Materials Chemistry and Physics. 2008;107(2–3):266-73.
[145] Pourjavadi A, Kurdtabar M, Mahdavinia RG, Hosseinzadeh H. Synthesis and super-swelling behavior of a novel protein-based superabsorbent hydrogel. Polymer Bulletin. 2006;57(6):813-24.
[146] Kiatkamjornwong S, Phunchareon P. Influence of reaction parameters on water absorption of neutralized poly (acrylic acid-co-acrylamide) synthesized by inverse suspension polymerization. Journal of Applied Polymer Science. 1999;72(10):1349-66.
[147] Dimonie MV, Boghina CM, Marinescu NN, Marinescu MM, Cincu CI, Oprescu CG. Inverse suspension polymerization of acrylamide. European Polymer Journal. 1982;18(7):639-45.
[148] Pang X, Cheng G, Li R, Lu S, Zhang Y. Bovine serum albumin-imprinted polyacrylamide gel beads prepared via inverse-phase seed suspension polymerization. Analytica Chimica Acta. 2005;550(1):13-7.
[149] Ahearn DG, Grace DT, Jennings MJ, Borazjani RN, Boles KJ, Rose LJ, et al. Effects of hydrogel/silver coatings on in vitro adhesion to catheters of bacteria associated with urinary tract infections. Current microbiology. 2000;41(2):120-5.
[150] Kopecek J. Hydrogels: From soft contact lenses and implants to self-assembled nanomaterials. Journal of Polymer Science Part A: Polymer Chemistry. 2009;47(22):5929-46.
[151] Corkhill PH, Hamilton CJ, Tighe BJ. Synthetic hydrogels VI. Hydrogel composites as wound dressings and implant materials. Biomaterials. 1989;10(1):3-10.
[152] Peppas NA. Hydrogels and drug delivery. Current opinion in colloid & interface science. 1997;2(5):531-7.
[153] Hoare TR, Kohane DS. Hydrogels in drug delivery: progress and challenges. Polymer. 2008;49(8):1993-2007.
[154] Sassi AP, Lin S, Alonso-Amigo MG, Hooper HH. Thermoreversible hydrogels comprising linear copolymers and their use in electrophoresis. Google Patents; 1997.
[155] Ratner BD, Hoffman AS. Synthetic hydrogels for biomedical applications. Hydrogels for medical and related applications. 1976;31:1-36.
[156] Collier Iv LW, Yahiaoui A, Johns EM, Durrance DH. Absorbent diapers having a nonwoven fabric linings for more dryness comfort feel. Google Patents; 1997.

[157] Umachitra G. Disposable baby diaper--a threat to the health and environment. Journal of environmental science & engineering. 2012;54(3):447-52.
[158] Choudhury NA, Sampath S, Shukla AK. Hydrogel-polymer electrolytes for electrochemical capacitors: an overview. Energy & Environmental Science. 2009;2(1):55-67.
[159] Wijesekara I, Pangestuti R, Kim S-K. Biological activities and potential health benefits of sulfated polysaccharides derived from marine algae. Carbohydrate Polymers. 2011;84(1):14-21.
[160] Lee KY, Mooney DJ. Alginate: properties and biomedical applications. Progress in polymer science. 2012;37(1):106-26.
[161] Scott JE. Periodate oxidation, pK a and conformation of hexuronic acids in polyuronides and mucopolysaccharides. Biochimica et Biophysica Acta (BBA)-General Subjects. 1968;170(2):471-3.
[162] McHugh DJ. A guide to the seaweed industry: Food and Agriculture Organization of the United Nations Rome, Italy; 2003.
[163] Pawar SN, Edgar KJ. Alginate derivatization: a review of chemistry, properties and applications. Biomaterials. 2012;33(11):3279-305.
[164] Augst AD, Kong HJ, Mooney DJ. Alginate hydrogels as biomaterials. Macromolecular bioscience. 2006;6(8):623-33.
[165] Braccini I, Pérez S. Molecular basis of Ca2+-induced gelation in alginates and pectins: the egg-box model revisited. Biomacromolecules. 2001;2(4):1089-96.
[166] Draget KI, Skjåk-Bræk G, Stokke BT. Similarities and differences between alginic acid gels and ionically crosslinked alginate gels. Food Hydrocolloids. 2006;20(2):170-5.
[167] Paul W, Sharma CP. Chitosan and alginate wound dressings: a short review. Trends Biomater Artif Organs. 2004;18(1):18-23.
[168] Matthew IR, Browne RM, Frame JW, Millar BG. Tissue response to a haemostatic alginate wound dressing in tooth extraction sockets. British Journal of Oral and Maxillofacial Surgery. 1993;31(3):165-9.
[169] Nallamuthu N, Braden M, Patel MP. Dimensional changes of alginate dental impression materials. Journal of Materials Science: Materials in Medicine. 2006;17(12):1205-10.
[170] Tønnesen HH, Karlsen J. Alginate in drug delivery systems. Drug development and industrial pharmacy. 2002;28(6):621-30.
[171] Sirviö JA, Kolehmainen A, Liimatainen H, Niinimäki J, Hormi OEO. Biocomposite cellulose-alginate films: promising packaging materials. Food chemistry. 2014;151:343-51.
[172] Prouse RE, West AA, King DA, Poulson R. Method of making paper from water insoluble alginate fibers and the paper produced. Google Patents; 1978.
[173] F. Gibbs SKIACNMB. Encapsulation in the food industry: a review. International journal of food sciences and nutrition. 1999;50(3):213-24.
[174] Glicksman M. Utilization of seaweed hydrocolloids in the food industry. Twelfth International Seaweed Symposium: Springer; 1987. p. 31-47.
[175] Rinaudo M, Pavlov G, Desbrieres J. Influence of acetic acid concentration on the solubilization of chitosan. Polymer. 1999;40(25):7029-32.
[176] Jayakumar R, Prabaharan M, Kumar PTS, Nair SV, Tamura H. Biomaterials based on chitin and chitosan in wound dressing applications. Biotechnology advances. 2011;29(3):322-37.
[177] Kurita K, Sannan T, Iwakura Y. Studies on chitin. VI. Binding of metal cations. Journal of Applied Polymer Science. 1979;23(2):511-5.
[178] Bernkop-Schnürch A, Dünnhaupt S. Chitosan-based drug delivery systems. European Journal of Pharmaceutics and Biopharmaceutics. 2012;81(3):463-9.
[179] Croisier F, Jérôme C. Chitosan-based biomaterials for tissue engineering. European Polymer Journal. 2013;49(4):780-92.
[180] Wu T, Zivanovic S. Determination of the degree of acetylation (DA) of chitin and chitosan by an improved first derivative UV method. Carbohydrate Polymers. 2008;73(2):248-53.
[181] Armisén R. Agar and agarose biotechnological applications. Hydrobiologia. 1991;221(1):157-66.
[182] Al Mousa AA, Al-Deyab SS. Antimicrobial hydrogel wound dressing. Google Patents; 2011.

[183] Rezanejade Bardajee G, Hooshyar Z, Pourhasan Y. The Effect of Multidentate Biopolymer Based on Polyacrylamide Grafted onto Kappa-Carrageenan on the Spectrofluorometric Properties of Water-Soluble CdS Quantum Dots. International Journal of Spectroscopy. 2011;2011.
[184] Campo VL, Kawano DF, da Silva DB, Carvalho I. Carrageenans: Biological properties, chemical modifications and structural analysis–A review. Carbohydrate Polymers. 2009;77(2):167-80.
[185] Skjåk-Bræk G, Zanetti F, Paoletti S. Effect of acetylation on some solution and gelling properties of alginates. Carbohydrate Research. 1989;185(1):131-8.
[186] Coleman RJ, Lawrie G, Lambert LK, Whittaker M, Jack KS, Grøndahl L. Phosphorylation of alginate: synthesis, characterization, and evaluation of in vitro mineralization capacity. Biomacromolecules. 2011;12(4):889-97.
[187] Alban S, Schauerte A, Franz G. Anticoagulant sulfated polysaccharides: Part I. Synthesis and structure–activity relationships of new pullulan sulfates. Carbohydrate Polymers. 2002;47(3):267-76.
[188] Rowley JA, Madlambayan G, Mooney DJ. Alginate hydrogels as synthetic extracellular matrix materials. Biomaterials. 1999;20(1):45-53.
[189] Donati I, Draget KI, Borgogna M, Paoletti S, Skjåk-Bræk G. Tailor-made alginate bearing galactose moieties on mannuronic residues: selective modification achieved by a chemoenzymatic strategy. Biomacromolecules. 2005;6(1):88-98.
[190] Sinquin A, Hubert P, Dellacherie E. Amphiphilic derivatives of alginate: evidence for intra-and intermolecular hydrophobic associations in aqueous solution. Langmuir. 1993;9(12):3334-7.
[191] Pelletier S, Hubert P, Lapicque F, Payan E, Dellacherie E. Amphiphilic derivatives of sodium alginate and hyaluronate: synthesis and physico-chemical properties of aqueous dilute solutions. Carbohydrate Polymers. 2000;43(4):343-9.
[192] Sinquin A, Hubert P, Marchal P, Choplin L, Dellacherie E. Rheological properties of semi-dilute aqueous solutions of hydrophobically modified propylene glycol alginate derivatives. Colloids and Surfaces A: Physicochemical and Engineering Aspects. 1996;112(2):193-200.
[193] Babak VG, Skotnikova EA, Lukina IG, Pelletier S, Hubert P, Dellacherie E. Hydrophobically associating alginate derivatives: surface tension properties of their mixed aqueous solutions with oppositely charged surfactants. Journal of colloid and interface science. 2000;225(2):505-10.
[194] Yeom CK, Lee KH. Characterization of sodium alginate membrane crosslinked with glutaraldehyde in pervaporation separation. Journal of Applied Polymer Science. 1998;67(2):209-19.
[195] Leone G, Torricelli P, Chiumiento A, Facchini A, Barbucci R. Amidic alginate hydrogel for nucleus pulposus replacement. Journal of Biomedical Materials Research Part A. 2008;84(2):391-401.
[196] Shah SB, Patel CP, Trivedi HC. Ceric-induced grafting of acrylate monomers onto sodium alginate. Carbohydrate Polymers. 1995;26(1):61-7.
[197] Işıklan N, Kurşun F, İnal M. Graft copolymerization of itaconic acid onto sodium alginate using ceric ammonium nitrate as initiator. Journal of Applied Polymer Science. 2009;114(1):40-8.
[198] Işıklan N, Kurşun F, İnal M. Graft copolymerization of itaconic acid onto sodium alginate using benzoyl peroxide. Carbohydrate Polymers. 2010;79(3):665-72.
[199] Kim JH, Lee SB, Kim SJ, Lee YM. Rapid temperature/pH response of porous alginate-g-poly (N-isopropylacrylamide) hydrogels. Polymer. 2002;43(26):7549-58.
[200] Grasselli M, Diaz LE, Cascone O. Beaded matrices from cross-linked alginate for affinity and ion exchange chromatography of proteins. Biotechnology techniques. 1993;7(10):707-12.
[201] Moe ST, Skjåk-Bræk G, Smidsrød O. Covalently cross-linked sodium alginate beads. Food Hydrocolloids. 1991;5(1):119-23.
[202] de Koning HWM, Chamuleau RAFM, Bantjes A. Crosslinked agarose encapsulated sorbents resistant to steam sterilization. Preparation and mechanical properties. Journal of Biomedical Materials Research. 1984;18(1):1-13.
[203] Bezbradica DI, Mateo C, Guisan JM. Novel support for enzyme immobilization prepared by chemical activation with cysteine and glutaraldehyde. Journal of Molecular Catalysis B: Enzymatic. 2014;102:218-24.

[204] Dillon GP, Yu X, Sridharan A, Ranieri JP, Bellamkonda RV. The influence of physical structure and charge on neurite extension in a 3D hydrogel scaffold. Journal of Biomaterials Science, Polymer Edition. 1998;9(10):1049-69.
[205] Jayakumar R, Nagahama H, Furuike T, Tamura H. Synthesis of phosphorylated chitosan by novel method and its characterization. International Journal of Biological Macromolecules. 2008;42(4):335-9.
[206] Rinaudo M, Le Dung P, Gey C, Milas M. Substituent distribution on O, N-carboxymethylchitosans by 1H and 13C NMR. International Journal of Biological Macromolecules. 1992;14(3):122-8.
[207] Le Dung P, Milas M, Rinaudo M, Desbrières J. Water soluble derivatives obtained by controlled chemical modifications of chitosan. Carbohydrate Polymers. 1994;24(3):209-14.
[208] Desbrieres J, Martinez C, Rinaudo M. Hydrophobic derivatives of chitosan: characterization and rheological behaviour. International Journal of Biological Macromolecules. 1996;19(1):21-8.
[209] Mi F-L, Wu S-J, Lin F-M. Adsorption of copper (II) ions by a chitosan–oxalate complex biosorbent. International Journal of Biological Macromolecules. 2015;72:136-44.
[210] Dang JM, Sun DDN, Shin-Ya Y, Sieber AN, Kostuik JP, Leong KW. Temperature-responsive hydroxybutyl chitosan for the culture of mesenchymal stem cells and intervertebral disk cells. Biomaterials. 2006;27(3):406-18.
[211] Zhu B, Wei C, Hou C, Gu Q, Chen D. Preparation and characterization of hydroxybutyl chitosan. e-Polymers. 2010;10(1):883-92.
[212] Rees DA, Williamson FB, Frangou SA, Morris ER. Fragmentation and Modification of r-Carrageenan and Characterisation of the Polysaccharide Order-Disorder Transition in Solution. European Journal of Biochemistry. 1982;122(1):71-9.
[213] Guiseley KB. Modified kappa-carrageenan. Google Patents; 1978.
[214] Tarı Ö, Pekcan Ö. Swelling of iota-carrageenan gels prepared with various CaCl2 content: A fluorescence study. e-Polymers. 2008;8(1):1-10.
[215] Ciancia M, Noseda MD, Matulewicz MC, Cerezo AS. Alkali-modification of carrageenans: mechanism and kinetics in the kappa/iota-, mu/nu-and lambda-series. Carbohydrate Polymers. 1993;20(2):95-8.
[216] Viana AG, Noseda MD, Duarte MER, Cerezo AS. Alkali modification of carrageenans. Part V. The iota–nu hybrid carrageenan from Eucheuma denticulatum and its cyclization to iota-carrageenan. Carbohydrate Polymers. 2004;58(4):455-60.
[217] Navarro DA, Stortz CA. Microwave-assisted alkaline modification of red seaweed galactans. Carbohydrate Polymers. 2005;62(2):187-91.
[218] Hosseinzadeh H, Pourjavadi A, Mahdavinia GR, Zohuriaan-Mehr MJ. Modified carrageenan. 1. H-CarragPAM, a novel biopolymer-based superabsorbent hydrogel. Journal of Bioactive and Compatible Polymers. 2005;20(5):475-90.
[219] Pourjavadi A, Harzandi AM, Hosseinzadeh H. Modified carrageenan 3. Synthesis of a novel polysaccharide-based superabsorbent hydrogel via graft copolymerization of acrylic acid onto kappa-carrageenan in air. European Polymer Journal. 2004;40(7):1363-70.
[220] Prasad K, Meena R, Siddhanta AK. Microwave-induced rapid one-pot synthesis of κ-carrageenan-g-PMMA copolymer by potassium persulphate initiating system. Journal of Applied Polymer Science. 2006;101(1):161-6.
[221] Pourjavadi A, Barzegar S, Zeidabadi F. Synthesis and properties of biodegradable hydrogels of κ-carrageenan grafted acrylic acid-co-2-acrylamido-2-methylpropanesulfonic acid as candidates for drug delivery systems. Reactive and Functional Polymers. 2007;67(7):644-54.
[222] Tümtürk H, Karaca N, Demirel G, Şahin F. Preparation and application of poly (N, N-dimethylacrylamide-co-acrylamide) and poly (N-isopropylacrylamide-co-acrylamide)/κ-Carrageenan hydrogels for immobilization of lipase. International Journal of Biological Macromolecules. 2007;40(3):281-5.
[223] Daniel-da-Silva AL, Lopes AB, Gil AM, Correia RN. Synthesis and characterization of porous κ-carrageenan/calcium phosphate nanocomposite scaffolds. J Mater Sci. 2007;42(20):8581-91.

[224] Yuan H, Zhang W, Li X, Lü X, Li N, Gao X, et al. Preparation and in vitro antioxidant activity of κ-carrageenan oligosaccharides and their oversulfated, acetylated, and phosphorylated derivatives. Carbohydrate Research. 2005;340(4):685-92.
[225] Yuan H, Song J, Zhang W, Li X, Li N, Gao X. Antioxidant activity and cytoprotective effect of κ-carrageenan oligosaccharides and their different derivatives. Bioorganic & medicinal chemistry letters. 2006;16(5):1329-34.
[226] He G, Cheng C, Lu R. [Studies on biological effects of kappa-selenocarrageenan on human breast cancer cell line BCaP-37]. Zhonghua yu fang yi xue za zhi [Chinese journal of preventive medicine]. 1997;31(2):103-6.
[227] Jiang Y-P, Guo X-K. O-maleoyl derivative of low-molecular-weight κ-carrageenan: Synthesis and characterization. Carbohydrate Polymers. 2005;61(4):441-5.
[228] Chou AI, Nicoll SB. Characterization of photocrosslinked alginate hydrogels for nucleus pulposus cell encapsulation. Journal of Biomedical Materials Research Part A. 2009;91(1):187-94.
[229] Rouillard AD, Berglund CM, Lee JY, Polacheck WJ, Tsui Y, Bonassar LJ, et al. Methods for photocrosslinking alginate hydrogel scaffolds with high cell viability. Tissue Engineering Part C: Methods. 2010;17(2):173-9.
[230] Chou AI, Akintoye SO, Nicoll SB. Photo-crosslinked alginate hydrogels support enhanced matrix accumulation by nucleus pulposus cells in vivo. Osteoarthritis and Cartilage. 2009;17(10):1377-84.
[231] Gulrez SKH, Phillips GO, Al-Assaf S. Hydrogels: methods of preparation, characterisation and applications: INTECH Open Access Publisher; 2011.
[232] Kim JJ, Park K. Smart hydrogels for bioseparation. Bioseparation. 07-1998;7(4-5):177-84.
[233] Yong Qiu KP. Environment-sensitive hydrogels for drug delivery. Advanced Drug Delivery Reviews. 2001;53(2001):321–39.
[234] Gupta P, Vermani K, Garg S. Hydrogels: from controlled release to pH-responsive drug delivery. Drug Discovery Today. 2002;7(10):569-79.
[235] Best JP, Neubauer MP, Javed S, Dam HH, Fery A, Caruso F. Mechanics of pH-Responsive Hydrogel Capsules. Langmuir. 2013;29(31):9814-23.
[236] Khare AR, Peppas NA. Release behavior of bioactive agents from pH-sensitive hydrogels. Journal of Biomaterials Science, Polymer Edition. 1993;4(3):275-89.
[237] Freitas RFS, Cussler EL. Temperature sensitive gels as extraction solvents. Chemical Engineering Science. 1987;42(1):97-103.
[238] Bromberg LE, Ron ES. Temperature-responsive gels and thermogelling polymer matrices for protein and peptide delivery. Advanced Drug Delivery Reviews. 1998;31(3):197-221.
[239] Feil H, Bae YH, Feijen J, Kim SW. Molecular separation by thermosensitive hydrogel membranes. Journal of Membrane Science. 1991;64(3):283-94.
[240] Takashima Y, Hatanaka S, Otsubo M, Nakahata M, Kakuta T, Hashidzume A, et al. Expansion–contraction of photoresponsive artificial muscle regulated by host–guest interactions. Nat Commun. 2012;3(1270).
[241] Suzuki A, Tanaka T. Phase transition in polymer gels induced by visible light. Nature. 1990;346(6282):345-7.
[242] Lee KK, Cussler EL, Marchetti M, McHugh MA. Pressure-dependent phase transitions in hydrogels. Chemical Engineering Science. 1990;45(3):766-7.
[243] Mahkam M. Novel pH-sensitive hydrogels for colon-specific drug delivery. Drug delivery. 2010;17(3):158-63.
[244] Hanneke ML, Mark JHC, ávan Lankvelt BM, Martin WM. Tuning the LCST of poly (2-oxazoline) s by varying composition and molecular weight: alternatives to poly (N-isopropylacrylamide)? Chemical Communications. 2008(44):5758-60.
[245] Miguel SP, Ribeiro MP, Brancal H, Coutinho P, Correia IJ. Thermoresponsive chitosan–agarose hydrogel for skin regeneration. Carbohydrate Polymers. 2014;111:366-73.
[246] Crompton KE, Goud JD, Bellamkonda RV, Gengenbach TR, Finkelstein DI, Horne MK, et al. Polylysine-functionalised thermoresponsive chitosan hydrogel for neural tissue engineering. Biomaterials. 2007;28(3):441-9.

[247] Katono H, Maruyama A, Sanui K, Ogata N, Okano T, Sakurai Y. Thermo-responsive swelling and drug release switching of interpenetrating polymer networks composed of poly (acrylamide-co-butyl methacrylate) and poly (acrylic acid). Journal of Controlled Release. 1991;16(1):215-27.
[248] Savina I, Galaev IYU. Smart polymers for bioseparation and other biotechnological applications. Smart Polymers and their Applications. 2014:408.
[249] Yang S, Liu G, Cheng Y, Zheng Y. Electroresponsive behavior of sodium alginate-g-poly (acrylic acid) hydrogel under DC electric field. Journal of Macromolecular Science®, Part A: Pure and Applied Chemistry. 2009;46(11):1078-82.
[250] Bentz DP, Weiss WJ. Internal Curing: A 2010 State-of-the-Art Review. In: Interagency N, editor.2011. p. 82.
[251] Mechtcherine V, Gorges M, Schröfl C, Assmann A, Brameshuber W, Bettencourt Ribeiro V, et al. Effect of Internal Curing by Using Superabsorbent Polymers (SAP) on Autogenous Shrinkage and Other Properties of a High-performance Fine-grained Concrete: Results of a RILEM Round-robin Test, TC 225-SAP. Mater Struct. 2014;47(3):541-62.
[252] Mechtcherine V, Dudziak L, Hempel S. Mitigating early age shrinkage of Ultra-High Performance Concrete by using Super Absorbent Polymers (SAP). In: Sato R, Maekawa K, Tanabe T, Sakata K, Nakamura H, Mihashi H, editors. Creep, Shrinkage and Durability Mechanics of Concrete and Concrete Structures. Ise-Shima: Taylor & Francis; 2009. p. 847-53.
[253] Craeye B, De Schutter S. Experimental evaluation of mitigation of autogenous shrinkage by means of a vertical dilatometer for concrete. In: Jensen OM, Lura P, Kovler K, editors. International RILEM conference on Volume changes of hardening concrete: testing and mitigation. Lyngby: RILEM Publications S.A.R.L.; 2006. p. 21-30.
[254] Jensen OM, Hansen PF. Water-entrained cement-based materials I. Principles and theoretical background. Cem Concr Res. 2001;31(4):647-54.
[255] Jensen OM, Hansen PF. Water-entrained cement-based materials II. Experimental observations. Cem Concr Res. 2002;32(6):973-8.
[256] Igarashi S, Watanabe A. Experimental study on prevention of autogenous deformation by internal curing using super-absorbent polymer particles. In: Jensen OM, Lura P, Kovler K, editors. International RILEM Conference on Volume Changes of Hardening Concrete: Testing and Mitigation. Lyngby: RILEM Publications S.A.R.L.; 2006. p. 77-86.
[257] Assmann A. Physical properties of concrete modified with superabsorbent polymers. Stuttgart: Stuttgart University; 2013.
[258] Schröfl C, Mechtcherine V, Gorges M. Relation between the molecular structure and the efficiency of superabsorbent polymers (SAP) as concrete admixture to mitigate autogenous shrinkage. Cement and Concrete Research. 2012;42(6):865-73.
[259] Powers TC, Brownyard TL. Studies of the physical properties of hardened Portland cement paste. Cornell: Portland Cement Association, Research Laboratories; 1948.
[260] Snoeck D. Self-Healing and Microstructure of Cementitious Materials with Microfibres and Superabsorbent Polymers. Ghent: Ghent University; 2015.
[261] Lura P, Ye G, Cnudde V, Jacobs P. Preliminary results about 3D distribution of superabsorbent polymers in mortars. In: Sun W, van Breugel K, Miao C, Ye G, Chen H, editors. International Conference on Microstructure Related Durability of Cementitious Composites. Nanjing2008. p. 1341-8.
[262] Mönnig S. Water saturated super-absorbent polymers used in high strength concrete. Otto-Graf-Journal. 2005;16:193-202.
[263] Reinhardt HW, Assmann A. Enhanced durability of concrete by superabsorbent polymers. In: Brandt AM, Olek J, Marshal IH, editors. International Symposium Brittle Matrix Composites 9. Warsaw: Woodhead Publishing; 2009. p. 291-300.
[264] Snoeck D, Steuperaert S, Van Tittelboom K, Dubruel P, De Belie N. Visualization of water penetration in cementitious materials with superabsorbent polymers by means of neutron radiography. Cement and Concrete Research. 2012;42(8):1113-21.

[265] Wyrzykowski M, Lura P. Reduction of autogenous shrinkage in OPC and BFSC pastes with internal curing. In: Quattrone M, John VM, editors. XIII International Conference on Durability of Building Materials and Components. São Paulo2014. p. 1010-7.
[266] Almeida FDCR, Klemm AJ. Effect of superabsorbent polymers (SAP) on fresh state mortars with ground granulated blast-furnace slag (GGBS). 5th International Conference on Durability of Concrete Structures. Shenzhen2016. p. 1-7.
[267] Lura P, Durand F, Loukili A, Kovler K, Jensen OM. Compressive strength of cement pastes and mortars with superabsorbent polymers. In: Jensen OM, Lura P, Kovler K, editors. International RILEM Conference on Volume Changes of Hardening Concrete: Testing and Mitigation. Lyngby: RILEM Publications SARL; 2006. p. 117-25.
[268] Klemm AJ, Sikora KS. The effect of Superabsorbent Polymers (SAP) on microstructure and mechanical properties of fly ash cementitious mortars. Constr Build Mater. 2013;49:134-43.
[269] Snoeck D, Schaubroeck D, Dubruel P, De Belie N. Effect of high amounts of superabsorbent polymers and additional water on the workability, microstructure and strength of mortars with a water-to-cement ratio of 0.50. Construction and Building Materials. 2014;72:148-57.
[270] Dudziak L, Mechtcherine V. Enhancing early-age resistance to cracking in high-strength cement based materials by means of internal curing using super absorbent polymers. In: Brameshuber W, editor. International RILEM Conference on Material Science. Aachen: RILEM Publications S.A.R.L.; 2010. p. 129-39.
[271] Lura P, Jensen OM, Igarashi S. Experimental observation of internal curing of concrete. Mater Struct. 2007;40(2):211-20.
[272] Hasholt MT, Jespersen MHS, Jensen OM. Mechanical properties of concrete with SAP part I: Development of compressive strength. In: Jensen OM, Hasholt MT, Laustsen S, editors. International RILEM Conference on Use of Superabsorbent Polymers and Other New Additives in Concrete. Lyngby: RILEM Publications SARL; 2010. p. 117-26.
[273] Mönnig S, Lura P. Superabsorbent polymers—an additive to increase the freeze-thaw resistance of high strength concrete. Advances in construction materials 2007: Springer; 2007. p. 351-8.
[274] Mechtcherine V, Schröfl C, Wyrzykowski M, Gorges M, Cusson D, Margeson J, et al. Effect of superabsorbent polymers (SAP) on the freeze-thaw resistance of concrete: results of a RILEM interlaboratory test Mater Struct. 2017:accepted.
[275] P. Lura GY, V. Cnudde, P. Jacobs. Preliminary results about 3D distribution of superabsorbent polymers in mortars. In: W. Sun KvB, C. Miao, G. Ye and H. Chen, editor. International Conference on Microstructure Related Durability of Cementitious Composites: RILEM Publications; 2008. p. 8.
[276] Snoeck D, Tittelboom KV, Steuperaert S, Dubruel P, Belie ND. Self-healing cementitious materials by the combination of microfibres and superabsorbent polymers. Journal of Intelligent Material Systems and Structures. 2012.
[277] Snoeck D, Schaubroeck D, Dubruel P, De Belie N. Effect of high amounts of superabsorbent polymers and additional water on the workability, microstructure and strength of mortars with a water-to-cement ratio of 0.50. Construction and Building Materials. 2014;72(0):148-57.
[278] Lee HXD, Wong HS, Buenfeld NR. Potential of superabsorbent polymer for self-sealing cracks in concrete. Advances in Applied Ceramics. 2010;109(5):296-302.
[279] Lee HXD, Wong HS, Buenfeld NR. Self-sealing cement-based materials using superabsorbent polymers. In: Jensen OM, Hasholt MT, Laustsen S, editors. International RILEM Conference on Use of Superabsorbent Polymers and Other New Additives in Concrete. Lyngby: RILEM Publications SARL; 2010. p. 171-8.
[280] Lee HXD, Wong HS, Buenfeld NR. Self-sealing of cracks in concrete using superabsorbent polymers. Cem Concr Res. 2016;79:194-208.
[281] Song XF, Wei JF, He TS. A method to repair concrete leakage through cracks by synthesizing super-absorbent resin in situ. Constr Build Mater. 2009;23(1):386-91.

[282] Kim JS, Schlangen E. Super absorbent polymers to simulate self healing in ECC. In: van Breugel K, Ye G, Yuan Y, editors. 2nd International Symposium on Service Life Design for Infrastructures. Delft: RILEM Publications SARL; 2010. p. 849-58.
[283] Snoeck D, De Belie N. Repeated autogenous healing in strain-hardening cementitious composites by using superabsorbent polymers. J Mater Civ Eng. 2015;04015086:1-11.
[284] Snoeck D, Dewanckele J, Cnudde V, De Belie N. X-ray computed microtomography to study autogenous healing of cementitious materials promoted by superabsorbent polymers. Cem Concr Comp. 2016;65:83-93.
[285] Fan S, Li M. X-ray computed microtomography of three-dimensional microcracks and self-healing in engineered cementitious composites. Smart Mater Struct. 2015;24(1):015021.
[286] Kong X-M, Zhang Z-L, Lu Z-C. Effect of pre-soaked superabsorbent polymer on shrinkage of high-strength concrete. Mater Struct. 2015;48(9):2741-58.
[287] AzariJafari H, Kazemian A, Rahimi M, Yahia A. Effects of pre-soaked super absorbent polymers on fresh and hardened properties of self-consolidating lightweight concrete. Constr Build Mater. 2016;113:215-20.
[288] Laustsen S, Hasholt MT, Jensen OM. Void structure of concrete with superabsorbent polymers and its relation to frost resistance of concrete. Mater Struct. 2015;48(1-2):357-68.
[289] Yao Y, Zhu Y, Yang Y. Incorporation of SAP particles as controlling pre-existing flaws to improve the performance of ECC. Constr Build Mater. 2011;28(1):139-45.
[290] Hasholt MT, Jensen OM, Kovler K, Zhutovsky S. Can superabsorbent polymers mitigate autogenous shrinkage of internally cured concrete without compromising the strength? Construction and Building Materials. 2012;31:226-30.
[291] Hasholt MT, Jespersen MHS, Jensen OM. Mechanical properties of concrete with SAP. Part I: Development of compressive strength. Use of Superabsorbent Polymers and Other New Additives in Concrete. 2010.

II. Experimental section

II.1. Overview of applied materials

Acetic acid, Sigma-Aldrich (Bornem, Belgium)

Acetone, Univar (Anderlecht, Belgium)

Acrylamide (AM), Janssen Chimica (Geel, Belgium)

2-Acrylamido-2-methylpropane sulfonic acid (AMPS), Sigma-Aldrich (Bornem, Belgium)

Acrylic acid (AA), Acros Organics (Geel, Belgium)

Agarose (Aga), Sigma-Aldrich (Bornem, Belgium)

Ammonium persulfate (APS), Sigma-Aldrich (Bornem, Belgium)

1-Butyl-3-methylimidazolium chloride (BMImCl), Solvionic (Toulouse, France)

Calcium chloride (CaCl2), Acros Organics (Geel, Belgium)

Chitosan (Chi), Sigma-Aldrich (Bornem, Belgium)

Commercial SAP A (copolymer of acrylamide and sodium acrylate), BASF (BASF Construction Chemicals GmbH, Trostberg, Germany)

Commercial SAP B (cross-linked potassium salt polyacrylate), BASF (BASF Construction Chemicals GmbH, Trostberg, Germany)

Deuterium chloride (DCl), Eurisotop (Saint-Aubin Cedex, France)

Deuterium oxide (D2O), Eurisotop (Saint-Aubin Cedex, France)

Dialysis membranes (Spectra/Por® 4, MWCO 12,000-14,000 Da), Polylab (Antwerp, Belgium)

2-(dimethylamino)ethyl methacrylate (DMAEMA), Sigma-Aldrich (Bornem, Belgium)

Dimethylaminopropyl methacrylamide (DMAPMA), Sigma-Aldrich (Bornem, Belgium)

4-Dimethylaminopyridine (DMAP), Sigma-Aldrich (Bornem, Belgium)

Dimethylformamide (DMF), Acros Organics (Geel, Belgium)

Dimethyl sulfoxide (DMSO), Acros Organics (Geel, Belgium)

Dimethyl sulfoxide-d6 (d-DMSO), Eurisotop (Saint-Aubin Cedex, France)

Hydrochloric acid (HCl), Sigma-Aldrich (Bornem, Belgium)

Hydrogen peroxide (H_2O_2), Sigma-Aldrich (Bornem, Belgium)

Methacrylic anhydride (MAAH), Sigma-Aldrich (Bornem, Belgium)

N,N'-methylene bisacrylamide (MBA), Merck (Nottingham, UK)

Nitric acid (HNO_3, analytical grade), Chem Lab (Zedelgem, Belgium)

Paper filters (retention of 8 – 12 µm), Munktell filters (Bärenstein, Germany)

Phenothiazine, Sigma-Aldrich (Bornem, Belgium)

Release foil, James Walker Benelux (Wilrijk, Belgium)

Sodium alginate (NaAlg), Sigma-Aldrich (Bornem, Belgium)

Sodium hydroxide (NaOH), Sigma-Aldrich (Bornem, Belgium)

Sulfur trioxide pyridine complex (SO_3.Py), Acros Organics (Geel, Belgium)

Tea bags, Cilia (Germany)

N,N,N',N'- tetramethylethylene-diamine (TEMED), Acros Organics (Geel, Belgium)

All materials were used as received unless stated otherwise.

II.2. Overview of synthesis methodologies

II.2.1. Development of poly(acrylic acid) SAPs

A poly(acrylic acid) (p(AA)) network is developed by combining acrylic acid (AA) with the bifunctional cross-linker N,N'-methylene bisacrylamide (MBA) (0.2 mol% as a function of the total amount of added monomer). The following methods to develop SAPs have been partially based on techniques from literature [1] and further fine-tuned and adapted for other monomers. A low amount of cross-linker was selected to create polymers with superabsorbent swelling properties. The redox initiator pair ammonium persulfate (APS) and N,N,N',N'-tetramethylethylene diamine (TEMED) was added to initiate the polymerization. APS was added at a concentration of 2 w/v% (0.6 mol%) with respect to the total weight of the monomers and the cross-linker. TEMED was added in a 1/1 vol% (0.8/1 mol%) ratio with respect to APS. The first choices of the initiator-pair concentration were based on previous literature regarding the synthesis of a pH-sensitive superporous hydrogel system based on AA and acrylamide (AM) [2]. To perform the polymerization in water (250 g of monomers and cross-linker/L) under nitrogen (N_2) atmosphere to avoid inhibition of oxygen, a three-neck flask was used. APS was added after flushing by using a syringe through a septum. The synthesis was performed at 45°C while stirring continuously during 24 hours. Subsequently, the SAP was removed from the flask and purified by incubation in water during 24 hours. Finally, the product was lyophilized by means of a Christ freeze-dryer alpha 2-4-LSC and grinded to a powder with an A11 basic Analytical Mill.

II.2.2. Development of poly(acrylic acid-co-acrylamide) SAPs

The SAPs were polymerized starting from the monomers AA and acrylamide (AM) with varying molar ratios (25/75 – 50/50 – 75/25). In order to obtain a network, the polymers were synthesized in the presence of the cross-linker MBA in altering molar fractions (0.2, 2 or 10 mol% as a function of the total amount of added monomers). The redox initiator pair APS and TEMED was added to initiate the polymerization. APS was added at a concentration of 2 w/v% (0.6 – 0.7 mol%) with respect to the total weight of the monomers and the cross-linker depending on the composition of the copolymer. TEMED was added in a 1/1 vol% (0.8/1 mol%) ratio with respect

to APS. A three-neck flask was used to perform the polymerization in water (250 g of monomers and cross-linker/L) under nitrogen (N_2) atmosphere to avoid inhibition of oxygen at 45°C while stirring continuously. APS was added after flushing by using a syringe through a septum. After 24 hours, the SAP was removed from the flask and purified by incubation in water during 24 hours. Finally, the product was lyophilized by means of a Christ freeze-dryer alpha 2-4-LSC and grinded to a fine powder with an A11 basic Analytical Mill.

II.2.3. Development of poly(dimethylaminoethyl methacrylate) SAPs

The SAPs were developed by combining 2-(dimethylamino)ethyl methacrylate (DMAEMA) with the bifunctional cross-linker MBA in altering molar fractions (2 and 4 mol% as a function of the total amount of added DMAEMA). The redox initiator pair APS and TEMED was added to initiate the polymerization. APS was added at a concentration of 2 w/v% (1.4 and 1.1 mol% respectively for 2 and 4 mol% MBA) with respect to the total combined weight of the monomers and cross-linker. TEMED was added in a 1/1 vol% (0.8/1 and 1/1 mol% respectively) ratio with respect to APS. A three-neck flask was used to perform the polymerization in water (250 g of monomers and cross-linker/L) under nitrogen (N_2) atmosphere to avoid inhibition of oxygen. APS was added after flushing by using a syringe through a septum. The reaction was performed at 45°C while stirring continuously. After 24 hours, the SAP was removed from the flask and purified by incubation in water during 24 hours. Finally, the product was lyophilized by means of a Christ freeze-dryer alpha 2-4-LSC and grinded to a fine powder with an A11 basic Analytical Mill.

II.2.4. Synthesis of calcium alginate

For the development of calcium alginate (CaAlg), a calcium chloride ($CaCl_2$, 100 mM) and a 1w/v% sodium alginate (NaAlg) aqueous solution were prepared. By adding the NaAlg solution drop-wise in the $CaCl_2$ solution, the Na cations are exchanged by Ca cations and an ionic network of CaAlg beads are formed which can easily be separated from the solution through filtration. Finally, the product was lyophilized by means of a Christ freeze-dryer alpha 2-4-LSC. The resulting dried material was grinded into a fine white powder with an A11 basic Analytical Mill.

II.2.5. Methacrylation of polysaccharides

II.2.5.1. Modification of alginate with methacrylic anhydride

A derivatization of alginate with methacrylic anhydride (MAAH), based on a reaction of the free hydroxyl moieties on the polysaccharide backbone with the anhydride, was performed to incorporate methacrylates enabling subsequent network formation. This has already been done previously in literature [3, 4]. A 2 w/v% sodium alginate solution was prepared in demineralized water using a mechanical stirrer. Subsequently, MAAH was added dropwise to the solution. The added amount corresponded to x equivalents of MAAH with respect to the hydroxyl moieties on the alginate backbone (x depending on the needed low or high degree of substitution). During the reaction, methacrylic acid was released which lowers the pH of the reaction. Therefore, the pH of the mixture was constantly monitored and increased to pH 8 by adding a 5 M sodium

hydroxide (NaOH) solution. The reaction was performed in a slightly alkaline environment to improve reactivity. On the other hand, the pH should not be too high in order to avoid hydrolysis of the ester in the reaction product. The mixture was stirred and kept at room temperature for 24 hours after addition of the MAAH. Afterwards, dialysis was performed during 72 hours while changing the dialysis water twice a day to remove unreacted agents. The resulting solution of modified alginate (algMOD) was frozen and the water removed via lyophilization using a Christ freeze-dryer alpha 2-4-LSC at -85 °C and 0.37 mbar.

II.2.5.2. Modification of agarose with methacrylic anhydride

Due to the low solubility of agarose in water, the methacrylation of this polysaccharide was carried out in dimethylsulfoxide (DMSO) (as described in [5]). A solution of 1.82 w/v% agarose in DMSO was prepared followed by stirring overnight at 60°C in a round-bottom flask with a mechanical stirrer. Next, 0.09 equivalents MAAH with respect to the hydroxyl functionalities were added (i.e. 1.83 ml per g agarose). 4-dimethylaminopyridine (0.02 w%) and phenothiazine (0.02 w%) were also added together with the MAAH as respectively a base catalyst and a radical scavenger. After overnight stirring, the mixture was precipitated in a tenfold excess of ice-cooled acetone. After filtration, the precipitant was dissolved in 1 L ultrapure water (highest level of purity) at 60 °C and dialysis was performed during 72 hours at 60 °C whilst changing the dialysis water twice per day. The resulting solution of modified agarose (agaMOD) was frozen and the water was removed via lyophilization.

II.2.5.3. Modification of chitosan with methacrylic anhydride

A 1.5 w/v% aqueous chitosan solution containing 2 w/v% acetic acid was prepared in a round-bottom flask using a mechanical stirrer. The acid was added to protonate the amine functionalities on the chitosan backbone to increase solubility. After overnight stirring, the pH of the solution was raised from 3 to 5 by adding a 5 M NaOH solution. Subsequently, 0.8 equivalents MAAH, with respect to the amine groups from chitosan, were added dropwise. This amounts to 0.589 g MAAH per g chitosan. The method was based on previous research by Lu et al [6]. The reaction was terminated after 3 hours and dialysis was performed on the reaction mixture during 72 hours while changing the dialysis water twice a day. After purification, the solution was frozen and the water removed via lyophilization.

II.2.5.4. Modification of κ-carrageenan backbone with methacrylic anhydride

A 1 w/v% aqueous κ-carrageenan solution was prepared in a round bottom flask with a mechanical stirrer. To this, 11 equivalents of MAAH per hydroxyl functionality was added which amounts to 12 ml per g of κ-carrageenan (method similar as [7]). The acidity of the mixture was constantly monitored and increased to pH 8 by adding a 5 M sodium hydroxide (NaOH) solution. The reaction was performed in a slightly alkaline environment to improve reactivity. On the other hand, the pH should not be too high to avoid hydrolysis of the ester in the reaction product. The mixture was stirred and kept at 50°C during 6 hours after addition of the MAAH. Afterwards, dialysis was performed during 72 hours while changing the dialysis water twice a day

to remove unreacted agents. The resulting solution of modified κ-carrageenan (carMOD) was frozen and the water removed via lyophilization using a Christ freeze-dryer alpha 2-4-LSC at -85 °C and 0.37 mbar.

II.2.6. Development of poly(algMOD_acrylic acid/2-acrylamido-2-methylpropane-sulfonic acid) SAPs

AlgMOD (1 w/v%, prepared as described in §II.2.5.1.) was dissolved in demineralized water in a three-neck flask. After stirring until a homogenous solution was obtained, acrylic monomers (7 w/v%) were added in different molar ratios as indicated in Table II.1:

Table II.1: poly(alg_AA/AMPS) superabsorbent polymer compositions.

AA/AMPS [mol%/mol%]	AA [mmol]	Mass AA [g/g algMOD]	AMPS [mmol]	Mass AMPS [g/g algMOD]
100/0	97.14	7	0	0
75/25	47.15	3.40	15.72	3.60
50/50	23.23	1.67	23.23	5.33
25/75	9.21	0.66	27.64	6.34
0/100	0	0	30.54	7

Subsequently, TEMED was added in 1/1 vol% with APS [2]. The reaction was performed under nitrogen atmosphere by flushing 3 times during 3 minutes with a vacuum pump and a N_2 balloon. The reaction was initiated at 45°C after thermal equilibration during 15 minutes. APS (2 w/v% compared to the combined weight of algMOD and the monomers) was subsequently added starting from an aqueous stock solution (10 w%) through a septum to initialize the polymerization. After 15 minutes, the onset of gelation was observed. 24 hours after the addition of APS, the hydrogel was removed from the flask and incubated during 24 hours in a 10-fold excess demineralized water to remove unreacted monomers which were not incorporated in the network. Subsequently, the hydrogel was frozen and the incorporated water removed via lyophilization. The resulting dried material was grinded into a fine white powder with an A11 basic Analytical Mill.

II.2.7. Development of poly(algMOD_acrylic acid/acrylamide) SAPs with a low and high degree of substitution

A three-neck flask was used for the synthesis. AlgMOD (1 w/v%) was dissolved in ultrapure water at 50 °C. The DS was determined as described in §II.3.5.1. After dissolution, both AA and AM (7 w/v% in total) were added in two different molar ratios, namely 100/0 and 75/25 [mol%/mol%]. Subsequently, TEMED was supplied to the mixture in the same volume as the theoretically necessary volume of APS (2 % compared to the combined weight of algMOD and the monomers). The reaction was performed under nitrogen atmosphere by flushing three times

during three minutes with a vacuum pump and a N_2 balloon. This ensured that the initiator (APS), did not react with any oxygen to inhibit the polymerization. APS was prepared as a 10 w% solution in ultrapure water and was added through a septum to initiate the polymerization. 30 minutes after addition of APS, the onset of gelation was noticed. After 24 hours, dialysis was performed during 24 hours. Finally, the material was filtered, frozen and freeze-dried via lyophilisation and grinded into a fine powder with an A11 basic Analytical Mill.

II.2.8. Synthesis of poly(algMOD/agaMOD/chiMOD – DMAEMA/DMAPMA)

The modified polysaccharides (algMOD, agaMOD or chiMOD) were dissolved in a solvent. Agarose and chitosan are troublesome to dissolve in water [8-10]. Therefore, AgaMOD and ChiMOD were dissolved respectively in DMSO and an aqueous acidic medium (6 v% acetic acid (AcOH)). The used solvent, the polymer concentration applied as well as the reaction temperature are specified in Table II.2. After dissolution, the monomers (i.e. DMAEMA versus dimethylaminopropyl methacrylamide (DMAPMA)) were added followed by TEMED, in the same volume as the theoretically necessary volume of APS (2 % of the total added amount of monomers and polysaccharide). Subsequently, an inert nitrogen atmosphere was created. Afterwards, APS (a 10 w% stock solution in ultrapure water) was added through a septum. The gel started to form after a few minutes. The final hydrogel was removed 24 h after the addition of APS and placed in a beaker with a 10-fold excess demineralized water during 24 hours. In case of cross-linked AgaMOD, the material was washed several times followed by dialysis during 3 days. The hydrogels were then frozen and dried by lyophilization and grinded into a fine powder with an A11 basic Analytical Mill.

Table II.2: Overview of algMOD, agaMOD or chiMOD-based SAPs crosslinking conditions in the presence of DMAEMA or DMAPMA.

Modified Polysaccharide	Solvent	T	Polysaccharide	DMAEMA /DMAPMA	TEMED	APS
AlgMOD	H_2O	50 °C	2 w%	14 w%	0.48 v%	0.32 w%
AgaMOD	DMSO	60 °C	2 w%	6 w%	0.24 v%	0.16 w%
ChiMOD	6 v% aq. AcOH	35 °C	2 w%	14 w%	0.96 v%	0.64 w%

II.2.9. Sulfation of methacrylated alginate

The sulfation was performed in dimethylformamide (DMF). First the methacrylated alginate was sulfated in an ionic liquid medium. To a solution of premelted 1-butyl-3-methylimidazolium chloride (BMImCl, 98% pure) (950 mg) at 90°C, algMOD (50 mg) was added in a Schlenk tube. After dissolution, 4-dimethylaminopyridine (DMAP, 99% pure) (5mg) was added to the mixture, followed by a suspension of sulfur trioxide pyridine complex (SO_3.Py, technical grade, 48.8-50.3% active SO_3) in DMF (0.5 ml). For sulfation targeting at around 9-10 wt%S, a weight ratio of algMOD:SO_3.Py of 1:5 was used with a sulfation time of 1h at 45°C under atmospheric pressure.

When targeting a sulfation of 6-7 wt%S, a ratio of 1:2.5 was used with a sulfation time of 1h at 45°C. After dilution with water (10 ml) and cooling to room temperature, the solution pH was adjusted to 7-8 with NaOH (3N). The final solution was dialyzed against distilled water for 72h to remove any remaining products before freeze-drying.

II.2.10. UV polymerization of methacrylated κ-carrageenan

The carMOD is dissolved in water (10 w/v%), followed by addition of an Irgacure®2959 solution (0.8 w/v%), taking into account the DS calculated with respect to the hydroxyl moieties present and using 5 mol% Irgacure®2959 with respect to the methacrylate functionalities present. Afterwards, the mixture is flushed with N_2-gas to remove oxygen. Then, the solution is spread out in a rectangular rubber mold between two glass plates which are covered with a release foil. The glass plates are placed in between UV lamps ($\lambda_{operating}$ = 300 – 400 nm, intensity of 9 – 10 mW/cm² per unit) during 90 minutes to make sure the gel is completely formed after which the gel is removed from the glass plates, frozen and freeze-dried.

II.3. Overview of applied characterization methods

II.3.1. Freeze drying

The SAP was freeze-dried using a Christ freeze-dryer alpha 2-4-LSC at -85 °C and 0.37 mbar.

II.3.2. Gel fraction assessment

After polymerization, unreacted particles were removed from the end product via dialysis. By measuring the dry weight of the sample before and after purification during 24 hours, the gel fraction could be determined (in triplicate) using equation (II.1):

$$G\ [\%] = {}^{W}/_{W_0} \tag{II.1}$$

With W = weight of the dry insoluble part of the sample [mg]
W_0 = initial dry weight of the sample [mg]

II.3.3. Particle size distribution obtained via optical microscopy

To examine the resulting particle diameter of all grinded materials, a Zeiss Axiotech optical microscope was used together with the digital image capturing software ZEN core and the analysis software ImageJ. The particles were spread on a microscope slide to clearly distinguish them, followed by observation with a 100- or 200-fold magnification (depending on the particle size). To analyze the images with ImageJ, first the appropriate scale bar was applied, followed by changing the image type to 8-bit color and calibrating the image. Subsequently, the brightness and threshold of the image were adjusted to obtain a clear distinction between particles and

background. The areas of the particles were then analyzed by the software which enables to calculate a theoretical diameter assuming perfect round particles.

II.3.4. Attenuated total reflectance Fourier transform infrared measurements

The SAP powder was characterized using ATR-IR spectroscopy. A PerkinElmer Frontier FT-IR (midIR) combined with a MKII Golden Gate set-up equipped with a diamond crystal from Specac was used to determine the chemical composition of the SAPs. The spectra were measured with a wavenumber window between 4000 and 600 cm^{-1}. The results were analyzed with the PerkinElmer Spectrum Analysis software.

The healing products after water permeability measurements were dispersed in KBr (Merck, Darmstadt, Germany) tablets and transmission was recorded between 4000 and 600 cm^{-1} using a Fourier transform IR (FT-IR) spectrophotometer (Perkin Elmer Instruments, Waltham, US). The resolution of the measurements was 0.25 cm^{-1}. The data were analyzed using the SpectrumOne software.

II.3.5. Nuclear magnetic resonance spectroscopy

II.3.5.1. Assessment of degree of substitution via ^{1}H-NMR spectroscopy

The ^{1}H-NMR spectra from the samples dissolved in D_2O were recorded at room temperature on a Varian Inova 400 MHz spectrometer using a 5 mm four-nucleus PFG probe. Free induction decays were collected with water suppression and using the following acquisition parameters: a 90° pulse of 6.35 µs, a spectral width of 6.4 kHz, an acquisition time of 3 s, a preparation delay of 12s and 64 accumulations. A line-broadening factor of 1 Hz was applied before Fourier transformation to the frequency domain.

To determine the degree of substitution of AgaMOD, a small amount of material (10 - 15 mg) was dissolved in a mixture of deuterated DMSO (d-DMSO) and D_2O (10 v% D_2O), to suppress the peaks of the hydroxyl functionalities on the agarose repeating units. Potassium iodide (10 w/v% relative to the agaMOD) was added to disrupt the double helices which can result in peak broadening. Potassium iodide adheres to the polymer chains which results in a negative charge and therefore repelling behavior of the double helices. The measurement was done at 60 °C. The samples were analyzed with a 300 MHz Bruker spectrometer.

ChiMOD

ChiMOD was dissolved in D_2O acidified with deuterium chloride (DCl, 2 w/v%) to increase solubility. The measurement was done at room temperature with a 300 MHz Bruker spectrometer.

CarMOD

CarMOD was dissolved in D_2O. The measurement was done at 50°C with a 500 MHz Bruker spectrometer.

II.3.5.2. Assessment of cross-linking efficiency through High Resolution Magic-Angle Spinning NMR spectroscopy

HR-MAS NMR spectroscopy of the developed SAPs was performed on a Bruker Avance II 700 spectrometer (700.13 MHz) using a HR-MAS probe equipped with a ^{1}H, ^{13}C, ^{119}Sn and gradient channel. The spinning rate was set to 6 kHz. Samples were prepared by introducing a small amount of freeze-dried material inside a 4 mm zirconium oxide MAS rotor (50 µL). 30 µL D_2O was added to the rotor, allowing the samples to swell. The samples were homogenized by manual stirring prior to analysis. A teflon® coated cap was used to close the rotor.

II.3.6. Scanning electron microscopy energy-dispersive spectroscopy (SEM-EDS)

Scanning electron microscopy (SEM) analysis on the obtained healing products after water permeability was performed on a JEOL JSM-5600 instrument. The apparatus was used in the secondary electron mode (SEI). The SEM instrument was equipped with an electron microprobe JED 2300 and an energy-dispersive spectroscopy (EDS) detector for elemental analysis at four different spots (129 µm x 95µm) in mapping mode. Prior to analysis, the samples were coated with a thin gold layer (ca. 20 nm) using a plasma magnetron sputter coater.

II.3.7. Thermogravimetric analysis (TGA)

The thermal properties of the healing products after water permeability were analyzed using thermogravimetric analysis (TGA) using a TA-instruments Q-50 Thermogravimetric Analyzer. The samples were placed in platina sample holders and subsequently heated to 1000°C at a heating rate of 10°C/min. All TGA analyses were performed under nitrogen atmosphere (60 mL/min). The obtained data were analyzed using TA instruments Universal Analysis 2000 software.

II.3.8. Determination of Ca and Na cations in alginate samples by inductively coupled plasma optical emission spectroscopy

The mass percentages of Ca^{2+} and Na^{+} in sodium alginate and calcium alginate samples were determined before and after performing swelling tests in cement filtrate solutions using inductively coupled plasma optical emission spectroscopy (ICP-OES) through a Spectro Arcos Optical Emission Spectrometer (Spectro, Germany). Before analysis, freeze-dried samples (0.03 - 0.07g, 3 of each material) were dissolved in a solution containing 5 mL HNO3 and 1 mL H2O2. Yttrium was added to all solutions as an internal standard, in order to correct for possible instrument instabilities and/or matrix effects.

II.3.9. Determination of sulfation degree of modified alginate by high-performance anion-exchange chromatography

The linked ester sulfate group content in the samples was determined using high-performance anion-exchange chromatography (HPAEC) by measuring the difference between the total sulfur contents present in the hydrolyzed sample and the non-treated sample. These measurements

were performed by Ifremer (Dr. Sylvia Colliec-Jouault) according to a procedure described earlier in literature [11]. An aqueous solution of an internal standard, KNO_3 (10 g/L), was added to an aqueous solution of the sample (2 mg/mL). The mixture was hydrolyzed with HCl (1M) at 133°C for 4h20m. After cooling to room temperature and adding water (4.5 ml), 800 µl of the sample was analyzed by HPAEC (in triplicate). Prior to injection, all samples were filtered through membrane filters with 0.45 µm pore size. The sulfate peak was attributed with a retention time reference using a Na_2SO_4 standard, investigated over the concentration range 1 – 8 mM.

II.3.10. Dynamic vapor sorption measurements

DVS was applied to measure the moisture uptake capacity at different relative humidities (RHs). The equipment consists of a Cahn microbalance, a temperature-controlled housing and mass flow controllers which control the appropriate flow of the wet and dry N_2 gas. The benefit of this technique is the control over both the relative humidity as well as the temperature (i.e. 21°C). For the DVS analysis, approximately 5 – 10 mg freeze-dried SAP was introduced in the sample pan. A first step (RH of 0%) was required to start with a completely dry material. Afterwards, the humidity was varied in systematic steps. Every subsequent step was initiated when the change of the sample mass as a function of time was lower than 0.002 mg/min. After an equilibrium value was obtained at the highest RH, desorption was realized in consecutive RH steps similar to the sorption process until full desorption was realized. If required, the equilibrium values were calculated from the weight versus time curves by extrapolation using the exponential function presented in equation (II.2):

$$m(t) = a * (1 - b * \exp(-c * t)) \qquad \text{(II.2)}$$

in which m(t) is the mass of the sample at time t, while the coefficients a, b and c can be determined by means of non-linear curve fitting via Microsoft Excel.

II.3.11. Swelling studies

II.3.11.1. Swelling study in aqueous solutions with a varying pH

The swelling capacity of the SAPs was measured as the mass change between the freeze-dried and the swollen (cfr. saturated) state. A mass of 0.15 – 0.20 g polymer was incubated in 75 – 100 mL of an aqueous solution at various pH-values ranging from 1 to 13. Depending on the pH targeted, NaOH or HCl was added to the aqueous solution. Regarding suitable media for testing behavior of SAP, using buffers would be useless as these all consist of different cations present. Using acidified and basified cement filtrate or acidified and basified aqueous solutions is more representative but is not completely representative to mortar but gives a good indication how the SAP will normally react in the fresh mortar and when water infiltrates in the present cracks. After one day incubation the swelling will reach an equilibrium and a funnel and a filter were used to capture the water that was not absorbed by the SAPs. By calculating the difference between the initially added and the filtered water, the residual water inside the material could be determined together with the swelling capacity of the material (in triplicate) using equation (II.3):

$$Swelling\ capacity = {}^{(m_0 - m_{filter})}/_{m_{SAP}} \quad \text{(II.3)}$$

in which m_0 is the initially added water mass [g], m_{filter} represents the mass of the solution going through the filter [g] and m_{SAP} is the added mass of dried SAP (i.e. 0.15 - 0.20 g). The filtration paper was typically saturated prior to filtration to exclude its influence on the mass of the filtered solution.

II.3.11.2. Swelling study in cement filtrate solutions

Cement filtrate (CF) was made by mixing 10 g ordinary Portland cement (OPC) and 100 mL demineralized water for three hours with a mechanical stirrer, followed by filtration to remove the cement particles and collecting the solution. HCl was added if required to adjust the pH to the targeted values (pH 9 - 12). NaOH was added to the CF solution if needed to investigate the possible degradation effect of the SAP at pH 13. This is useful to gain an improved understanding of the swelling effect at extreme basic condition. The same principle (0.15 – 0.20 g polymer incubated in 75 – 100 mL cement filtrate solution) was used as described in §II.3.11.1. All swelling tests were performed in triplicate.

II.3.12. Bending and compression strength measurements

Mortar prisms were manufactured by a standard mortar mixing procedure, as described in EN 196-1 to investigate the influence of the addition of SAPs on the flexural and compression strength of mortar. First, 450 g ordinary Portland cement (22 m%) and the required amount of SAP (0, 0.5 or 1.0 m% with respect to the added amount of cement, corresponding respectively to 0, 2.25 or 4.5 g SAP) were mixed together using a standard mortar mixer. Then 225 mL water (11 m%, W/C = 0.5) and optionally an additional amount of water (corresponding to the added amount of SAP, added on top of the total mixture) was brought into contact with the dry mixture and mixed at 140 rpm for 30s. Subsequently, 1350 g silica sand 0/2 (67 m%) was steadily added during the next 30 s with the same rotational speed. The mixer was brought to a high speed (285 rpm) for an additional 30s. The mixing was subsequently stopped for 90s. The first 30s, the mortar was scraped from the bowl and then left resting for 60s. Afterwards, the mixing was continued for 60s at high speed, following the method described in EN 196-1. The workability was measured by means of a jolting table as described in EN 12350-5. The samples were then molded as described in EN 196-1. The resulting samples (160 x 40 x 40 mm^3) were stored in a climate room with a relative humidity of 95 ± 5% and a temperature of 20 ± 2 °C for 28 days.

Flexural and compressive strength of mortar was measured (in triplicate) after 28 days by means of a three-point-bending test (performed in triplicate) on 160 × 40 × 40 mm^3 mortar beams followed by a compression test on the resulting halves (6 samples in total per series) following the standard NBN EN 196-1. The strength tests were performed with a servo-hydraulic testing machine Walter + Bai DB 250/15. The results were analyzed by using the software package Proteus® 10.1. Univariate ANOVA tests with two factors, followed by a Tukey post-hoc test were

performed in the statistical program SPSS to identify significant strength differences between the mortars containing different SAPs or different SAP quantities ($p < 0.05$).

II.3.13. Air void analysis

A quantitative analysis to determine the air voids was possible with the RapidAir 457 apparatus. The test was performed on cylindrical mortar specimens (diameter 70 mm, height 30 mm). The technique required careful polishing of the sample surface since scratches have to be avoided and air voids must have sharp edges [12]. To enhance the contrast, the polished surfaces were colored with black ink and white barium sulfate ($BaSO_4$) powder was distributed on top to fill the air voids. After removing the excess powder with a steel blade, the specimens were ready for testing. All samples were analyzed in two perpendicular directions using 3 probe lines per frame with a total traverse length of 2415 mm and a scanned area of 50 × 50 mm². With the recorded total chord length of air voids T_a (mm) and paste T_p (mm), the total surface distance traversed across T_{tot} (mm), the air content can be carefully characterized as described in equation (II.4).

$$A = \frac{T_a}{T_{tot}} * 100 \qquad \text{(II.4)}$$

II.3.14. Self-sealing study on mortars containing SAPs by water permeability

Mortar specimens were mixed as described in section §3.12. and casted in a PVC-tube with addition of internal reinforcement. The dimension of the cylindrical samples used in the permeability tests was 78 mm in diameter and 20 mm in height. After 48 hours, these samples were demolded and kept in a room with a humidity of 95 ± 5% and a temperature of 20 ± 2 °C. Permeability tests were performed, starting at an age of 28 days after cracking cylindrical specimens at the age of 14 days by means of a crack width-controlled splitting test (Walter + Bai DB 250/15). The crack width was controlled during the splitting test by connecting two linear variable difference transducers (LVDTs) (Solartron AX/0.5/S; Solartron Metrology, West Sussex, UK; with an accuracy of 1 µm) at the front and back of the sample. The crack opened with a velocity of 0.001 mm/s and was stopped when a crack width of 300 µm was reached. The residual crack widths after relaxation of the sample ranged between 150 and 245 µm, measured by a Leica S8 APO optical microscope with a DFC 295 camera. After splitting, the samples were taped at the side to avoid the entrance of epoxy in the crack and glued with epoxy into a poly(vinylchloride) (PVC) tube to exclude side effects during the permeability tests. The samples were vacuum-saturated (NBN B 24-213 [13]) with water by filling the vacuum chamber with water and keeping the vacuum state for 2.5h, then restoring the atmospheric pressure and keeping the samples submerged for 24h. The mortars were then placed into the water permeability test setup at an age of 28 days. The water permeability coefficient could be calculated by creating a water column at the top of the sample and thus generating water pressure followed by measuring the descent of that water column over time. Rubber seals between plexiglass and PVC rings ensured a water-tight setup. At the top opening, a glass pipette with an inner diameter of 10 mm was positioned and covered to avoid evaporation. A

line of millimeter paper was stuck to the pipette to measure the descent of the water column. At the bottom part, a rubber hose was attached and positioned level with the lower part of the mortar cylinder. The method is presented in Figure II.1. The used water permeability setup has already been described in detail by Van Tittelboom et al. [14, 15].

The self-sealing efficiency was measured as the decrease in water flow through the crack over time. Starting from Darcy's law, an expression for the coefficient of water permeability k (m/s) is found using equation (II.5):

$$k = \frac{a*L}{A*t_f} * \ln\left(\frac{h_0}{h_f}\right) \quad \text{(II.5)}$$

in which a is the cross-sectional area of the fluid column [m^2], L is the thickness of the specimen [m], A represents the surface area of the sample subjected to the flow [m^2], t_f is the measured time [s], h_0 is the initial pressure head [m] and h_f represents the remaining pressure head [m]. Permeability readings for all specimens (≥ 3 samples per series) were taken every day during 28 days. On the 28th day (at an age of 56 days), the average coefficients of water permeability of the samples were compared. Measurements were done in triplicate. Again, the significant differences are identified.

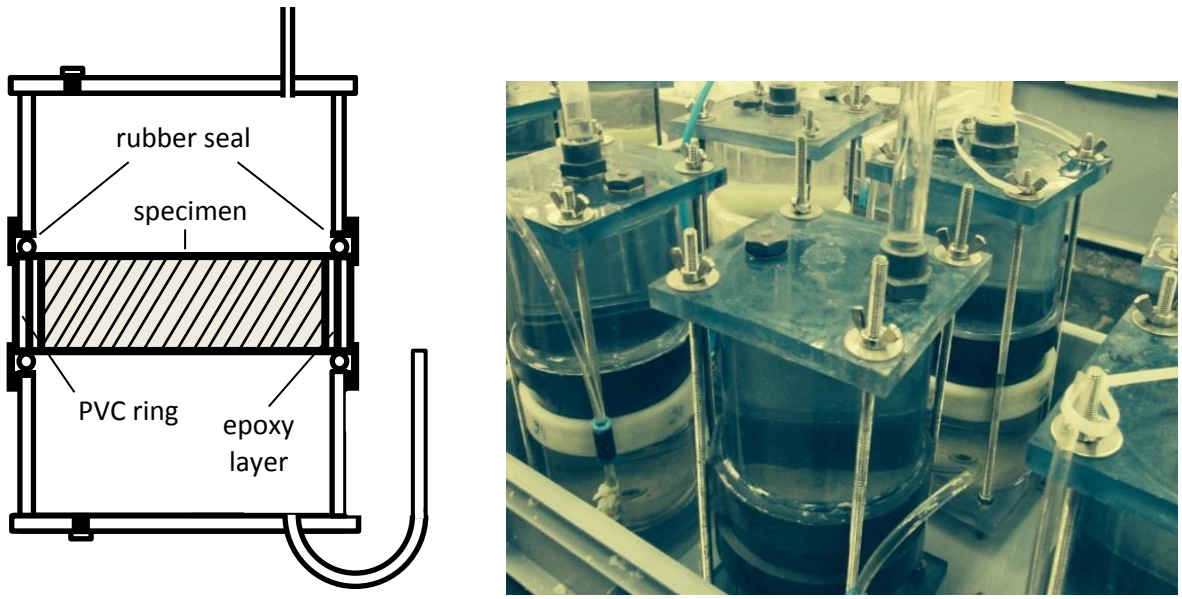

Figure II.1: Water permeability set-up for mortar samples.

II.3.15. Combined self-sealing and -healing study

To test the self-sealing and -healing capacity of SAP-containing mortar, mortar samples with additional fibers were produced based on the methodology described by Snoeck et al. [16]. SAPs were added to the reference mixture (without SAPs) in the amounts of 0.5, 0.7, 1.0 and 1.3 m%

with respect to the cement weight. First, the cement (334.0 g, 29.8 m%), the fly ash (334.0 g, 29.8 m%) and, if applicable, the SAPs were shortly mixed. Then, the water (200.6 g, 17.9 m%) and polycarboxylate superplasticizer (3.0 g, 0.3 m%) were added and mixed for 30 s at 140 rpm. Next, fine silica sand (234.0, 20.9 m%) was added during the following 30 s while mixing. Subsequently, the speed was increased up to 285 rpm for 30 s, after which the mixture was scraped from the edges of the mixing bowl for 30 s. Then, a rest period of 60 s was included. Finally, poly(vinylalcohol) (PVA) fibers (14.3 g, 1.3 m%) were added during 30 s while mixing at a speed of 140 rpm, after which the speed was increased again to 285 rpm for another 60 s. The molds with dimensions of 160 x 40 x 10 mm³ (seven per series), were filled and after compaction, the samples were stored in a climate chamber for 24 hours at a RH of 95 ± 5% and a temperature of 20 ± 2 °C. The samples were demolded after one day and stored until the age of 28 days in the climate chamber. At the age of 28 days, multiple cracks were formed in the samples by use of a four-point-bending test powered by a servo-hydraulic testing system (Walter + Bai DB 250/15). This test is shown schematically in Figure II.2. Four-point-bending tests have been used extensively by different research groups to identify the self-healing potential of SAPs [17, 18].

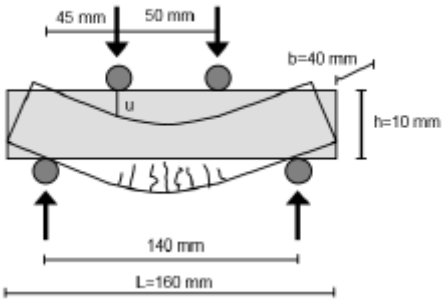

Figure II.2: Schematic representation of the four-point-bending test [16].

The displacement rate was fixed at a low value of 0.0015 mm/s to simulate a quasi-static load. The first three samples per test series were loaded until failure occurred and the maximum possible strain was reached at the bottom side of the specimen. The other four samples were subjected to the quasi-static load upon achieving a strain equal to 1% at the bottom side. This strain was theoretically calculated from the curvature and vertical displacement during loading. After cracking, all samples were subjected to wet-dry cycles for 28 days (alternately stored in water for 12 hours, followed by a period of 12 hours at a RH of 60%). At the age of 56 days, the four samples that were loaded until a strain of approximately 1% were reloaded in the same four-point-bending test to the point of failure. As such, a loading and reloading cycle were obtained for each of these samples.

The combination of the crack formation and reloading cycle after healing (see Figure II.3) gives the possibility to compare different mechanical properties. The most important parameters comprise the first-cracking strength σ_{fc}, the regain in first-cracking strength (regain in σ_{fc}) and the amount of multiple cracking (MC) immediately after failure and after reloading (loaded to obtain a strain of 1%, followed by a healing period of 28 days during wet-dry cycles and subsequent

reloading until failure). Equations II.6 – II.9, by using the points indicated in Figure II.3, were used to identify these properties for all specimens (measurements performed in triplicate).

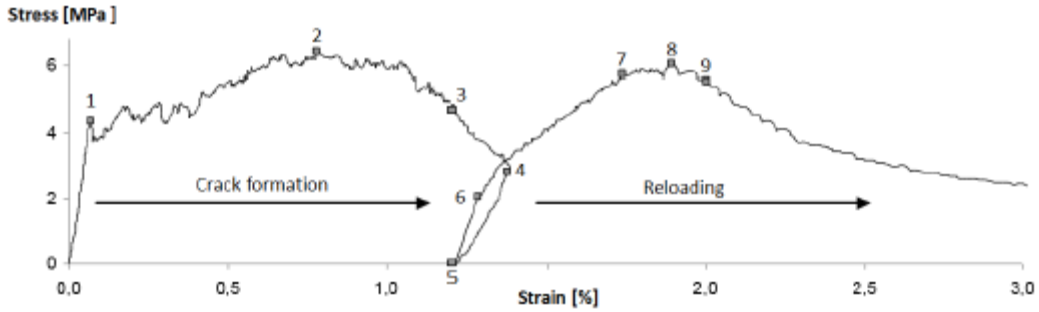

Figure II.3: Stress-strain curve of a specimen cracked up to approximately 1% strain and reloaded after a healing period of 28 days.

First-cracking strength:

$$\sigma_{fc} = \sigma_{[1]} \tag{II.6}$$

Regain in first-cracking strength:

$$Regain\ in\ \sigma_{fc} = \frac{\sigma_{[6]}}{\sigma_{[1]}} \tag{II.7}$$

Peak strength:

$$\sigma_p = \sigma_{[2]} \tag{II.8}$$

Multiple cracking:

$$\varepsilon_{mc} = \varepsilon_{[3]} - \varepsilon_{[1]} \tag{II.9}$$

Crack width determination

First, the cracks were visualized during the self-healing period by performing optical microscopy using a Leica S8 APO microscope with a DFC 295 camera. Images of all cracks were captured with a 6.3x optical zoom, after which they were analyzed with the software package ImageJ. Every crack was measured at five different locations, always with the same spacing between the measuring points. Subsequently, a comparison was made at different ages (3, 7, 14 and 28 days healing after the start-up of the wet-dry cycles or 28 days with fully cracked samples from the start) to calculate the degree of crack sealing.

II.3.16. Statistical analysis

Statistical assays were performed when possible. A univariate ANOVA test, followed by a Tukey (if equal variances were assumed) or Dunnett's T3 post-hoc test were performed in the statistical program SPSS to identify potential significant differences ($p < 0.05$). All standard deviations reported were calculated based on single values.

II.4. Theoretical discussion of the used methods

II.4.1. Structure confirmation through infrared spectroscopy

Infrared spectroscopy is a qualitative technique to determine the structure of the produced SAPs. It deals with the infrared region of the electromagnetic spectrum. An infrared beam reflects from the surface of the SAP, whereby it will be partially absorbed inside the molecule. The energy of these absorptions is corresponding to vibrational modes of present chemical bonds. As such, the absorption of the SAP as a function of the wavelength provides information on the moieties present in the SAP.

II.4.2. Determination of the cross-linking efficiency by high resolution magic-angle spinning nuclear magnetic resonance spectroscopy

HR-MAS ^{1}H-NMR spectroscopy was performed to have quantitative data on the double bond consumption. It is a technique that is able to measure samples in high-resolution NMR spectroscopy. By the high frequency spinning of the sample in the magnetic field, the obtained lines become more narrow, which increases the resolution of the measurement and thus improves the analysis of the spectrum.

II.4.3. Scanning electron microscopy energy-dispersive spectroscopy (SEM-EDS)

With SEM, an electron beam is scanned across the surface of the sample. When an electron strikes the sample, it penetrates and interacts elastically and inelastically, from where various types of radiation emerge. The detection of these signals creates the micrograph. There are three types of signals which provide the largest amount of information: secondary electrons, backscattered electrons and X-rays.
Secondary electrons (low energy, < 50 eV) are ejected from the outer shell of the atoms by inelastic scattering and due to being very surface sensitive let create a micrograph with a high resolution.

Backscattered electrons are especially useful for heavy elements and consist of high-energy electrons. They are reflected by elastic scattering interactions and the escape depth can be greater than for secondary electrons. Consequently, the resolution can decrease [19-21].
SEM-EDS is a technique able to detect all elements from carbon to uranium, with a detection limit of circa 0.2 m% for most elements [20]. EDS analysis was conducted by emission of X-rays.

II.4.4. Thermogravimetric analysis (TGA)

TGA gives a software-controlled measurement and analysis of the weight loss of the SAP as a function of an increasing temperature under an inert atmosphere (N_2). It allows to calculate the degradation temperature of polymers, gives an indication on the chemical composition and the amount of non-organic residue.

II.4.5. Inductively coupled plasma optical emission spectroscopy (ICP-OES)

ICP is a dominant source to obtain a fast spectroscopic multi-element analysis with a low detection limit due to large signals and limited background noise as well as high precision.
ICP-OES allows to monitor emission from different elements either sequentially or simultaneously. Atom lines are most intense for elements with high ionization potentials and alkali metals. There are two major differences between ICP-OES and ICP-MS (mass spectroscopy). The first difference is that, for the latter technique, ions from the sample must be physically transported from the plasma to the mass spectrometer. In the former technique, the collections of photons is nonintrusive. The second difference lies in the emission intensity being strongly dependent on the fraction of excited ions (ICP-OES), while for MS, the signals are dependent on ionization, not excitation [22].

II.4.6. High-performance anion-exchange chromatography (HPAEC)

HPAEC is used to separate anionic analytes or analytes which can be ionized at extreme alkaline conditions (> pH 12). It uses strong alkaline conditions to create anions from those latter analytes which would not be anionic at neutral pH. The difference in pKa and the difference in interaction with a cation-exchange resin gives rise to a variation of elution times during HPAEC. The non-porous nature of the resin imparts highly effective separation of a wide variety of carbohydrates including polysaccharides [23].

II.4.7. Moisture uptake capacity determination by dynamic vapor sorption (DVS) measurements

The DVS equipment consists of a Cahn microbalance, a temperature-controlled housing and mass flow controllers which control the appropriate flow of the wet and dry N_2 gas. The benefit of this technique is the control over both the relative humidity as well as the temperature. This technique allows to measure sorption and desorption processes in a non-destructive way, by weight changes on a balanced system. It also allows fast kinetics due to a continuous measurement. By the constant N_2 gas flow, an optimal mass transfer rate is ensured to and from the SAP.

II.4.8. References

[1] Noppakundilograt S, Nanakorn P, Jinsart W, Kiatkamjornwong S. Synthesis of acrylamide/acrylic acid-based aluminum flocculant for dye reduction and textile wastewater treatment. Polymer Engineering & Science. 2010;50(8):1535-46.
[2] Shivakumar NVGaHG. Investigation of Swelling Behavior and Mechanical Properties of a pH-Sensitive Superporous Hydrogel Composite. Iranian Journal of Pharmaceutical Research. 2012;11(2):481-93.
[3] Rouillard AD, Berglund CM, Lee JY, Polacheck WJ, Tsui Y, Bonassar LJ, et al. Methods for photocrosslinking alginate hydrogel scaffolds with high cell viability. Tissue Engineering Part C: Methods. 2010;17(2):173-9.
[4] Chou AI, Nicoll SB. Characterization of photocrosslinked alginate hydrogels for nucleus pulposus cell encapsulation. Journal of Biomedical Materials Research Part A. 2009;91(1):187-94.

[5] Paepe ID, Declercq H, Cornelissen M, Schacht E. Novel hydrogels based on methacrylate-modified agarose. Polymer International. 2002;51(10):867-70.
[6] Yu LMY, Kazazian K, Shoichet MS. Peptide surface modification of methacrylamide chitosan for neural tissue engineering applications. Journal of Biomedical Materials Research Part A. 2007;82A(1):243-55.
[7] Mihaila SM, Gaharwar AK, Reis RL, Marques AP, Gomes ME, Khademhosseini A. Photocrosslinkable Kappa-Carrageenan Hydrogels for Tissue Engineering Applications. Advanced healthcare materials. 2013;2(6):895-907.
[8] Rinaudo M. Main properties and current applications of some polysaccharides as biomaterials. Polymer International. 2008;57(3):397-430.
[9] Dutkiewicz JK. Superabsorbent materials from shellfish waste—a review. Journal of Biomedical Materials Research. 2002;63(3):373-81.
[10] Jayakumar R, Prabaharan M, Kumar PTS, Nair SV, Tamura H. Biomaterials based on chitin and chitosan in wound dressing applications. Biotechnology advances. 2011;29(3):322-37.
[11] Chopin N, Sinquin C, Ratiskol J, Zykwinska A, Weiss P, Cérantola S, et al. A Direct Sulfation Process of a Marine Polysaccharide in Ionic Liquid. BioMed research international. 2015;2015.
[12] Jakobsen UH, Pade C, Thaulow N, Brown D, Sahu S, Magnusson O, et al. Automated air void analysis of hardened concrete — a Round Robin study. Cement and Concrete Research. 2006;36(8):1444-52.
[13] Nbn B. B 24-213. Belgische norm: Proeven op metselstenen-Wateropslorping onder vacuum. 1976.
[14] Van Tittelboom K, De Belie N, De Muynck W, Verstraete W. Use of bacteria to repair cracks in concrete. Cement and Concrete Research. 2010;40(1):157-66.
[15] Van Tittelboom K, De Belie N, Van Loo D, Jacobs P. Self-healing efficiency of cementitious materials containing tubular capsules filled with healing agent. Cement and Concrete Composites. 2011;33(4):497-505.
[16] Snoeck D, De Belie N. Repeated autogenous healing in strain-hardening cementitious composites by using superabsorbent polymers. Journal of Materials in Civil Engineering. 2015;28(1):04015086.
[17] Kim JS, Schlangen H. Self-healing in ECC stimulated by SAP under flexural cyclic load. ICSHM 2011: Proceedings of the 3rd International Conference on Self-Healing Materials, Bath, UK, 27-29 June 20112011.
[18] Yao Y, Zhu Y, Yang Y. Incorporation superabsorbent polymer (SAP) particles as controlling pre-existing flaws to improve the performance of engineered cementitious composites (ECC). Construction and Building Materials. 2012;28(1):139-45.
[19] Goldstein J, Newbury DE, Echlin P, Joy DC, Romig Jr AD, Lyman CE, et al. Scanning electron microscopy and X-ray microanalysis: a text for biologists, materials scientists, and geologists: Springer Science & Business Media; 2012.
[20] Loria EA. SCANNING ELECTRON-MICROSCOPY AND X-RAY-MICROANALYSIS-GOLDSTEIN, JI, NEWBURY, DE, ECHLIN, P, JOY, DC, FIORI, C, LIFSHIN, E. MINERALS METALS MATERIALS SOC 420 COMMONWEALTH DR, WARRENDALE, PA 15086; 1983.
[21] Flegler SL, Heckman Jr JW, Klomparens KL. Scanning and transmission electron microscopy: an introduction. Oxford University Press(UK), 1993. 1993:225.
[22] Olesik JW. Elemental Analysis Using ICP-OES and ICP/MS. Analytical Chemistry. 1991;63(1):12A-21A.
[23] Lee YC. High-performance anion-exchange chromatography for carbohydrate analysis. Analytical Biochemistry. 1990;189(2):151-62.

III. Development and implementation of synthetic SAPs for self-sealing and self-healing of cracks in mortar

III.1 Using cross-linked poly(acrylic acid) as a synthetic superabsorbent polymer

The present work will start with the synthesis and characterization of an internal and active system for self-healing of cracks in concrete by incorporating a synthetic superabsorbent polymer (SAP) based on acrylic acid (AA) during the mixing process. AA and its sodium or potassium salts are some of the most often used monomers for the industrial production of SAPs [1]. Poly(acrylic acid) (pAA) has already been used for metal ion recovery [2] and for creating multiwalled carbon-nanotubes (MWNTs) composite-coated glassy-carbon electrodes for the voltammetric detection of dopamine and uric acid [3, 4]. Acrylates have been often combined with polysaccharides and used in a plethora of applications going from drug release [5-10], removal or adsorption of metal ions and dyes [11-13] to agricultural use [14-16]. They have also been used already in concrete for different applications [17-20]. The most often used technique to prepare acrylic-based synthetic SAPs is by a free-radical polymerization of vinyl monomers in the presence of a multifunctional cross-linker [1, 21].

In a first part, a cross-linked polymer network based on AA has been created by using a synthetic bifunctional cross-linker N,N'-methylene bisacrylamide (MBA) to result in p(AA). As mentioned in [1], pAA has been very often used for the synthesis of SAPs [22, 23]. As such, it is a good choice to start with and investigate what possibilities it has. The chemical structure of the SAP has been verified by attenuated total reflectance-infrared (ATR-IR) spectroscopy. The cross-linking efficiency has been determined by high resolution magic-angle spinning (HR-MAS) ^{1}H-NMR spectroscopy. It is also important to quantify its moisture uptake capacity by dynamic vapor sorption (DVS), as for the intended application, cracks are not always directly in contact with water and it is important to know how strong these SAPs could swell in a moist environment and to partially seal off the cracks. The swelling capacity has been investigated in aqueous solutions with a varying pH to investigate the effect of pH on swelling behavior and on possible degradation of the polymer and in a cement filtrate solution to get an idea of its behavior in mortar. Subsequently, the influence of this SAP on the bending and compressive strength by incorporation in mortar has been evaluated. The results have been compared to commercially available synthetic SAPs to indicate their potential for the envisaged application [24].

III.1.1. Development of the synthetic acrylate-based p(AA_{100})_0.2 SAPs

Poly(acrylic acid) (p(AA)) based materials were synthesized starting from acrylic acid (AA) and N,N'-methylene bisacrylamide (MBA) by a free radical cross-linking reaction. The obtained material was ductile and had a white colour. After polymerization, the obtained SAPs were incubated in water for purification. Finally, the SAP was freeze-dried and grinded to a fine powder prior to characterization. The obtained gel fraction was 95 ± 1 %, indicating that a high yield was obtained for the polymerization. This was a qualitative proof regarding the polymerization efficiency. Further quantitative results have been discussed in § III.1.2. Additionally, most of the particle sizes varied between 30 and 240 µm in diameter (10% of the particle diameters ≤ 33 – 34 µm, 50% ≤ 137 µm and 90% ≤ 243 – 244 µm).

When comparing the obtained data with commercial SAPs, the synthesized SAPs had a similar diameter range as the so-called SAP A (copolymer of acrylamide and sodium acrylate, particle size of 100.0 ± 21.5 µm [24]). SAP B, a cross-linked potassium salt poly(acrylate), on the other hand, was characterized by a larger particle size of 476.6 ± 52.9 µm [24]. These two SAPs were indicated to be best performing for internal curing and self-healing according to Snoeck et al. [25].

III.1.2. Chemical structure elucidation and assessment of the polymerization efficiency of the SAPs developed

ATR-IR spectroscopy was performed on the resulting SAPs. The OH – stretch, corresponding with the carboxylic acid, was laying between 3400 cm^{-1} and 2400 cm^{-1} and was clearly visible (Figure III.1). The peak at 1695 cm^{-1} could be attributed to the C=O stretch of both the secondary amide groups from the cross-linker as well as the carboxylic acid from the monomer, while the C-O stretch of the acrylic acid corresponded with the signal at 1410 cm^{-1}. The latter already provided a qualitative indication of the presence of both the monomer as well as the cross-linker in the final product.

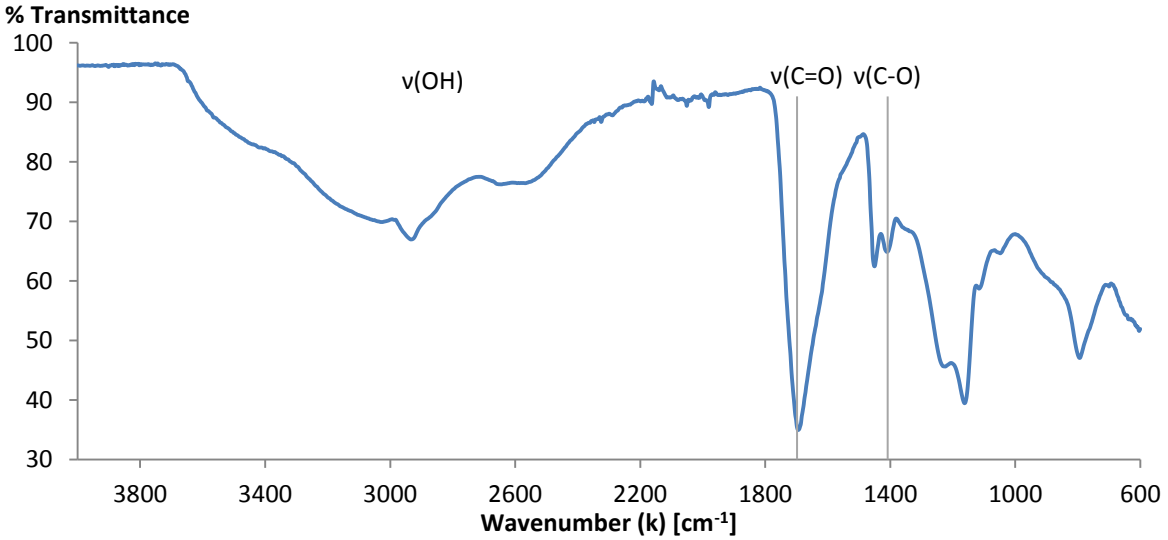

Figure III.1: ATR-IR spectrum obtained for the p(AA_{100})_0.2 SAPs.

To assess the polymerization efficiency, high resolution magic-angle spinning (HR-MAS) ^{1}H-NMR spectroscopy was applied. The signals related to the H-atoms of the C=C double bonds corresponding to AA and MBA prior to polymerization appeared between 5.9 – 6.4 ppm and 5.7 – 6.2 ppm respectively [26]. When investigating the spectrum after polymerization (Figure III.2), it could be observed that these peaks had completely disappeared. This was especially visible within the area between 6 – 6.5 ppm. HR-MAS ^{1}H-NMR spectroscopy could thus be considered as an additional and quantitative tool to confirm the successful synthesis of the p(AA_{100})_0.2 SAPs.

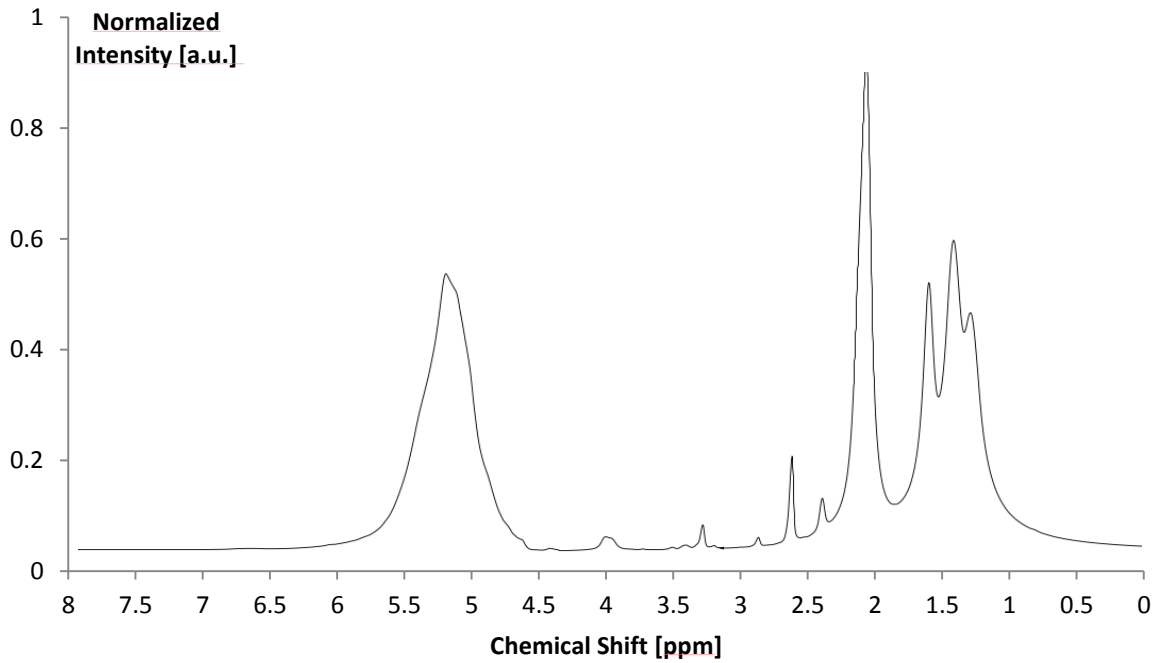

Figure III.2: HR-MAS ^{1}H-NMR spectra of p(AA_{100})_0.2 after polymerization. The peaks corresponding with the H-atoms of the C=C double bonds (5.5-6.5 ppm) have completely disappeared.

III.1.3. Moisture uptake capacity measurements

When cracking occurs, the incorporated SAPs will not be in direct contact with water at all times. It is therefore important to observe and measure the moisture uptake capacity in a humid environment. If the SAP is able to swell substantially, partial crack sealing would still be possible, even when no water is able to reach the SAP. This has also been proven in Snoeck et al. by partial sealing at 60 and 90% RH [25]. Interestingly, DVS (with steps of 0, 30, 60, 90, 95% RH) enables to determine the equilibrium moisture content as a function of the relative humidity (i.e. sorption isotherms).

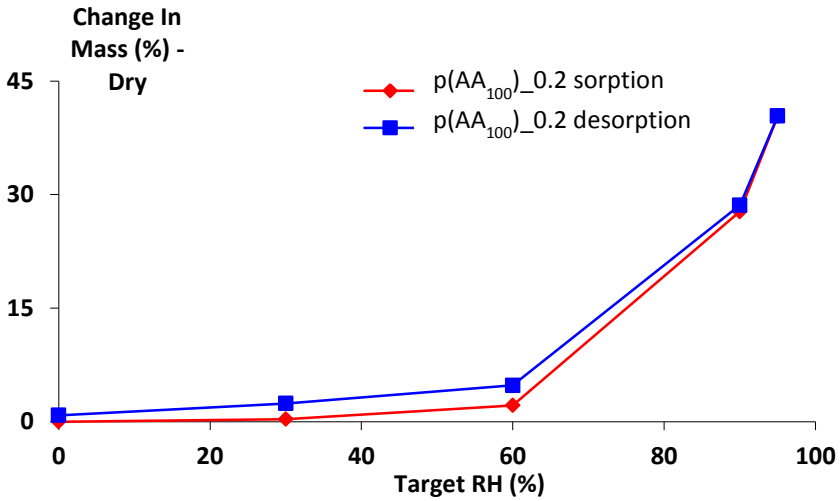

Figure III.3: Moisture uptake capacity at varying RH values for p(AA_{100})_0.2

As illustrated in Figure III.3, the moisture uptake capacity was very low at RHs up to 60% (i.e. 2% of the original weight of the SAP). A substantial increase occurred at higher RH, being 28% at 90% RH up to 40% at 95% RH. The latter implied that the SAP could only take up less than half its own weight in moisture at high RH and could only aid to a limited extent in blocking the crack when no external water is available. Interestingly, the level of hysteresis was negligible with a maximum up to 3%. Thus, the initially absorbed moisture at a certain RH can be fully desorbed when the RH level decreases again and can thus be entirely available to be delivered to the remaining unreacted cement particles. When comparing the obtained moisture uptake capacity results to the values of the commercial SAPs, both SAP A and B had an overall superior moisture uptake (they both have an uptake of 25, 85 and 125% the original weight of the SAP at 60, 90 and 95% RH).

III.1.4. Swelling capacity measurements in aqueous and cement filtrate solutions

In order to define the SAP swelling capacity, the materials developed were incubated during 24 hours in aqueous solutions of varying pH (3, 6, 8, 10, 12 and 13) and in a cement filtrate solution (CF). The latter enabled to assess the pH-responsiveness of the SAP and the possible degradation (e.g. through hydrolysis). As indicated in Figure III.4, the swelling capacity of the SAP was 31 ± 1 g_{water}/g_{SAP} at a pH 3. However, acrylic acid has a pKa value of 4.25 [27], implying that the carboxylic acids become negatively charged at a pH above this value. This was indicated by the swelling capacity which increased steadily up to 46 ± 2 g_{water}/g_{SAP} at pH 8. This anticipated trend was also observed in other research during which the pH-responsiveness of polyether-modified poly(acrylic acid) was tested [28]. No significant change could be distinguished between pH 8 and 10, as anticipated. At pH 12, however, the swelling capacity increased extremely up to 393 ± 14 g_{water}/g_{SAP}, which again dropped to 55 ± 4 g_{water}/g_{SAP} at pH 13.

Interestingly, the maximal swelling of p(AA_{100})_0.2 was substantially higher than the water uptake capacity of the commercially available SAPs in demineralized water (i.e. a swelling of 305 ± 4 g_{water}/g_{SAP} for SAP A and 283 ± 2 g_{water}/g_{SAP} for SAP B respectively [24]). Zohuriaan-Mehr et al. also synthesized poly(acrylic acid) with MBA and combined it with kaolin. Looking at the swelling capacity of their reference material (250 g_{water}/g_{SAP}), the swelling potential obtained for p(AA_{100})_0.2 is superior. The same authors also reported a study varying the amount and type of cross-linker (using 1,4-butanediol diacrylate (BDDA) as alternative cross-linker in addition to MBA). The maximal swelling capacity for the materials with MBA was up to 350 g_{water}/g_{SAP} which is comparable but still lower than what was obtained for p(AA_{100})_0.2. However, addition of the lowest amount of BDDA led to a superior swelling capacity of 575 g_{water}/g_{SAP} [29].

The swelling in cement filtrate was very limited, being 12 ± 1 g_{water}/g_{SAP}. In cement filtrate solution (pH 12.6), the acid groups are converted into carboxylate moieties. These groups repel each other and increase the volume of the swollen polymer. However, in cement filtrate solution this effect is counterbalanced. Indeed, the presence of dissolved cations in cement filtrate

(K^+, Na^+, Mg^{2+} and Ca^{2+}) counter this repelling effect, thereby decreasing the swelling capacity. Secondly, the presence of divalent cations (Mg^{2+} and Ca^{2+}) exert an additional reductive effect on the swelling properties [30, 31], these cations form strong electrostatic interactions with the carboxylate groups present and can therefore act as physical cross-linkers. Consequently, there is less opportunity for the repelling negative charges to increase the volume of the swollen SAP, which results in a low swelling capacity. The swelling capacity in CF was substantially lower than for the commercial SAPs (i.e. 61 ± 1 g_{water}/g_{SAP} for SAP A and 58 ± 2 g_{water}/g_{SAP} for SAP B [24]). This makes the synthesized ones promising as they should swell less during mixing in mortar and create smaller macro-pores. This was investigated further in §III.1.5.

The increase in swelling degree in the aqueous solution at pH 12 can be attributed to hydrolysis of the cross-linker. MBA becomes less stable and the internal amide groups will start to hydrolyze into carboxylates (and primary amines). In a first stage, some of the links are broken, leading to a more open structure and more possibility for swelling, which leads to the extreme increase in swelling capacity. However, from a critical point onwards, too many bonds are broken, thereby compromising the network integrity, which causes the swelling capacity to drop again at pH 13. In cement filtrate (pH around 12.6), the network started to degrade, and as was identified qualitatively by IR, part of the amide groups was hydrolyzed, corresponding with the condition obtained during incubation in the aqueous solutions with pH between 12 and 13.

Degradation phenomena were demonstrated by IR spectroscopy as presented in Figure III.5. After incubation in the different aqueous (and cement filtrate) solutions, the materials were freeze-dried and ATR-IR spectroscopy was performed. In the original IR spectrum of $p(AA_{100})\_0.2$, a few important signals could be distinguished (see also Table III.1). At 794 cm^{-1}, a broad peak could be observed which corresponded to the out-of-plane bending vibration γ(N-H) of amides from the cross-linker. Around 1410 cm^{-1}, the symmetric COO^- stretching ν_s(C-O) from acrylic acid was present. At 1695 cm^{-1} a strong peak could be distinguished which could be attributed to the C=O stretch from both the secondary amide groups from the cross-linker as well as the carboxylic acid from the monomer. When looking at the spectrum after incubation at pH 3, the above-mentioned peaks remained visible and no changes could be observed (data not shown). However, in the spectrum after incubation at pH 12, a peak at 1550 cm^{-1} became apparent, which was originally overlapping with the shoulder of the C=O stretch from the cross-linker. This asymmetric COO^- stretch ν_{as}(C-O) from the acrylates became much more pronounced compared to the C=O stretch of the secondary amides because the internal amide groups became hydrolyzed, which caused the network links to break partially. The alkaline hydrolysis of amide moieties into acrylates has been introduced already in literature [32]. This was also confirmed by the out-of-plane bending vibration γ(N-H) of the amides at 794 cm^{-1} which was far less pronounced. As ATR-IR spectroscopy is a qualitative technique, care must be taken with the interpretation of “more or less pronounced”. Only the comparison between peaks can be semi-quantitative [33, 34].

At pH 13, the observed effects were even more pronounced. The ν_s(C-O) was strongly present, to such an extent that the ν_{as}(C-O) was almost completely hidden, while the C=O stretch was

very weak. In addition, a very sharp peak arised at 876 cm^{-1} which was related to γ(N-H) from primary amines, the second functionality formed by the hydrolysis of the internal amide groups from the cross-linker.

On the other hand, when looking at the spectrum after incubation in cement filtrate solution, both the ν_s(C-O) and ν_{as}(C-O) were strongly present, while the sharp peak of γ(N-H) at 876 cm^{-1} was only weakly visible. This corresponded with a condition between pH 12 and 13 of the aqueous solutions. This makes these p(AA_{100})_0.2 SAPs in their current form not suitable for the envisaged application. Interestingly, SAP B is a cross-linked poly(acrylate) which is used commercially for a plethora of applications including the targeted purpose, as reflected by its incorporation in mortar [24]. The difference with the synthesized SAP could perhaps be found in the type of cross-linker or the density of the network. SAP A on the other hand, is a copolymer of acrylamide and sodium acrylate which is prone to alkaline hydrolysis. This leads to the formation of additional acrylate moieties and greater swelling potential at increased pH. Interestingly, previous research performed on these commercial SAPs indicated they are not prone to degradation in cement filtrate [25].

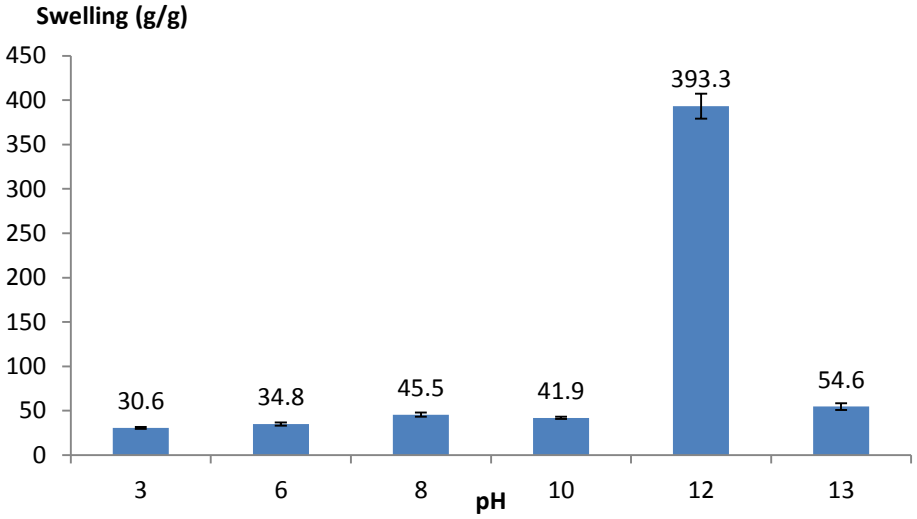

Figure III.4: Swelling capacity of p(AA_{100})_0.2 SAPs in aqueous solutions with varying pH.

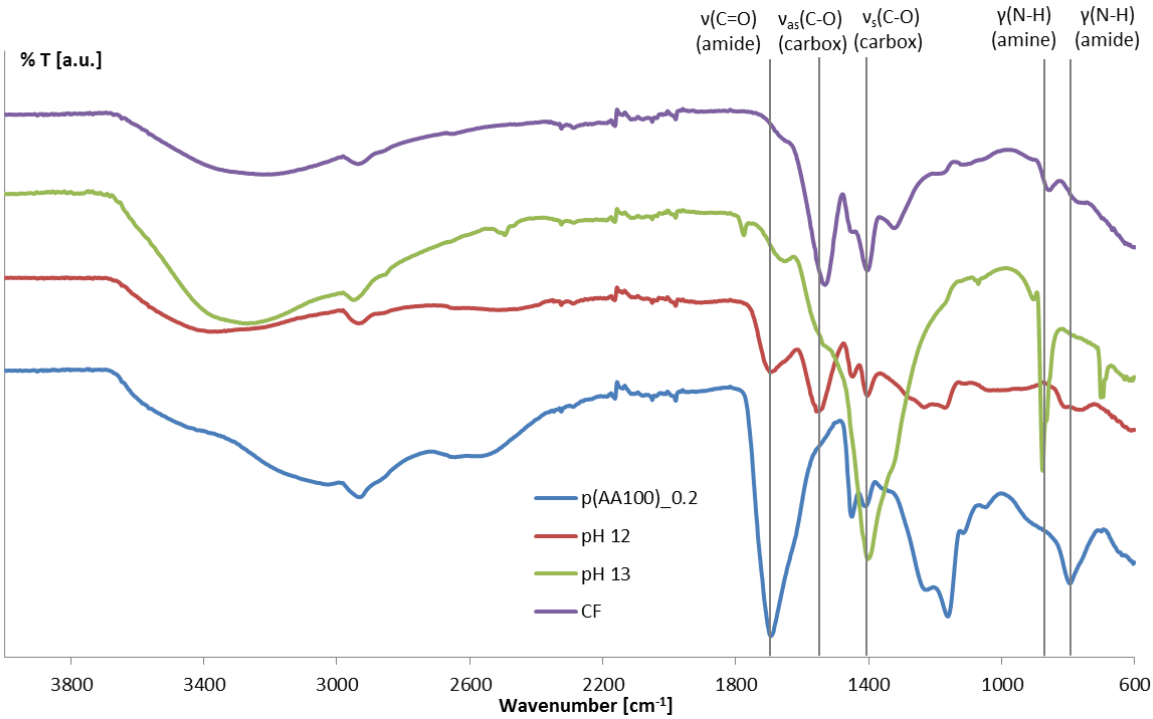

Figure III.5: ATR-IR spectra of p(AA_{100})_0.2 before and after incubation in aqueous solutions at pH 12, 13 and in cement filtrate solution.

Table III.1: Characteristic signals of p(AA_{100})_0.2 particles before and after swelling in aqueous and CF solutions at varying pH values.

Frequency	Assignment	p(AA_{100}) _0.2	pH 12.0	pH 13.0	CF (pH 12.6)
794 cm^{-1}	γ(N-H) amide (1°/2°)*	m, br	w	/	w
876 cm^{-1}	γ(N-H) amine (1°)	/	/	s, shp	w
1400-1410 cm^{-1}	ν_s(C-O) carboxylate	w	w	vs	m
1550 cm^{-1}	ν_{as}(C-O) carboxylate	sh	m	sh	s
1695 cm^{-1}	ν(C=O) amide (2°) + carboxylate	vs	m	/	/

w: weak, m: medium, s: strong, vs: very strong, sh: shoulder, shp: sharp, br: broad
* 1° and 2° represent primary and secondary amide respectively

III.1.5. Effect of the p(AA_{100})_0.2 SAPs on the mechanical strength of mortar samples

Next, the effect of the SAPs developed on the mechanical properties of mortar samples was assessed. To this end, mortar was made with and without p(AA_{100})_0.2 (0, 0.5 and 1m% SAPs relative to the added cement amount) and three-point bending and compressive strength tests were performed. As the SAPs absorb mixing water, there was a negative effect on the mortar workability. As a result, additional water was added (30 and 50 mL on top upon addition of 0.5 and 1 m% of SAP respectively) to compensate for the presence of the SAPs and to create mixtures exhibiting a similar workability (with a flow around 210 mm) as the reference material with a water-to-cement ratio of 0.50.

Interestingly, Figure III.6 indicates that there was no significant reduction ($p < 0.05$) on the bending strength when adding 0.5 m% SAP. There was, however, a small significant reduction (13%) when 1 m% SAP was added to the mortar. However, the compressive strength was significantly reduced for both 0.5 and 1 m% SAP (6 and 22% reduction, respectively) albeit very limited for addition of 0.5 m% SAP. This means that a higher addition led to a more severe decrease in strength, as expected. Nevertheless, adding 0.5 m% to mortar led to only a very small, but significant decrease in the compressive strength. The required amount of SAP for self-healing mortar or concrete (0.5 – 1 m%) is higher than what is used for mitigating autogenous shrinkage (0.3 m%). The effect of an increase in compressive strength by an increased degree of hydration cannot counterbalance the increased void volume and thus the reduced strength [30, 35, 36]. When comparing the obtained data with the results for mortars containing commercial SAPs [24], the results showed that mortar samples containing p(AA_{100})_0.2 were characterized by a similar bending strength behavior as with SAP A (0% and 14% reduction upon addition of 0.5 m% and 1 m% SAP A), but performed inferior compared to SAP B (no bending strength reduction upon addition of 1 m% of SAP B). For the compressive strength, p(AA_{100})_0.2 performed superior compared to SAP A (35% and 55% reduction upon addition of 0.5 m% and 1 m% SAP A) and SAP B upon addition of 0.5 m% (20% reduction). It performed similar compared to the addition of 1 m% SAP B (20% reduction). Overall, p(AA_{100})_0.2 showed a smaller reducing effect on the mortar strength than SAP A and had a similar effect as SAP B.

The stronger decrease in compressive strength compared to flexural strength is related to the irregularity of the shape of the SAP particles. As the SAPs and thus macro pores are irregular in shape, the compressive loads are not transferred by dome action, which would be the case for spherical SAPs. This causes the compressive strength to be lower for irregular shaped SAPs. This parameter is not of influence on the bending strength. For the bending strength, the total amount of air voids and macro pores in the cross-sectional area of the tensile plane is more important. This is why the bending strength is generally less influenced [25].

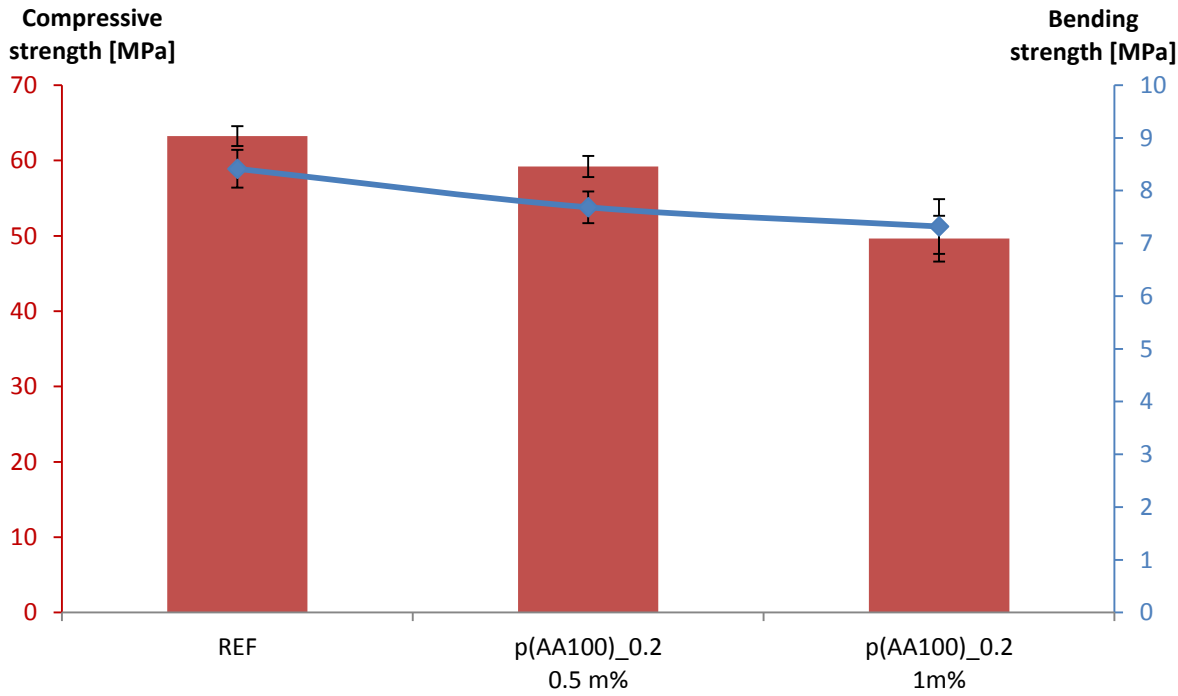

Figure III.6: Effect of p(AA_{100})_0.2 weight fraction on the bending and compressive strength of mortar.

III.1.6. Conclusion and future perspectives

Cross-linked poly(acrylic acid) has been synthesized successfully by combining acrylic acid and N,N'-methylene bisacrylamide as cross-linker in a free radical cross-linking reaction. A high gel fraction of 95% was obtained while infrared spectroscopy confirmed the chemical structure and the cross-linking efficiency was indicated by high resolution magic-angle spinning (HR-MAS) ^{1}H-NMR spectroscopy. Subsequently, the maximum moisture uptake capacity determined through dynamic vapor sorption measurements was 40% of the SAP's original weight at a relative humidity of 95%. Furthermore, hysteresis was negligible, which indicated that all moisture taken up at a high RH is released again at low RH rendering this SAP a moisture reservoir. The moisture uptake capacity was less than for commercial SAPs A and B (up to 125% their weight at 95% RH). The SAPs showed a swelling capacity up to 46 times their own weight at neutral pH. Increasing the pH to alkaline conditions resulted in a substantial increase of the water uptake up to 393 ± 14 g_{water}/g_{SAP}, followed by a distinct drop at pH 13. The latter was attributed to hydrolysis of the internal amide groups from the cross-linker which first resulted in a less dense cross-linked network and more swelling, followed by a disintegrated network of which only parts remained intact, as illustrated via infrared spectroscopy. Alkaline hydrolysis of amide moieties has already been reported earlier in literature [32]. The maximal swelling of p(AA100)_0.2 was substantially higher than the water uptake capacity of the commercially available SAPs (i.e. a swelling of 305 ± 4 g_{water}/g_{SAP} for SAP A and 283 ± 2 g_{water}/g_{SAP} for SAP B, respectively [24]).

As a final proof-of-concept, the SAPs were incorporated in mortar to assess their effect on the bending and compressive strength of the mortar samples. The results showed that the bending strength was affected significantly for addition of 1 m% SAP only (decrease limited to 13%),

while the compressive strength was not reduced upon addition of 0.5 m% SAP. However, the significant decrease of the compressive strength (with 22%) associated with the addition of 1 m% SAP while maintaining workability with additional water, indicated that there was a significant compressive strength reduction upon adding 1 m%. The synthesized p(AA_{100})_0.2 outperformed commercial SAP A (compressive strength reduction of 55% upon addition of 1 m% SAP) and SAP B for an addition of 0.5 m% and showed a similar mortar strength reduction compared to when 1 m% SAP B was added (20% reduction). Given its low swelling capacity at neutral pH, a high amount of SAP (≥ 1 m%) would probably be required to result in self-sealing. As a result, no further tests were performed using these SAPs, despite the promising compressive strength results upon addition of 0.5 m%. To conclude, p(AA_{100})_0.2 can thus be considered as an initial reference material to be further improved for self-healing purposes.

However, a few problems still need to be tackled in the upcoming sections. More specifically, a low swelling capacity was observed at neutral pH, for which a high swelling is needed to enable self-sealing of cracks. In addition, the material started to degrade in alkaline conditions and finally, there was a significant effect on the mortar strength due to an increased macro-pore formation, which should be minimized by decreasing the swelling at a high pH. In the second part of this chapter, acrylamide (AM) has been introduced to create a copolymer of AA and AM. Incorporating AM is anticipated to increase the swelling capacity, as it is also a hydrophilic monomer which will not become charged within the explored pH-range. As such, the swelling of the SAP is less affected by the presence of cations (cfr. addition of NaOH to result in an alkaline pH in aqueous solutions or the presence of multivalent cations in CF solution) which in the case of AA leads to additional physical cross-linking [37-39]. In a third part, a different approach has been elaborated and a basic monomer has been combined with MBA (i.e. dimethylaminoethyl methacrylate, DMAEMA). This material swells less in alkaline conditions and more upon decreasing the pH, which could assist in obtaining increased swelling and therefore improved self-sealing properties.

III.1.7. References

[1] Mohammad J. Zohuriaan-Mehr KK. Superabsorbent Polymer Materials: A Review. Iranian Polymer Journal. 2008;17((6)):451-77.
[2] Abdelaal MY, Makki MSI, Sobahi TRA. Modification and characterization of polyacrylic acid for metal ion recovery. American Journal of Polymer Science. 2012;2(4):73-8.
[3] Liu A, Honma I, Zhou H. Simultaneous voltammetric detection of dopamine and uric acid at their physiological level in the presence of ascorbic acid using poly(acrylic acid)-multiwalled carbon-nanotube composite-covered glassy-carbon electrode. Biosensors and Bioelectronics. 2007;23(1):74-80.
[4] Liu A, Watanabe T, Honma I, Wang J, Zhou H. Effect of solution pH and ionic strength on the stability of poly(acrylic acid)-encapsulated multiwalled carbon nanotubes aqueous dispersion and its application for NADH sensor. Biosensors and Bioelectronics. 2006;22(5):694-9.
[5] Bukhari SMH, Khan S, Rehanullah M, Ranjha NM. Synthesis and characterization of chemically cross-linked acrylic acid/gelatin hydrogels: effect of pH and composition on swelling and drug release. International Journal of Polymer Science. 2015.
[6] Liang R, Yuan H, Xi G, Zhou Q. Synthesis of wheat straw-g-poly (acrylic acid) superabsorbent composites and release of urea from it. Carbohydrate Polymers. 2009;77(2):181-7.
[7] Yin L, Fei L, Cui F, Tang C, Yin C. Superporous hydrogels containing poly(acrylic acid-co-acrylamide)/O-carboxymethyl chitosan interpenetrating polymer networks. Biomaterials. 2007;28(6):1258-66.
[8] Pourjavadi A, Barzegar S, Zeidabadi F. Synthesis and properties of biodegradable hydrogels of κ-carrageenan grafted acrylic acid-co-2-acrylamido-2-methylpropanesulfonic acid as candidates for drug delivery systems. Reactive and Functional Polymers. 2007;67(7):644-54.
[9] Sadeghi M, Hosseinzadeh H. Synthesis of Starch—Poly(Sodium Acrylate-co-Acrylamide) Superabsorbent Hydrogel with Salt and pH-Responsiveness Properties as a Drug Delivery System. Journal of Bioactive and Compatible Polymers. 2008;23(4):381-404.
[10] Katono H, Maruyama A, Sanui K, Ogata N, Okano T, Sakurai Y. Thermo-responsive swelling and drug release switching of interpenetrating polymer networks composed of poly (acrylamide-co-butyl methacrylate) and poly (acrylic acid). Journal of Controlled Release. 1991;16(1):215-27.
[11] Singh T, Singhal R. Poly (acrylic acid/acrylamide/sodium humate) superabsorbent hydrogels for metal ion/dye adsorption: Effect of sodium humate concentration. Journal of Applied Polymer Science. 2012;125(2):1267-83.
[12] Gupta VK, Agarwal S, Singh P, Pathania D. Acrylic acid grafted cellulosic Luffa cylindrical fiber for the removal of dye and metal ions. Carbohydrate Polymers. 2013;98(1):1214-21.
[13] Blanchard E, Gautreaux G, Harper R, Lofton J. Cross dyeing fiber blends of polyurethane, polyacrylate or butadiene-acrylonitrile copolymer coated cotton fibers with disperse and reactive dyes. Google Patents; 1974.
[14] Varennes Ad, Queda C. Application of an insoluble polyacrylate polymer to copper-contaminated soil enhances plant growth and soil quality. Soil Use and Management. 2005;21(4):410-4.
[15] Wenhua Z, Pute W, Hao F, Fuli X, Baifeng L, Rongchang N. Effects of super absorbent polyer of sodium polyacrylate usedin soil on the growth and yield of winter wheat. Transactions of the Chinese Society of Agricultural Engineering. 2008;2008(5).
[16] Guiwei Q. Study on Remediation Effect of Ammonium Polyacrylate on Soil Polluted by Exogenous Compound Heavy Metals. Journal of Anhui Agricultural Sciences. 2007;35(20):6211.
[17] Schröfl C, Mechtcherine V, Gorges M. Relation between the molecular structure and the efficiency of superabsorbent polymers (SAP) as concrete admixture to mitigate autogenous shrinkage. Cement and Concrete Research. 2012;42(6):865-73.
[18] Mechtcherine V, Reinhardt H-W. Application of super absorbent polymers (SAP) in concrete construction: state-of-the-art report prepared by Technical Committee 225-SAP: Springer Science & Business Media; 2012.

[19] Chen D-p, Qian C-x, Gao G-b, Zhao H-k. Mechanism and effect of SAP for reducing shrinkage and cracking of concrete. Journal of Functional Materials. 2007;38(3):475.
[20] Jensen OM, Hansen PF. Water-entrained cement-based materials: II. Experimental observations. Cement and Concrete Research. 2002;32(6):973-8.
[21] Ahmed EM. Hydrogel: Preparation, characterization, and applications: A review. Journal of advanced research. 2015;6(2):105-21.
[22] Janković B, Adnađević B, Jovanović J. Application of model-fitting and model-free kinetics to the study of non-isothermal dehydration of equilibrium swollen poly (acrylic acid) hydrogel: Thermogravimetric analysis. Thermochimica Acta. 2007;452(2):106-15.
[23] Don T-M, Huang M-L, Chiu A-C, Kuo K-H, Chiu W-Y, Chiu L-H. Preparation of thermo-responsive acrylic hydrogels useful for the application in transdermal drug delivery systems. Materials Chemistry and Physics. 2008;107(2–3):266-73.
[24] Snoeck D, Dubruel P, De Belie N. How to seal and heal cracks in cementitious materials by using superabsorbent polymers. Application of Superabsorbent Polymers and Other New Admixtures in Concrete Construction: RILEM Publications; 2014. p. 375-84.
[25] Snoeck D. Self-healing and microstructure of cementitious materials with microfibres and superabsorbent polymers. PhD thesis: Ghent University; 2015.
[26] Raina J-B, Tapiolas D, Willis BL, Bourne DG. Coral-associated bacteria and their role in the biogeochemical cycling of sulfur. Applied and environmental microbiology. 2009;75(11):3492-501.
[27] Michaels AS, Morelos O. Polyelectrolyte Adsorption by Kaolinite. Industrial & Engineering Chemistry. 1955;47(9):1801-9.
[28] Bromberg L, Temchenko M, Hatton TA. Dually Responsive Microgels from Polyether-Modified Poly(acrylic acid): Swelling and Drug Loading. Langmuir. 2002;18(12):4944-52.
[29] Kabiri K, Omidian H, Hashemi SA, Zohuriaan-Mehr MJ. Synthesis of fast-swelling superabsorbent hydrogels: effect of crosslinker type and concentration on porosity and absorption rate. European Polymer Journal. 2003;39(7):1341-8.
[30] Snoeck D, Schaubroeck D, Dubruel P, De Belie N. Effect of high amounts of superabsorbent polymers and additional water on the workability, microstructure and strength of mortars with a water-to-cement ratio of 0.50. Construction and Building Materials. 2014;72(0):148-57.
[31] Hancock RD, Martell AE. Ligand design for selective complexation of metal ions in aqueous solution. Chemical Reviews. 1989;89(8):1875-914.
[32] Athawale VD, Lele V. Factors influencing absorbent properties of saponified starch-g-(acrylic acid-co-acrylamide). Journal of Applied Polymer Science. 2000;77(11):2480-5.
[33] Schulz H, Baranska M, Quilitzsch R, Schütze W. Determination of alkaloids in capsules, milk and ethanolic extracts of poppy (Papaver somniferum L.) by ATR-FT-IR and FT-Raman spectroscopy. Analyst. 2004;129(10):917-20.
[34] Huber W, Bubendorf A, Grieder A, Obrecht D. Monitoring solid phase synthesis by infrared spectroscopic techniques. Analytica Chimica Acta. 1999;393(1):213-21.
[35] Hasholt MT, Jensen OM, Kovler K, Zhutovsky S. Can superabsorbent polymers mitigate autogenous shrinkage of internally cured concrete without compromising the strength? Construction and Building Materials. 2012;31:226-30.
[36] Hasholt MT, Jespersen MHS, Jensen OM. Mechanical properties of concrete with SAP. Part I: Development of compressive strength. Use of Superabsorbent Polymers and Other New Additives in Concrete. 2010.
[37] Pourjavadi A, Jahromi PE, Seidi F, Salimi H. Synthesis and swelling behavior of acrylatedstarch-g-poly (acrylic acid) and acrylatedstarch-g-poly (acrylamide) hydrogels. Carbohydrate Polymers. 2010;79(4):933-40.
[38] Tomar RS, Gupta I, Singhal R, Nagpal AK. Synthesis of poly (acrylamide-co-acrylic acid) based superabsorbent hydrogels: Study of network parameters and swelling behaviour. Polymer-Plastics Technology and Engineering. 2007;46(5):481-8.
[39] Rabat NE, Hashim S, Majid RA. Effect of Different Monomers on Water Retention Properties of Slow Release Fertilizer Hydrogel. Procedia Engineering. 2016;148:201-7.

III.2 Introducing acrylamide to create poly(acrylic acid-co-acrylamide) copolymer networks

Next to acrylic acid and its salts, acrylamide is also often used as starting monomer for superabsorbent polymers. It has been proven extensively that the incorporation of acrylamide (AM) forms strong gels with substantial swelling potential [1-4]. Additionally, AM is a hydrophilic monomer, which is not charged within the pH-range of interest. Acrylic acid (AA), on the other hand, becomes charged at pH values exceeding its pKa (pH > 4.25). These charges attract cations in the swelling media due to the addition of NaOH for alkaline aqueous solutions and the presence of mono- and multivalent cations in cement filtrate solution. This leads to a decreased swelling due to a screening effect of the counter ion on the poly-anion chain [5]. In case of multivalent cations, a physical cross-linking in addition to covalent cross-linking is thereby introduced. The presence of AM could potentially solve the limited swelling and moisture uptake capacity associated with the previously described poly(acrylic acid) gel [6-8]. Acrylamide has been often described in literature in combination with many different materials. Acrylamide – sodium methacrylate copolymers have been characterized in detail [9]. They showed that an increase of the ionic concentration of a salt solution led to a decreased swelling due to a shielding effect of the ions of sodium methacrylate by counter ions. Another study showed the potential of a graft copolymerization of cottonseed protein with acrylic acid and acrylamide [10]. The resulting superabsorbent polymer could reach swelling equilibrium in minutes and exhibited swelling capacity (up to 376 g/g). Furthermore, acrylamide/2-acrylamido-2-methylpropane sulfonic acid and associated sodium salt superabsorbent copolymer nanocomposites have already been used as fire retardants [11].

The present part of this chapter reports on the development and the characterization of a cross-linked copolymer network consisting of among others acrylic acid and acrylamide, cross-linked by using a synthetic bifunctional cross-linker (N,N'-methylene bisacrylamide (MBA)) in various concentrations. The chemical structure and cross-linking efficiency of the synthesized SAPs has been verified through attenuated total reflectance-infrared (ATR-IR) spectroscopy and high resolution magic-angle spinning (HR-MAS) ^{1}H-NMR spectroscopy respectively. In addition, the sorption and desorption of moisture at different relative humidities has been determined by dynamic vapor sorption (DVS) measurements. The swelling capacity of the SAPs has been analyzed over the entire pH-range in order to gain insight in the SAP swelling behavior as a function of pH. Based on these results, the two best performing SAPs have been selected for further characterization. First, the two selected SAPs have been characterized by comparing their swelling capacity at varying pH-values in aqueous solutions and (acidified) cement filtrate. In a second part, the mechanical properties of mortar mixtures in the absence and presence of SAPs have been compared by performing flexural and compressive strength tests. The sealing

This work has been published as: Mignon Arn, Graulus Geert-Jan, Snoeck Didier, Martins José, Dubruel Peter, De Belie Nele, Van Vlierberghe Sandra (2015). pH-sensitive superabsorbent polymers : a potential candidate material for self-healing concrete. Journal of materials science, 50(2):970-979.
Mignon Arn, Snoeck Didier, Schaubroeck David, Luickx Nathalie, Dubruel Peter, Van Vlierberghe Sandra and De Belie Nele (2015). pH-responsive superabsorbent polymers: A pathway to self-healing of mortar. Reactive and Functional Polymers, 93, 68-76.

efficiency and the potential for self-healing has been subsequently measured through a water permeability set-up. Potentially formed healing products have been identified thoroughly by scanning electron microscopy energy-dispersive spectroscopy (SEM-EDS), ATR-IR spectroscopy and thermogravimetric analysis (TGA).

III.2.1. Development of synthetic p(AA/AM) SAPs

Starting from acrylic acid (AA) and acrylamide (AM) in combination with the cross-linker N,N'-methylene bisacrylamide (MBA), a free radical precipitation polymerization was performed to develop pH-responsive superabsorbent copolymer networks. As the materials are intended for concrete applications, the effect of the polymer network composition on the swelling capacity was examined. Table III.2 gives an overview of the chemical composition of the different SAPs obtained.

Table III.2: Overview of theoretical chemical composition and gel fraction of the developed SAPs. The molar cross-linker fraction was added with respect to the total monomer amount.

Sample	AA mol%	AA mol%	AM mol%	Gel fraction (%)
$p(AA_{75}/AM_{25})\_0.2_{a,b,c}$	75	25	0.2	87 ± 2
$p(AA_{75}/AM_{25})\_2_{b,c}$	75	25	2	91 ± 3
$p(AA_{75}/AM_{25})\_10_{a,b}$	75	25	10	80 ± 4
$p(AA_{50}/AM_{50})\_0.2_{c}$	50	50	0.2	89 ± 2
$p(AA_{50}/AM_{50})\_2_{b,c}$	50	50	2	92 ± 2
$p(AA_{50}/AM_{50})\_10_{c}$	50	50	10	93 ± 1
$p(AA_{25}/AM_{75})\_0.2_{a}$	25	75	0.2	75 ± 10

The gel fraction was determined for all SAPs developed as indicated in Table III.2. The results illustrated that for all samples, relatively high gel fractions were obtained ranging from 74 to 95%. The effect of two parameters was described: the co-monomer ratio and the cross-linker amount. The results indicated that varying the cross-linker fraction did not affect the gel fraction to a significant extent. However, when comparing the gel fractions of the samples with varying co-monomer ratios, a significant difference could be observed ($p < 0.05$). The correlation, as calculated with the univariate ANOVA test, between the monomer ratio and cross-linker amount was not significant. The Tukey post-hoc test showed that samples $p(AA_{75}/AM_{25})\_0.2$, $p(AA_{75}/AM_{25})\_2$, $p(AA_{75}/AM_{25})\_10$ and $p(AA_{50}/AM_{50})\_0.2$, $p(AA_{50}/AM_{50})\_2$, $p(AA_{50}/AM_{50})\_10$

could be seen as one subset, and p(AA_{25}/AM_{75})_0.2 as a different. P(AA_{75}/AM_{25})_10 was significantly different from p(AA_{50}/AM_{50})_0.2 and p(AA_{50}/AM_{50})_10. Moreover, p(AA_{25}/AM_{75})_0.2 also differed significantly from p(AA_{50}/AM_{50})_0.2,_2,_10 and p(AA_{75}/AM_{25})_ 2. The SAPs could be grouped by the use of this Tukey post-hoc test (see Table III.2, subscript indicating groups of no significant difference).

III.2.2. Chemical structure elucidation and assessment of the cross-linking efficiency

ATR-IR spectroscopy results of the SAPs starting formulation (Figure III.7) revealed that a higher molar fraction of acrylic acid present in the starting formulation (Figure III.7a) resulted in a broader O-H stretch between 3400 cm^{-1} and 2400 cm^{-1}. This could be attributed to hydrogen-bond formation of acid moieties. In addition, as anticipated, the N-H stretch deduplication (at 3170 cm^{-1} and 3340 cm^{-1} corresponding to the primary amide) became more distinguishable with an increase of the molar fraction of acrylamide. The peak at 1650 cm^{-1} could be attributed to the C=O stretch while symmetric and asymmetric stretching of COO^- corresponded with the signals at 1420 cm^{-1} and 1590 cm^{-1}, respectively. The peak at 1296 cm^{-1} present in the fingerprint area could be attributed to the C-O stretch. After polymerization, an additional peak at 2930 cm^{-1} was observed (see Figure III.7b) which could be assigned to the C-H stretching of CH_2 groups arising from the polymerization reaction. ATR-IR spectroscopy thus indicated the successful conversion of the carbon-carbon double bonds from the starting monomers into CH_2 single bonds. The results obtained are in good agreement with previous literature reports [12-14].

In order to assess the polymerization efficiency, HR-MAS ^{1}H-NMR spectroscopy was applied. The signals appearing between 5.4 and 6.4 ppm (Figure III.8) were related to the H-atoms of the C=C double bonds and corresponded to the monomers and the cross-linker prior to polymerization. Typically, an additional peak was anticipated at 4.65 ppm, related to the H-atoms corresponding to the methylene part of the cross-linker. However, as this signal is typically apparent in the vicinity of the water peak, which is suppressed during the measurement, the signal was not visible (Figure III.8). The H-peaks corresponding to the C-C single bonds were located between 1.5 and 2.5 ppm. Interestingly, upon comparing HR-MAS ^{1}H-NMR spectra of a blend of the starting compounds with the SAPs obtained after polymerization and purification (Figure III.8 illustrates as an example p(AA_{75}/AM_{25})_0.2), the peaks between 5.5 and 6.4 ppm did completely disappear. Together with the broad peaks that appeared in the 1.5 - 2.5 ppm area, these findings indicated that the combination of the polymerization and a subsequent purification was successful. Interestingly, as the methylene peak from the cross-linker had shifted from 4.65 ppm to 5.1 ppm due to the network formation, the signal could be distinguished after network formation.

HR-MAS ^{1}H-NMR spectroscopy could thus be considered as a complementary tool for gel fraction experiments to study the success of SAP development.

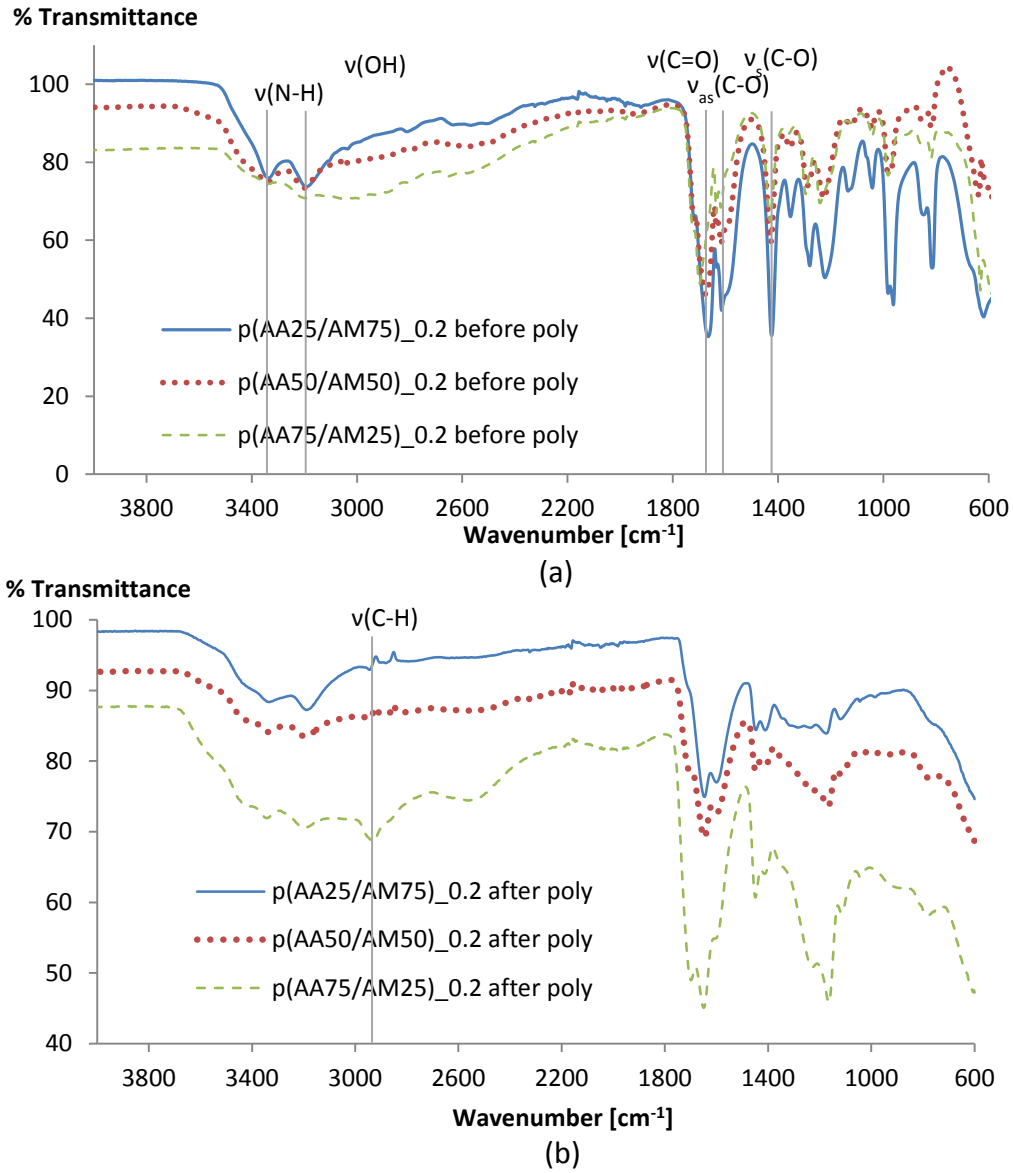

Figure III.7: Comparison of ATR-IR spectra with varying monomer ratio: a) before polymerization, b) after polymerization.

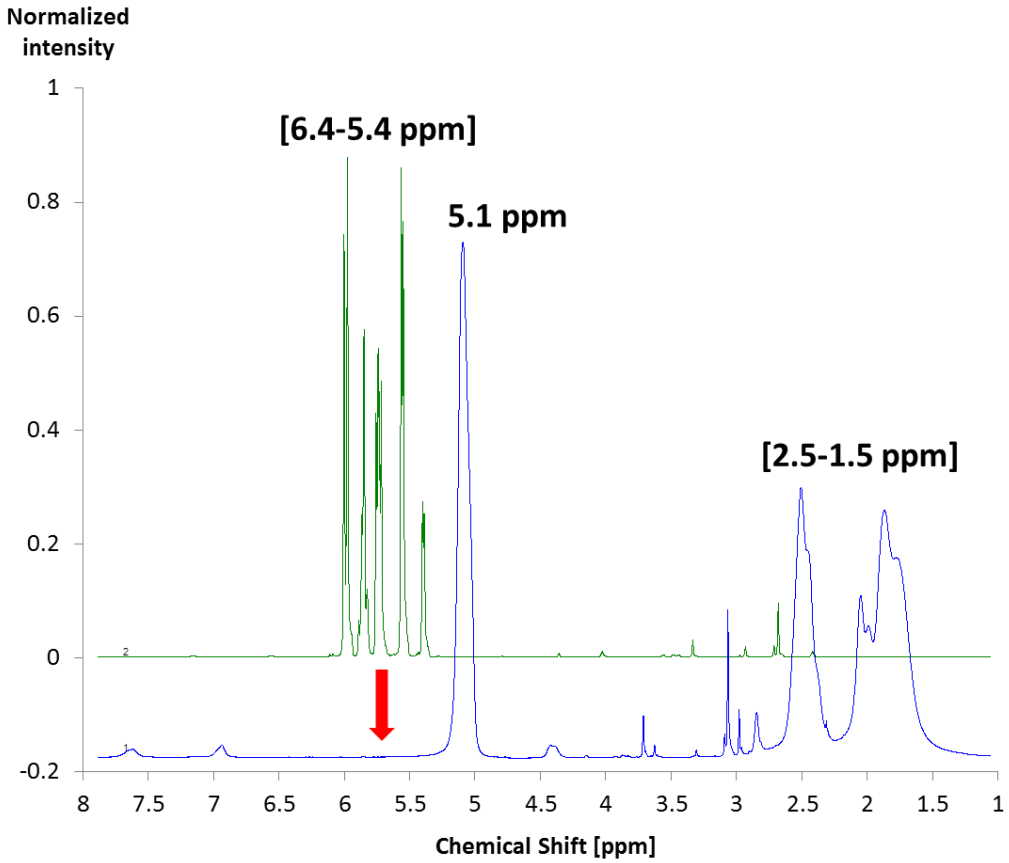

Figure III.8: HR-MAS ^{1}H-NMR spectra of p(AA_{75}/AM_{25})_0.2 prior to (upper curve) and after polymerization (lower curve). The arrow indicates the disappearance of the peaks characteristic for the H-atoms of the C=C double bonds.

III.2.3. Moisture uptake capacity measurements

First, two SAPs with varying monomer molar fractions in the presence of a constant cross-linker amount (p(AA_{50}/AM_{50})_0.2 versus p(AA_{75}/AM_{25})_0.2, see Table III.2) were evaluated and compared. The results (shown in Figure III.9) indicated that both materials took up up to 30% their own weight at a RH of 95%. For the selected two materials, an additional step at 98% RH was measured. It was found that now over 90% of their own weight was taken up. However, it could be questioned if measurements at such high RH are useful as this comes very close to full submersion in aqueous solutions which is determined by swelling capacity measurements in §III.2.4. This implied that in environments showing high humidity (up to 95%), the developed SAPs could only partially serve as a moisture reservoir. Interestingly, the level of hysteresis was negligible (i.e. up to 7% at 90% RH) implying that all moisture initially absorbed by the material again desorbs completely. Interestingly, the results showed that varying the co-monomer molar ratios did not influence the moisture uptake capacity. This parameter, however, had a large influence on the swelling capacity in aqueous environments as discussed further. The results indicated that the moisture uptake capacity was limited and insufficient to enable significant self-sealing of cracks.

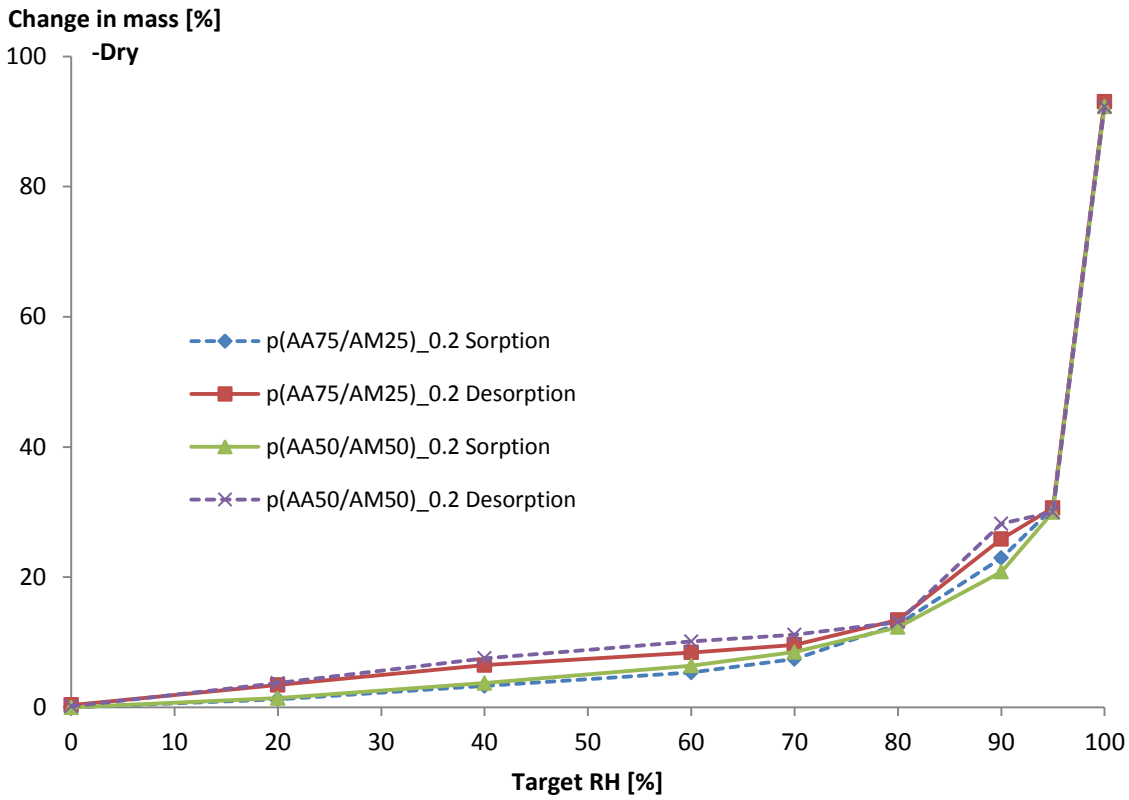

Figure III.9: Sorption and desorption isotherms of p(AA_{75}/AM_{25})_0.2 and p(AA_{50}/AM_{50})_0.2 measured by means of dynamic vapor sorption.

Table III.3 shows a comparison of the moisture uptake capacity at different RHs upon varying the molar fraction of the cross-linker (i.e. p(AA_{50}/AM_{50})_0.2, p(AA_{50}/AM_{50})_2 and p(AA_{50}/AM_{50})_10 presented in Table III.2). The results indicated that the difference in moisture uptake capacity between p(AA_{50}/AM_{50})_0.2 and p(AA_{50}/AM_{50})_2 was negligible. The moisture uptake capacity of p(AA_{50}/AM_{50})_10, however, was slightly higher compared to the materials cross-linked to a lower extent. In order to further elucidate the latter phenomenon, the material morphology was characterized and compared using optical microscopy (see Figure III.10).

Both p(AA_{50}/AM_{50})_0.2 as well as p(AA_{50}/AM_{50})_2 showed similar size distributions. The more cross-linked sample (i.e. p(AA_{50}/AM_{50})_10)), however, was characterized by smaller particle sizes and a limited amount of clusters resulting in a larger surface area and thus a superior ability to absorb moisture (Figure III.10c and III.10d). Over 95% of the obtained particle sizes ranged from 3 to 134 µm, 1 to 101 µm and 3 to 74 µm for p(AA_{50}/AM_{50})_0.2, p(AA_{50}/AM_{50})_2 and p(AA_{50}/AM_{50})_10, respectively.

Table III.3: Effect of cross-linker concentration on SAP water sorption behavior. '_X' represents the cross-linker concentration, expressed as molar fraction relative to the total amount of monomers.

Moisture uptake [%]	p(AA_{50}/AM_{50})_0.2	p(AA_{50}/AM_{50})_2	p(AA_{50}/AM_{50})_10
0% RH	0	0	0
20% RH	1.43	1.88	3.45
40% RH	3.73	4.35	6.04
60% RH	6.40	7.09	9.13
70% RH	8.50	9.19	11.39
80% RH	12.31	13.43	14.59
90% RH	20.82	19.80	19.02

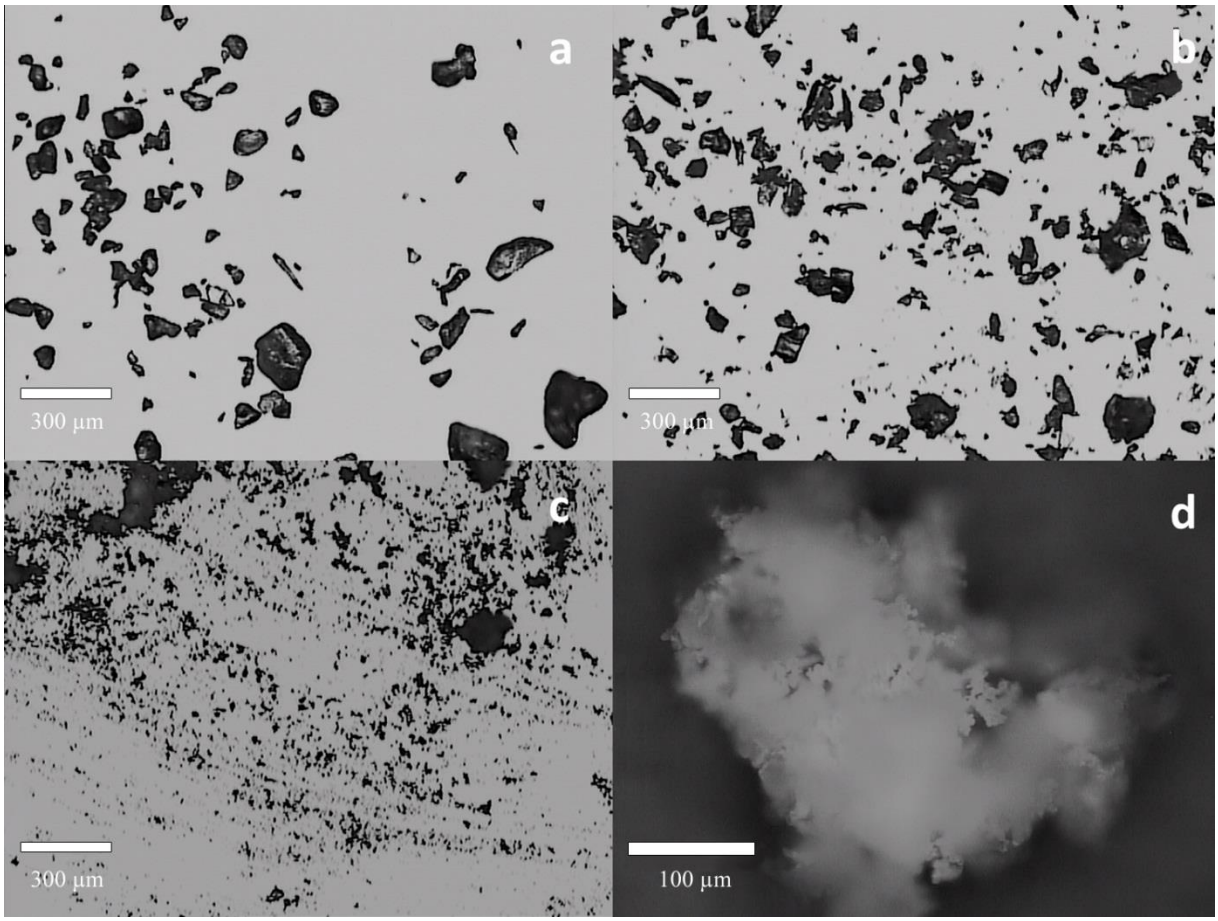

Figure III.10: Optical microscopy images of a) p(AA_{50}/AM_{50})_0.2, b) p(AA_{50}/AM_{50})_2, c) p(AA_{50}/AM_{50})_10 and d) a zoom of clustered powder of p(AA_{50}/AM_{50})_10.

III.2.4. Swelling capacity measurements

Swelling tests in aqueous solutions

First, the effect of the cross-linker fraction present (0.2, 2 and 10 mol% MBA relative to the total amount of added monomers, see Figure III.12a) on the swelling capacity was evaluated (schematic representation of the swelling of the SAP presented in Figure III.11). As anticipated, the lowest concentration of MBA resulted in the highest swelling capacity (i.e. 433.7 ± 15.1 g_{water}/g_{SAP} at pH 12). The materials containing 2 and 10 mol% MBA showed maximum swelling capacities at pH 12 of 56.3 ± 3.4 g_{water}/g_{SAP} and 17.9 ± 3.3 g_{water}/g_{SAP} respectively. Due to these low swelling capacities, the different pH-responsive swelling steps (which could be distinguished in the presence of 0.2 mol% MBA) could not be observed in the presence of 10 mol% MBA and became slightly apparent when 2 mol% MBA was applied. The results indicated that a cross-linker fraction of 10 mol% did not lead to materials showing superabsorbent behavior.

For $p(AA_{75}/AM_{25})\_0.2$, multiple regions could be distinguished. Between pH 3 and 5, the swelling increased from 16.5 ± 0.1 to 60.6 ± 4.7 g_{water}/g_{SAP}. The latter could be explained considering the pK_a of acrylic acid (i.e. 4.25) [15], which resulted in carboxylic acid moieties starting to deprotonate (cfr. conversion of -COOH into $-COO^-$) in the above-mentioned pH-range. Due to the presence of repelling negative charges, the polymer network volume increased, creating the possibility to absorb more water. Figure III.11a gives an overview of the chemical composition of the SAPs, while Figure III.11b schematically represents the effect of the deprotonated acid moieties. At pH 5, most of the carboxylic acids were deprotonated and no significant swelling capacity changes could be detected upon further increasing the pH to 9. From that point onwards, the swelling capacity increased again, yet extremely, up to a pH of 12 (cfr. maximal swelling of 433.7 ± 15.1 g_{water}/g_{SAP}). Finally, a distinct drop in the swelling capacity (i.e. from 433.7 ± 15.1 to 84.3 ± 11.2 g_{water}/g_{SAP}) was observed when increasing the pH from 12 to 13. The effects at high pH-values (pH 9 and higher) could be ascribed to the hydrolysis of amide groups [16-19]. This results in two counterbalancing effects. First, the amide groups started to hydrolyze forming carboxylic acids which were negatively charged in the above-mentioned pH range (i.e. pH 9 to 12). Consequently, the formed carboxylates repelled one another which resulted in an additional swelling effect. However, as the cross-linker also contains two amide moieties, the network junction knots also started to hydrolyze which initially resulted in a swelling increase but from a critical point onwards (i.e. above pH 12) in a drastic swelling decrease because of degradation to such an extent that the network integrity is lost as schematically illustrated in Figure III.13. This effect is explained in greater depth with ATR-IR spectroscopy when comparing the obtained results with the swelling capacity measurements in CF solutions.

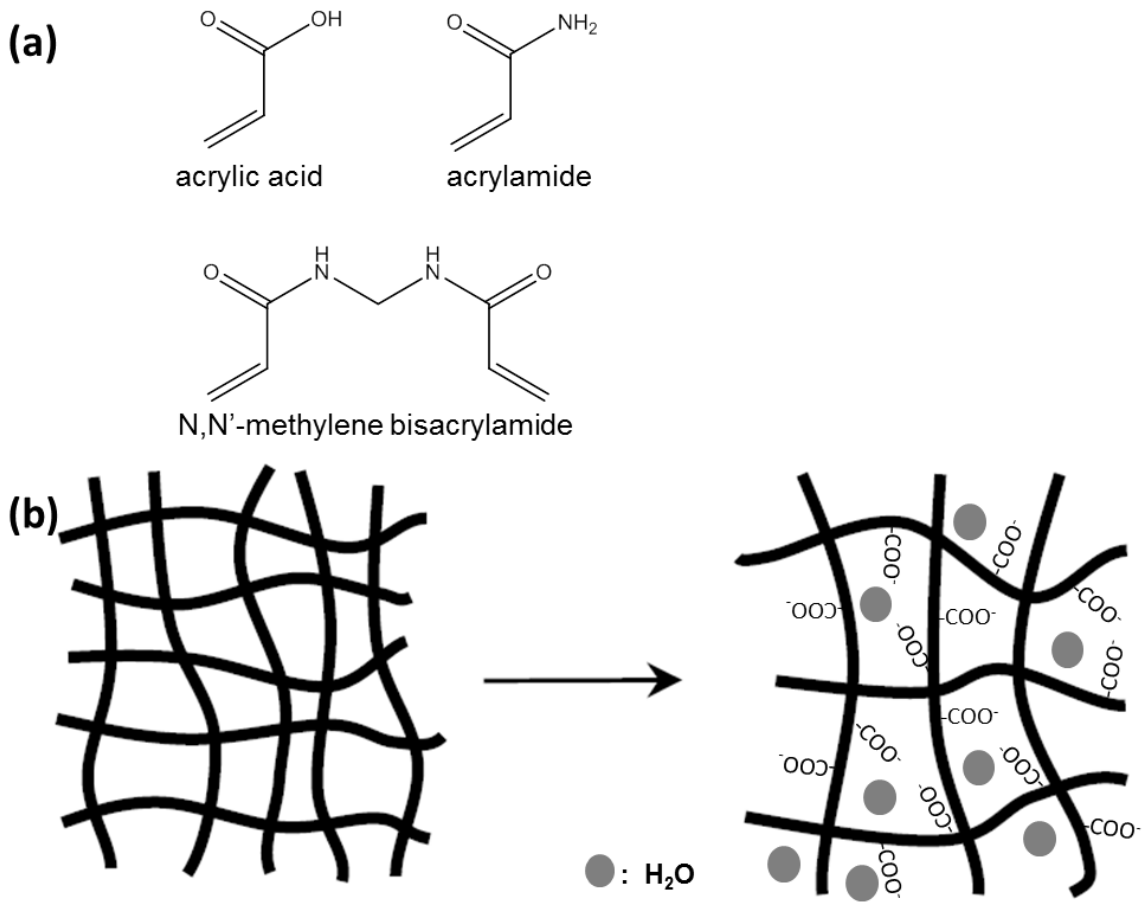

Figure III.11: (a) Chemical structures showing the starting compounds, (b) Schematic representation of the SAP swelling due to the presence of repellant negatively charged carboxylate moieties.

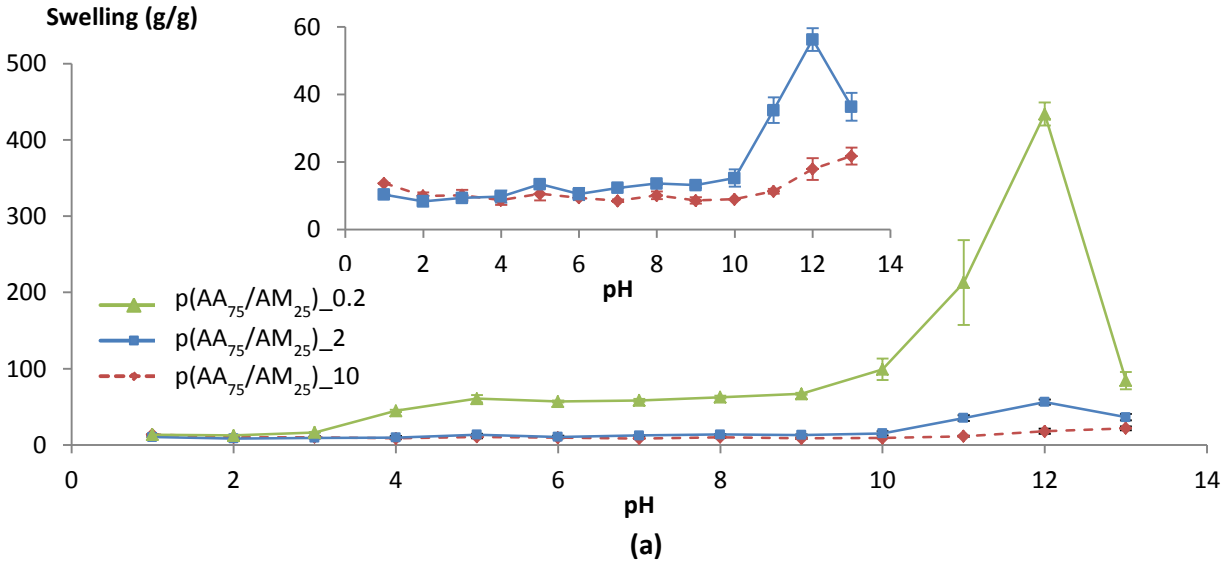

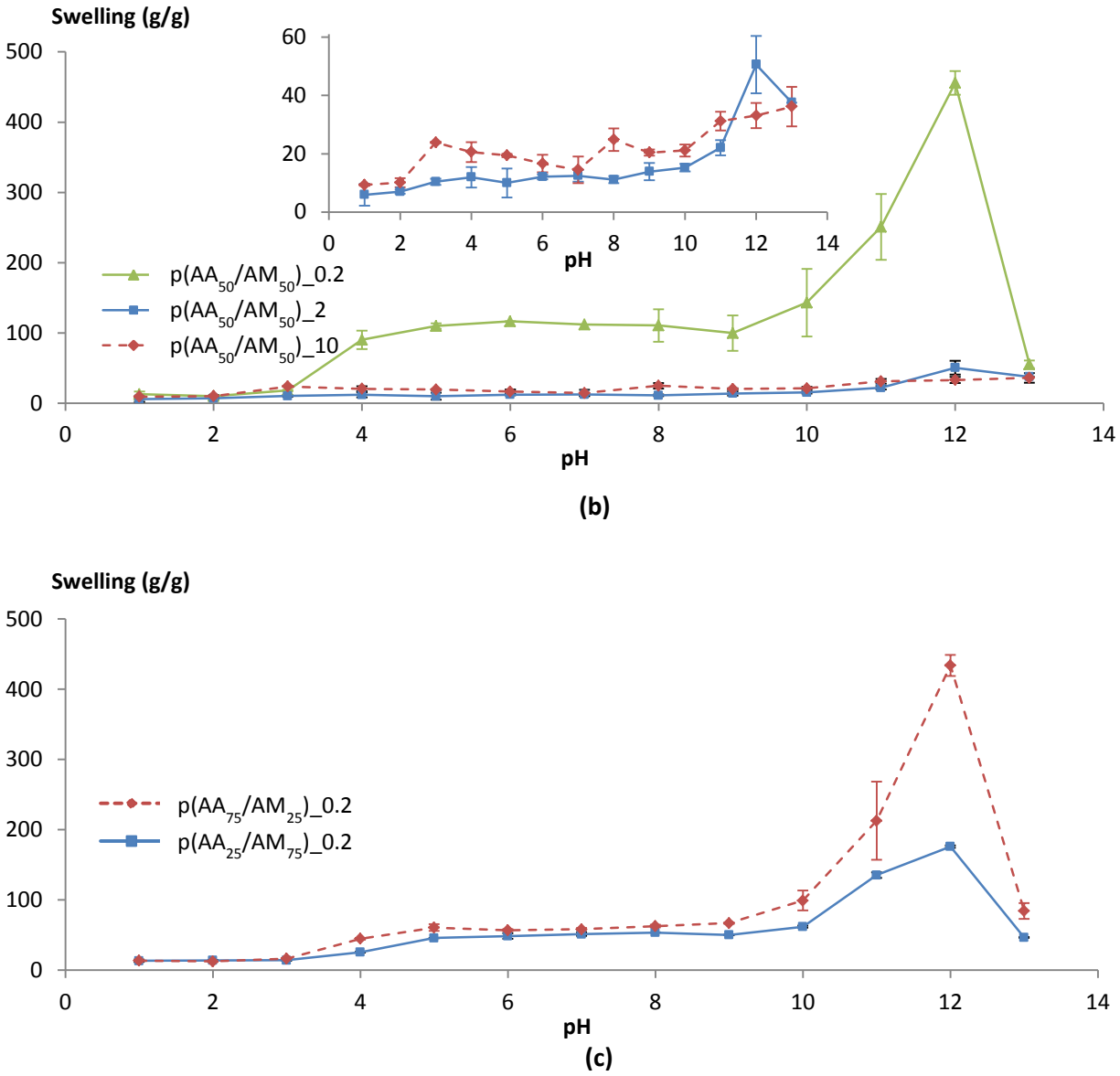

Figure III.12: Swelling capacity curves of a) 75/25 samples series with 0.2, 2 and 10 mol% MBA, b) 50/50 samples series with 0.2, 2 and 10 mol% MBA, c) $p(AA_{75}/AM_{25})\_0.2$ versus $p(AA_{25}/AM_{75})\_0.2$.

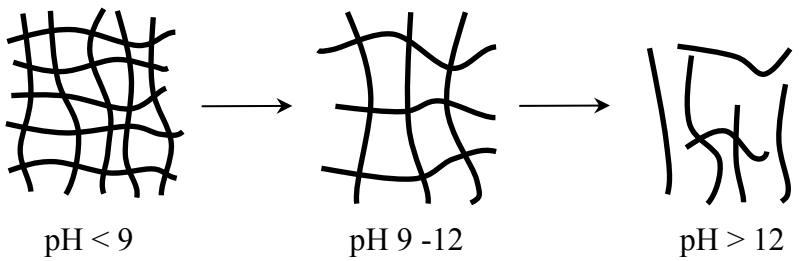

Figure III.13: Rupture of the polymer network at high alkaline conditions due to hydrolysis.

A similar analysis could be made when considering the molar ratio of 50 mol% acrylic acid and 50 mol% acrylamide (see Figure III.12b). The lowest cross-linker fraction (i.e. 0.2 mol% MBA) resulted, as anticipated, in the highest swelling capacity. The swelling potential of $p(AA_{50}/AM_{50})\_10$ and $p(AA_{50}/AM_{50})\_2$ were similar throughout the entire pH-range evaluated. As shown in Figure III.10, the $p(AA_{50}/AM_{50})\_10$ particles were characterized by smaller dimensions than $p(AA_{50}/AM_{50})\_0.2$ and $p(AA_{50}/AM_{50})\_2$. Smaller particles lead to a higher active surface and more possibility for swelling. As such, for equal particle sizes, $p(AA_{50}/AM_{50})\_10$ would have given rise to even lower swelling potential. Similar trends could be observed for $p(AA_{50}/AM_{50})\_0.2$. Around pH 4 and 9, an increase occurred in swelling capacity while a distinct decrease in swelling again was observed above pH 12. Figure III.12c illustrates the effect of varying monomer fractions keeping the cross-linking density constant.

Swelling tests in cement filtrate solutions

As the previous results indicated that a higher percentage of MBA led to polymers lacking superabsorbent properties, for swelling experiments in (acidified) cement filtrate only $p(AA_{50}/AM_{50})\_0.2$ and $p(AA_{75}/AM_{25})\_0.2$ were tested.

Considering the targeted application, swelling tests were performed in (acidified) cement filtrate (CF) solutions (varying the pH from 9 to 12 while pure cement filtrate was characterized by a pH of 12.6). Previously, the pH-responsiveness of a series of SAPs was already evaluated in aqueous solutions. However, in order to assess the effect of the presence of salts and ions in CF solutions on the pH-responsive swelling capacity of the SAPs, the results of both series of swelling experiments were compared herein (see Figure III.14).

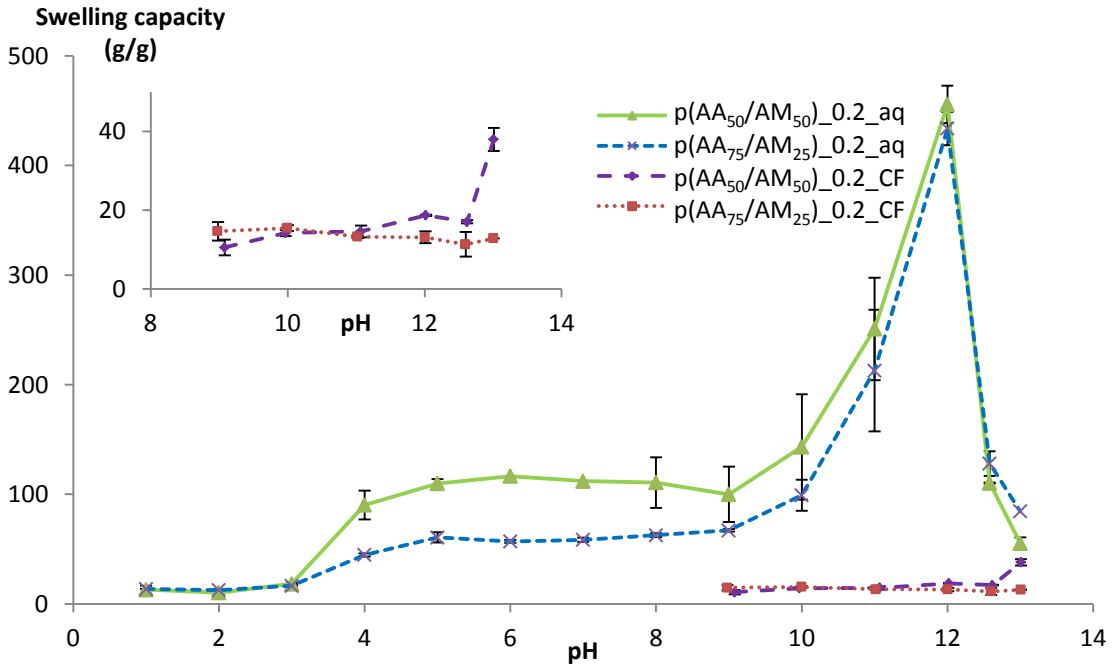

Figure III.14: Comparison between the swelling characteristics of $p(AA_{50}/AM_{50})\_0.2$ and $p(AA_{75}/AM_{25})\_0.2$ in aqueous solutions versus (acidified/basified) CF.

Two important observations could be made in the (acidified) cement filtrate (CF) solutions. First, the results showed that the swelling capacities in CF were much lower compared to aqueous solutions. Secondly, the swelling degree of both SAPs in CF solutions was hardly influenced by the pH (within the pH range 9-12.6).

When exceeding the pKa of AA (pH > 4.25 [20]), the carboxylic acids were converted into carboxylate groups. These groups start to repel each other and increase the volume of the swollen polymer. In cement filtrate, however, this behavior which is distinctive for aqueous solutions, was counteracted. First, the presence of dissolved cations in the cement filtrate (K^+, Na^+, Mg^{2+} and Ca^{2+}) countered this repelling effect and decreased the swelling capacity. Secondly, the presence of divalent cations (Mg^{2+} and Ca^{2+}) exerted an additional reductive effect on the swelling properties [21, 22]. It has already been proven before by Schröfl et al. that the presence of Ca^{2+} ions would lead to a decreased swelling and a difference in kinetics [23]. These cations formed strong electrostatic interactions with the carboxylate groups present and could therefore act as a physical cross-linker. Consequently, there was less opportunity for the repelling negative charges to increase the volume of the swollen SAP, which resulted in a low swelling degree.

To explain the second observation, a resumption of the observed trends in aqueous solutions should be made. Due to hydrolysis of the acrylamides into carboxylate groups (at pH > 9), the above-mentioned repellant effect increased to a great extent. However, as the cross-linker also contains two internal amide moieties, the network junction knots also started to hydrolyze from a critical point onwards (i.e. above pH 12) resulting in a drastic swelling decrease due to degradation (cfr. decrease of the network integrity), as described earlier. Interestingly, inside CF solutions (pH 9 – 12.6) this hydrolysis trend was not observed. It can be anticipated that an internal shielding effect occurred due to the presence of dissolved cations in the cement filtrate which could lead to a pH-delayed hydrolysis.

To compare the hydrolysis with the swelling capacity at the highest pH-value (pH 13) in aqueous solutions, an additional measurement was performed for both SAPs at pH 13 by addition of NaOH to cement filtrate. At this pH, the swelling capacity of p(AA_{50}/AM_{50})_0.2 already increased while p(AA_{75}/AM_{25})_0.2 still showed less to no change in swelling. In order to verify the observed postponed hydrolysis trend, IR spectroscopy was performed on the dried SAPs after swelling in both the aqueous as well as the CF solutions at varying pH-values (see Table III.4. and Figure III.15 for p(AA_{50}/AM_{50})_0.2; p(AA_{75}/AM_{25})_0.2 showed similar results, data not shown). To clarify the results, it should be noted that a primary amide (present in AM) is more prone to hydrolysis than a secondary amide (present in MBA) due to steric effects [24, 25]. At high pH-values, the formed products after hydrolysis are a carboxylate and ammonia (from AM) on the one hand and a carboxylate and a primary amine (from MBA) on the other hand. Ammonia is typically not visible via IR spectroscopy.

P(AA_{50}/AM_{50})_0.2 showed a broad out-of-plane bending vibration γ(N-H) at 783 cm^{-1} which corresponded to amides. Furthermore, a small peak could be distinguished at 1414 cm^{-1} which was characteristic for the symmetric COO^- stretching ν_s(C-O) from acrylic acid. A third important peak corresponded to the bending deformation δ(N-H) of the primary amides at 1597 cm^{-1}. After

swelling in an aqueous solution at pH 10.0, the same peaks were still observed (data not shown). However, at a pH of 12.0, a few interesting phenomena occurred. The γ(N-H) at 783 cm^{-1} became very weak while ν_s(C-O) was more pronounced as reflected by the additional peak at 1548 cm^{-1} which correlated with the asymmetric COO^- stretching ν_{as}(C-O) and was indicative for the onset of hydrolysis of the acrylamides. Further increase of the pH to 12.7 resulted in both ν_s(C-O) as well as ν_{as}(C-O) becoming very strong. Moreover, an additional sharp peak at 878 cm^{-1} corresponding to the out-of-plane bending vibration γ(N-H) of primary amines could be distinguished. The latter was illustrative for the onset of hydrolysis of the cross-linker (MBA) and the corresponding polymer network degradation. This was even more pronounced at pH 13.0.

Similarly, in cement filtrate solutions with a pH of 10.0, there were no differences regarding the characteristic signals in the IR spectrum compared to the non-swollen p(AA_{50}/AM_{50})_0.2. CF at pH 12.5 exhibited the initial hydrolysis with the disappearance of γ(N-H) and the appearance of ν_s(C-O) and ν_{as}(C-O), while no amine signal became apparent (as opposed to the aqueous solution at pH 12.7). At pH 13.0, the peaks of ν_s(C-O) and ν_{as}(C-O) were again more pronounced, while still no amine peak was visible.

The results showed that the cross-linker was not yet affected by hydrolysis when exposed to extremely high pH-values inside CF solutions. It could be anticipated that the latter was related to the presence of divalent cations. These results were very promising as the SAPs did not show hydrolysis inside mortar.

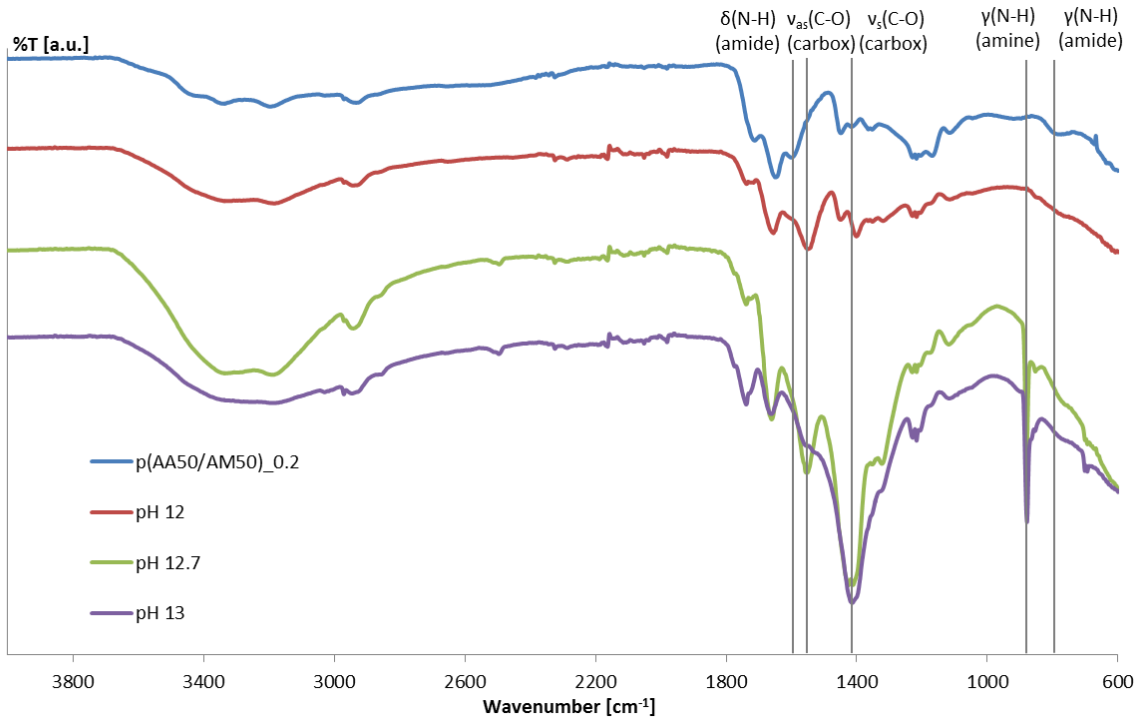

(a)

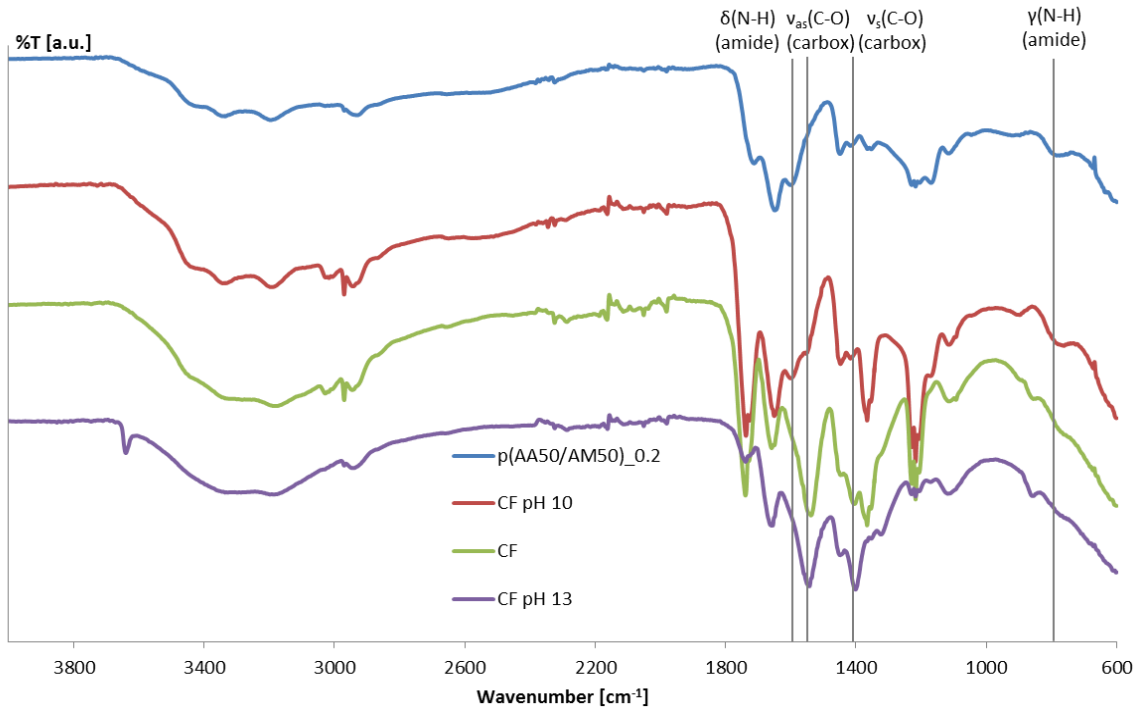

(b)

Figure III.15: The IR spectra showing the characteristic signals as depicted in Table III.4 (a) shows dry p(AA_{50}/AM_{50})_0.2 (blue) and immersed in an aqueous solution of pH 12 (red), pH 12.7 (green) and pH 13 (purple). (b) shows dry p(AA_{50}/AM_{50})_0.2 (blue) and immersed in a cement filtrate solution of pH 10 (red), pH 12.7 (no additional HCl or NaOH, green) and pH 13 (purple).

III.2.5. Evaluation of mechanical strength of SAP-containing mortar samples

Three-point bending and compressive strength tests were performed to determine the mechanical properties of mortar samples in the presence of SAPs with varying concentrations. As the SAPs absorb mixing water, there was a negative effect on the mortar workability. Additional water was added to compensate for the presence of the SAPs and to create mixtures exhibiting a similar workability (flow of 210 mm) as the reference material with a water-to-cement ratio of 0.50. The swelling capacity in CF provided a good indication of the additional amount of water required in mortar. For comparison, additional mortar mixtures were also developed using superplasticizer instead of additional water to improve the workability. The results of the three-point bending and compressive strength tests are shown in Table III.5.

First, the obtained values in mixtures with additional water were compared. Both the effects of the type of SAP as well as the applied amount of SAP in the different mixtures were assessed. The results indicated that compared to the reference, p(AA_{50}/AM_{50})_0.2 and p(AA_{75}/AM_{25})_0.2 both showed a significant reduction ($p < 0.05$) of the bending and compressive strength. Addition of a higher amount of SAP resulted in a more significant ($p < 0.05$) decrease of the sample strength. When comparing p(AA_{50}/AM_{50})_0.2 and p(AA_{75}/AM_{25})_0.2, a significant difference of the mechanical strength was only observed upon addition of 1 m%.

Table III.4: Characteristic signals of IR spectra of dried p(AA_{50}/AM_{50})_0.2 particles after swelling in aqueous and CF solutions at varying pH values indicating the postponed hydrolysis behavior in CF solutions.

Frequency	Assignment	p(AA_{50}/AM_{50})_0.2	pH 10.0	pH 12.0	pH 12.7	pH 13.0	CF pH 10.0	CF (pH 12.5)	CF pH 13.0
783 cm^{-1}	γ(N-H) amide (1°/2°)*	m, br	m, br	w	/	/	m, br	/	/
878 cm^{-1}	γ(N-H) amine (1°)	/	/	/	s, shp	s, shp	/	/	/
1400-1414 cm^{-1}	ν_s(C-O) carboxylate	w	w	m	vs	vs	w	m	s
1541-1548 cm^{-1}	ν_{as}(C-O) carboxylate	/	sh	s	s	w	sh	s	s
1597 cm^{-1}	δ(N-H) amide (1°)	s	s	/	/	/	s	/	/

w: weak, m: medium, s: strong, vs: very strong, sh: shoulder, shp: sharp, br: broad
* 1° and 2° represent primary and secondary amide respectively

These observations could be explained by the hydration degree of the binder. The hydration process of a mixture determines an important parameter in moisture transport processes, namely the microstructural development. Inside mortar, the SAPs swell due to the presence of additional water, which is released during internal curing [26], leading to continued hydration and as such, to a decreased micro-porosity. Literature reports indicate that this decrease in the number of micro-pores is related to two effects. First, the existing pores are filled with hydration products because of internal curing. Secondly, initially formed micro-cracks in the interior are reduced due to a decrease in autogenous shrinkage [27]. However, the water-filled SAPs are drained for this micro-pore filling thereby creating voids, which directly affects the mechanical properties of the cementitious material [28]. SAPs thus exert both a positive and a negative effect on the strength of mortar. Previous literature reports have shown that the addition of SAPs can lead to a decrease of the flexural and compressive strength [29-32]. The SAP voids can form a pathway for cracks and reduce the cross-sectional area [21, 32, 33].

Independent of the amount of SAPs added, SAP voids are created, leading to a decrease in strength of the mortar. The introduction of a higher amount of SAPs results in more voids, thus leading to a more severe effect on the strength [29-32]. To confirm this, air void analysis was performed on the sample containing p(AA_{75}/AM_{25})_0.2 at a concentration of 0.5 m% and the obtained result was compared to the result of the reference samples. The results showed that the air content increased from 4.0 ± 0.0 to 6.6 ± 0.7 upon introducing SAPs. As indicated by Laustsen et al., this increase in air content can lead to a reduction in strength [28].

Nowadays, SAPs are already used in mortar for internal curing. The percentages of SAPs required for this application generally amounts to 0.2 – 0.3% by mass of cement [34, 35]. However, for the envisaged application, a higher fraction of SAP (up to 1% by mass of cement) is required [36] which results in a stronger decrease in strength. As the swelling capacity of p(AA_{50}/AM_{50})_0.2 in CF was slightly higher compared to p(AA_{75}/AM_{25})_0.2, p(AA_{50}/AM_{50})_0.2 resulted in the creation of larger SAP voids, which explained the mutual difference in strength reduction for a 1 m% addition. The observed difference was not yet significant upon addition of 0.5 m% SAPs. Interestingly, the in-house synthesized SAPs showed similar effects on the strength as mortar samples containing commercially available SAPs with additional water [21]. Mixtures with p(AA_{50}/AM_{50})_0.2 (at a concentration of 0.5 m%) and p(AA_{75}/AM_{25})_0.2 show acceptable strengths for structural applications such as reservoirs, swimming pools, road stabilization, etc. Further work will focus on reducing this negative effect on the strength.

In a subsequent step, mortars were created exhibiting the same workability by the addition of a superplasticizer in the absence of additional water. The samples exhibited a higher bending and compressive strength at the age of 28 days as shown in Table III.5, which was due to a lower effective water-to-binder ratio [21]. A drawback, however, was the high degree of segregation of the SAPs from the mixture. The samples containing 1 m% of p(AA_{50}/AM_{50})_0.2 did not result in a similar workability (flow of 210 mm) as the reference samples upon addition of the maximum suggested amount of superplasticizer. Normal dosage for Glenium® 51 (modified polycarboxylic-ether, chloride-free, concentration of 35%) is between 0.5 and 1.6 liters per 100 kg cement for these types of mortar mixtures as suggested by the manufacturer. Additionally, literature has

previously correlated the use of superplasticizer with the possibility of a delayed setting and hardening [21]. Therefore, the results with superplasticizer were not taken into account for further investigations on self-sealing through water permeability assays.

Table III.5: Results of mechanical three-point bending and compressive strength tests. "/" indicates no strength reduction.

$p(AA_{50}/AM_{50})\_0.2$		Bending strength [MPa]	Compressive strength [MPa]
0.5 m%	(+ 60 mL water)	6.6 ± 0.4 (-1%)	47.0 ± 1.3 (-26%)
1 m%	(+ 130 mL water)	5.0 ± 0.1 (-25%)	30.6 ± 0.7 (-52%)
0.5 m%	(+ 6 mL superplast)	7.4 ± 0.4 (/)	64.1 ± 2.5 (/)
$p(AA_{75}/AM_{25})\_0.2$			
0.5 m%	(+ 55 mL water)	6.5 ± 0.6 (-3%)	51.9 ± 0.9 (-19%)
1 m%	(+ 95 mL water)	5.8 ± 0.1 (-13%)	44.2 ± 0.9 (-31%)
0.5 m%	(+ 3 mL superplast)	7.5 ± 0.3 (/)	73.7 ± 1.6 (/)
1 m%	(+ 7 mL superplast)	7.1 ± 0.3 (/)	57.2 ± 4.0 (/)
Reference			
No SAP	No extra water	6.7 ± 0.4	63.8 ± 1.9

III.2.6. Self-sealing and potential self-healing properties of mortar containing SAPs

Water permeability measurements indicate the self-sealing effect of SAPs present inside cylindrical mortar samples [37]. Figure III.16 shows water permeability measurements in the presence of a variable amount and type of SAP, compared to the reference samples. The cracked starting and end values of the developed samples refer to the k-value at day 1 and after day 28, respectively (age of the samples were 28 and 56 days). The crack widths are indicated between brackets. The other two results represent the data for the uncracked samples at the same measurement times.

Significant differences were observed between the reference and the samples containing 0.5 m% SAP for *uncracked* samples, in contrast to samples containing 1 m% SAP. At the end of the measurements, significantly different k-values were found between the reference and 0.5 m% SAP and between 0.5 m% versus 1 m% SAP. The addition of SAPs resulted in SAP voids after hydration, as described earlier (see §III.2.5.). The latter results in a reduction of the cross-sectional area, which explains the higher k-values of mortars containing SAPs. No differences could be found in the uncracked samples between $p(AA_{50}/AM_{50})\_0.2$ and $p(AA_{75}/AM_{25})\_0.2$.

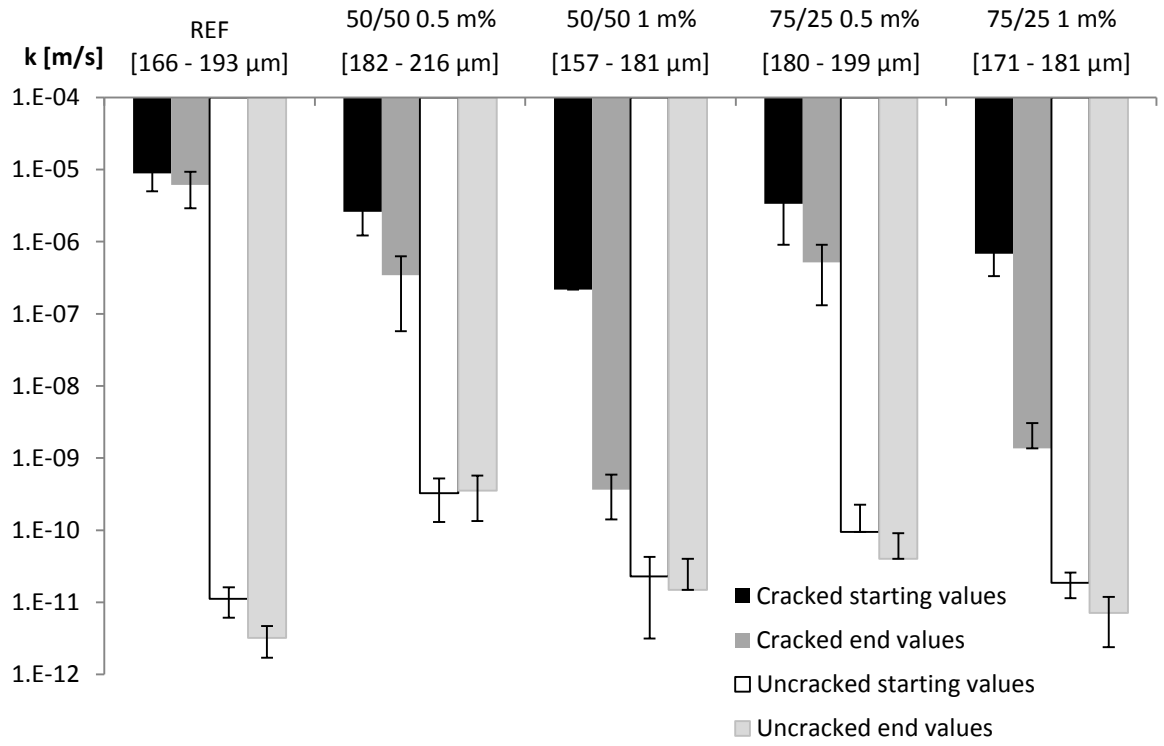

Figure III.16: Water permeability results for mortars with and without the addition of SAPs . The samples p(AA_{50}/AM_{50})_0.2 and p(AA_{75}/AM_{25})_0.2 have been abbreviated in the graph to 50/50 and 75/25 for reasons of clarity. The range of length values between brackets show the range of the crack widths.

As anticipated, *cracked* reference samples did not show significant sealing as indicated by their k-values after 28 days and 56 days. Interestingly, upon addition of any amount or type of SAPS, a significant ($p < 0.05$, addition of 0.5 m% SAP) or a very significant ($p < 0.01$, addition of 1 m% SAP) closure of the cracks was observed after 28 days. Cracked samples containing 0.5 m% SAP showed no significant difference with the reference sample at the onset of the measurements (starting value), in contrast with the end of the measurements (end value). The latter implies that even 0.5 m% SAP resulted in a stronger sealing effect over a period of 28 days compared to the reference samples. As anticipated, addition of 1 m% SAP resulted in a higher extent of closure compared to the reference and the samples containing 0.5 m% SAP. More SAP equals a higher swelling potential and as such, a stronger blockage of the cracks and potential to stimulate further cement hydration and $CaCO_3$ precipitation. Thus, a higher amount of SAP led to a significantly ($p < 0.05$) strong self-sealing effect, almost reaching the k-values of uncracked samples, especially in the case of p(AA_{50}/AM_{50})_0.2.

The results showed that the addition of SAPs resulted in a certain degree of crack closure, with a higher fraction of SAP leading to more self-sealing. Interestingly, for various samples containing 1 m% SAP, stalactites were observed due to leaching from the sealed cracks. These stalactites are representative for healing products formed in the crack, as illustrated in Figure III.17.

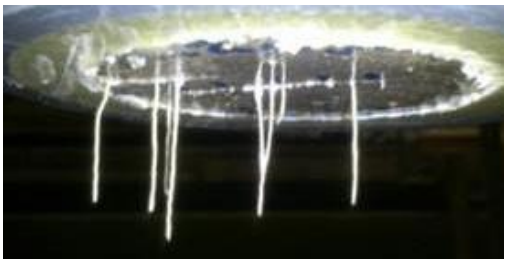

Figure III.17: Formation of stalactites at the bottom of the water permeability samples upon addition of 1 m% p(AA_{50}/AM_{50})_0.2 and 1 m% p(AA_{75}/AM_{25})_0.2.

SEM-EDS measurements were performed to identify the chemical composition of the formed stalactites. As indicated in Figure III.18, the leached products were highly crystalline while EDS analysis confirmed the presence of Ca, C and O in high fractions (i.e. 22 – 33%, 19 – 24% and 44 – 55% respectively), together with some small traces of Na, Mg, Al and Si (i.e. 0.2 – 0.8 %). The traces could be correlated to the mortar as small leached ions could be entrapped inside the formed crystals. The pronounced presence of Ca, C and O provides a first indication that the formed stalactites were composed of different types of $CaCO_3$, CaO and/or $Ca(OH)_2$.

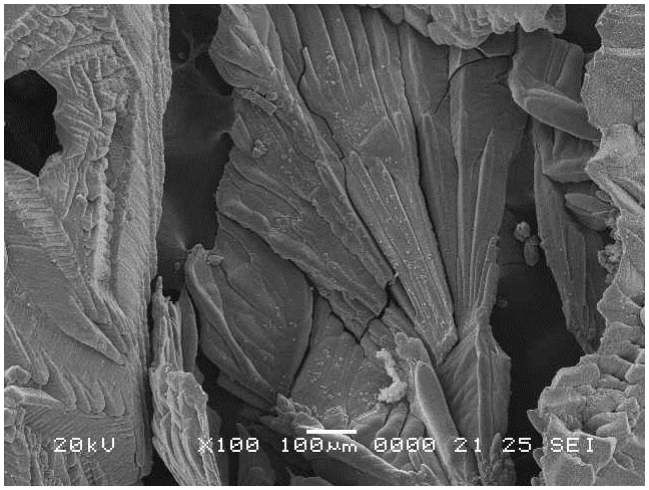

Element	Atom%
C K	20.61
O K	55.34
Na K	0.48
Mg K	0.28
Al K	0.18
Si K	0.6
Ca K	21.76
Au M	0.75
Total	100

Element	Atom%
C K	19.13
O K	45.8
Na K	0.27
Mg K	0.73
Al K	0.21
Si K	0.15
Ca K	31.99
Au M	1.72
Total	100

Element	Atom%
C K	19.72
O K	43.68
Na K	0.38
Mg K	0.41
Al K	0.31
Ca K	33.38
Au M	2.14
Total	100

Element	Atom%
C K	23.99
O K	50.05
Na K	0.51
Mg K	0.79
Al K	0.23
Ca K	22.45
Au M	1.97
Total	100

Figure III.18: SEM micrograph and EDS analysis of the formed stalactites.

Subsequently, the materials were subjected to FT-IR spectroscopy and TGA. The FT-IR spectrum of the stalactites is shown in Figure III.19. The peaks at 1428 cm^{-1}, 878 cm^{-1} and 714 cm^{-1} corresponding to stretching v_3 (C-O) and bending v_2 and v_4 respectively were characteristic absorption bands of calcium carbonate, more specifically calcite [38, 39]. The spectrum of the stalactites (dashed blue line) shows a higher absorption at 3400 cm^{-1} in comparison to $CaCO_3$ (full green line), which could be attributed to the presence of more adsorbed water. Compared to the spectrum of calcium hydroxide ($Ca(OH)_2$, dotted red line) the IR spectrum of the stalactites lacks the typical steep absorption peak at 3640 cm^{-1}. However, small fractions of $Ca(OH)_2$ can always convert to $CaCO_3$ by reaction with CO_2 [40]. This technique could not exclude the presence of CaO. As a result, TGA experiments were also performed to further identify the chemical composition of the stalactites.

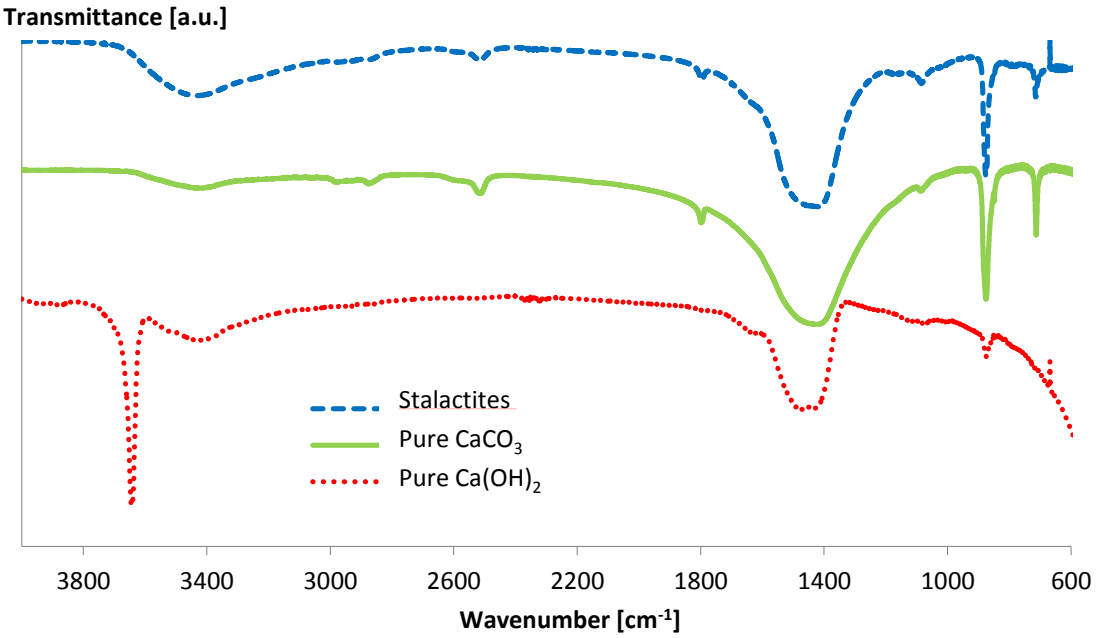

Figure III.19: ATR-IR spectrum of the formed stalactites. The IR spectra of $CaCO_3$ and $Ca(OH)_2$ are also included as references.

TGA only showed one peak corresponding with weight loss (see Figure III.20). As indicated by literature, the latter is completely related to the loss of carbon dioxide (CO_2) gas [41-43] (see equation (III.1)):

$$CaCO_{3\,(s)} \xrightarrow{\Delta T} CaO_{(s)} + CO_{2\,(g)} \qquad \text{(III.1)}$$

By comparing the molecular weights of $CaCO_3$ and CaO (i.e. 100.1 g/mol and 56.1 g/mol respectively), the decrease from 550 °C till 710 °C corresponded almost fully with $CaCO_3$, as described in literature [44]. No weight loss related to the presence of $Ca(OH)_2$ was observed with TGA at its characteristic degradation temperature range (i.e. 320 - 510 °C). Small amounts of CaO were present which could not be degraded using TGA (T < 1000°C). The latter, however, explains the difference between the theoretical amount of CO_2 loss (mol. weight of 44 g/mol) and the total obtained residue.

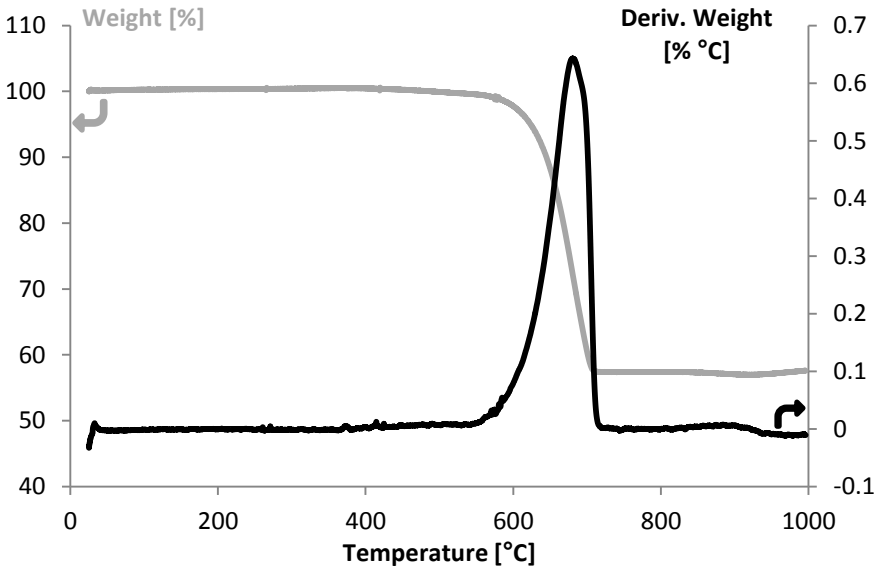

Figure III.20: TGA of the formed stalactites.

The combination of the above-mentioned tests confirmed the formation of the healing product $CaCO_3$ and small amounts of CaO, which leached out from the crack. Together with the water permeability results, this supports the strong self-sealing and potential self-healing capacity for cracks upon addition of 1 m% of the synthesized SAPs inside mortar.

III.2.7. Conclusions and future perspectives

In the present work, a free radical precipitation polymerization was successfully applied for synthesizing a range of (superabsorbent) polymers composed of acrylic acid, acrylamide and N,N'-methylene bisacrylamide as cross-linker. Interestingly, dynamic vapor sorption measurements indicated that water uptake capacities up to 31% were obtained with a RH of 95%. When going to even higher RH, up to 90% of the SAPs own weight could be taken up depending on the applied cross-linking density while possessing a negligible hysteresis. Moreover, the developed materials showed a strong pH-sensitivity and reached swelling capacities up to 450 g_{water}/g_{SAP} in aqueous solutions.

Based on these results, the two best performing SAPs (i.e. p(AA_{50}/AM_{50})_0.2 and p(AA_{75}/AM_{25})_0.2) were chosen for further characterization and linked to potential self-sealing and self-healing of cracks in concrete. The swelling experiments of these two SAPs showed that due to the presence of divalent cations, the swelling capacity in CF solutions was significantly lower compared to in aqueous solutions. The observed hydrolysis in aqueous solutions at extreme alkaline conditions was postponed in CF solutions and the degradation of the polymer network was absent in CF which could be explained by a shielding effect due to the presence of divalent cations in the cement filtrate as indicated by ATR-IR spectroscopy. Bending and compression strength tests in mortar showed that a higher fraction of SAP resulted in a greater decrease in strength (up to 52% loss of compression strength). Conversely, the addition of higher SAP amounts resulted in a stronger self-sealing effect compared to reference samples without SAP. Interestingly, stalactites were observed after performing water permeability tests on

samples containing 1 m% SAP. In-depth characterization showed that the latter mainly consisted of healing products ($CaCO_3$ and small fractions of CaO). Despite a partial decrease in mortar strength, the synthesized SAPs exhibited a strong self-sealing and potential self-healing effect on cracks and can be considered as promising materials for the envisaged application. However, further development is necessary to create materials that have a less severe effect on the mortar strength. Therefore, in a third part of this chapter, a pH-responsive basic monomer (i.e. dimethylaminoethyl methacrylate) is introduced to ensure a low swelling capacity at alkaline mixing conditions and a greater swelling upon infiltration of water into the crevices.

III.2.8. References

[1] Özeroglu C, Birdal A. Swelling properties of acrylamide-N, N'-methylene bis (acrylamide) hydrogels synthesized by using meso-2, 3-dimercaptosuccinic acid-cerium (IV) redox couple. Express Polym Lett. 2009;3:168-76.
[2] Boyde TRC. Swelling and contraction of polyacrylamide gel slabs in aqueous solutions. Journal of Chromatography A. 1976;124(2):219-30.
[3] Baker JP, Hong LH, Blanch HW, Prausnitz JM. Effect of Initial Total Monomer Concentration on the Swelling Behavior of Cationic Acrylamide-Based Hydrogels. Macromolecules. 1994;27(6):1446-54.
[4] Pekcan Ö, Kara S. Photon transmission technique for monitoring swelling of acrylamide gels formed with various crosslinker contents. Polymer. 2001;42(25):10045-53.
[5] Li A, Wang A, Chen J. Studies on poly (acrylic acid)/attapulgite superabsorbent composites. II. Swelling behaviors of superabsorbent composites in saline solutions and hydrophilic solvent–water mixtures. Journal of Applied Polymer Science. 2004;94(5):1869-76.
[6] Pourjavadi A, Jahromi PE, Seidi F, Salimi H. Synthesis and swelling behavior of acrylatedstarch-g-poly (acrylic acid) and acrylatedstarch-g-poly (acrylamide) hydrogels. Carbohydrate Polymers. 2010;79(4):933-40.
[7] Tomar RS, Gupta I, Singhal R, Nagpal AK. Synthesis of poly (acrylamide-co-acrylic acid) based superabsorbent hydrogels: Study of network parameters and swelling behaviour. Polymer-Plastics Technology and Engineering. 2007;46(5):481-8.
[8] Rabat NE, Hashim S, Majid RA. Effect of Different Monomers on Water Retention Properties of Slow Release Fertilizer Hydrogel. Procedia Engineering. 2016;148:201-7.
[9] Murali Mohan Y, Keshava Murthy PS, Mohana Raju K. Synthesis, characterization and effect of reaction parameters on swelling properties of acrylamide–sodium methacrylate superabsorbent copolymers. Reactive and Functional Polymers. 2005;63(1):11-26.
[10] Zhang B, Cui Y, Yin G, Li X, Liao L, Cai X. Synthesis and swelling properties of protein-poly(acrylic acid-co-acrylamide) superabsorbent composite. Polymer Composites. 2011;32(5):683-91.
[11] Limparyoon N, Seetapan N, Kiatkamjornwong S. Acrylamide/2-acrylamido-2-methylpropane sulfonic acid and associated sodium salt superabsorbent copolymer nanocomposites with mica as fire retardants. Polymer Degradation and Stability. 2011;96(6):1054-63.
[12] Sadeghi M, Hosseinzadeh H. Synthesis of Starch—Poly(Sodium Acrylate-co-Acrylamide) Superabsorbent Hydrogel with Salt and pH-Responsiveness Properties as a Drug Delivery System. Journal of Bioactive and Compatible Polymers. 2008;23(4):381-404.
[13] Nesrinne S, Djamel A. Synthesis, characterization and rheological behavior of pH sensitive poly(acrylamide-co-acrylic acid) hydrogels. Arabian Journal of Chemistry. 2013(0).
[14] Abd Alla SG, Sen M, El-Naggar AWM. Swelling and mechanical properties of superabsorbent hydrogels based on Tara gum/acrylic acid synthesized by gamma radiation. Carbohydrate Polymers. 2012;89(2):478-85.
[15] Rived F, Rosés M, Bosch E. Dissociation constants of neutral and charged acids in methyl alcohol. The acid strength resolution. Analytica Chimica Acta. 1998;374(2–3):309-24.
[16] Kulkarni RV, Sa B. Polyacrylamide-Grafted-Alginate-Based pH-Sensitive Hydrogel Beads for Delivery of Ketoprofen to the Intestine: in Vitro and in Vivo Evaluation. Journal of Biomaterials Science, Polymer Edition. 2009;20(2):235-51.
[17] Kurenkov VF, Hartan HG, Lobanov FI. Alkaline Hydrolysis of Polyacrylamide. Russian Journal of Applied Chemistry. 2001;74(4):543-54.
[18] Rabbii MEZaA. Alkaline Hydrolysis of Polyacrylamide and Study on Poly(acrylamide-co-sodium acrylate) Properties. Iranian Polymer Journal. 2002;11(4):269-75.
[19] Rahna K Shamsudeen SNVGJ. Equilibrium swelling conductivity and electroactive characteristics of polyacrylamide hydrogels. Indian Journal of Engineering & Materials Sciences. 2006;13(2006):62-8.
[20] Morris GE, Vincent B, Snowden MJ. Adsorption of Lead Ions ontoN-Isopropylacrylamide and Acrylic Acid Copolymer Microgels. Journal of colloid and interface science. 1997;190(1):198-205.

[21] Snoeck D, Schaubroeck D, Dubruel P, De Belie N. Effect of high amounts of superabsorbent polymers and additional water on the workability, microstructure and strength of mortars with a water-to-cement ratio of 0.50. Construction and Building Materials. 2014;72(0):148-57.
[22] Hancock RD, Martell AE. Ligand design for selective complexation of metal ions in aqueous solution. Chemical Reviews. 1989;89(8):1875-914.
[23] Schröfl C, Mechtcherine V, Gorges M. Relation between the molecular structure and the efficiency of superabsorbent polymers (SAP) as concrete admixture to mitigate autogenous shrinkage. Cement and Concrete Research. 2012;42(6):865-73.
[24] Slebocka-Tilk H, Bennet AJ, Keillor JW, Brown RS, Guthrie JP, Jodhan A. Oxygen-18 exchange accompanying the basic hydrolysis of primary, secondary, and tertiary toluamides. 2. The importance of amine leaving abilities from the anionic tetrahedral intermediate. Journal of the American Chemical Society. 1990;112(23):8507-14.
[25] DeRuiter J. Amides and related functional groups. 2005.
[26] Jensen O, Lura P. Techniques and materials for internal water curing of concrete. Mat Struct. 2006;39(9):817-25.
[27] P. Lura GY, V. Cnudde, P. Jacobs. Preliminary results about 3D distribution of superabsorbent polymers in mortars. In: W. Sun KvB, C. Miao, G. Ye and H. Chen, editor. International Conference on Microstructure Related Durability of Cementitious Composites: RILEM Publications; 2008. p. 8.
[28] Laustsen S, Hasholt M, Jensen O. Void structure of concrete with superabsorbent polymers and its relation to frost resistance of concrete. Mat Struct. 2013;48(1-2):357-68.
[29] Mechtcherine V, Dudziak L, Hempel S. Mitigating early age shrinkage of ultra-high performance concrete by using super absorbent polymers (SAP). Creep Shrinkage and Durability Mechanics of Concrete and Concrete Structures–CONCREEP-8, Tanabe T et al (eds) Taylor & Francis Group, London, UK. 2009:847-53.
[30] Jensen OM, Hansen PF. Water-entrained cement-based materials: I. Principles and theoretical background. Cement and Concrete Research. 2001;31(4):647-54.
[31] Jensen OM, Hansen PF. Water-entrained cement-based materials: II. Experimental observations. Cement and Concrete Research. 2002;32(6):973-8.
[32] Hasholt MT, Jensen OM, Kovler K, Zhutovsky S. Can superabsorbent polymers mitigate autogenous shrinkage of internally cured concrete without compromising the strength? Construction and Building Materials. 2012;31:226-30.
[33] Snoeck D, Steuperaert S, Van Tittelboom K, Dubruel P, De Belie N. Visualization of water penetration in cementitious materials with superabsorbent polymers by means of neutron radiography. Cement and Concrete Research. 2012;42(8):1113-21.
[34] Nestle N, Kühn A, Friedemann K, Horch C, Stallmach F, Herth G. Water balance and pore structure development in cementitious materials in internal curing with modified superabsorbent polymer studied by NMR. Microporous and Mesoporous Materials. 2009;125(1–2):51-7.
[35] Mechtcherine V, Gorges M, Schroefl C, Assmann A, Brameshuber W, Ribeiro A, et al. Effect of internal curing by using superabsorbent polymers (SAP) on autogenous shrinkage and other properties of a high-performance fine-grained concrete: results of a RILEM round-robin test. Mat Struct. 2014;47(3):541-62.
[36] Snoeck D, Van Tittelboom K, De Belie N, Steuperaert S, Dubruel P. The use of superabsorbent polymers as a crack sealing and crack healing mechanism in cementitious materials. Concrete Repair, Rehabilitation and Retrofitting III: 3rd International Conference on Concrete Repair, Rehabilitation and Retrofitting, ICCRRR-3, 3-5 September 2012, Cape Town, South Africa: CRC Press; 2012. p. 58.
[37] Lee HXD, Wong HS, Buenfeld NR. Potential of superabsorbent polymer for self-sealing cracks in concrete. Advances in Applied Ceramics. 2010;109(5):296-302.
[38] Andersen FA, Brecevic L. Infrared spectra of amorphous and crystalline calcium carbonate. Acta Chem Scand. 1991;45:1018-24.
[39] Lane MD, Christensen PR. Thermal infrared emission spectroscopy of anhydrous carbonates. Journal of Geophysical Research: Planets (1991–2012). 1997;102(E11):25581-92.

[40] Teir S, Eloneva S, Fogelholm C-J, Zevenhoven R. Dissolution of steelmaking slags in acetic acid for precipitated calcium carbonate production. Energy. 2007;32(4):528-39.
[41] Haselbach L. Potential for Carbon Dioxide Absorption in Concrete. Journal of Environmental Engineering. 2009;135(6):465-72.
[42] Faatz M, Gröhn F, Wegner G. Amorphous Calcium Carbonate: Synthesis and Potential Intermediate in Biomineralization. Advanced Materials. 2004;16(12):996-1000.
[43] Oniyama E, Wahlbeck PG. Application of transpiration theory to TGA data: Calcium carbonate and zinc chloride. Thermochimica Acta. 1995;250(1):41-53.
[44] Villain G, Thiery M, Platret G. Measurement methods of carbonation profiles in concrete: Thermogravimetry, chemical analysis and gammadensimetry. Cement and Concrete Research. 2007;37(8):1182-92.

III.3 Introducing a basic monomer to induce pH-responsiveness in the synthetic SAP

As was seen in the previous chapter, a decrease in the mortar strength still remains an issue as the used superabsorbent polymers (SAPs) already swell during the mixing. When they then release their water during the hardening, they leave behind macro pores. This leads to a porous matrix and this negatively influences the mortar strength. This negative influence is especially pronounced when high amounts of SAP (up to 1 m% in function of the added cement) are needed for the intended application [1, 2]. To solve this issue, a different monomer is introduced into the SAP in this chapter. By using a basic monomer such as 2-(dimethylamino)ethyl methacrylate (DMAEMA), the SAP will on the one hand not swell substantially upon exposure to a pH above its pKa value of 8.4 [3] (cfr. the pH of fresh mortar is very alkaline, pH 12.5 – 13). On the other hand, when water infiltrates a crack, the SAP will swell more given the more neutral pH of infiltrating water (i.e. 7 – 9).

Poly(DMAEMA) has already been used as a copolymer combined with N-isopropylacrylamide (NIPAAm) to create hydrogels with both pH- as well as temperature sensitivity [4]. Another study showed the use of NIPAAm, acrylic acid (AA) and DMAEMA as starting monomers for the development of a multi-responsive adaptive liquid microlens [5]. Other research has indicated the usefulness of grafting p(DMAEMA) from a poly(thiophene) backbone to create a reversible pH-response in different aqueous solutions rendering it attractive for fabricating functional polymer composites [6]. A copolymer of hydroxyethyl methacrylate (HEMA) and DMAEMA has even been reported as a sensor for CO_2-detection [7].

As DMAEMA shows already high potential for a multiplicity of applications, it is also interesting to investigate the effect of this ‘smart’ pH-sensitive SAP for the self-sealing and -healing of cracks in concrete. Herein, DMAEMA has been cross-linked with the synthetic cross-linker N,N’-methylene bisacrylamide. The chemical structure of the obtained SAP has been elucidated by ATR-IR spectroscopy while its cross-linking efficiency has been investigated using high-resolution magic angle spinning proton nuclear magnetic resonance (HR-MAS ^{1}H-NMR) spectroscopy. Additionally, dynamic vapor sorption (DVS) experiments and swelling tests in aqueous solutions of varying pH (and cement filtrate solution) have been used to indicate the moisture uptake capacity and pH-responsiveness of cross-linked poly(dimethylaminoethyl methacrylate) (p(DMAEMA)_x). Finally, the effect of these SAPs on the bending and compressive strength of mortar samples has been tested to provide an idea on their usefulness for applications in construction. The latter characteristics has also been compared with the outcome upon applying commercially available synthetic SAPs [8].

III.3.1. Development of cross-linked p(DMAEMA)

The poly(dimethylaminoethyl methacrylate) (p(DMAEMA)) based materials were synthesized with a varying fraction of N,N'-methylene bisacrylamide (MBA). A high amount of cross-linker of at least 2 mol% (compared to the total added amount of DMAEMA) was required to obtain a polymer with gel-like characteristics. The concentration of cross-linker was also doubled (4 mol%) to determine the influence of a denser network on the characteristics of the SAP. The gel fraction was calculated (75 ± 8 % and 72 ± 2 %, respectively for p($DMAEMA_{100}$)_2 and p($DMAEMA_{100}$)_4) and was found to be rather low compared to other SAPs where they aim at higher than 85% [9, 10] (no significant differences were found between both values).

The ground SAP showed a wide particle size distribution (Table III.6). This could be related to the hardness of the SAP and thus the time needed to grind these materials. When comparing with commercial SAPs, the synthesized SAPs were in good agreement with the dimensions of SAP A (cfr. particle size of 100.0 ± 21.5 µm [8]). SAP B, on the other hand, is characterized by a larger particle size of 476.6 ± 52.9 µm [8]. The latter could have an influence on some properties such as the moisture uptake capacity as described further (see §III.3.3.).

Table III.6: Particle size distribution of the p(DMAEMA)_x SAPs. The d_x stands for the diameter of sieve where 10%, 50% and 90% will constitute the eluate.

Sample	d_{10} [µm]	d_{50} [µm]	d_{90} [µm]
p($DMAEMA_{100}$)_2	14	83	151
p($DMAEMA_{100}$)_4	15	36	91

III.3.2. Chemical structure elucidation of cross-linked p(DMAEMA)

ATR-IR spectroscopy (Figure III.21) indicated the presence of a C=O stretch (ν(C=O)) at 1720 cm^{-1} which is characteristic for the esters present in DMAEMA. The C=C stretch corresponding with the double bonds from the unreacted monomer and the cross-linker was no longer visible (around 1650 cm^{-1}). The C-N stretch (ν(C=N)) of DMAEMA could be observed at 1145 cm^{-1}. The C=O stretch of the secondary amide groups of the cross-linker were overlapping with the shoulder of the C=O ester stretch. The IR spectroscopy results are a first indication that the synthesis was successful.

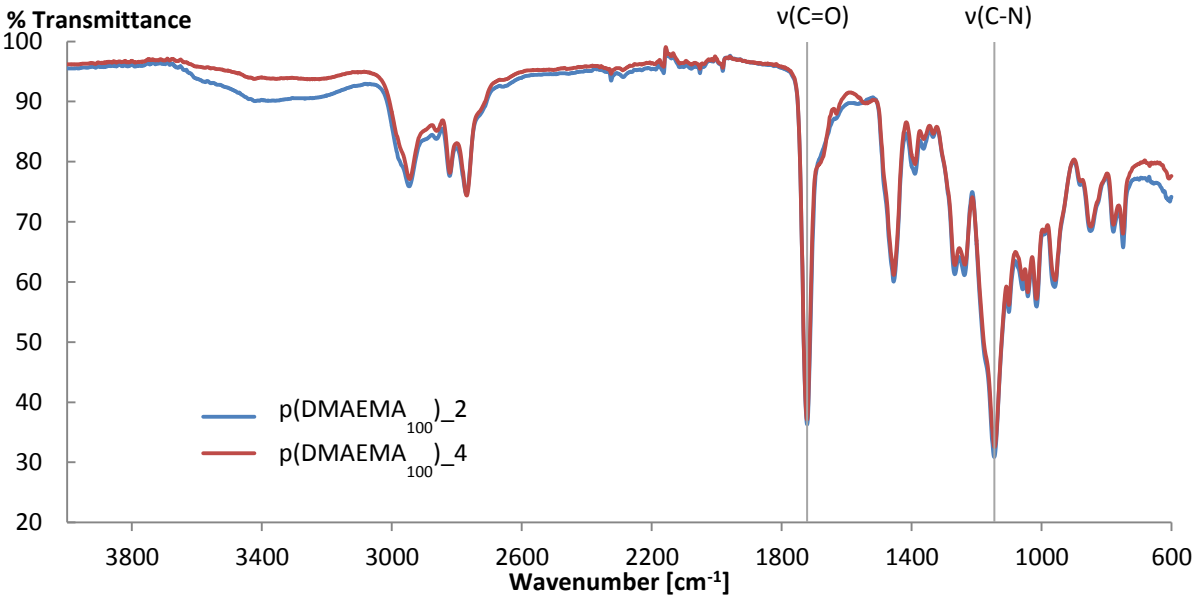

Figure III.21: ATR-IR spectra obtained for the p(DMAEMA)_x SAPs.

Additionally, HR-MAS ^{1}H-NMR spectroscopy was performed to assess the cross-linking efficiency of the reaction. As indicated in the spectrum in Figure III.22, the peaks corresponding with the protons from the C=C double bond (5.7 – 6.2 ppm) were only visible to a limited extent. Indeed, they had mainly shifted to the right (1.5 – 2.5 ppm) as they became alkane protons, located adjacent to an electronegative group. The above-mentioned techniques clearly prove their use as complementary tools to confirm the successful polymerization of the p(DMAEMA)_x SAPs.

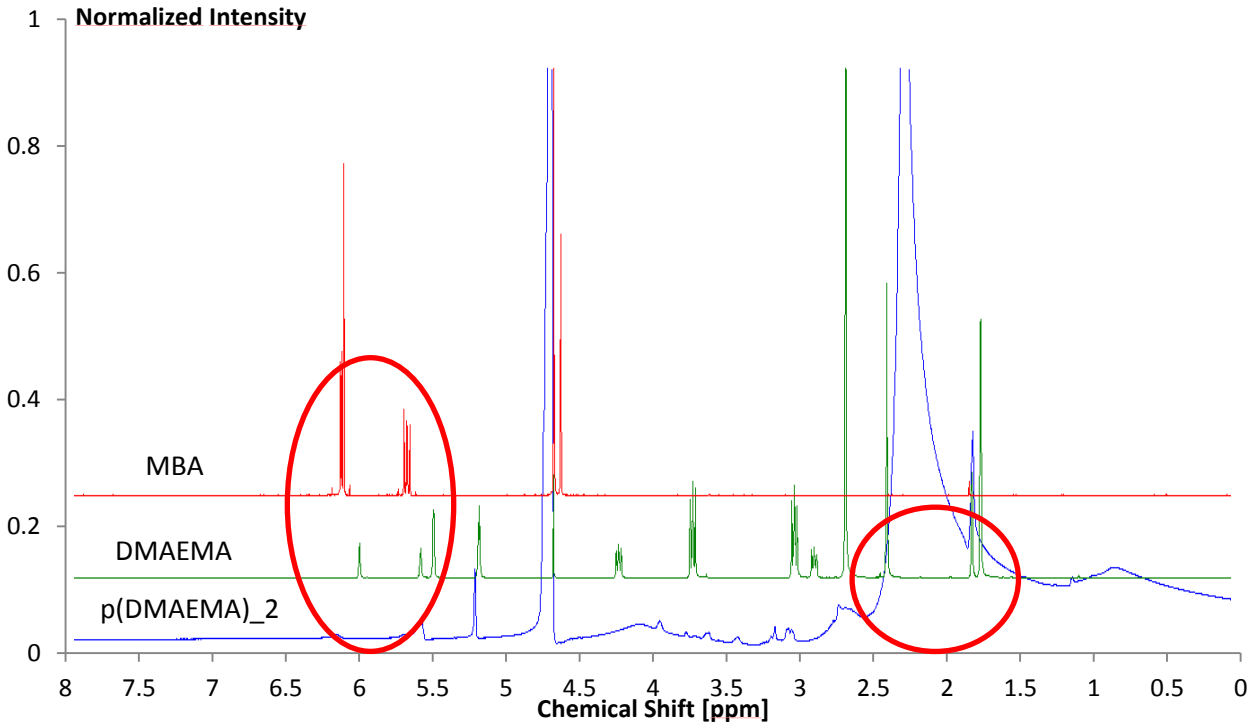

Figure III.22: HR-MAS ^{1}H-NMR spectrum of MBA, DMAEMA and p(DMAEMA$_{100}$)_2 from top to bottom. The peaks indicative for the protons from the C=C double bonds (5.7 – 6.2 ppm) become negligibly small.

III.3.3. Dynamic vapor sorption measurements to identify the moisture uptake capacity of the synthesized SAPs

Dynamic vapor sorption experiments indicated that both polymers showed a moisture uptake capacity up to 45% of their original weight at 95% RH (Figure III.23 and Table III.7). It could be noticed that a double amount of cross-linker resulted in a small increase in moisture uptake. This difference could be explained by the particle morphology. The p(DMAEMA$_{100}$)_4 particles were smaller, leading to a larger surface area and thus a somewhat higher moisture uptake capacity. Additionally, there was no hysteresis whatsoever, which implies that all moisture absorbed at high RH could be desorbed again. This is useful as the SAPs can thus be used as moisture reservoirs, and deliver their absorbed moisture back to the matrix when the RH is decreasing again. When comparing these results with commercial SAPs, the latter took up more moisture at 60% RH [8]. Similarly, at ≥ 90% RH, (as an indication, the yearly average RH in Brussels, Belgium is around 85% [11, 12]) the moisture uptake capacity was higher for commercially available SAPs. However, irrespective of their higher moisture uptake potential, the partial self-sealing potential of the commercial SAPs remains still limited.

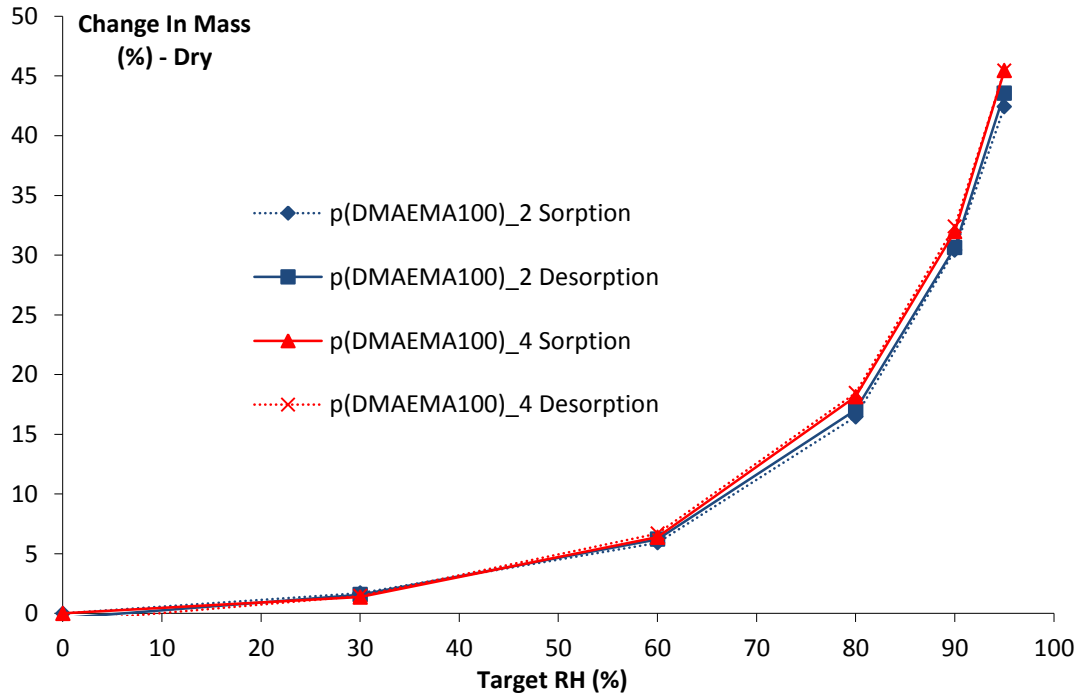

Figure III.23: Moisture uptake capacity measurements of p(DMAEMA$_{100}$)_2 and p(DMAEMA$_{100}$)_4 (sorption and desorption) where a negligible hysteresis is visible.

Table III.7: Effect of concentration of the cross-linker on the p(DMAEMA) moisture sorption behavior. The results from the commercial SAPs were obtained from [8].

Moisture uptake capacity [%]	p(DMAEMA$_{100}$)_2 Sorption	p(DMAEMA$_{100}$)_4 Sorption	SAP A *copolymer of acrylamide and sodium acrylate*	SAP B *cross-linked potassium salt poly(acrylate)*
60% RH	6	6	26	28
90% RH	30	32	83	84
95% RH	42	45	130	119

III.3.4. Swelling capacity of the cross-linked p(DMAEMA) SAPs

As indicated in the swelling experiments (Figure III.24), the materials showed a pH-responsive behavior. Both p(DMAEMA$_{100}$)_2 as well as p(DMAEMA$_{100}$)_4 exhibited a low swelling at the most alkaline conditions (i.e. 12 ± 1 g_{water}/g_{SAP} and 15 ± 2 g_{water}/g_{SAP} respectively) and an increase in swelling down to a pH of 10 (39 ± 1 g_{water}/g_{SAP} and 25 ± 1 g_{water}/g_{SAP} respectively), at which the material with a lower MBA concentration led to a higher swelling as anticipated due to its less dense network. A further increase of the swelling occurred at pH 3 (i.e. 68 ± 1 g_{water}/g_{SAP} and 42 ± 2 g_{water}/g_{SAP} respectively). The latter showed the pH-sensitivity of p(DMAEMA)_x. The tertiary amine moieties become more protonated at a lower pH. These positive charges repel each other, creating a more open structure which can take up additional water.

Commercially available SAPs showed a swelling exceeding 4 times that reached for p(DMAEMA$_{100}$)_2 at pH 3 (i.e. a swelling of 305 ± 4 g_{water}/g_{SAP} for SAP A and 283 ± 2 g_{water}/g_{SAP} for SAP B respectively [8]). However, these commercial SAPs retain a high swelling capacity also at alkaline conditions, as indicated in cement filtrate solutions, whereas this was lower for the synthesized SAPs due to its pH-responsiveness. As anticipated, due to the presence of the dissolved cations in cement filtrate (K^+, Na^+, Mg^{2+} and Ca^{2+}), the swelling was substantially lower than in aqueous solutions (i.e. 61 ± 1 g_{water}/g_{SAP} for SAP A and 58 ± 2 g_{water}/g_{SAP} for SAP B [8]). However, the in-house synthesized SAPs have a more limited water uptake capacity in cement filtrate solution (13 ± 1 g_{water}/g_{SAP} and 14 ± 0 g_{water}/g_{SAP} for p(DMAEMA$_{100}$)_2 and p(DMAEMA$_{100}$)_4 respectively), which makes them still promising. Indeed, they swell less during mortar mixing thereby creating smaller pores during the hardening compared to commercial SAPs. The latter is anticipated to result in a lower influence on the bending and compression strength of mortar with the addition of SAPs as discussed in the upcoming section. When cracks occur, p(DMAEMA$_{100}$)_2 are exposed to the lower pH of infiltrating water resulting in increased swelling, especially when rain with a low pH (cfr. acid rain) starts to infiltrate the crack.

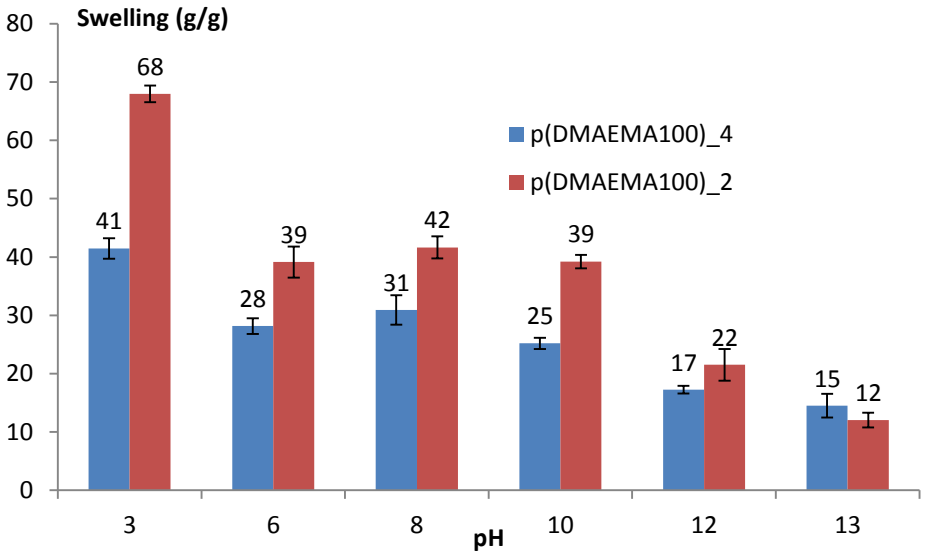

Figure III.24: Effect of cross-linker concentration on the swelling capacity measurements in aqueous solutions with a varying pH.

After incubation in the different solutions, the SAPs were freeze-dried and characterized using ATR-IR spectroscopy to identify potential degradation through hydrolysis, especially at extreme alkaline conditions. As indicated in Figure III.25, almost no differences between the spectra were visible, even at extremely alkaline conditions (cfr. aqueous solution of pH 13 and CF solution). A minor difference could be observed at 876 cm^{-1} at which the peak corresponding with γ(N-H) from the primary amines seemed to be slightly more pronounced. However, the signals at 1550 cm^{-1} and especially at 1410 cm^{-1} associated with the asymmetric (ν_{as}(C-O)) and symmetric (ν_{s}(C-O)) C-O stretch, related to hydrolysis, were not stronger present than the original spectrum, so as a result, it could be concluded that these materials showed a negligible amount of hydrolysis distinguishable through ATR-IR spectroscopy.

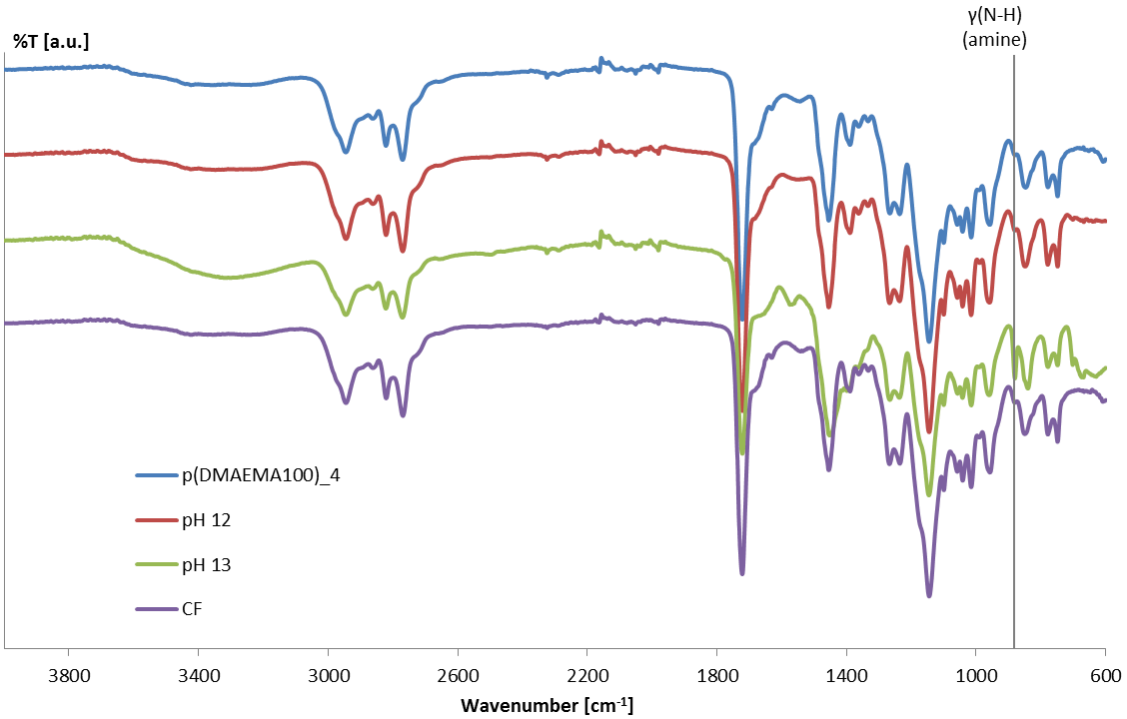

Figure III.25: ATR-IR spectra from the freeze-dried SAPs after incubation in various solutions showing the absence of hydrolysis occurring in alkaline conditions.

III.3.5. Determination of the flexural and compressive strength in mortar after addition of cross-linked p(DMAEMA) SAPs

Flexural and compressive strength tests were performed on mortar samples with and without (i.e. reference) addition of SAPs (Table III.8). As the SAPs absorb mixing water, there was a negative effect on the mortar workability. Additional water was thus added to compensate for the presence of the SAPs and to create mixtures exhibiting a similar workability (slump around 210 mm, S4 slump class) as the reference material with a water-to-cement ratio of 0.5. No significant differences were found on the bending strength of the samples investigated. However, the compressive strength showed (limited) significant reductions upon addition of 0.5 m% SAP (compared to the added amount of cement) for both p(DMAEMA$_{100}$)_2 as well as p(DMAEMA$_{100}$)_4 (cfr. 11% and 9% reduction, respectively). Addition of 1 m% SAP resulted in an even more severe decrease (24% and 19% reduction, respectively), implying they could only be used for applications for which the compressive strength is of an inferior importance when compared to water tightness such as swimming pools, reservoirs, etc [13]. Interestingly, when comparing both SAPs, a small significant difference was found in the compressive strength upon addition of 1 m% SAP. This could be explained by the particle size which was larger for the p(DMAEMA$_{100}$)_2 SAPs resulting in the formation of less, but larger pores, compared to more, but smaller pores for the p(DMAEMA$_{100}$)_4.

Commercial SAPs (for a similar mortar workability) did not result in a reduction of the bending strength of the mortar samples either [8]. However, SAP A showed an extremely severe effect (up to 55% reduction by the addition of 1 m% SAP) on the compressive strength. SAP B

performed superior as it showed comparable results as p(DMAEMA$_{100}$)_2 and p(DMAEMA$_{100}$)_4 upon addition of 1 m% SAP. Interestingly, the p(DMAEMA)_x SAPs had a more limited strength reduction compared to the commercial SAPs upon addition of 0.5 m%.

Table III.8: Three-point bending and compressive strength of mortar samples w/o addition of p(DMAEMA)_x SAPs.

p(DMAEMA100)_2		Bending strength [MPa]	Compressive strength [MPa]
0.5 m%	(+ 25 mL water)	7.7 ± 0.5 (/)	56.5 ± 1.7 (-11%)
1 m%	(+ 40 mL water)	6.3 ± 0.5 (-17%)	48.3 ± 2.0 (-24%)
p(DMAEMA100)_4			
0.5 m%	(+ 25 mL water)	7.1 ± 0.7 (-7%)	57.9 ± 2.3 (-9%)
1 m%	(+ 50 mL water)	7.3 ± 0.4 (-4%)	51.4 ± 1.0 (-19%)
SAP A			
0.5 m%	(+ 73 mL water)	7.8 ± 0.0 (/)	41.7 ± 0.9 (-35%)
1 m%	(+ 134 mL water)	6.6 ± 0.1 (-14%)	28.9 ± 1.7 (-55%)
SAP B			
0.5 m%	(+ 22 mL water)	8.0 ± 0.1 (/)	51.2 ± 1.1 (-20%)
1 m%	(+ 43 mL water)	7.7 ± 0.1 (/)	51.3 ± 0.4 (-20%)
Reference			
No SAP	/	6.7 ± 0.4	63.8 ± 1.9

III.3.6. Conclusion and future perspectives

In the present work, 2-(dimethylamino)ethyl methacrylate (DMAEMA) was combined with a varying amount of N,N'-methylene bisacrylamide (MBA, 2 and 4 mol% with respect to monomer present) as a bifunctional cross-linker to successfully synthesize two superabsorbent polymer networks as proven by the complementary results obtained from ATR-IR spectroscopy for polymer structure elucidation and HR-MAS ^{1}H-NMR spectroscopy to assess the cross-linking efficiency. Interestingly, dynamic vapor sorption measurements indicated that these materials showed moisture uptake capacities up to 45% their own weight at a high RH with a slightly higher uptake for p(DMAEMA$_{100}$)_4. The latter was related to their smaller particle size resulting in a larger surface area. The obtained results were compared with commercial SAPs including SAP A (i.e. a copolymer of acrylamide and sodium acrylate) and SAP B (i.e. a cross-linked potassium salt poly(acrylate)). The commercial SAPs showed superior moisture uptake capacities

to the synthesized p(DMAEMA)_x SAPs (120 – 129% vs. 42 – 45% respectively at a RH of 95%), implying they could aid more in the partial sealing of cracks when no water can infiltrate, although their sealing potential when no direct water could enter the crack remains limited. The synthesized SAPs showed a negligible hysteresis, indicating that the amount of moisture taken up could also be desorbed again completely, meaning they could be used as a water reservoir.

The SAPs showed a strong pH-sensitivity as anticipated, due to the pH-responsive nature of DMAEMA. Swelling capacities up to 68 times their own weight in aqueous solutions were obtained. The lower the cross-linker fraction, the higher the swelling potential as anticipated due to a less dense network formation. The swelling potential was lower compared to the commercial SAPs. However, due to its pH-sensitivity, p(DMAEMA)_x swells less during the mixing process of mortar (up to 14 times its weight in cement filtrate solutions) compared to the commercial SAPs (i.e. 61 ± 1 g_{water}/g_{SAP} for SAP A and 58 ± 2 g_{water}/g_{SAP} for SAP B). This should lead to smaller pores in the mortar matrix and thus less effect on the mortar strength. Even at extremely alkaline conditions, these p(DMAEMA)_x polymers showed almost no sign of hydrolysis as proven by ATR-IR spectroscopy.

Finally, three-point bending and compressive strength experiments in mortar showed that no significant differences were obtained for the flexural strength, even for mortars containing up to 1 m% SAP. There was, however, a significant decrease (up to 24%) in compressive strength. Conversely, by comparing with the commercial SAPs, SAP A had a negative effect on the compressive strength (up to 55% decrease), while SAP B performed similar compared to synthesized p($DMAEMA_{100}$)_x upon addition of 1 m%. Upon addition of 0.5 m%, the novel SAPs performed superior, rendering them promising for applications in mortar or concrete. However, due to the limited swelling capacity, high amounts of SAP would be necessary for full self-sealing and -healing of cracks. As an addition of 1 m% already led to 24% decrease in compressive strength, no further self-sealing and -healing tests were performed. Future work could incorporate these experiments to validate this assumption. In the next chapter, all synthetic materials developed have been compared to identify the ‘best’ SAPs so far. Subsequently, a new part of this work will elucidate the potential of polysaccharides as natural cross-linker to create semi-synthetic SAPs.

III.3.7. References

[1] Hasholt MT, Jespersen MHS, Jensen OM. Mechanical properties of concrete with SAP. Part I: Development of compressive strength. Use of Superabsorbent Polymers and Other New Additives in Concrete. 2010.
[2] Snoeck D, Schaubroeck D, Dubruel P, De Belie N. Effect of high amounts of superabsorbent polymers and additional water on the workability, microstructure and strength of mortars with a water-to-cement ratio of 0.50. Construction and Building Materials. 2014;72(0):148-57.
[3] Creutz S, Jérôme R. Effectiveness of block copolymers as stabilizers for aqueous titanium dioxide dispersions of a high solid content. Progress in Organic Coatings. 2000;40(1–4):21-9.
[4] Wang B, Xu X-D, Wang Z-C, Cheng S-X, Zhang X-Z, Zhuo R-X. Synthesis and properties of pH and temperature sensitive P(NIPAAm-co-DMAEMA) hydrogels. Colloids and Surfaces B: Biointerfaces. 2008;64(1):34-41.
[5] Dong L, Agarwal AK, Beebe DJ, Jiang H. Adaptive liquid microlenses activated by stimuli-responsive hydrogels. Nature. 2006;442(7102):551-4.
[6] Wang M, Zou S, Guerin G, Shen L, Deng K, Jones M, et al. A Water-Soluble pH-Responsive Molecular Brush of Poly(N,N-dimethylaminoethyl methacrylate) Grafted Polythiophene. Macromolecules. 2008;41(19):6993-7002.
[7] Herber S, Olthuis W, Bergveld P, van den Berg A. Exploitation of a pH-sensitive hydrogel disk for CO2 detection. Sensors and Actuators B: Chemical. 2004;103(1–2):284-9.
[8] Snoeck D, Dubruel P, De Belie N. How to seal and heal cracks in cementitious materials by using superabsorbent polymers. Application of Superabsorbent Polymers and Other New Admixtures in Concrete Construction: RILEM Publications; 2014. p. 375-84.
[9] Ahmed EM. Hydrogel: Preparation, characterization, and applications: A review. Journal of advanced research. 2015;6(2):105-21.
[10] Bukhari SMH, Khan S, Rehanullah M, Ranjha NM. Synthesis and characterization of chemically cross-linked acrylic acid/gelatin hydrogels: effect of pH and composition on swelling and drug release. International Journal of Polymer Science. 2015.
[11] World Weather and Climate Information. Average humidity in Brussels. https://weather-and-climate.com/average-monthly-Humidity-perc,Brussels,Belgium, accessed on 01/06/2016.
[12] ClimaTemps. Relative Humidity. http://www.climatemps.com/. 04/08/2016.
[13] Perkins PH. Swimming Pools: Design and Construction: CRC Press; 2000.

III.4 Comparison of properties of developed and commercially available SAPs

The previous parts of chapter III described the synthesis and the characterization of synthetic SAPs based on a cross-linked network starting from respectively acrylic acid (AA) (§III.1.), a combination of AA and acrylamide (AM) (§III.2.) and 2-(dimethylamino)ethyl methacrylate (DMAEMA) (§III.3.) using N,N'-methylene bisacrylamide (MBA) as cross-linker. First, AA was combined with 0.2 mol% MBA with respect to the monomer present. In a second part, AM was also added to create a strong gel with substantial swelling potential (up to 111 ± 23 g_{water}/g_{SAP} compared to 46 ± 2 g_{water}/g_{SAP} for pure AA at pH 8). The AA/AM co-monomer ratio was varied between 75/25, 50/50 and 25/75 while the effect of the cross-linker amount was also assessed (i.e. 0.2, 2 and 10 mol%). A variation of the monomer ratio provided an indication of the potential of AM, while a variation of the amount of cross-linker enabled identification of the difference in swelling and moisture uptake potential when applying a low and a high cross-linker amount. The results showed that only the lowest cross-linker concentration (i.e. 0.2 mol%) led to superabsorbent properties. As a result, two materials were selected for further characterization including $p(AA_{75}/AM_{25})\_0.2$ and $p(AA_{50}/AM_{50})\_0.2$. $P(AA_{25}/AM_{75})\_0.2$ was not chosen to characterize further as it had a limited maximal swelling degree (176 ± 2 g_{water}/g_{SAP} compared to 456 ± 17 g_{water}/g_{SAP} for $p(AA_{50}/AM_{50})\_0.2$). The last section (§III.3.) covered the introduction of the pH-responsive, basic monomer DMAEMA in order to increase swelling upon decreasing the pH to around 7 – 8 as it was anticipated that this would reduce pore formation occurring during hardening of mortar samples. Again, the cross-linker amount was varied (2 and 4 mol%) to influence the swelling and the mechanical mortar strength. Cross-linker concentrations as low as 0.2 mol% did not give rise to SAPs with gel-like characteristics.

Chemical structure elucidation occurred through attenuated total-reflectance infrared spectroscopy, which indicated that all monomers were incorporated in the polymer networks thereby creating the targeted SAPs. In addition, high resolution magic-angle spinning (HR-MAS) ^{1}H-NMR spectroscopy enabled the quantification of the cross-linking efficiency. As anticipated, the signals corresponding with the H-atoms from C=C (5.5 – 6.5 ppm) shifted towards the peaks characteristic for H-atoms from C-C (1.5 – 2.5 ppm). For a limited number of SAPs, a negligible amount of the former H-atoms were remaining (i.e. $p(DMAEMA_{100})\_x$).

In the upcoming section, a comparative study has been presented by providing an overview of the most relevant synthetic SAPs together with their moisture uptake capacity, their swelling capacity and the resulting strength upon incorporation in mortar in order to identify the best performing synthetic SAPs and to compare their potential with their commercially available counterparts. In this comparative study, the synthetic SAPs have been compared to data obtained for commercial SAP A (copolymer of acrylamide and sodium acrylate) and SAP B (cross-linked potassium salt poly(acrylate)) [1].

III.4.1. Comparative assessment of the moisture uptake capacity of synthetic SAPs

A first important aspect associated with SAPs is their moisture uptake capacity, which could be determined by dynamic vapor sorption measurements. Interestingly, all materials showed a negligible hysteresis, implying that the moisture taken up by the SAPs at a high relative humidity (RH) will also be completely desorbed upon decreasing RH. The latter is relevant for the envisaged application as constructions which are not exposed to water can still retain a certain amount of moisture from air, at a high RH (≥ 90%). When the RH drops again, they are able to deliver the moisture to remaining unreacted cement particles, thereby contributing to the development of self-healing concrete.

Table III.9: Comparative study of the moisture uptake capacity of the most relevant synthetic SAPs at 60, 90 and 95% relative humidity (RH). The values are compared to the data from two commercial SAPs [1].

Moisture uptake capacity [%]	60% RH	90% RH	95% RH
p(AA_{100})_0.2	2	28	40
p(AA_{50}/AM_{50})_0.2	6	21	30
p(AA_{75}/AM_{25})_0.2	5	23	31
p($DMAEMA_{100}$)_2	6	30	42
p($DMAEMA_{100}$)_4	6	32	46
SAP A	26	83	129
SAP B	28	84	120

When comparing the moisture sorption data (Table III.9), particularly the values for a RH of 60% are of relevance for application in countries with a low RH (e.g. New York is characterized by an annual RH of 58%, while Athens corresponds with 62% [2]), while a RH of 90% is close to for example the annual average RH in Brussels being 83% [2, 3]. As this average RH varies from month to month, it is important to obtain a general idea of the moisture uptake capacity so a RH of 90% was also selected. A RH of 95% might be important in rainy weather conditions for SAPs to be applied in constructions where no direct water can infiltrate the concrete cracks. Table III.9 shows that at 60% RH, all moisture sorption values were low compared to the commercial SAPs, with p(AA_{100})_0.2 exhibiting the lowest moisture uptake (i.e. 2%). The moisture uptake of the other SAPs ranged between 5 and 6%. It could be discussed whether the value of p(AA_{100})_0.2 was significantly lower than the others as it lies close to the detection limit of the equipment (2 – 3% for SAPs). It could however be concluded that all synthesized SAPs had a lower moisture uptake capacity than the commercial SAPs (26 – 28%). It is more important to compare the uptake values at higher RH. At 90% RH, p(AA_{50}/AM_{50})_0.2 and p(AA_{75}/AM_{25})_0.2 only took up 21

and 23% of water vapor respectively, while p(AA_{100})_0.2, p($DMAEMA_{100}$)_2 and p($DMAEMA_{100}$)_4 showed values increasing up to 28%, 30 and 32% respectively. This was expected as the latter three materials constitute pH-responsive monomers which become charged upon contact with moisture, while the first two SAPs partly contain AM, which does not possess this pH-sensitivity. The SAPs still had a 2 – 3 times lower moisture uptake than what was found for the commercial SAPs (83 – 84%). When further increasing the RH to 95%, a similar trend could be observed. P(AA_{50}/AM_{50})_0.2 and p(AA_{75}/AM_{25})_0.2 showed sorption levels of 30 and 31% respectively, while p(AA_{100})_0.2 had a moisture uptake capacity of 40% versus 42 and 46% for p($DMAEMA_{100}$)_2 and p($DMAEMA_{100}$)_4 respectively. A similar explanation could be given as for 90% RH. Again, these values were 3 – 4 times lower than the values for SAP A and B (129 and 120% respectively). It can be concluded that particularly at high RH, p($DMAEMA_{100}$)_2 and p($DMAEMA_{100}$)_4 exhibited more sorption compared to the other synthetic SAPs, closely followed by p(AA_{100})_0.2. These results are in agreement with moisture uptake results for copolymers of AA and AM with montmorillonite at a RH of 90%, as described earlier in literature [4]. Interestingly, they observed a higher moisture uptake capacity at 60% RH (around 40%). This could either be related to the use of montmorillonite as this clay also possesses substantial swelling potential [5] or to the use of a different moisture uptake capacity technique by adding a thermo-transducer as moisture sensor. The synthesized SAPs took up more moisture compared to poly(propylene glycol)/poly(acrylic acid) interpenetrating polymer network hydrogels which have been studied earlier in literature [6]. Nonetheless, the synthesized SAPs are outperformed by the commercial SAPs and further optimization is required (see chapter IV).

III.4.2. Comparative evaluation of the swelling potential

The most important characteristic of a SAP, prior to incorporation in mortar is its swelling capacity as a function of pH. Fresh mortar is characterized by an extremely alkaline pH around 12.5 – 13. However, external water entering cracks has a lower pH depending on the environment and the degree of leaching of ions from the matrix (cfr. neutral to slightly alkaline pH). First, the swelling potential of p(AA_{100})_0.2 has been compared with p(AA_{50}/AM_{50})_0.2 and p(AA_{75}/AM_{25})_0.2. As anticipated, the AM-based materials both outperformed p(AA_{100})_0.2 at any pH (except for p(AA_{50}/AM_{50}) _0.2 at pH 13) as p(AA_{100})_0.2 was affected by the presence of cations (cfr. addition of NaOH to reach alkaline pH) which leads to a shielding effect of the counter ion towards the poly-anion chain [7]. Addition of AM led to increased swelling. When comparing both p(AA_{50}/AM_{50})_0.2 and p(AA_{75}/AM_{25})_0.2, no significant difference ($p < 0.05$) could be found at pH 12 (i.e. 433.7 ± 15.1 g_{water}/g_{SAP} and 455.8 ± 17.0 g_{water}/g_{SAP}) at which maximal swelling occurred. The extremely high swelling of these three polymers at pH 12 was the result of hydrolysis of the amide groups [8-11]. First, the amide moieties of AM started to hydrolyze, while further increasing the pH led to the hydrolysis of the internal secondary amide moieties of MBA. By hydrolyzing the cross-linker, the network first started to become less dense (cfr. extremely high swelling at pH 12) followed by a severe degradation of the network (at pH 13). However, upon decreasing the pH to 10 (or 8), the swelling capacity of p(AA_{50}/AM_{50}) _0.2 becomes superior compared to p(AA_{75}/AM_{25}) _0.2. At this point, there was no hydrolysis and the superior swelling potential of the higher molar concentration of AM would be related to the

screening effect of the Na^+ cation on the AA [12-14]. Only at pH 13, p(AA_{75}/AM_{25})_0.2 exhibited more swelling. The higher swelling was an indication that the network had degraded less for p(AA_{75}/AM_{25})_0.2 than p(AA_{50}/AM_{50}) _0.2. However, as already mentioned earlier, it is especially important to obtain a high swelling at neutral to slightly alkaline pH in aqueous solutions (infiltrating water in cracks) instead of in cement filtrate (CF) solutions (during the mixing process). Swelling in cement filtrate solutions was for all SAPs studied rather low (between 12 and 17 g_{water}/g_{SAP}), with a significantly higher swelling only for p(AA_{50}/AM_{50})_0.2. Table III.10 shows that the swelling capacity of p(AA_{50}/AM_{50})_0.2 was superior over all synthetic SAPs compared. In case of lower cross-linker concentrations (p($DMAEMA_{100}$)_2 versus p($DMAEMA_{100}$)_4), the swelling capacity rose at pH ≤ 12. Interestingly, p($DMAEMA_{100}$)_2 only outperformed p(AA_{50}/AM_{50})_0.2 at pH 3 (cfr. 68.0 ± 1.4 vs. 18.2 ± 1.0) due to its pH-responsiveness, rendering these SAPs interesting for the ingress of and swelling in acidic rain. However, generally, rain has a pH closer to 6 – 7, at which p(AA_{50}/AM_{50})_0.2 showed far superior swelling. Overall, p(AA_{50}/AM_{50})_0.2 possessed the highest swelling capacity of all synthetic SAPs studied at neutral to slightly alkaline pH, followed by p(AA_{75}/AM_{25})_0.2. P($DMAEMA_{100}$)_2 is especially useful to be applied in very acidic conditions.

When comparing the obtained data with the swelling capacity of the commercial SAPs in aqueous solutions (i.e. 305 ± 4 g_{water}/g_{SAP} for SAP A and 283 ± 2 g_{water}/g_{SAP} for SAP B [1]) and CF solutions (i.e. 61 ± 1 g_{water}/g_{SAP} for SAP A and 58 ± 2 g_{water}/g_{SAP} for SAP B [1]) it was found that both SAP A and B exhibited a lower maximal swelling capacity compared to p(AA_{100})_0.2, p(AA_{75}/AM_{25})_0.2 and p(AA_{50}/AM_{50})_0.2. However, these values were obtained at pH 12, at which part of the SAP was already hydrolyzed. At neutral pH, the commercial SAPs showed superior swelling properties. This was also observed for other tested poly(acrylate) and poly(acrylic acid-co-acrylamide) SAPs in literature. Their swelling capacity in demineralized water goes up to 200 – 300 g_{water}/g_{SAP} [15]. This is higher than what was found around neutral pH for the synthesized SAPs. So further optimization is still necessary. Interestingly, the superior swelling potential in CF solutions for SAP A and B (4 – 6 times higher than the synthesized SAPs) is disadvantageous as this suggests they already swell extensively during mixing in mortar, which would lead to extensive macro-pore formation and thus a severe decrease in mortar strength (as discussed further in §III.4.3.). The swelling values of the synthetic SAPs were however comparable to what was found in a synthetic pore solution [15]. Interestingly, when comparing these data with the DVS results, some differences can be observed, which can be explained based on two phenomena. First, there was no variation between the moisture uptake capacity of p($DMAEMA_{100}$)_2 and p($DMAEMA_{100}$)_4, because the moisture uptake is not influenced by the cross-linking density (Table III.3, §III.2.3.). The network density, on the other hand, does have an influence on the swelling capacity. Secondly, p(AA_{100})_0.2 took up more moisture compared to p(AA_{75}/AM_{25})_0.2 or p(AA_{50}/AM_{50})_0.2 because in water vapor, no cations are present which can result in a screening effect. Additionally, the carboxylate moieties will be able to take up more moisture than the amides.

Finally, when comparing the degradation of the synthesized SAPs in CF, p(AA_{100})_0.2 was prone to hydrolysis. However, the sharp peak of γ(N-H) at 876 cm^{-1}, resulting from the primary amine formed by hydrolysis of the internal amide groups from the cross-linker, was only visible to a

minor extent. This also explained the swelling trend upon varying pH (§III.2.4.). A similar conclusion could be drawn for p(AA_{75}/AM_{25})_0.2 and p(AA_{50}/AM_{50})_0.2, for which the ν_{as}(C-O) and ν_s(C-O) peaks from the acrylates became apparent while the sharp peak of γ(N-H) at 876 cm^{-1} was not clearly visible, even in a CF solution at pH 13 (with additional NaOH). Interestingly, both p($DMAEMA_{100}$)_2 and p($DMAEMA_{100}$)_4 did not show a significant degree of hydrolysis, which makes them more interesting should the swelling capacity be further increased.

Table III.10: Comparative study of the swelling capacity of the synthetic SAPs in both aqueous solutions of varying pH as well as in cement filtrate solution (CF). The maximal value per material is underlined.

Aq. Sol.	p(AA_{100})_0.2	p(AA_{50}/AM_{50})_0.2	p(AA_{75}/AM_{25})_0.2	p($DMAEMA_{100}$)_2	p($DMAEMA_{100}$)_4
pH 3	30.6 ± 1.1	18.2 ± 1.0	16.5 ± 0.1	<u>68.0 ± 1.4</u>	<u>41.5 ± 1.8</u>
pH 6	34.8 ± 1.8	116.55 ± 0.0	56.9 ± 1.4	39.1 ± 2.7	28.2 ± 1.4
pH 8	45.5 ± 2.3	110.6 ± 23.0	62.7 ± 1.8	41.7 ± 1.9	30.9 ± 2.5
pH 10	41.9 ± 1.3	143.2 ± 48.2	99.2 ± 14.2	39.2 ± 1.1	25.2 ± 1.0
pH 12	<u>393.3 ± 14.0</u>	<u>455.8 ± 17.0</u>	<u>433.7 ± 15.1</u>	21.5 ± 2.7	17.3 ± 0.7
pH 13	54.6 ± 3.8	55.3 ± 5.5	128.0 ± 1.4	12.0 ± 1.3	14.5 ± 2.0
CF	11.8 ± 0.6	17.1 ± 0.4	12.8 ± 0.0	13.3 ± 0.9	14.0 ± 0.3

III.4.3. Bending and compressive strength of SAP-containing mortar

After extensive SAP characterization, the discussion focuses on the incorporation of these SAPs in mortar for potentially identifying a reduction of the mortar strength. As the latter is mortar batch-dependent, the reference was included for each of the samples evaluated (see Table III.11).

When comparing the AA-containing SAPs, the addition of 0.5 m% (with respect to the added amount of cement) did not result in a decrease of the bending strength of mortar. However, the addition of 1 m% SAP resulted in a significant decrease of the bending strength with 13% for p(AA_{100})_0.2 and p(AA_{75}/AM_{25})_0.2 and up to 25% for p(AA_{50}/AM_{50})_0.2. In addition, for all SAPs evaluated, a compressive strength reduction was observed, albeit limited upon introducing 0.5 m% p(AA_{100})_0.2 (i.e. 6%) while the addition of 1 m% resulted in a more significant strength reduction (i.e. 22%). The effect is related to the irregularity of the shape of the SAP particles, which causes the compressive strength to be lower than what would be the case for spherical SAPs. For the bending strength, two influences need to be taken into account. Internal curing provided by the SAPs would increase the bending strength, but the presence of macro-pores in the cross-sectional area decreases the bending strength. This is why the bending strength is generally less influenced.

For the AM-containing materials, even the addition of 0.5 m% SAP already resulted in a severe decrease of the compressive strength although p(AA_{75}/AM_{25})_0.2 performed better compared to p(AA_{50}/AM_{50})_0.2. The latter was anticipated, due to the distinct presence of (multivalent) cations. The presence of dissolved cations in the cement filtrate (K^+, Na^+, Mg^{2+} and Ca^{2+}) counter the repelling effect of the carboxylate moieties and decrease the swelling capacity in CF substantially. Secondly, the presence of divalent cations (Mg^{2+} and Ca^{2+}) exerts an additional reductive effect on the swelling properties due to electrostatic interactions [16, 17]. As such, the higher molar fraction of AA/AM in p(AA_{75}/AM_{25})_0.2 would lead to a lower swelling in CF and thus in mortar, which would result in the formation of smaller macro-pores and a more limited effect on the compressive strength of mortar. The same explanation applies for p(AA_{100})_0.2, which contains the highest fraction of carboxylate moieties. Additionally, the limited effect on the mortar strength of p(AA_{100})_0.2 could also be related to its low swelling capacity compared to the AA/AM-based SAPs. The higher swelling capacity of p(AA_{50}/AM_{50})_0.2 and p(AA_{75}/AM_{25})_0.2 led to a strong water uptake during mixing, which resulted in the formation of larger pores and thus a more severe drop in the compressive strength of the mortar samples.

From a mechanical point-of-view, it was anticipated that the p(DMAEMA)-based SAPs would perform superior as they showed a pH-responsive behavior resulting in more swelling in a aqueous solution with a lower pH compared to upon exposure to alkaline conditions during mixing. As indicated in Table III.11, no significant differences could be observed between the flexural strengths of the different mortar samples, while a minor reduction of the compressive strength was obtained upon introducing 0.5 m% SAP (i.e. 9 and 11% for p($DMAEMA_{100}$)_4 and p($DMAEMA_{100}$)_2 respectively). However, the addition of 1 m% SAP resulted in a decrease (19 and 24% respectively) in the same order of magnitude as observed for p(AA_{100})_0.2. The less dense network, being p($DMAEMA_{100}$)_2, showed a more pronounced effect on the compressive strength compared to p($DMAEMA_{100}$)_4 due to its higher swelling capacity, albeit limited. Upon comparing the effect of the synthesized SAPs on the mortar strength with the commercial SAPs, the latter did not show any effect on the bending strength upon addition of 0.5 m%, while 1 m% of SAP A led to a bending strength reduction of 14%. However, both SAPs had a significant effect on the compressive strength. Mortars with SAP A showed an extremely severe reduction in compressive strength (i.e. 35 and 55% upon addition of 0.5 and 1 m% respectively), which was inferior to all synthesized SAPs. Mortars with SAP B showed a reduction of 20% upon addition of 0.5 m% SAP, performing worse than p(AA_{100})_0.2, p($DMAEMA_{100}$)_2 and p($DMAEMA_{100}$)_4 and were comparable to p(AA_{75}/AM_{25})_0.2. Addition of 1 m% SAP B led to an identical reduction of 20%, similar as p(AA_{100})_0.2 and p($DMAEMA_{100}$)_4 and slightly better than p($DMAEMA_{100}$)_2. In conclusion, p($DMAEMA_{100}$)_4 performed superior when considering all aspects associated with mortar strength, closely followed by p(AA_{100})_0.2 and SAP B. SAP A is not useful for the targeted application of self-healing of cracks and p(AA_{50}/AM_{50})_0.2 also had a severe effect on the strength.

As already discussed earlier in literature, the effect SAPs have on mortar depends strongly on the required amount. To mitigate autogenous shrinkage, only small amounts (0.1 – 0.3 m%) are needed, which often leads to no or only a limited compressive strength reduction [18-20].

However, for the intended application, high amounts of SAP are required (up to 1 m%) which causes a more severe effect on the strength [16, 21]. Interestingly, p($DMAEMA_{100}$)_4 and p(AA_{100})_0.2 could compete with commercial SAP B regarding their effect on the mortar strength although they had a more limited swelling capacity compared to the latter. Due to this low swelling, they were not tested for their self-sealing potential by water permeability tests. Only p(AA_{75}/AM_{25})_0.2 and p(AA_{50}/AM_{50})_0.2, which had superior swelling capacities, were tested for self-sealing purposes.

Table III.11: Comparative study of the bending and compressive strength of mortar samples upon SAP addition. The colors indicate the percentage strength reduction: (x < 10%), (10% < x < 20%), (20% < x < 30%) and (x > 30%).

Sample	Added percentage of SAP	Bending strength [MPa]	Compressive strength [MPa]	Batch
Reference 1	No SAP	8.4 ± 0.4 6.7 ± 0.4 7.6 ± 1.1 7.7 ± 0.4	63.2 ± 1.3 63.8 ± 1.9 63.8 ± 1.9 65.4 ± 3.2	1 2 3 4
p(AA_{100})_0.2	0.5 m%	7.7 ± 0.3 (-9%)	59.2 ± 1.4 (-6%)	1
	1 m%	7.3 ± 0.5 (-13%)	49.6 ± 3.0 (-22%)	1
p(AA_{50}/AM_{50})_0.2	0.5 m%	6.6 ± 0.4 (-1%)	47.0 ± 1.3 (-26%)	2
	1 m%	5.0 ± 0.1 (-25%)	30.6 ± 0.7 (-52%)	2
p(AA_{75}/AM_{25})_0.2	0.5 m%	6.5 ± 0.6 (-3%)	51.9 ± 0.9 (-19%)	2
	1 m%	5.8 ± 0.1 (-13%)	44.2 ± 0.9 (-31%)	2
p($DMAEMA_{100}$)_2	0.5 m%	7.7 ± 0.5 (/)	56.5 ± 1.7 (-11%)	3
	1 m%	6.3 ± 0.5 (-17%)	48.3 ± 2.0 (-24%)	3
p($DMAEMA_{100}$)_4	0.5 m%	7.1 ± 0.7 (-7%)	57.9 ± 2.3 (-9%)	3
	1 m%	7.3 ± 0.4 (-4%)	51.4 ± 1.0 (-19%)	3
SAP A	0.5 m%	7.8 ± 0.0 (/)	41.7 ± 0.9 (-35%)	4
	1 m%	6.6 ± 0.1 (-14%)	28.9 ± 1.7 (-55%)	4
SAP B	0.5 m%	8.0 ± 0.1 (/)	51.2 ± 1.1 (-20%)	4
	1 m%	7.7 ± 0.1 (/)	51.3 ± 0.4 (-20%)	4

III.4.4. Evaluation of valorization opportunities of synthetic SAPs

Not only the SAP's characteristics, but also its cost is an important factor, in particular with respect to assessment of their commercialization potential. Taking into account the cost accounted for by bulk manufacturers for monomer and cross-linker production, an estimate was made for the additional price for SAP modification per m³ concrete upon introducing SAPs. Considering a cement content of 300 kg/m³ of concrete and upon addition of 1 m% SAP versus cement weight, the additional cost associated with the use of SAPs in concrete could be calculated (Table III.12).

Table III.12: Additional cost, calculated by using bulk prices for the monomers and cross-linker, associated with the application of synthetic SAPs in concrete.

Price	p(AA_{100}) _0.2	p(AA_{50}/AM_{50}) _0.2	p(AA_{75}/AM_{25}) _0.2	p($DMAEMA_{100}$) _2	p($DMAEMA_{100}$) _4
€/kg	0.9	1.3	1.1	2.7	2.9
€/m³ concrete	2.7	3.9	3.3	8.2	8.6

These additional cost values can be compared with the cost of different self-healing mechanisms (comparative study performed by Snoeck et al. [22]) such as the use of autonomous polymeric healing by capsules containing polyurethane [23] (€ 630 /m³ concrete), bacterial healing through encapsulation in diatomaceous earth (€ 11.3 – 50.9 /m³ concrete), microcapsules (€ 154.8 – 469.2 /m³ concrete) or SAPs [24] (€ 35.7 – 81 /m³ concrete) or the use of SAPs separately with (€ 70.2 /m³ concrete) or without (€ 9 /m³ concrete) additional microfibers. The last price was calculated for commercial SAP B. Table III.12 indicates that most of the synthetic SAPs developed are rather cost-effective and even outperform commercially available SAPs [22]. However, these prices do not take into account any profit nor production margins. If a production margin for the manufacturer of 50% of the bulk price is taken and a profit margin of 20% of the bulk price, the prices of the synthesized SAPs would be € 1.5 – 4.9 /kg or € 4.6 – 15 /m³ concrete. This would imply that the prices of p(AA_{100})_0.2, p(AA_{50}/AM_{50}) _0.2 and p(AA_{75}/AM_{25}) _0.2 would be lower than for SAP B and especially more cost-effective compared to all other self-healing systems. The prices of p($DMAEMA_{100}$)_2 and p($DMAEMA_{100}$)_4 are about 1.5 times higher than for SAP B, but still lower than for all other self-healing systems. The cost of p(AA_{100})_0.2 was the lowest, followed closely by p(AA_{75}/AM_{25})_0.2 and p(AA_{50}/AM_{50})_0.2. The latter is related to the higher price of acrylamide compared to acrylic acid. DMAEMA, on the other hand, is the most expensive monomer employed for the production of synthetic SAPs herein. Normal concrete has a price of approximately € 65 /m³ concrete. This means that the price would go up with 7 – 23 %. This is definitely an acceptable surplus as manual injection of one crack per m³ concrete in a tunnel would cost € 120 – 140 /m³, which is far more expensive [22].

III.4.5. Conclusion

It can be concluded that although the cost of p(AA_{100})_0.2 is extremely low, it was prone to hydrolysis and had a limited swelling capacity which makes them inappropriate for the envisaged application. P(AA_{50}/AM_{50})_0.2 has proven to be a material with a superior swelling capacity compared to the other synthesized SAPs, which on the other hand resulted in a severe decrease of the compressive strength of mortar. P(AA_{75}/AM_{25})_0.2 is more cost-effective and showed a less severe effect on the compressive strength. It possessed, however, a smaller swelling capacity at neutral pH compared to p(AA_{50}/AM_{50})_0.2. Interestingly, despite their effect on the strength, both p(AA_{50}/AM_{50})_0.2 and p(AA_{75}/AM_{25})_0.2 showed a strong self-sealing capacity as indicated by water permeability (Figure III.16, §III.2.6.). The latter was only performed on these materials, as the other SAPs still require further improvement regarding their swelling properties. Therefore, this parameter was not taken into account for the comparative study. Both AA/AM-based SAPs also showed an inferior moisture uptake capacity at high RH compared to p(AA_{100})_0.2. this parameter is however less important for the envisaged application than the swelling capacity. P($DMAEMA_{100}$)_2 performed better compared to p($DMAEMA_{100}$)_4 when considering its swelling capacity and showed a similar moisture uptake capacity at high RH. Addition of both these DMAEMA-based SAPs led to a similar decrease in the mortar strength. As a result, the greater swelling capacity and lower cost (albeit a substantially higher cost than for p(AA_{100})_0.2) renders p($DMAEMA_{100}$)_2 more attractive than p($DMAEMA_{100}$)_4. It is not straightforward to select the most appropriate material fulfilling all requirements since a superior performance with respect to one parameter is often associated with inferior performance considering another parameter. If the effect on the mortar strength could be minimized, p(AA_{50}/AM_{50})_0.2 and p(AA_{75}/AM_{25})_0.2 SAPs would be performing best for the synthesized SAPs. When comparing the obtained data to what was obtained for commercial SAPs, it was found that the latter showed a superior moisture uptake capacity. On the other hand, p(AA_{100})_0.2, p(AA_{50}/AM_{50})_0.2 and p(AA_{75}/AM_{25})_0.2 showed a stronger maximal swelling capacity than the commercial SAPs, but it should be noted that this was achieved at pH 12, at which the synthesized SAPs already showed partial hydrolysis. When comparing at neutral pH, the commercial SAPs still showed a superior swelling. P(AA_{100})_0.2, p($DMAEMA_{100}$)_2 and p($DMAEMA_{100}$)_4 showed a better performance regarding the compressive strength of mortar upon addition of 0.5 m% SAP than commercial SAP B. When adding 1 m%, only p($DMAEMA_{100}$)_4 and p(AA_{100})_0.2 performed similar to SAP B. SAP A, on the other hand, performed worse than all synthesized SAPs. Finally, the prices of p(AA_{100})_0.2, p(AA_{50}/AM_{50})_0.2 and p(AA_{75}/AM_{25})_0.2 are estimated to be cheaper than SAP B, while p($DMAEMA_{100}$)_2 and p($DMAEMA_{100}$)_4 are about 1.5 times more expensive. Nevertheless, these prices are still much lower than for other healing systems and manual injection.

III.4.6. References

[1] Snoeck D, Dubruel P, De Belie N. How to seal and heal cracks in cementitious materials by using superabsorbent polymers. Application of Superabsorbent Polymers and Other New Admixtures in Concrete Construction: RILEM Publications; 2014. p. 375-84.
[2] ClimaTemps. Relative Humidity. http://www.climatemps.com/. 04/08/2016.
[3] World Weather and Climate Information. Average humidity in Brussels. https://weather-and-climate.com/average-monthly-Humidity-perc,Brussels,Belgium, accessed on 01/06/2016.
[4] Gao D, Heimann RB, Lerchner J, Seidel J, Wolf G. Development of a novel moisture sensor based on superabsorbent poly(acrylamide)-montmorillonite composite hydrogels. J Mater Sci. 2001;36(18):4567-71.
[5] Segad M, Jönsson B, Åkesson T, Cabane B. Ca/Na Montmorillonite: Structure, Forces and Swelling Properties. Langmuir. 2010;26(8):5782-90.
[6] Kim SJ, Lee KJ, Kim SI. Water sorption of poly(propylene glycol)/poly(acrylic acid) interpenetrating polymer network hydrogels. Reactive and Functional Polymers. 2003;55(1):69-73.
[7] Li A, Wang A, Chen J. Studies on poly (acrylic acid)/attapulgite superabsorbent composites. II. Swelling behaviors of superabsorbent composites in saline solutions and hydrophilic solvent–water mixtures. Journal of Applied Polymer Science. 2004;94(5):1869-76.
[8] Kulkarni RV, Sa B. Polyacrylamide-Grafted-Alginate-Based pH-Sensitive Hydrogel Beads for Delivery of Ketoprofen to the Intestine: in Vitro and in Vivo Evaluation. Journal of Biomaterials Science, Polymer Edition. 2009;20(2):235-51.
[9] Kurenkov VF, Hartan HG, Lobanov FI. Alkaline Hydrolysis of Polyacrylamide. Russian Journal of Applied Chemistry. 2001;74(4):543-54.
[10] Rabbii MEZaA. Alkaline Hydrolysis of Polyacrylamide and Study on Poly(acrylamide-co-sodium acrylate) Properties. Iranian Polymer Journal. 2002;11(4):269-75.
[11] Rahna K Shamsudeen SNVGJ. Equilibrium swelling conductivity and electroactive characteristics of polyacrylamide hydrogels. Indian Journal of Engineering & Materials Sciences. 2006;13(2006):62-8.
[12] Pourjavadi A, Jahromi PE, Seidi F, Salimi H. Synthesis and swelling behavior of acrylatedstarch-g-poly (acrylic acid) and acrylatedstarch-g-poly (acrylamide) hydrogels. Carbohydrate Polymers. 2010;79(4):933-40.
[13] Tomar RS, Gupta I, Singhal R, Nagpal AK. Synthesis of poly (acrylamide-co-acrylic acid) based superabsorbent hydrogels: Study of network parameters and swelling behaviour. Polymer-Plastics Technology and Engineering. 2007;46(5):481-8.
[14] Rabat NE, Hashim S, Majid RA. Effect of Different Monomers on Water Retention Properties of Slow Release Fertilizer Hydrogel. Procedia Engineering. 2016;148:201-7.
[15] Lee HXD, Wong HS, Buenfeld NR. Potential of superabsorbent polymer for self-sealing cracks in concrete. Advances in Applied Ceramics. 2010;109(5):296-302.
[16] Snoeck D, Schaubroeck D, Dubruel P, De Belie N. Effect of high amounts of superabsorbent polymers and additional water on the workability, microstructure and strength of mortars with a water-to-cement ratio of 0.50. Construction and Building Materials. 2014;72(0):148-57.
[17] Hancock RD, Martell AE. Ligand design for selective complexation of metal ions in aqueous solution. Chemical Reviews. 1989;89(8):1875-914.
[18] Schröfl C, Mechtcherine V, Gorges M. Relation between the molecular structure and the efficiency of superabsorbent polymers (SAP) as concrete admixture to mitigate autogenous shrinkage. Cement and Concrete Research. 2012;42(6):865-73.
[19] Hasholt MT, Jensen OM, Kovler K, Zhutovsky S. Can superabsorbent polymers mitigate autogenous shrinkage of internally cured concrete without compromising the strength? Construction and Building Materials. 2012;31:226-30.
[20] Mechtcherine V, Schroefl C, Gorges M. Effectiveness of various superabsorbent polymers (SAP) in mitigating autogenous shrinkage of cement-based materials. Mechanics and Physics of Creep, Shrinkage, and Durability of Concrete: Proceedings of the Ninth International Conference on Creep,

Shrinkage, and Durability Mechanics (CONCREEP-9), September 22-25, 2013 Cambridge, Massachusetts: ASCE Publications; 2013. p. 324.
[21] Kovler K. Effect of superabsorbent polymers on the mechanical properties of concrete. Application of Super Absorbent Polymers (SAP) in Concrete Construction: Springer; 2012. p. 99-114.
[22] Snoeck D. Self-healing and microstructure of cementitious materials with microfibres and superabsorbent polymers. PhD thesis: Ghent University; 2015.
[23] Van Tittelboom K. Self-Healing Concrete through Incorporation of Encapsulated Bacteria-or Polymer-Based Healing Agents. PhD thesis Ghent University; 2012.
[24] Wang J. Self-healing concrete by means of immobilized carbonate precipitating bacteria. PhD thesis: Ghent University; 2013.

IV. Implementation of polysaccharides to create semi-synthetic SAPs for self-sealing and self-healing of cracks in mortar

IV.1 The high potential of biopolymers for sustainable concrete repair

Nowadays, reports have been presented in literature regarding synthetic superabsorbent polymers (SAPs) used in concrete for various applications such as internal curing [1, 2], frost resistance [3, 4] and crack-sealing and -healing [5-7]. Synthetic SAPs have already been proven to be promising as a smart internal solution for self-sealing of cracks in mortar, as indicated in §III.2. However, as already mentioned earlier, these materials often compromise the material strength, which is undesired in the construction industry. On the one hand, the SAP particles cause internal curing by releasing their entrained mixing water, stimulating the densification and further hydration of the cementitious matrix, and reducing autogenous shrinkage and hence the risk of early age cracking. These consequences can lead to an increase of the overall material strength. Conversely, after the release of the entrained water by the SAPs, air-filled macropores remain present in the matrix, which generally lead to a decrease of the overall concrete strength [3, 8, 9]. As for self-sealing [10] and self-healing applications [5, 9] high SAP amounts are required (up to 1 % relative to cement mass), the macropore formation becomes more critical especially when high amounts of additional water are used to compensate for the loss in workability.

The previous chapter focused on the effect of changing the used monomers (i.e. acrylic acid (AA) in §III.1., a copolymer of AA and acrylamide in §III.2. and dimethylaminoethyl methacrylate in §III.3.). Instead, in the present chapter, natural polysaccharides have been introduced to act as multi-functional cross-linker to replace the synthetic bifunctional cross-linker N,N'-methylene bisacrylamide (MBA) (as implemented in §III.1–3). More specifically, the potential of a novel biopolymer (i.e. alginate) has been evaluated in this first part of the chapter because of several benefits associated with the use of polysaccharides. Indeed, in addition to its low cost [11], polysaccharides might also contribute to a sustainable approach for concrete repair through natural materials.

Sodium alginate is a water-soluble anionic polysaccharide extracted from the cell walls of brown algae. It is a linear copolymer composed of mannuronic and guluronic acid, covalently linked in varying sequences and blocks and is commercially available as a sodium salt (NaAlg). Interestingly, when NaAlg is combined with multivalent cations such as calcium (originating from salts such as calcium chloride, $CaCl_2$), a physically cross-linked network is formed, which becomes insoluble in water in the absence of monovalent cations. Alginate has only been reported scarcely so far in combination with concrete. It has been described that alginate can form gels upon contact with cementitious materials and has the ability to protect microorganisms (*Sporosarcina pasteurii*) [12]. However, they have not been used as the main healing agent. The healing mechanism relies on bacteria-induced self-healing. In earlier research of our group

This work has been published as: Mignon Arn, Snoeck Didier, D'Halluin Kenny, Balcaen Lieve, Vanhaecke Frank, Dubruel Peter, Van Vlierberghe Sandra and De Belie Nele (2016). Alginate biopolymers: Counteracting the impact of superabsorbent polymers on mortar strength. Construction and Building Materials, 110, 169-174.

ureolytic bacteria (*Bacillus sphaericus*) have been incorporated in a cross-linked Pluronic F-127 bismethacrylate hydrogel to realize a smart, two-step self-healing approach [13, 14]. However, a severe effect on the strength was observed, so a need for a superior hydrogel is necessary.

The present work aims to evaluate the potential of both NaAlg as well as physically cross-linked CaAlg as SAPs to establish a sustainable approach towards self-sealing and -healing concrete without impairing mechanical strength. To this end, (cross-linked) alginate has herein been characterized by first using dynamic vapor sorption measurements to determine the moisture uptake capacity. Subsequently, the swelling properties in both demineralized water as well as in cement filtrate solution have been tested. In a final part, the mechanical properties of mortar mixtures in the absence and in the presence of SAPs have been examined by performing flexural and compressive tests. All properties have been compared with those obtained before using commercially available synthetic SAPs from BASF (SAP A, a copolymer of acrylamide and sodium acrylate, particle size of 100.0 ± 21.5 µm and SAP B, a cross-linked potassium salt poly(acrylate), particle size of 476.6 ± 52.9 µm) [15]. The results acquired when using alginate are anticipated to provide an indication of the applicability of biopolymers in the field of self-sealing and self-healing concrete and will therefore assist in guiding future research in the field.

IV.1.1. Moisture uptake capacity measurements

Over 95% of the obtained CaAlg particle sizes ranged from 2 to 85 µm for NaAlg and from 2 to 101 µm for CaAlg. In order to assess the potential superabsorbent properties of NaAlg and CaAlg, dynamic vapor sorption (DVS) measurements have been performed. The technique enables to determine the equilibrium moisture content as a function of the relative humidity (RH), as depicted in sorption isotherms (see Figure IV.1).

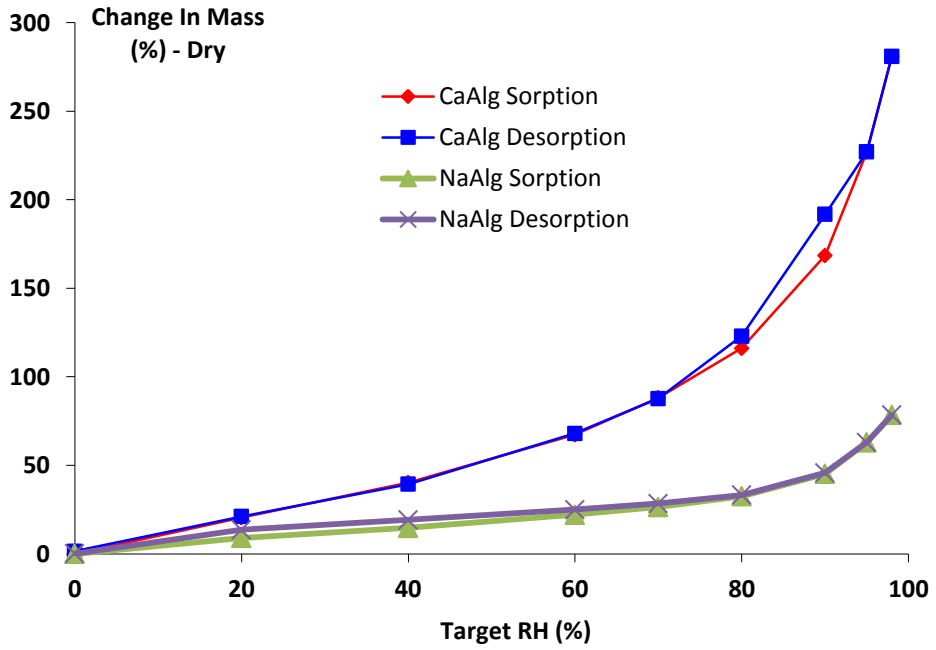

Figure IV.1: Moisture uptake capacity measurements of CaAlg and NaAlg with a varying relative humidity.

The results showed that only negligible hysteresis occurs for both sample types, implying that all initially absorbed moisture again desorbs at similar RH levels. This also implies that in conditions where no water is available to reach the crack, the SAPs can still retain moisture from the air. Secondly, as CaAlg is a physically cross-linked polymer, it forms a 3D structure rendering it possible to absorb moisture within its pores. Additionally, as CaAlg contains a higher concentration of cations (Ca^{2+} and Na^{+}, see further Table IV.2) than NaAlg, there was a stronger moisture uptake capacity for the former due to osmosis [16]. While NaAlg showed a maximal moisture uptake capacity of 78% at 98% RH of the dry polymer weight, this amount was already taken up by CaAlg at a RH between 60 and 70%.

Table IV.1: Most relevant moisture uptake capacity values for NaAlg and CaAlg and commercially available synthetic SAPs (results for SAP A and B obtained from [15]).

Moisture uptake capacity [%]	NaAlg (%)	CaAlg (%)	SAP A (%)	SAP B (%)
60% RH	22	67	26	28
90% RH	46	169	83	84
95% RH	63	227	130	119
98% RH	78	281	394	394

The moisture uptake capacity values of NaAlg and CaAlg were compared with commercially available synthetic SAPs (see Table IV.1). SAP A and B showed similar results, while CaAlg outperformed the other polymers as it showed more than twice the moisture uptake capacity at 60% and 90% RH compared to SAP A and B. At a RH 95%, CaAlg still outperformed the commercial SAPs. This could again be related to the high presence of cations in CaAlg as explained above. At 98% RH, the amount taken up is lower than for SAP A and B but still amounts to almost three times its own weight. The reason why the commercial SAPs now showed a superior moisture uptake at 98% RH could be related to the high humidity of 98% leading to condensation and approaching the situation of full submersion, for which the commercial SAPs also show superior swelling. Overall, it could be concluded that the moisture uptake capacity for CaAlg was very promising at RH up to 90% as it could take up 67 and 169% its own weight at 60 and 90% RH respectively.

IV.1.2. Swelling experiments on the alginate-based polymers

In order to gain insight in the swelling behavior of NaAlg and CaAlg in mortar, the swelling capacity of both materials was assessed in demineralized water and cement filtrate (CF) solution. As NaAlg is a linear, water-soluble polymer, no swelling could be recorded in demineralized water. CaAlg showed a swelling capacity of 72.0 ± 2.5 g_{water}/g_{SAP}, which was, however, lower compared to commercially available synthetic SAPs (respectively 305 ± 3.7 g_{water}/g_{SAP} for SAP A and 283.2 ± 2.4 g_{water}/g_{SAP} for SAP B) [5].

In CF solutions, two interesting observations could be made. First, NaAlg becomes insoluble due to the presence of multivalent cations in CF (especially Ca^{2+} [17, 18]), which replace part of the Na^{+} cations thereby creating a physically cross-linked hydrogel. The formed hydrogel showed a swelling capacity of 67.0 ± 2.3 g_{water}/g_{SAP} in CF, in the same order as reported for commercially available synthetic SAPs (61.0 ± 1.0 g_{water}/g_{SAP} and 58.4 ± 1.7 g_{water}/g_{SAP} for respectively SAP A and B) [5] and in the same order as the swelling of CaAlg in demineralized water. Conversely, CaAlg showed a swelling capacity in CF which dropped down to 12.0 ± 2.3 g_{water}/g_{SAP}. It could be anticipated that the latter observation was the result of additional crosslinking of CaAlg upon incubation in the Ca^{2+}-containing cement filtrate solution, since more extensive crosslinking is concomitant with a reduced swelling degree [19, 20]. In order to validate this hypothesis, inductively coupled plasma optical emission spectroscopy (ICP-OES) measurements have been performed on NaAlg and CaAlg before and after swelling in cement filtrate solutions to determine the total content of Ca^{2+} and Na^{+} present (see Table IV.2).

Table IV.2: ICP-OES measurements on NaAlg and CaAlg before and after swelling tests in CF.

Sample	% Ca^{2+}	% Na^{+}
NaAlg	0.2 ± 0.0	8.7 ± 0.4
CaAlg	4.0 ± 1.2	7.5 ± 2.2
NaAlg (CF)	9.8 ± 0.9	1.7 ± 0.4
CaAlg (CF)	11.5 ± 1.8	0.3 ± 0.1

Before incubation in CF, an initial amount of 8.7% Na^{+} in NaAlg and a negligible amount of Ca^{2+} (0.2%) was measured. The CaAlg beads showed, as anticipated, a higher amount of Ca^{2+} (4.0%). The amount of Na^{+} (7.5%), however, did not decrease significantly. After incubation in CF, the amount of Na^{+} decreased (down to 1.7 and 0.3 % in NaAlg and CaAlg, respectively) due to an exchange of Na^{+} by Ca^{2+}. In addition, the Ca^{2+} amount increased to 9.8 and 11.5% for NaAlg and CaAlg, respectively. Although these values were not significantly different ($p > 0.05$), it could be anticipated that CaAlg was more densely cross-linked in CF (cfr. 11.5% Ca^{2+}) compared to NaAlg (cfr. 9.8% Ca^{2+}). Indeed, an increase in the average Ca^{2+} content of 1.7% could already result in an extensively lower swelling. Previously, Acatürk et al. showed that an increase in Ca^{2+} fraction by 1% could result in a decrease of the swelling capacity of alginate with a factor four [20].

IV.1.3. Evaluation of mechanical strength of mortar containing NaAlg and CaAlg

Three-point bending and compressive strength tests were performed to determine the mechanical properties of mortar upon addition of NaAlg or CaAlg. Additional water was added to compensate for the absorption of mixing water by the polymers and to create mixtures exhibiting a similar workability (flow around 210 mm, Table IV.3) as the reference material with a water-to-cement ratio of 0.50 [9]. Although the swelling capacity of CaAlg in demineralized water or CF was lower compared to the commercially available SAPs A and B, it was useful to

compare the effect on the strength upon applying an equal dosage. Previous results [7, 18] already showed that addition of synthesized SAPs provided a strong self-sealing efficiency using 1 m% relative to cement mass, although they only swelled up to around 100 times their own weight which is three times lower compared to the commercially available SAPs. The bending strength results of the different materials were compared using a univariate ANOVA test.

A significant bending strength reduction was obtained for NaAlg (0.5 m% relative to cement mass) and CaAlg (1 m% relative to cement mass) compared to the reference sample. However, the addition of 0.5 m% CaAlg did not result in a significant reduction in bending strength. The significant difference between CaAlg (0.5 m%) and NaAlg (0.5 m%) could be explained by the higher swelling capacity of NaAlg in CF. When comparing with equally added amounts of commercially available SAPs and addition of extra water to maintain workability (Table IV.3), the results showed that SAP B had slightly (significant) higher bending strengths than the alginates.
Upon considering the compressive strengths, significant differences could be observed between the reference, NaAlg (0.5 m%: 10% reduction versus 1 m%: 28% reduction) and CaAlg (1 m%: 15% reduction). Additionally, significant differences were obtained between NaAlg (0.5 m%) and CaAlg (0.5 m%), and between CaAlg (0.5 m%) and CaAlg (1 m%). The latter difference could be explained by a higher addition of polymer creating more pores after release of their absorbed water. NaAlg (1 m%) had a significant effect on the compressive strength compared to the reference and all other alginate-containing samples.

Overall, the results could be linked with the above-mentioned results for the absorption capacity. Indeed, a higher swelling capacity in CF was related to an increased amount of additional water required (30 and 65 mL for 0.5 and 1 m% NaAlg respectively versus 10 and 15 mL for CaAlg). This caused increased pore formation in mortar and as such, a more severe effect on the strength. Interestingly, when comparing the results with the commercially available SAPs, it was shown that SAP A and B both required a higher amount of additional water (73 and 134 mL for 0.5 and 1 m% SAP A and 22 and 43 mL for SAP B) compared to CaAlg (which is expected as CaAlg had a lower swelling capacity in CF) and as such resulted in significantly lower compressive strengths compared to the mortar samples containing alginate, except for 1 m% NaAlg (cfr. strength reductions of 36% and even 56% upon addition of 0.5 and 1 m% SAP A relative to the cement mass respectively and a reduction of 20% for SAP B upon using 0.5 and 1 m%). The lower strength of mortar with NaAlg (1 m%) was again related to its high amount of additional water due to a comparable swelling in CF as SAP A and B. The difference in additional water between SAP A and B despite their similar swelling in CF could be related to the particle size of SAP A being 5 times lower than SAP B, creating a larger specific surface available for mixing water to be taken up SAP B [21, 22]. In mortar, there was less mixing water available and a reduced spatial freedom for swelling. Interestingly, the compressive strength reduction of CaAlg-containing samples was very limited even upon addition of 1 m%. The obtained data, together with the required amount of additional water and workability is found in Table IV.3.

Table IV.3: Results of mechanical three-point bending and compressive strength tests.

NaAlg		Bending strength [MPa]	Compressive strength [MPa]
0.5 m%	30	6.8 ± 0.3 (-12%)	58.9 ± 0.4 (-10%)
1 m%	65	7.2 ± 0.3 (-6%)	47.2 ± 1.0 (-28%)
CaAlg			
0.5 m%	10	7.3 ± 0.4 (-5%)	65.8 ± 2.0 (/)
1 m%	15	6.6 ± 0.2 (-14%)	55.8 ± 2.3 (-15%)
SAP A			
0.5 m%	73	7.8 ± 0.0 (/)	41.7 ± 0.9 (-35%)
1 m%	134	6.6 ± 0.1 (-14%)	28.9 ± 1.7 (-55%)
SAP B			
0.5 m%	22	8.0 ± 0.1 (/)	51.2 ± 1.1 (-20%)
1 m%	43	7.7 ± 0.1 (/)	51.3 ± 0.4 (-20%)
Reference			
No SAP		7.7 ± 0.4	65.4 ± 3.2

IV.1.4. Conclusions

The current work showed that CaAlg exhibits a strong moisture uptake capacity, exceeding that of commercially available synthetic SAPs. Indeed, CaAlg took up 67%, 169% and 227% its own weight in moisture at 60%, 90% and 95% RH respectively. Both NaAlg and CaAlg were shown to be very promising to be added to mortar. NaAlg became insoluble due to the divalent cations present in CF, creating a physically cross-linked hydrogel. Mortars with CaAlg were concomitant with only a small reduction of 15% in compressive strength upon addition of a high amount (i.e. 1% relative to cement mass). NaAlg led to a stronger decrease in strength (up to 28% for 1% addition) due to the higher water uptake capacity and, as such, a stronger macro-pore formation. Conversely, an equal addition of commercially available synthetic SAPs resulted in a compressive strength reduction up to 20% or even 55%, for SAP B and A respectively as they required a higher amount of additional water. The present work aims to pave the way towards further research covering these high-potential biopolymers for sustainable concrete repair without impairing the strength. The further potential of polysaccharides has been examined more profoundly in the next parts of this chapter.

IV.1.5. References

[1] Mechtcherine V, Gorges M, Schroefl C, Assmann A, Brameshuber W, Ribeiro A, et al. Effect of internal curing by using superabsorbent polymers (SAP) on autogenous shrinkage and other properties of a high-performance fine-grained concrete: results of a RILEM round-robin test. Mat Struct. 2014;47(3):541-62.
[2] Viktor Mechtcherine LD, Joachim Schulze. Internal curing by super absorbent polymers (SAP) – effects on material properties of self-compacting fibre-reinforced high performance concrete. In: O. M. Jensen PL, K. Kovler, editor.: RILEM Publications SARL; 2006. p. 87 - 96.
[3] Laustsen S, Hasholt M, Jensen O. Void structure of concrete with superabsorbent polymers and its relation to frost resistance of concrete. Mat Struct. 2013;48(1-2):357-68.
[4] Jensen OM. Use of superabsorbent polymers in concrete. Concrete International. 2013;35(1):48-52.
[5] Snoeck D, Van Tittelboom K, Steuperaert S, Dubruel P, De Belie N. Self-healing cementitious materials by the combination of microfibres and superabsorbent polymers. Journal of Intelligent Material Systems and Structures. 2014;25(1):13-24.
[6] Snoeck D, Van Tittelboom K, De Belie N, Steuperaert S, Dubruel P. The use of superabsorbent polymers as a crack sealing and crack healing mechanism in cementitious materials. Concrete Repair, Rehabilitation and Retrofitting III: 3rd International Conference on Concrete Repair, Rehabilitation and Retrofitting, ICCRRR-3, 3-5 September 2012, Cape Town, South Africa: CRC Press; 2012. p. 58.
[7] Mignon A, Graulus G-J, Snoeck D, Martins J, De Belie N, Dubruel P, et al. pH-sensitive superabsorbent polymers: a potential candidate material for self-healing concrete. J Mater Sci. 2014;50(2):970-9.
[8] Hasholt MT, Jensen OM, Kovler K, Zhutovsky S. Can superabsorbent polymers mitigate autogenous shrinkage of internally cured concrete without compromising the strength? Construction and Building Materials. 2012;31:226-30.
[9] Snoeck D, Schaubroeck D, Dubruel P, De Belie N. Effect of high amounts of superabsorbent polymers and additional water on the workability, microstructure and strength of mortars with a water-to-cement ratio of 0.50. Construction and Building Materials. 2014;72(0):148-57.
[10] Snoeck D, Steuperaert S, Van Tittelboom K, Dubruel P, De Belie N. Visualization of water penetration in cementitious materials with superabsorbent polymers by means of neutron radiography. Cement and Concrete Research. 2012;42(8):1113-21.
[11] Tally M, Atassi Y. Optimized synthesis and swelling properties of a pH-sensitive semi-IPN superabsorbent polymer based on sodium alginate-g-poly(acrylic acid-co-acrylamide) and polyvinylpyrrolidone and obtained via microwave irradiation. Journal of polymer research. 2015;22(9):1-13.
[12] Harbottle MJ, Zhang J, Gardner DR. Combined physical and biological gel-based healing of cementitious materials. ICSHM 2013: Proceedings of the 4th International Conference on Self-Healing Materials, Ghent, Belgium, June 16-20, 2013: Ghent University; Delft University of Technology; 2013.
[13] Wang J, Dewanckele J, Cnudde V, Van Vlierberghe S, Verstraete W, De Belie N. X-ray computed tomography proof of bacterial-based self-healing in concrete. Cement and Concrete Composites. 2014;53(0):289-304.
[14] Wang J, Snoeck D, Van Vlierberghe S, Verstraete W, De Belie N. Application of hydrogel encapsulated carbonate precipitating bacteria for approaching a realistic self-healing in concrete. Construction and Building Materials. 2014;68(0):110-9.
[15] Snoeck D, Dubruel P, De Belie N. How to seal and heal cracks in cementitious materials by using superabsorbent polymers. Application of Superabsorbent Polymers and Other New Admixtures in Concrete Construction: RILEM Publications; 2014. p. 375-84.

[16] Lu X, Boo C, Ma J, Elimelech M. Bidirectional diffusion of ammonium and sodium cations in forward osmosis: Role of membrane active layer surface chemistry and charge. Environmental science & technology. 2014;48(24):14369-76.
[17] Andersson K, Allard B, Bengtsson M, Magnusson B. Chemical composition of cement pore solutions. Cement and Concrete Research. 1989;19(3):327-32.
[18] Mignon A, Snoeck D, Schaubroeck D, Luickx N, Dubruel P, Van Vlierberghe S, et al. pH-responsive superabsorbent polymers: A pathway to self-healing of mortar. Reactive and Functional Polymers. 2015;93(0):68-76.
[19] Sriamornsak P, Kennedy RA. Swelling and diffusion studies of calcium polysaccharide gels intended for film coating. International Journal of Pharmaceutics. 2008;358(1–2):205-13.
[20] Takka F, Acarturk, S. Calcium alginate microparticles for oral administration: II effect of form ulation factors on drug release and drug entrapment efficiency. Journal of Microencapsulation. 1999;16(3):291-301.
[21] Kabiri K, Omidian H, Hashemi SA, Zohuriaan-Mehr MJ. Synthesis of fast-swelling superabsorbent hydrogels: effect of crosslinker type and concentration on porosity and absorption rate. European Polymer Journal. 2003;39(7):1341-8.
[22] Zhao Y, Su H, Fang L, Tan T. Superabsorbent hydrogels from poly(aspartic acid) with salt-, temperature- and pH-responsiveness properties. Polymer. 2005;46(14):5368-76.

IV.2 Introducing a carboxylic and sulfonic acid to a methacrylated alginate backbone

The previous part of this chapter has shown that polysaccharides and especially alginate, are very promising as starting materials for self-sealing and -healing of cracks. However, instead of the weak electrostatic bonds present within calcium alginate which are prone to disintegration in the presence of monovalent cations [1], covalent linkages generally result in mechanically superior SAPs [2]. One way to create covalent bonds in a SAP network based on polysaccharides is by first modifying them with methacrylic anhydride (MAAH) [3, 4]. MAAH can be used to enable cross-linking of the polysaccharides. In the case of alginate, the hydroxyl groups react with the anhydride resulting in methacrylated alginate, as seen in Figure IV.2. These methacrylate functions can be used to execute a free radical polymerization in the presence of acrylic monomers.

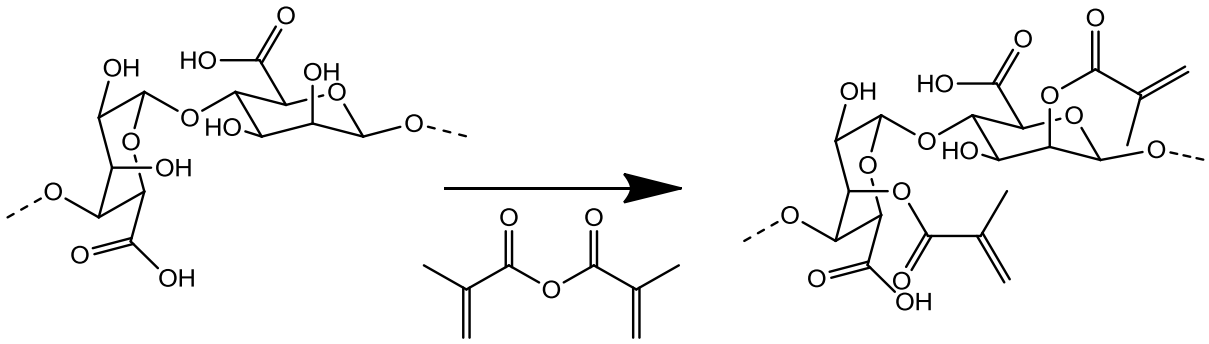

Figure IV.2: Methacrylation of alginate. Activated double bonds are incorporated in the alginate backbone to serve as a functional handle for a free radical polymerization.

Acrylic acid (AA) has already been proven to be a widespread used monomer for the development of synthetic SAPs, often in combination with other acrylic monomers such as acrylamide [5-9]. Another interesting monomer is 2-acrylamido-2-methylpropanesulfonic acid (AMPS) as this hydrophilic, sulfonic acid possesses a large swelling capacity and has already been used in a variety of applications going from water treatment [10, 11] and drug delivery [12] towards other biomedical applications [13-15] and personal care [16-18].

The present topic therefore reports on the development and characterization of SAPs based on methacrylated alginate as backbone combined with a varying molar fraction of AA and/or AMPS. The degree of methacrylation after modification has been determined by proton nuclear magnetic resonance spectroscopy. The chemical structure of the synthesized SAPs has been verified through attenuated total reflectance-infrared (ATR-IR) spectroscopy. High resolution

This work has been published as: Mignon Arn, Devisscher Dries, Graulus Geert-Jan, Stubbe Birgit, Martins José, Dubruel Peter, De Belie Nele and Van Vlierberghe Sandra (2017) Combinatory approach of methacrylated alginate and acid monomers for concrete applications, Carbohydrate polymers, 155, 448-455

magic-angle spinning (HR-MAS) ^{1}H-NMR spectroscopy and gel fraction have been used to identify the polymerization efficiency. In addition, the sorption and desorption of moisture at different relative humidities has been measured by dynamic vapor sorption (DVS) measurements. It is also important to identify the swelling degree in aqueous solutions (ultrapure water and demineralized water) and cement filtrate solutions. Additionally, the thermal stability has been evaluated using thermogravimetric analysis (TGA). Finally, the influence of these SAPs on the strength of mortar has also been determined.

IV.2.1. Methacrylation of alginate via modification with methacrylic anhydride

In a first step, alginate was methacrylated. The color of the mixture changed from clear, slightly yellow liquid to more cloudy, white as the reaction progressed. The final product, algMOD, was a soft white porous material after lyophilization. The degree of methacrylation (DM, also called degree of substitution DS), or thus the amount of double bonds incorporated on alginate had a strong influence on the physical properties as well as the swelling capacity of the formed SAP. For that reason, it was important to calculate the efficiency of the methacrylation. This is done by using ^{1}H NMR spectroscopy.

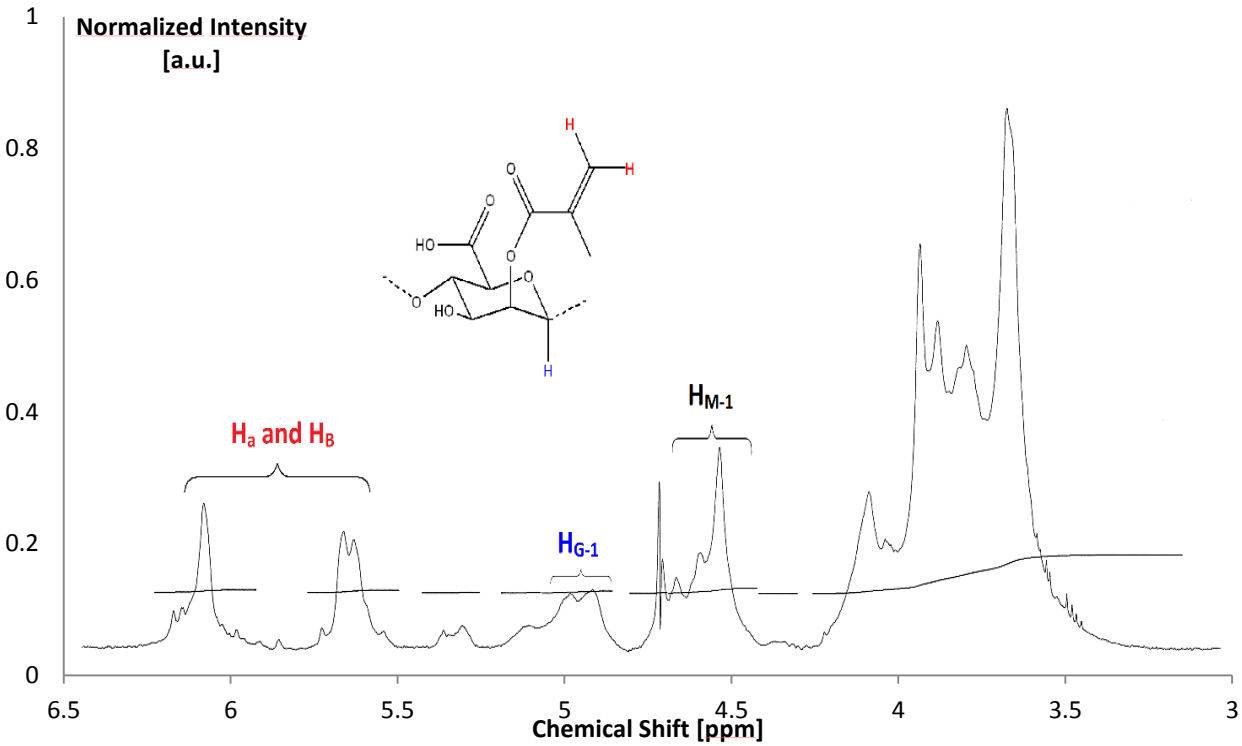

Figure IV.3: ^{1}H NMR spectrum of algMOD with annotation of the relevant peaks for the calculation of the DS.

The obtained spectra were analyzed by comparing the characteristic peaks of the methacrylate group corresponding to the vinyl protons at 5.73 and 6.16 ppm with the reference peak on the alginate backbone at 4.97 ppm. As this latter peak belongs to the proton of the anomeric carbon of the guluronic acid block (G-units), the G-value had to be calculated and incorporated as a correction factor due to the presence of mannuronic acid blocks (M-units). Therefore, the

relative proportion of the G-units compared to the total amount of G- and M-units had to be determined using equation (IV.1). Subsequently, the average of the peaks of the methacrylate groups was calculated and used to compute the degree of substitution (DS) value per repeating unit by applying equation (IV.2). To obtain the DS per hydroxyl group, this value had to be divided by two as the considered repeating unit (G-unit) possessed two hydroxyl groups.

$$G\ [\%] = \frac{H_{G-1}}{H_{M-1}+H_{G-1}} = \frac{I_{4.97ppm}}{I_{4.58ppm}+I_{4.97ppm}} * 100\% \quad \text{(IV.1)}$$

$$DS\ [\%] = G * \frac{\frac{H_a+H_b}{2}}{H_{G-1}} = G * \frac{\frac{I_{5.73ppm}+I_{6.16ppm}}{2}}{I_{4.97ppm}} \quad \text{(IV.2)}$$

The protons H_{G-1}, H_{M-1}, H_a and H_b were related to the intensity of their related peaks on the NMR spectrum, seen further in Figure IV.3. By equations (IV.1) and (IV.2) [19-21], a relative concentration of guluronic acid units or G-content of 30.5% and a DS of 18.7% in function of the present hydroxyl groups were calculated. This means that almost one in five functional hydroxyl groups or one in three repeating units (37.4%) have been modified. Afterwards, it was found by the group of prof. Adriaensens (appointed at UHasselt, where the ^{1}H-NMR measurements on methacrylated alginate were performed) that peaks nearby the reference peak could interfere with the calculations. This could lead to a less accurate integration and DS determination. To get around this problem, an alternative measurement was proposed. ^{13}C-NMR could resolve the issue of interfering peaks. This research is on-going and will in the near future indicate whether the ^{1}H-NMR gives an adequate determination of the DS.

IV.2.2. Development of the synthesized semi-synthetic SAPs

After modification, the methacrylated alginate (algMOD) was combined with the monomers (AA and AMPS) to create a cross-linked network gel by using a free radical precipitation polymerization as schematically presented in Figure IV.4. AMPS was selected as second monomer to compare the difference between a carboxylic acid and a sulfonic acid with respect to the swelling capacity and the influence on the mortar strength. AlgMOD with only AA formed a strong and transparent solid gel but a decrease in AA/AMPS ratio led to a more brittle gel. The composition and nomenclature of the SAPs is described in Table IV.4.

Table IV.4: Overview of theoretical chemical composition and gel fraction of the developed SAPs. The fraction algMOD was added on top of the total monomer amount.

Sample	$\frac{AlgMOD}{AA+AMPS}$ g/g	AA mol%	AMPS mol%	Gel fraction (%)
p(alg(1)_AA_{100}(7))_H	1/7	100	0	85 ± 1
p(alg(1)_AA_{75}/$AMPS_{25}$(7))	1/7	75	25	81 ± 3
p(alg(1)_AA_{50}/$AMPS_{50}$(7))	1/7	50	50	61 ± 2
p(alg(1)_AA_{25}/$AMPS_{75}$(7))	1/7	25	75	59 ± 1
p(alg(1)_$AMPS_{100}$(7))	1/7	0	100	43 ± 6

Gel fractions were determined and it could be clearly seen in Table IV.4 that a lower AA/AMPS ratio led to a significant decrease in the gel fraction. On the one hand, the materials containing more AMPS were more brittle and thus more prone to become damaged during purification. On top of this, the higher polarity of AMPS led to an increased repulsion between negatively charged carboxylate groups on the backbone and sulfonate moieties on the AMPS monomer. This hindered the cross-linking reaction, as the monomers had more difficulty to reach the alginate.

Smaller particles have a higher surface area, which can have an influence on for example the moisture uptake capacity. On top of this, when incorporated in mortar, these smaller particles led to more smaller pores compared to larger SAPs. All materials showed the same trends in particle size for d_{10} and d_{50} (Table IV.5). Approximately half of the particles had a diameter of 20 µm or lower. However, d_{90} showed a variation between the SAPs. A general remark that can be made is that the hardness of the formed SAP has an influence on the particle size distribution, as all SAPs were grinded immediately after freeze-drying. The difference for the current materials was quite limited and all diameters lay between 50 – 80 µm.

Table IV.5: Particle size ranges of the algMOD - AA/AMPS SAPs.

Sample	d_{10} [µm]	d_{50} [µm]	d_{90} [µm]
p(alg(1)_AA_{100}(7))_H	9	20	80
p(alg(1)_AA_{75}/$AMPS_{25}$(7))	8	20	47
p(alg(1)_AA_{50}/$AMPS_{50}$(7))	8	18	48
p(alg(1)_AA_{25}/$AMPS_{75}$(7))	10	21	75
p(alg(1)_$AMPS_{100}$(7))	10	20	67

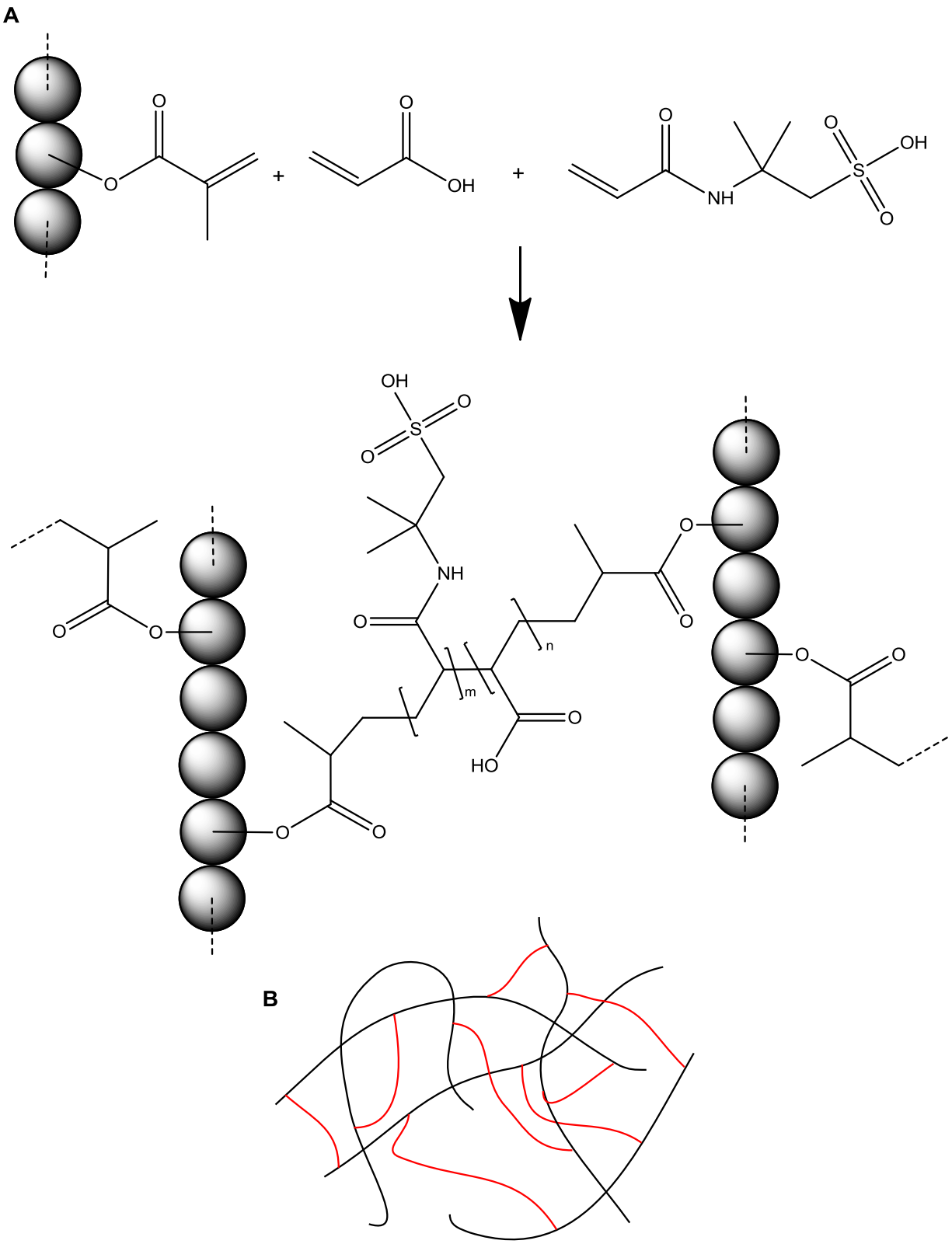

Figure IV.4: A) Schematic representation of the formation of a SAP with a methacrylated alginate (grey orb) and acrylic monomers (AA and AMPS). B) Example of a polymer network with the polysaccharide represented in black and the acrylic oligomers in red.

IV.2.3. Structure confirmation and cross-linking efficiency

Attenuated total reflectance infrared spectroscopy

ATR-IR spectroscopy was performed on all p(alg_AA/AMPS) SAPs as seen in Figure IV.5. At 1700 cm^{-1}, the carbon-oxygen double bond stretch vibration (ν(C=O)) became visible, especially in p(alg(1)_AA_{100}(7))_H. This peak is characteristic for the carbonyl bond in the acid moieties from both AA and the alginate backbone. The carbon-oxygen double bond stretch (ν(C=O)) and nitrogen-hydrogen bending vibration (δ(N-H)) related to the secondary amide bonds in the AMPS monomer could be defined at 1650 and 1550 cm^{-1}. The peaks at 1040 cm^{-1} and 1150 cm^{-1} corresponded to the absorption of the symmetric and asymmetric stretch vibration of the sulfur-oxygen bond in the "O=S=O" group of the sulfate (ν(O=S=O)). These four peaks became relatively more intense with a decreasing AA/AMPS ratio compared to the carbonyl peak at 1700 cm^{-1}. The incorporated methacrylate functions in algMOD after modification were distinguishable by two secondary ester peaks, related to the symmetric and asymmetric stretching vibration of the carbon-oxygen-carbon bonds in the ester functionality (ν(O=C-O)). They were visible around 1220 and 1170 cm^{-1} respectively but at lower AA/AMPS ratios, they were mostly hidden in the sulfate peak at 1150 cm^{-1}. Two broad bands could be seen at 3500-3100 cm^{-1} and 3400-2400 cm^{-1} respectively. These are attributed to the stretch vibration of the nitrogen-hydrogen (ν(N-H)) bond in the amide moieties of AMPS and the oxygen-hydrogen bond (ν(O-H)) in the carboxylic acids of AA and alginate.

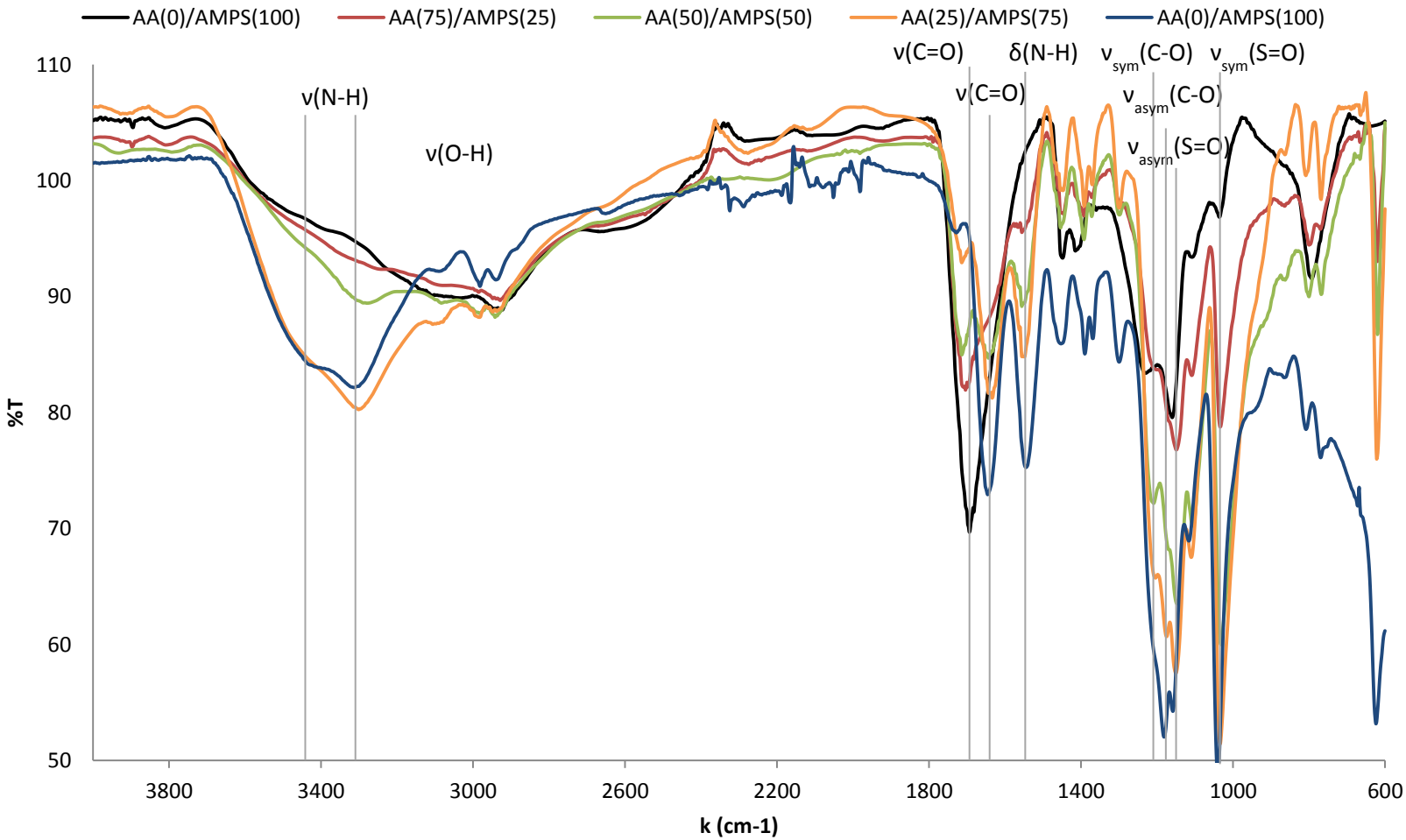

Figure IV.5: FTIR spectroscopy spectrum of the algMOD - AA/AMPS SAPs with annotation of several of the most relevant peaks. The samples are abbreviated by their molar ratio of the monomers as AA(x) /AMPS(y).

High resolution magic-angle spinning proton nuclear magnetic resonance spectroscopy

HR-MAS ^{1}H NMR spectroscopy was used as a technique to confirm the polymerization (cross-linking) efficiency. The peaks corresponding to protons connected to C=C double bonds from either the methacrylate groups created in algMOD or directly from the monomers lay in the range of 5.5 – 6.5 ppm (as can also be seen in Figure IV.3 for algMOD). After polymerization, these peaks completely disappeared. This can be seen in Figure IV.6, where p(alg(1)_AA_{50}/$AMPS_{50}$(7)) was shown as an example. These peaks has moved upfield (1.5 – 2.5 ppm) and have now become protons on an sp^3 carbon atom, adjacent to an electronegative group.

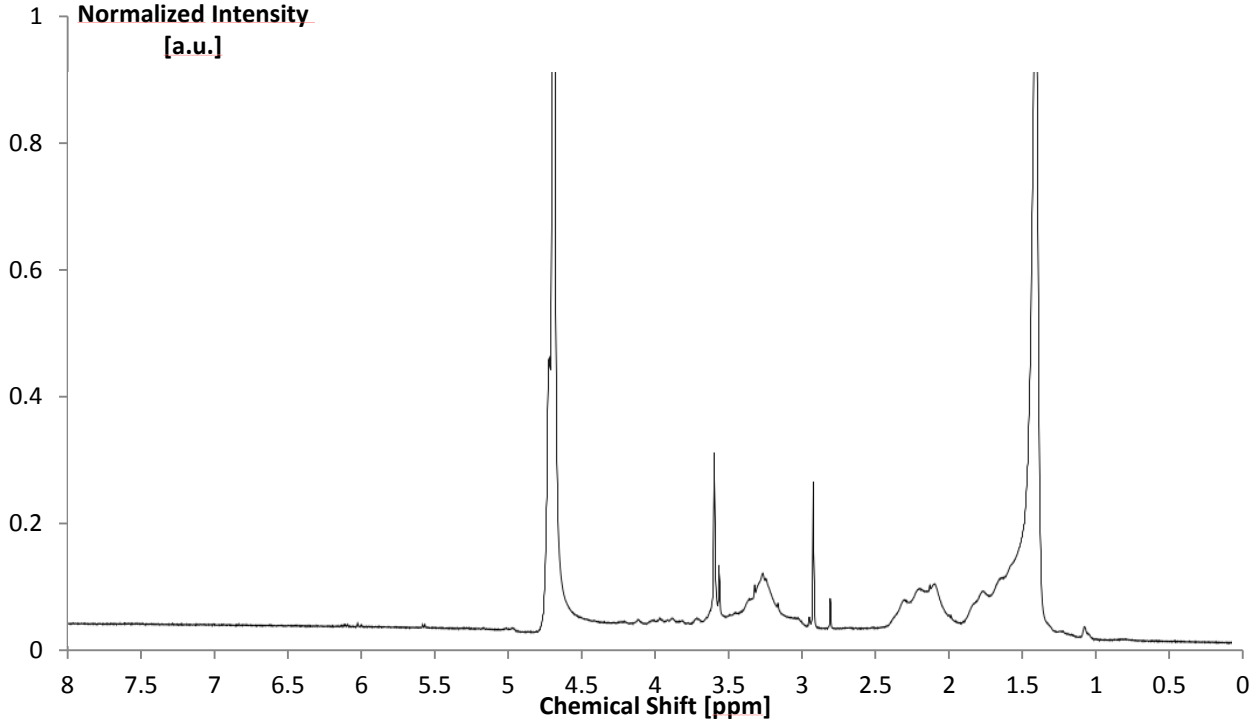

Figure IV.6: HR-MAS ^{1}H NMR spectrum of p(alg(1)_AA_{50}/$AMPS_{50}$(7)). The absence of peaks corresponding to double bond protons (situated between 5.5 and 6.5 ppm) from either algMOD, AA or AMPS confirms the successfulness of the cross-linking reaction.

IV.2.4. Determination of the moisture uptake capacity of the SAPs via dynamic vapor sorption

The moisture uptake capacity of the SAPs were assessed to identify the behavior in mortar or concrete, when no direct ingress of water or rain is possible upon crack formation. If these SAPs could already swell significantly in humid environments, the cracks may be partially sealed. The results are presented in Figure IV.7 and already showed that with a decrease of the AA/AMPS ratio, the moisture uptake capacity increased, especially at the high relative humidity (RH). The values ranged between 53.6 and 109.8% at a RH of 95%. All these values were already quite high (higher compared to the synthetic SAPs as seen in §III.4.). The materials with ≥ 50 mol% AMPS

could take up more than their original weight in moisture at this 95% RH. On top of this, these materials showed a negligible degree of hysteresis. As such, all moisture taken up can also be completely desorbed. Indeed, constructions that are not exposed to humid environments can thus still retain a certain amount of moisture from the air up to close to their own weight. In a subsequent stage, they are able to completely deliver this to remaining unreacted cement particles, which can lead to partial deposition of $CaCO_3$ from dissolved $Ca(OH)_2$ and CO_2 which, next to the further hydration of unreacted cement particles, contributes to the development of self-healing applications [22].

The reason for the higher moisture uptake capacity with a decrease in the AA/AMPS ratio could possibly be explained on the one hand by the higher polarity of the sulfonic acid compared to the carboxylic acid. On the other hand, the increase could also be related to the higher amount of sulfonic acid groups being ionized at the same pH. This effect is limited for the DVS results. However, this is more pronounced for the swelling capacity.

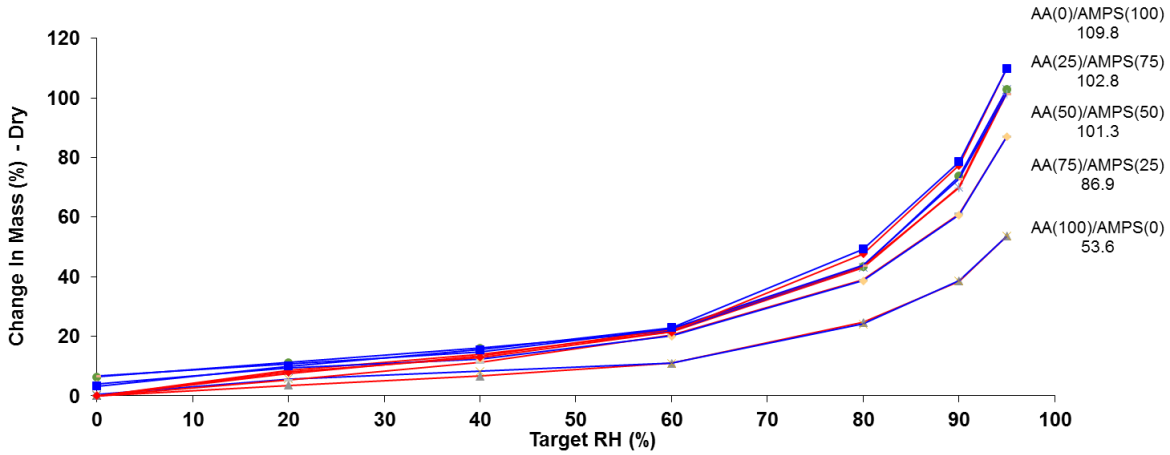

Figure IV.7: Sorption and desorption isotherms of the p(algMOD _AA/AMPS) materials measured by Dynamic Vapor Sorption. The samples are abbreviated by their molar ratio of the monomers as AA(x) /AMPS(y).

IV.2.5. Swelling capacity measurements on the synthesized semi-synthetic SAPs

The swelling potential of the SAPs upon 3h incubation was determined in three swelling media (i.e. ultrapure water, demineralized water and cement filtrate solution). As such, a difference in the ionic concentration was related to a variation in the swelling capacity. On the contrary, the molar variation also had a strong influence on the swelling degree. From this point onwards, the three most extreme samples were selected for further testing to see the most significant differences between p(alg(1)_AA_{100}(7))_H, p(alg(1)_AA_{50}/$AMPS_{50}$(7)) and p(alg(1)_$AMPS_{100}$(7)). It could be seen (Figure IV.8) that the swelling potential in cement filtrate was significantly ($p < 0.05$) lower as expected based on previous results obtained for synthetic SAPs due to the presence of Ca^{2+}, Mg^{2+} and other ions and due to the lower osmotic pressure in a solution with a high ion concentration [23]. No significant differences could be observed between ultrapure water and demineralized water except for p(alg(1)_$AMPS_{100}$(7)). Due to the high swelling of the latter, the relatively higher ionic concentration of demineralized water led to a swelling

reduction. An observed trend for the AA/AMPS ratio was that for all solutions, a decrease of the ratio led to an increase of the swelling capacity. This also added up with the explanation from the DVS results.

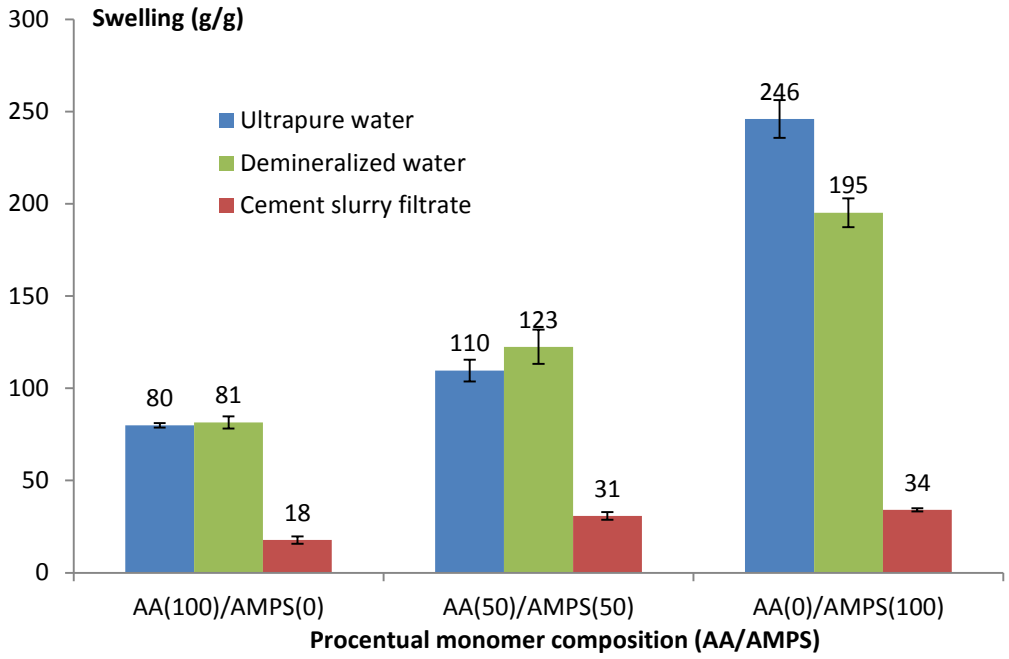

Figure IV.8: Swelling potential of the synthesized SAPs in ultrapure water, demineralized water and cement filtrate solution with a pH of 12.6. The samples are abbreviated by their molar ratio of the monomers as AA(x) /AMPS(y).

IV.2.6. Thermal stability of the SAPs by thermogravimetric analysis

The production of the SAPs occurred at 45°C and the temperature of concrete can raise up to 60°C during curing [24]. It is thus important that these polymers do not show thermal degradation at these increased temperatures. As such, TGA measurements were performed to determine the thermal stability (Figure IV.9). The results showed that at 100°C, over 90% of the material was maintained, while this loss can be attributed to residual water being present in the SAP as they were kept in the lab and no freeze drying step was performed right before the TGA measurements. Subsequently, the step at 200 – 250°C can be related to either the decarboxylation of the polymer and, when AMPS is present, the decomposition of sulfate groups. The last step around 360 – 450°C is the main chain C-C fission [25, 26].

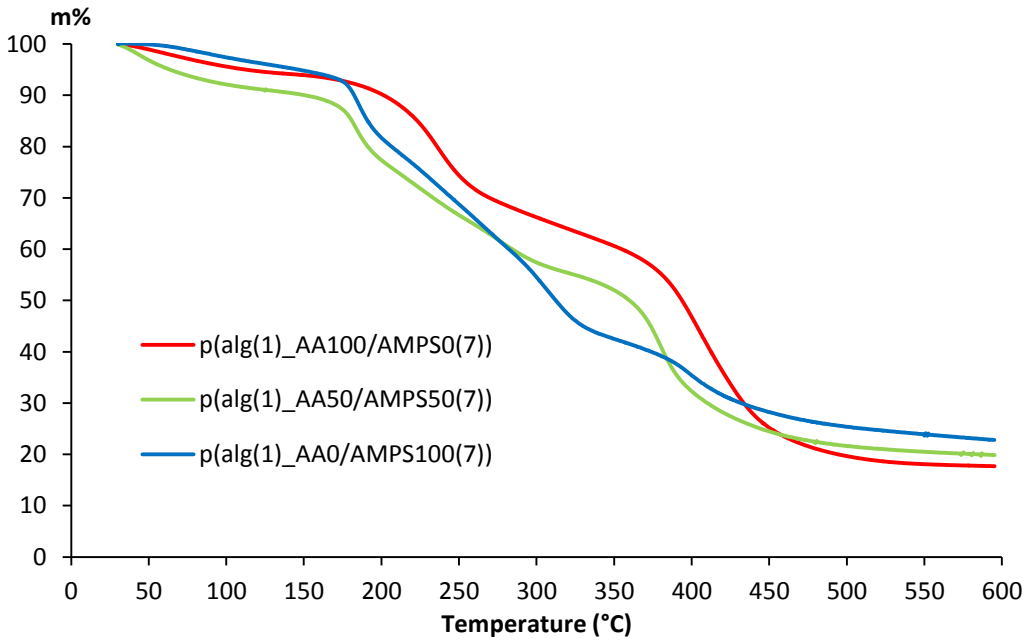

Figure IV.9: TGA plots displayed as the percentual weight as a function of temperature for p(alg(1)_AA_{100}/$AMPS_0$(7)), p(alg(1)_AA_{50}/$AMPS_{50}$(7)) and p(alg(1)_AA_0/$AMPS_{100}$(7)).

IV.2.7. Effect of SAPs on the flexural and compressive strength when incorporated in mortar

After a full characterization of the SAPs, the SAPs were incorporated into mortar and their effect on the flexural and compressive strength was investigated. The goal is to have as limited influence on the strength as possible upon incorporation of the SAPs in mortar. Interestingly, (Table IV.6) p(alg(1)_AA_{100}(7))_H had only a very limited compressive strength reduction up to 7% with an addition of 1 m% compared to the cement mass. The data indicated that SAPs with a higher molar fraction of AMPS led to weaker mortars compared to the reference for both the bending and compressive strength, up to the point that they were not useful anymore for the intended applications. For addition of 1 m% p(alg(1)_$AMPS_{100}$(7)) in function of the added amount of cement, the matrix just collapsed and was far too weak to test on its bending and compressive strength.

When looking at these samples using optical microscopy, it was observed that the SAPs containing a low AA/AMPS molar ratio showed a high degree of visible pores/cavities at the surface (Figure IV.10). These also showed a foaming formation during the mixing process. Together with the high swelling capacity of these SAPs compared to p(alg(1)_AA_{100}(7))_H, this could explain the severe decrease in the strength of the former.

Table IV.6: Information on the additional water and flow as well as the results of the three point bending and compression test on the mortar samples with 0.5 or 1 w% algMOD - AA/AMPS.

p(alg(1)_AA_{100}(7))_H		Bending strength [MPa]	Compressive strength [MPa]
0.5 m%	(+ 15 mL water)	6.8 ± 0.4 (-11%)	68.9 ± 1.6 (-6%)
1 m%	(+ 30 mL water)	7.6 ± 0.3 (/)	68.3 ± 0.6 (-7%)
p(alg(1)_AA_{50}/AM_{50}(7))			
0.5 m%	(+ 80 mL water)	6.3 ± 0.4 (-17%)	42.1 ± 1.4 (-42%)
1 m%	(+ 150 mL water)	5.1 ± 0.6 (-33%)	26.9 ± 0.2 (-63%)
p(alg(1)_$AMPS_{100}$(7))			
0.5 m%	(+ 100 mL water)	5.9 ± 0.3 (-22%)	36.6 ± 0.9 (-50%)
Reference			
No SAP	/	7.6 ± 0.5	73.1 ± 1.6

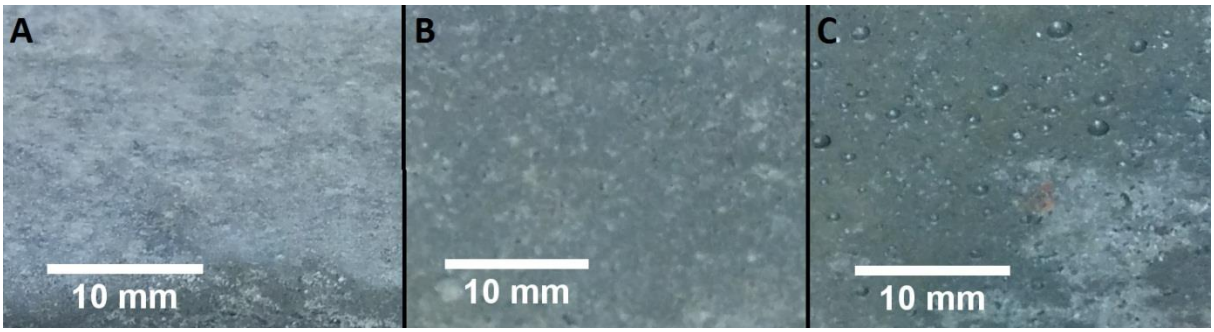

Figure IV.10: Microscopy performed on mortar samples containing no SAP (A), 1 m% of p(alg(1)_AA_{100}(7))_H (B) and 1 m% p(alg(1)_AA_{50}/$AMPS_{50}$(7)) (C). The cavities on the surface of the p(alg(1)_AA_{50}/$AMPS_{50}$(7)) sample are clearly visible.

IV.2.8. Conclusion and future perspectives

Alginate was successfully modified with methacrylic anhydride to create methacrylated alginate (algMOD) with a DS of 18.7% in function of the present hydroxyl groups. The combined effort of ATR-IR spectroscopy and HR-MAS ^{1}H-NMR spectroscopy could confirm the SAP structure and identify that the cross-linking efficiency was optimal, as no double bonds were remaining. These materials had gel fractions ranging between 85 and 43%, with a decreasing value for a decreasing AA/AMPS molar ratio. The SAPs showed a moisture uptake capacity going from 54 to

110% of their own weight at a RH of 95% with an increasing AMPS ratio. Interestingly, all materials showed a negligible hysteresis. This implied that they could be used as a reservoir. Additionally, all moisture taken up could also be completely desorbed. When investigating the swelling capacity, it was observed that an increase of the AMPS molar ratio led to an increased swelling, independent of the used solution up to a maximal swelling potential of 246 times its own weight for p(alg(1)_$AMPS_{100}$(7)). On top of this, these polymers showed a thermal stability higher than 100°C. This indicates that they do not degrade in temperatures encountered during production of or application in concrete. After incorporation of the SAPs in mortar, it was determined that a decrease of the AA/AMPS ratio would lead to an extremely severe decrease of the compressive strength. Interestingly, p(alg(1)_AA_{100}(7))_H showed only a very limited decrease in compressive strength (up to 7% decrease with an addition of 1 m% SAP), which would make these materials very interesting for the intended application. It is therefore useful to further test this material for its self-sealing and -healing potential. This is the subject of the following part of this chapter. The characteristics from p(alg(1)_AA_{100}(7))_H from this study have been compared to an identical material with a lower DS value of algMOD on the one hand and to a copolymers graft of AA and acrylamide on algMOD with a high (equal to the DS from this study) and a lower one. All these materials have also been tested on their self-sealing and -healing potential.

IV.2.9. References

[1] Bajpai SK, Sharma S. Investigation of swelling/degradation behaviour of alginate beads crosslinked with Ca2+ and Ba2+ ions. Reactive and Functional Polymers. 2004;59(2):129-40.
[2] Povh B, Rosina M. Scattering and structures: essentials and analogies in quantum physics: Springer Science & Business Media; 2005.
[3] Chou AI, Nicoll SB. Characterization of photocrosslinked alginate hydrogels for nucleus pulposus cell encapsulation. Journal of Biomedical Materials Research Part A. 2009;91(1):187-94.
[4] Chou AI, Akintoye SO, Nicoll SB. Photo-crosslinked alginate hydrogels support enhanced matrix accumulation by nucleus pulposus cells in vivo. Osteoarthritis and Cartilage. 2009;17(10):1377-84.
[5] Zhang B, Cui Y, Yin G, Li X, Liao L, Cai X. Synthesis and swelling properties of protein-poly(acrylic acid-co-acrylamide) superabsorbent composite. Polymer Composites. 2011;32(5):683-91.
[6] Mohammad J. Zohuriaan-Mehr KK. Superabsorbent Polymer Materials: A Review. Iranian Polymer Journal. 2008;17((6)):451-77.
[7] Zhou X, Weng L, Chen Q, Zhang J, Shen D, Li Z, et al. Investigation of pH sensitivity of poly(acrylic acid-co-acrylamide) hydrogel. Polymer International. 2003;52(7):1153-7.
[8] Nesrinne S, Djamel A. Synthesis, characterization and rheological behavior of pH sensitive poly(acrylamide-co-acrylic acid) hydrogels. Arabian Journal of Chemistry. 2013(0).
[9] Ding Y, Xiao C, An S, Jia G. Water-absorptive blend fibers of copoly(acrylic acid–acrylamide) and poly(vinyl alcohol). Journal of Applied Polymer Science. 2006;100(4):3353-7.
[10] Yu X-l, Liu X-h, Xia Z-r, Cheng D-b, Xiao S, Hu Z-j, et al. Synthesis and Water-retention Property of the PAA-AM-AMPS and PAA-AM Superabsorbent Polymer. Fine Chemicals. 2011;5:004.
[11] Kang G-d, Cao Y-m. Development of antifouling reverse osmosis membranes for water treatment: a review. Water research. 2012;46(3):584-600.
[12] Pourjavadi A, Barzegar S, Zeidabadi F. Synthesis and properties of biodegradable hydrogels of κ-carrageenan grafted acrylic acid-co-2-acrylamido-2-methylpropanesulfonic acid as candidates for drug delivery systems. Reactive and Functional Polymers. 2007;67(7):644-54.
[13] Keogh JR. Contacting blood with medical equipment having polymerized 2-acrylamido-2-methylpropanesulfonic acid on exposed surface. Google Patents; 1995.
[14] Keogh JR, Hobot CM, Eaton JW, Jevne AH, Bergan MA. Made from monomers such as N-(3-aminopropyl) methacrylamide hydrochloride, 2-acrylamido-2-methylpropanesulfonic acid, acrylamide and acrylic acid bonded to polymeric substrate surface; useful in medical devices. Google Patents; 1995.
[15] Anirudhan TS, Sandeep S. Synthesis and characterization of molecularly imprinted polymer of N-maleoylchitosan-grafted-2-acrylamido-2-methylpropanesulfonic acid and its controlled delivery and recognition of bovine serum albumin. Polymer Chemistry. 2011;2(9):2052-61.
[16] Cahalan PT, Coury AJ. Method of preparing tape electrode. Google Patents; 1986.
[17] Abdel-Azim AAA, Farahat MS, Atta AM, Abdel-Fattah AA. Preparation and properties of two-component hydrogels based on 2-acrylamido-2-methylpropane sulphonic acid. Polymers for Advanced Technologies. 1998;9(5):282-9.
[18] Lundmark LD, Melby A, Chun H-m. Method of imparting lubricity to keratinous substrates and mucous membranes. Google Patents; 1978.
[19] Grasdalen H. High-field, 1H-nmr spectroscopy of alginate: sequential structure and linkage conformations. Carbohydrate Research. 1983;118:255-60.
[20] Grasdalen H, Larsen B, Smidsrød O. A pmr study of the composition and sequence of uronate residues in alginates. Carbohydrate Research. 1979;68(1):23-31.
[21] Stubbe B. Development of biopolymer-based systems for burn wound treatment: Ghent University; 2016.
[22] Snoeck D, Van Tittelboom K, Steuperaert S, Dubruel P, De Belie N. Self-healing cementitious materials by the combination of microfibres and superabsorbent polymers. Journal of Intelligent Material Systems and Structures. 2014;25(1):13-24.

[23] Horkay F, Tasaki I, Basser PJ. Osmotic swelling of polyacrylate hydrogels in physiological salt solutions. Biomacromolecules. 2000;1(1):84-90.
[24] Ter Heide N. Crack healing in hydrating concrete. Delft University of Technology, Delft. 2005.
[25] Abdelaal MY, Makki MSI, Sobahi TRA. Modification and characterization of polyacrylic acid for metal ion recovery. American Journal of Polymer Science. 2012;2(4):73-8.
[26] Diao H, Yan F, Qiu L, Lu J, Lu X, Lin B, et al. High Performance Cross-Linked Poly(2-acrylamido-2-methylpropanesulfonic acid)-Based Proton Exchange Membranes for Fuel Cells. Macromolecules. 2010;43(15):6398-405.

IV.3 Investigating the introduction of acrylamide and a varying degree of substitution of the methacrylated alginate

Water permeability tests (see §III.2.6) have shown that the incorporation of synthetic SAPs based on acrylic acid (AA), acrylamide (AM) and N,N'-methylene bisacrylamide (MBA) in mortar samples resulted in a strong self-sealing effect of cracks (especially upon addition of 1 m% with respect to the cement mass). In addition, stalactite formation was observed, composed of $CaCO_3$ with small amounts of CaO. Despite these promising results, the bending and compressive strength of mortar drops severely upon introduction of the above-mentioned SAPs (up to 52% reduction of the compression strength upon addition of 1 m% SAP) [1, 2]. The previous sections (see §IV.1.) indicated that the use of polysaccharides could offer a valuable alternative in this respect. Resulting in only limited strength differences compared to reference samples, the incorporation of calcium alginate in mortar appeared to be a promising approach to obtain a minimal effect on the compressive strength of mortar [3]. In §IV.2., alginate was chemically modified using methacrylic anhydride to incorporate methacrylate moieties onto the alginate backbone resulting in algMOD. Interestingly, the methacrylates enabled subsequent co-polymerization with alternative functional monomers. A copolymer network with AA and/or 2-acrylamido-2-methylpropanesulfonic acid (AMPS) has been already synthesized onto the algMOD backbone. The results showed that in particular the combination with AA (p(alg(1)_AA_{100}(7))_H, see Table IV.4, §IV.2) induced a very limited strength reduction in mortar samples of 7% upon addition of 1 m% SAP with respect to the cement present. The present chapter is assessing the effect of varying the degree of substitution (DS) of algMOD (cfr. the number of incorporated methacrylates with respect to the OH groups present in alginate), thus the density of the polymer network, on the final SAP properties, the mortar strength upon incorporation of the SAPs and their self-sealing and -healing potential. In addition, both AA as well as AM have been incorporated to create a copolymer network to explore the effect of a natural backbone versus the synthetic crosslinker MBA (as described in §III.2.) on the different characteristics.

In summary, two algMOD derivatives with a varying DS have been co-polymerized with AA (and AM). After synthesis, gel fraction and particle size distribution have been determined. The chemical composition and cross-linking efficiency of these SAPs have been investigated by attenuated total reflectance infrared (ATR-IR) spectroscopy and high resolution magic-angle spinning proton nuclear magnetic resonance (HR-MAS ^{1}H-NMR) spectroscopy. Additionally, the moisture uptake capacity has been investigated by dynamic vapor sorption measurements. To identify the swelling capacity in different solutions, both aqueous as well as cement filtrate solutions have been used at varying pH-values by addition of hydrochloric acid or sodium hydroxide.
After full characterization, the SAPs have been incorporated in mortar to assess their effect on the flexural and compressive strength of mortar. Finally, the self-sealing and self-healing potential has been investigated using of a four-point-bending test.

IV.3.1. Methacrylation of alginate via modification with methacrylic anhydride

The degree of substitution (DS) of methacrylated alginate corresponds with the number of incorporated methacrylates with respect to the OH-moieties present in alginate and thus influences the density of the cross-linked network and therefore also the SAP properties. The DS has been determined through ^{1}H-NMR spectroscopy performed in collaboration with Prof. Adriaensens (appointed at UHasselt). As discussed earlier in §IV.2.1., ^{13}C-NMR spectroscopy will also be executed in future work to enable verification of the results obtained through ^{1}H-NMR spectroscopy. A representative spectrum of algMOD is presented in Figure IV.3 (§IV.2.1.).
Two algMOD batches with a DS of 19% and 9% (respectively high and low DS) have been used as starting materials for subsequent polymerization with AA or a combination of AA and AM, followed by SAP characterization and further use in mortar for evaluation of their influence on the mortar strength and self-sealing and -healing properties.

IV.3.2. Development of SAPs based on modified alginate and acrylic acid (and acrylamide)

The composition and gel fraction of all materials synthesized is listed in Table IV.7. To determine the reaction yield, the gel fractions of the SAPs were first determined. All values ranged between 85 and 93% indicating an efficient polymerization. There was no significant difference between p(alg(1)_AA_{100}(7))_H and p(alg(1)_AA_{100}(7))_L, while only a minor significant ($p < 0.05$) difference between p(alg(1)_AA_{75}/AM_{25}(7))_H and p(alg(1)_AA_{75}/AM_{25}(7))_L could be retrieved. The results were in excellent agreement with previous results based on AA and AA/AM with the synthetic cross-linker MBA for which gel fractions between 87 and 95% were obtained (§III.1. and §III.2.). These values give a qualitative prove of the polymerization efficiency. High resolution magic-angle spinning proton nuclear magnetic resonance (HR-MAS ^{1}H-NMR) spectroscopy provides a more quantitative prove.

Table IV.7: Chemical composition, degree of substitution and gel fraction of the developed SAPs.

Sample	$\frac{AlgMOD}{AA+AM}$ g/g	AA mol%	AM mol%	DS (/OH group)	Gel fraction (%)
p(alg(1)_AA_{100}(7))_H	1/7	100	0	19	85 ± 1
p(alg(1)_AA_{100}(7))_L	1/7	100	0	9	87 ± 1
p(alg(1)_AA_{75}/AM_{25}(7))_H	1/7	75	25	19	93 ± 2
p(alg(1)_AA_{75}/AM_{25}(7))_L	1/7	75	25	9	88 ± 1

After synthesis, the samples were freeze-dried and grinded. The particle size distribution is depicted in Table IV.8. The results show that the SAPs had similar sizes when considering d_{10} and d_{50}. Conversely, p(alg(1)_AA_{100}(7))_H showed a higher particle size for d_{90}. This difference could be related to the duration of the grinding process (correlated with the hardness of the polymers).

Table IV.8: Particle size distributions for the p(alg_AA/(AM)) SAPs.

Sample	d_{10} [µm]	d_{50} [µm]	d_{90} [µm]
p(alg(1)_AA_{100}(7))_H	10	34	223
p(alg(1)_AA_{100}(7))_L	11	25	69
p(alg(1)_AA_{75}/AM_{25}(7))_H	11	19	58
p(alg(1)_AA_{75}/AM_{25}(7))_L	12	27	71

IV.3.3. Chemical structure elucidation and assessment of the polymerization efficiency of the SAPs developed

In a first part, the SAPs were characterized by attenuated total reflectance infrared (ATR-IR) spectroscopy. As IR spectroscopy does not enable to detect changes in the algMOD DS, only a representative spectrum of each sample series (AA and AA/AM) is represented in Figure IV.11.

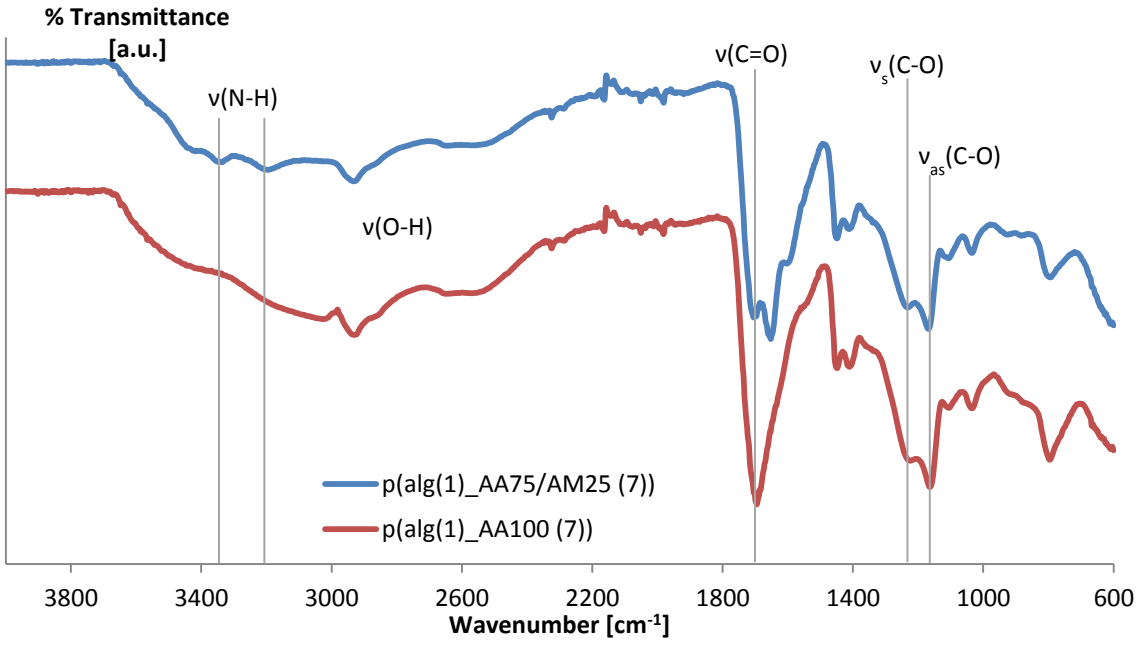

Figure IV.11: ATR-IR spectra of p(alg(1)_AA_{100} (7)) and p(alg(1)_AA_{75}/AM_{25} (7)) with designation of the relevant peaks and the corresponding bond vibrations as further described in Table IV.9.

The characteristic signals are listed in Table IV.9. The peaks related to the ester group of the modified alginate were present at 1170 and 1220 cm^{-1} and corresponded to the symmetric and asymmetric stretching vibration of the carbon-oxygen-carbon bonds (v(O=C-O)). At 1700 cm^{-1}, the carbon-oxygen double bond stretch vibration v(C=O) could be noticed which is related to the carboxylic acid moieties from both algMOD as well as AA. The broad oxygen-hydrogen stretch vibration v(O-H) of the carboxylic acid moieties was spread around 2400-3400 cm^{-1}. To identify AM, three characteristic signals could be found: the nitrogen-hydrogen stretch and the out-of-

plane equivalent (ν(N-H) and ν_{oop}(N-H)) on the one hand as well as the carbon-oxygen double bond stretch vibration ν(C=O) of the amide moiety.

Table IV.9: Relevant characteristic peaks visible in ATR-IR spectra from algMOD, AA and AM.

Wavenumber (cm^{-1}) AlgMOD	Vibration	Width	Functionality
1170	ν_{as}(C-O)	Sharp	Ester
1220	ν_{s}(C-O)	Sharp	Ester
1700-1720	ν(C=O)	Sharp	Carboxylic acid/ester
2400-3400	ν(O-H)	Broad	Carboxylic acid
Acrylic acid			
1700	ν(C=O)	Sharp	Carboxylic acid
2400-3400	ν(O-H)	Broad	Carboxylic acid
Acrylamide			
1625	ν_{oop}(N-H)	Sharp	Amide (out-of-plane)
1675	ν(C=O)	Sharp	Amide
3100-3500	ν(N-H)	Broad	Amide

In a second part, HR-MAS ^{1}H NMR spectroscopy indicated that the protons associated with the C=C double bonds in the range of 5.5 – 6.5 ppm had completely disappeared for p(alg(1)_AA_{75}/AM_{25}(7))_L while only a negligible amount of double bond protons remained for p(alg(1)_AA_{100} (7))_L (Figure IV.12). In addition, the peaks shifted to the lower ppm range (1.5 – 2.5 ppm) as anticipated after polymerization. The combination of ATR-IR spectroscopy and HR-MAS ^{1}H-NMR spectroscopy thus confirmed the chemical composition of the SAPs as well as their polymerization efficiency.

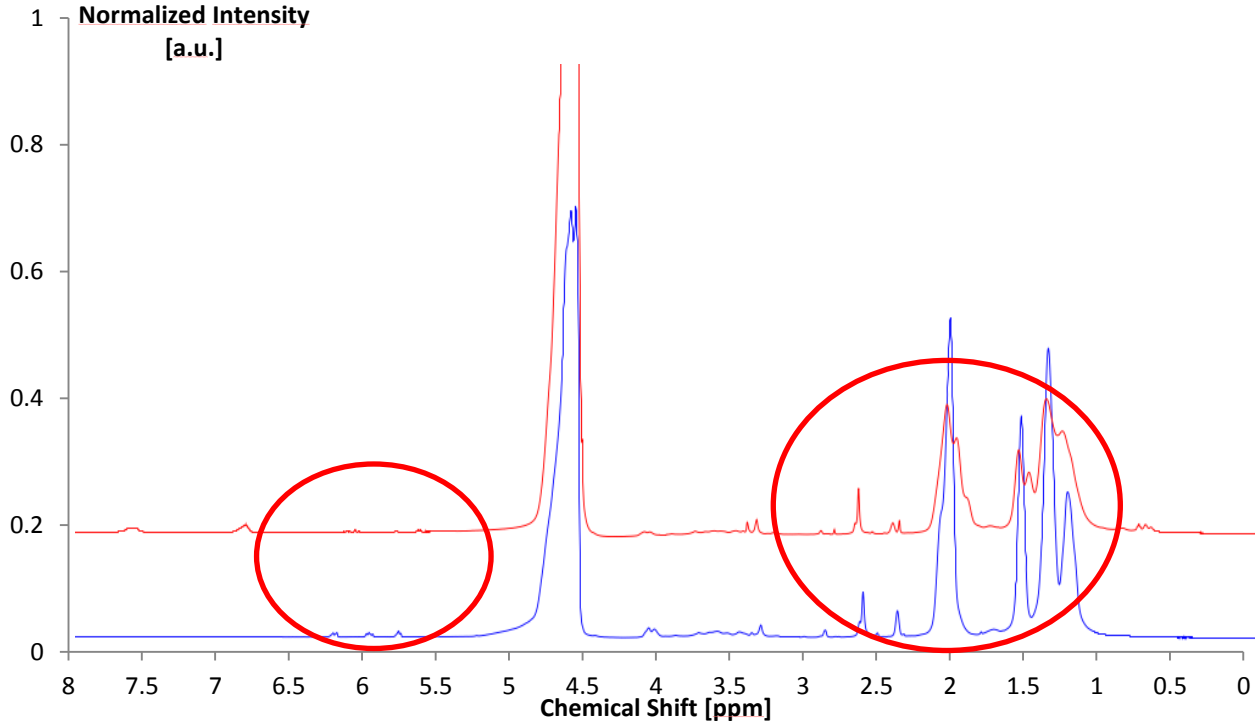

Figure IV.12: HR-MAS ^{1}H-NMR spectrum of p(alg(1)_AA_{75}/AM_{25}(7))_L (red) and p(alg(1)_AA100(7))_L (blue).

IV.3.4. Moisture uptake capacity determination via dynamic vapor sorption measurements

The DVS results are presented in Figure IV.13(a) for p(alg(1)_AA_{100}(7))_H and p(alg(1)_AA_{100}(7))_L and Figure IV.13(b) for p(alg(1)_AA_{75}/AM_{25}(7))_H and p(alg(1)_AA_{75}/AM_{25}(7))_L. The results show that the SAPs exhibited moisture uptake capacities ranging from 35.4 (p(alg(1)_AA_{75}/AM_{25}(7))_H) to 53.6% (p(alg(1)_AA_{100}(7))_H) of their own weight at a relative humidity (RH) of 95%. The materials containing only AA were characterized by a higher moisture uptake capacity, especially at RH ≥ 90%, as anticipated based on the higher amount of carboxylates present compared to the AA/AM blend. As in water vapor, no cations are present which can result in a screening effect towards AA [4-6], the carboxylates are able to take up more moisture than the amides. Only limited hysteresis was found for all SAPs studied, with a maximum of 3.5% for p(alg(1)_AA_{75}/AM_{25} (7))_L at 30% RH which was close to the detection limit for the DVS for these type of measurements (2 – 3%). The results described in §III.2.3. (Table III.3) showed that a difference in cross-linking density did not lead to a difference in moisture uptake capacity. In §III.3.3. (Table III.7), a variation of the cross-linking density also only led to a small change (close to detection limit) in moisture uptake capacity at 95% RH. Similarly, for the obtained results in the current part of the chapter, with a varying DS of algMOD a minor difference of the moisture uptake capacity at 95% RH was found being 4 and 6% for the AA/AM and AA-based SAPs, respectively.

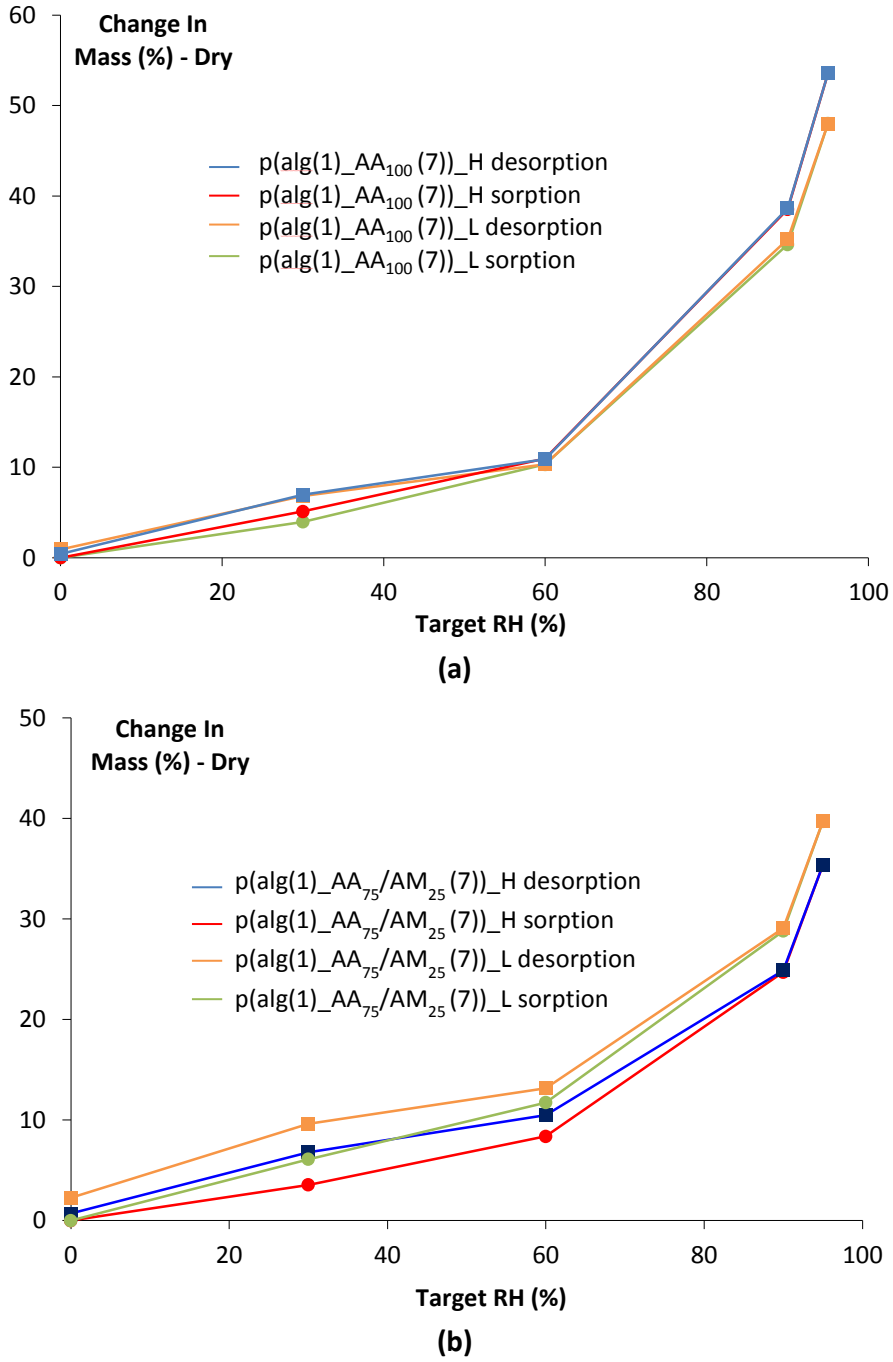

Figure IV.13: Moisture uptake capacity results of p(alg(1)_AA_{100}(7))_H and p(alg(1)_AA_{100}(7))_L (a) and p(alg(1)_AA_{75}/AM_{25}(7))_H and p(alg(1)_AA_{75}/AM_{25}(7))_L (b) obtained through dynamic vapor sorption measurements.

IV.3.5. Swelling capacity of the semi-synthetic SAPs

Swelling experiments were performed in both aqueous solutions of varying pH as well as cement filtrate solutions. In addition, potential SAP hydrolysis, in particular at extreme alkaline conditions, was investigated. Figure IV.14 depicts the effect of varying the DS of algMOD on the swelling degree of p(alg(1)_AA_{100}(7))_H and p(alg(1)_AA_{100}(7))_L. As the material with the lower DS algMOD followed a similar swelling trend as a function of the pH compared to the high DS material, the swelling was only depicted for a limited number of pH-values at which significant

differences were obtained (i.e. pH 2, 6, 10 and 12). As anticipated based on the monomer composition, p(alg(1)_AA_{100}(7))_H showed the same swelling trend in function of the pH as observed for p(AA_{100})_0.2 (see §III.1.4.). However, the absolute values were higher for the semi-synthetic SAPs due to the additional repelling carboxylate moieties present in algMOD (compared to the internal neutral amide moieties in MBA). Taking into account the DS of algMOD, for the high DS, 5 times more double bonds were present than for MBA. For the low DS, this corresponds with twice the amount of double bonds compared to MBA. Despite the increased amount of double bonds, the swelling at neutral to slightly alkaline pH (pH 6 – 10) was higher (49 to 52 g_{water}/g_{SAP} and 261 to 263 g_{water}/g_{SAP} for pH 6 and 10 for p(alg(1)_AA_{100}(7))_H and p(alg(1)_AA_{100}(7))_L respectively) than for p(AA_{100})_0.2 (Figure III.4, §III.1.4., 35 and 42 g_{water}/g_{SAP} for pH 6 and 10 respectively). At pH 12, the swelling became more pronounced for p(AA_{100})_0.2 (393 ± 14 g_{water}/g_{SAP}) than for p(alg(1)_AA_{100}(7))_H (99 ± 5 g_{water}/g_{SAP}). This could be related to the screening effect of a large amount of Na^+ cations [7, 8] towards the carboxylates in both AA as well as algMOD. Nevertheless, the decrease in DS led to a far superior swelling capacity, especially at pH 12, even outperforming the swelling of p(AA_{100})_0.2. The screening effect on the one hand and a more open structure due to a decrease in DS are two counteracting parameters to take into account.

When comparing p(alg(1)_AA_{100}(7))_H and p(alg(1)_AA_{100}(7))_L, a superior swelling capacity was found for p(alg(1)_AA_{100}(7))_L being more than 5 times the water uptake of p(alg(1)_AA_{100}(7))_H at pH 6 – 12 with no significant difference between pH 6 and 10 for both materials. The swelling of p(alg(1)_AA_{100}(7))_L increased from 21 ± 3 g_{water}/g_{SAP} at pH 2 to 263 ± 20 g_{water}/g_{SAP} at pH 10. A further increase was observed up to a maximum of 630 ± 31 g_{water}/g_{SAP} at pH 12.

When comparing the obtained swelling results of p(alg(1)_AA_{100}(7))_H in aqueous solutions at different pH values with the swelling capacity in ultrapure water (as described in section §IV.1.4.), the latter showed a swelling of 80 ± 1 g_{water}/g_{SAP}. This difference could be related to the particle size, as larger particles were obtained herein, which results in a smaller surface area, thus a lower final swelling degree [9]. The swelling capacity of p(alg(1)_AA_{100}(7))_H in cement filtrate was substantially lower (i.e. 12 ± 1 g_{water}/g_{SAP}) than p(alg(1)_AA_{100}(7))_L (23 ± 3 g_{water}/g_{SAP}), due to the presence of divalent ions, which has already been explained earlier (§III.2.4.). The observed trends could be explained by ATR-IR spectroscopy performed on the dried SAPs after incubation in the different solutions (Table IV.10). No difference in ATR-IR spectra could be observed when comparing the original material with the SAPs after incubation in solutions with varying pH up to 10. The first increase in swelling capacity from pH 2 to 6 was related to the pH-sensitivity of the acid moieties.

At pH 12, the symmetric and asymmetric carbon-oxygen bond stretch vibrations ν_s(C-O) and ν_{as}(C-O) of the carboxylates at 1410 and 1550 cm^{-1} respectively became more distinguishable while the carbon-oxygen double bond stretch vibration ν(C=O) at 1700 cm^{-1} became less visible. This effect was even more strongly pronounced at pH 13. Indeed, ν_s(C-O) and ν_{as}(C-O) became very strong while ν(C=O) disappeared completely. The latter could be explained by hydrolysis of the incorporated methacrylate ester from algMOD resulting in the formation of a carboxylate

and an alcohol moiety. As this gave rise to a less densely cross-linked network, the SAPs could absorb additional water. However, from a critical point onwards, too many linkages became hydrolyzed thereby impairing the network intactness resulting in a distinct decrease of the swelling capacity. This was particularly applicable at pH 13, since not only the ν_s(C-O) and ν_{as}(C-O) corresponding with the carboxylate became very strong, but also the broad oxygen-hydrogen stretch ν(O-H) associated with alcohols was more pronounced. Another indication further supporting our hypothesis, was the decrease in intensity of the symmetric and asymmetric carbon-oxygen bond stretch vibrations ν_s(C-O) and ν_{as}(C-O) of the ester at 1170 and 1220 cm^{-1} respectively. In CF solution, the same trends were observed as for alkaline aqueous solutions. Interestingly, the peaks associated with carboxylates were not as pronounced in CF solutions indicating that the degradation of the material was less severe in CF solution.

ATR-IR spectroscopy of p(alg(1)_AA_{100}(7))_L (Appendix Table S.1) indicated that at pH 12, ν_s(C-O) and ν_{as}(C-O) associated with the carboxylates became dominant, while ν(C=O) was suppressed by the shoulder of ν_{as}(C-O) from the carboxylates, albeit quite limited. The latter indicated that degradation phenomena already started from a pH of 12 for p(alg(1)_AA_{100}(7))_L in contrast with p(alg(1)_AA_{100}(7))_H , as anticipated based on the less dense network structure associated with the lower cross-linking degree (cfr. low DS algMOD). In CF solutions, a similar trend was observed for the degradation of low DS SAPs compared to their high DS counterparts.

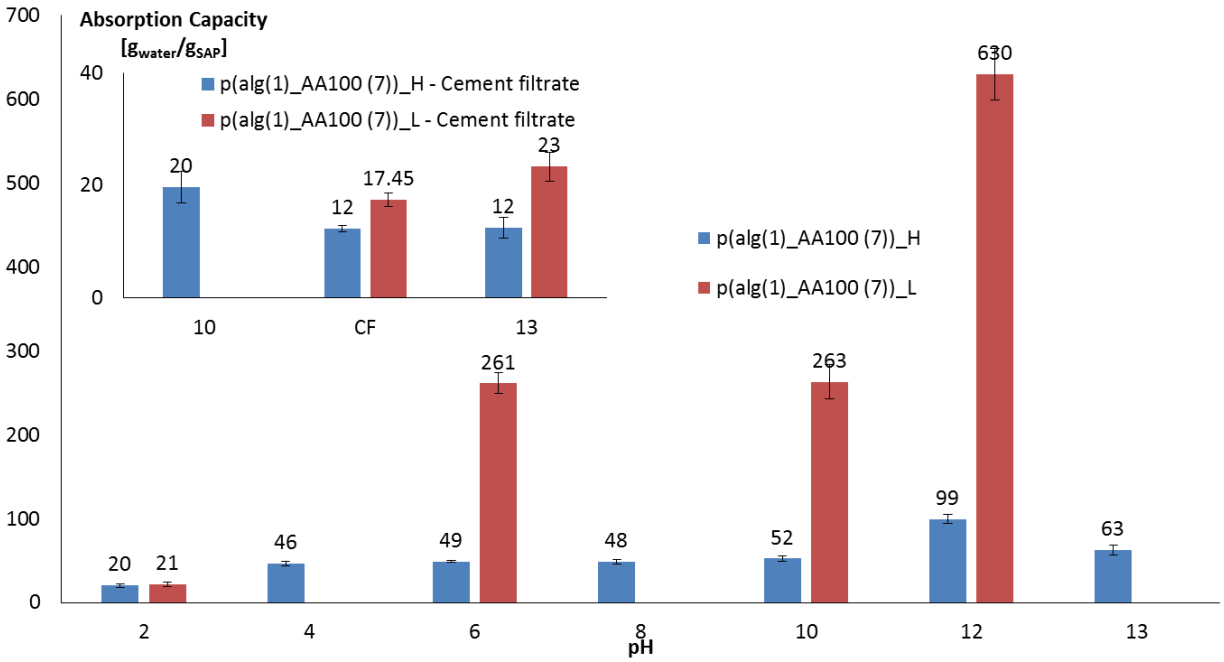

Figure IV.14: Comparison of the swelling capacity of p(alg(1)_AA_{100}(7))_H and p(alg(1)_AA_{100}(7))_L both in aqueous solutions at different pH as well as in (acidified and basified) cement filtrate solutions (inset).

Figure IV.15 shows the swelling potential of p(alg(1)_AA_{75}/AM_{25}(7))_H and p(alg(1)_AA_{75}/AM_{25}(7))_L SAPs in different aqueous and CF solutions. First of all, similar as in Figure IV.14, a decrease in DS led to an increase in the swelling capacity. Incubation of

p(alg(1)_AA_{75}/AM_{25}(7))_H in aqueous solutions was in agreement with the results obtained for p(AA_{75}/AM_{25})_0.2 (see §III.2.4.). An identical calculation for the amount of double bonds between MBA and algMOD could be made as performed earlier for the p(alg(1)_AA_{100}(7))_x series. Again, 5 times more double bonds were present in p(alg(1)_AA_{75}/AM_{25}(7))_H (DS of 19%) compared to MBA. For the low DS (9%), this was twice the amount of double bonds than MBA. Interestingly, the swelling capacity between pH 6 and 10 is not significantly different between p(alg(1)_AA_{75}/AM_{25}(7))_H and p(AA_{75}/AM_{25})_0.2. At pH ≥ 12, the swelling of p(AA_{75}/AM_{25})_0.2 became superior. The latter could again be related to a strong screening effect by Na^+ cations of p(alg(1)_AA_{75}/AM_{25}(7))_H due to the strong presence of carboxylate moieties in both the AA as well as the algMOD.

The overall swelling capacity of p(alg(1)_AA_{75}/AM_{25}(7))_H was higher compared to p(alg(1)_AA_{100}(7))_H. A similar explanation as described in §III.2. could explain this observed trend as a higher amount of carboxylates in p(alg(1)_AA_{100}(7))_H would lead to a stronger screening effect upon addition of NaOH to the aqueous solutions.

The ATR-IR spectra of p(alg(1)_AA_{75}/AM_{25}(7))_H (Table IV.11) showed additional peaks compared to p(alg(1)_AA_{100}(7))_H including the broad out-of-plane bending vibration γ(N-H) at 794 cm^{-1} and the carbon-oxygen double bond stretch vibration ν(C=O) peak at 1675 cm^{-1}, both characteristic for primary amides. Similar trends were observed for p(alg(1)_AA_{75}/AM_{25}(7))_H compared to p(alg(1)_AA_{100}(7))_H. The peaks associated with esters (ν_s(C-O), ν_{as}(C-O) and ν(C=O) at 1170, 1220 and 1700 cm^{-1} respectively) became weak at pH ≥ 12. In addition to the ester degradation, the amide moieties hydrolyzed thereby forming carboxylate functionalities and ammonia (NH_3). Although γ(N-H) became less apparent, ν(C=O), characteristic for the amide moieties, remained clearly visible, indicating that amides are less prone to degradation compared to ester functionalities which is also described in depth in literature [10-12]. This partial hydrolysis was also visualized by the more intense signals corresponding with carboxylates (ν_s(C-O) and ν_{as}(C-O) at 1410 and 1550 cm^{-1} respectively). In cement filtrate solutions, a similar trend was observed as found for the synthetic SAPs based on AA and AM. A delayed hydrolysis behavior is found, with less degradation in CF compared to alkaline aqueous solutions, due to the shielding effect from the present multivalent cations. The ATR-IR spectra of p(alg(1)_AA_{75}/AM_{25}(7))_H can be found in Table S.2.

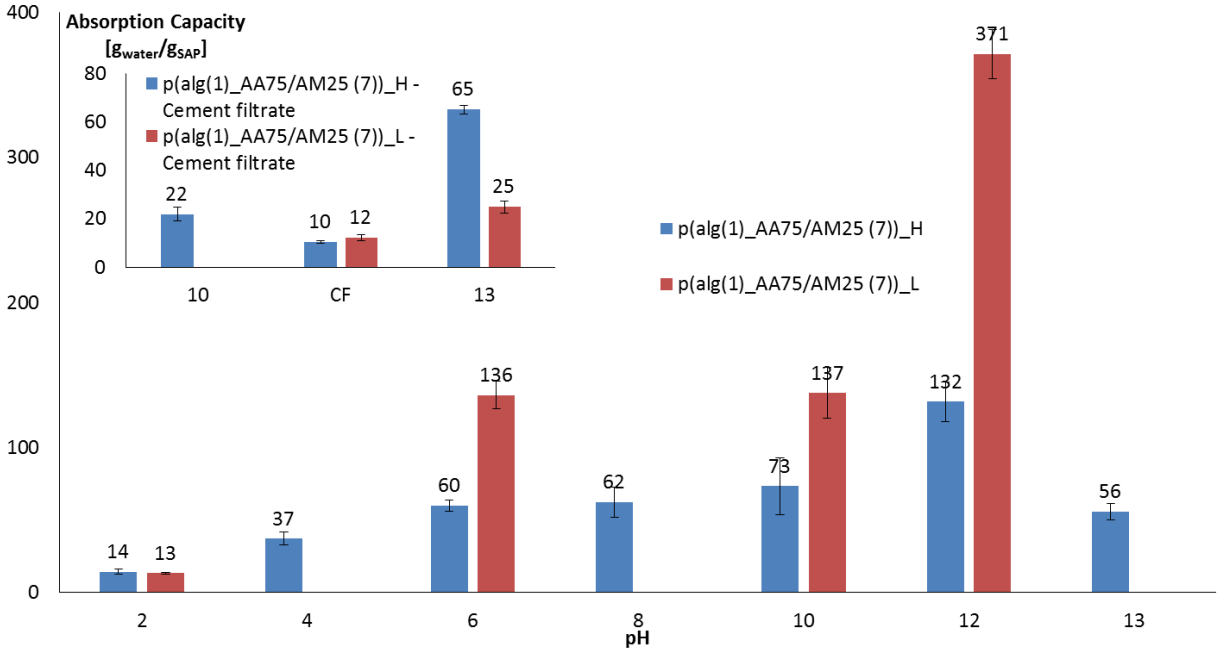

Figure IV.15: Comparison of the swelling capacity of p(alg(1)_AA_{75}/AM_{25}(7))_H and p(alg(1)_AA_{75}/AM_{25}(7))_L both in aqueous solutions as well as in (acidified/basified) cement filtrate solutions (inset).

Table IV.10: ATR-IR spectroscopy results obtained for dried SAPs after incubation of p(alg(1)_AA_{100}(7))_H in different solutions.

Frequency [cm^{-1}]	Assignment	Reference	pH 10	pH 12	pH 13.0	CF pH 10	CF (pH 12.6)	CF pH 13
1170	ν_{as}(C-O) ester	s	s	s	w	s	w	sh
1220	ν_{s}(C-O) ester	s	s	s	/	s	/	/
1410	ν_{s}(C-O) carboxylate	w	w	m	vs	w	vs	vs
1550	ν_{as}(C-O) carboxylate	sh	sh	m	vs	w	vs	vs
1700	ν(C=O) ester	vs	vs	s	/	vs	/	/

w: weak, m: medium, s: strong, vs: very strong, sh: shoulder, shp: sharp, br: broad
* 1° and 2° represent primary and secondary amide respectively

Table IV.11: ATR-IR spectroscopy results obtained for dried SAPs after incubation of p(alg(1)_ $AA_{75}/AM_{25}(7)$)_H in different solutions.

Frequency [cm^{-1}]	Assignment	Reference	pH 10	pH 12	pH 13	CF pH 10	CF (pH 12.5)	CF pH 13
794	γ(N-H) amide (1°)*	m, br	m, br	sh	sh	m, br	m, br	/
1170	ν_{as}(C-O) ester	s	s	w	w	s	sh	sh
1220	ν_{s}(C-O) ester	s	s	w	/	s	/	/
1410	ν_{s}(C-O) carboxylate	w	w	m	vs	w	s	vs
1550	ν_{as}(C-O) carboxylate	w	w	s	vs	w	vs	vs
1675	ν(C=O) amide	vs	vs	s	s	s	s	m
1700	ν(C=O) ester	vs	vs	/	/	s	sh	m

w: weak, m: medium, s: strong, vs: very strong, sh: shoulder, shp: sharp, br: broad
* 1° represents primary amide

IV.3.6. The effect of algMOD based SAPs on the flexural and compressive strength upon incorporation in mortar

All SAPs have been incorporated in mortar at a concentration of 0.5 and 1 m% with respect to the added amount of cement. Bending and compressive strength tests have been performed on the mortars to investigate the effect of the SAP addition (see Table IV.12). SAPs with a high DS led to a lower needed amount of additional water to mortar, resulting in a less pronounced effect on the mortar strength. Generally, the bending strength was only affected to a minor extent, except upon addition of 1 m% p(alg(1)_AA_{75}/AM_{25}(7))_L) for which the strength reduction amounted to 22%. The latter was also reflected in the compressive strength, as indicated by the observed reduction of 47% which is unacceptable for the targeted application. Unfortunately, a large variation on the compressive strength of the different references was found. It was considered best to compare the strength of the SAP containing specimens to the matching reference as the same materials and procedures were used and only the time of production was different. Nevertheless, it should be kept in mind that a result of for example 68 MPa for the mortar with p(alg(1)_AA_{100}(7))_H p(alg(1)_AA_{100}(7))_H compared to reference 3 (see Table IV.12) results in a 7% strength reduction, while this obtained value is actually higher than the strength of references 2 and 4. The low DS p(alg(1)_AA_{100}(7))_L did not result in a substantial strength reduction upon applying 0.5 m% SAP, but was concomitant with a reduction of 18% when introducing 1 m% SAP. The compressive strength reduction of p(alg(1)_AA_{100}(7))_H was very limited (as described in §IV.2.). Since p(alg(1)_AA_{100}(7))_L swells extremely in aqueous solutions and the strength reduction is limited, both p(alg(1)_AA_{100}(7))_H and p(alg(1)_AA_{100}(7))_L materials are likely to be very promising to be included in further self-healing tests. This is confirmed when comparing the obtained data to what was measured for commercial SAPs [13] (data shown in Table IV.3. in §IV.1.3.). The promising AA-based semi-synthetic SAPs outperformed both commercial SAPs.

When using p(alg(1)_AA_{75}/AM_{25}(7)), the effect on the mortar strength was more pronounced compared to the p(alg(1)_AA_{100}(7)) SAPs. This could be related to the shielding effect of the carboxylates in alginate and AA due to the presence of the divalent cations (Ca^{2+} and Mg^{2+}), which is not occurring for AM, causing the AA/AM-based SAPs to swell more thereby create larger macro-pores. This could also be seen by the amount of additional water which was higher when comparing equal DS values. The mortar strength of p(alg(1)_AA_{75}/AM_{25}(7))_H was acceptable upon addition of 0.5 m%, which was comparable as when adding 1 m% p(alg(1)_AA_{100}(7))_L. However, the other SAPs resulted in strength reductions down to 47%, indicating that the p(alg(1)_AA_{75}/AM_{25}(7)) SAPs were less promising. Nevertheless, they were also taken into account throughout future four-point-bending tests.

Table IV.12: Flexural and compressive strength of mortar samples upon addition of SAPs.

p(alg(1)_AA_{100}(7))_H		Bending strength [MPa]	Compressive strength [MPa]	Batch
0.5 m%	(+ 15 mL water)	6.8 ± 0.4 (-11%)	68.9 ± 1.6 (-6%)	3
1 m%	(+ 30 mL water)	7.6 ± 0.3 (/)	68.3 ± 0.6 (-7%)	3
p(alg(1)_AA_{100}(7))_L				
0.5 m%	(+ 25 mL water)	8.2 ± 0.1 (-2%)	64.2 ± 1.9 (/)	4
1 m%	(+ 60 mL water)	8.0 ± 0.4 (/)	55.0 ± 1.2 (-18%)	2
p(alg(1)_AA_{75}/AM_{25}(7))_H				
0.5 m%	(+ 25 mL water)	8.3 ± 0.3 (-2%)	56.9 ± 1.4 (-17%)	1
1 m%	(+ 40 mL water)	7.5 ± 0.3 (-13%)	49.3 ± 2.0 (-28%)	1
p(alg(1)_AA_{75}/AM_{25}(7))_L				
0.5 m%	(+ 33 mL water)	7.1 ± 0.7 (-7%)	49.1 ± 0.9 (-27%)	2
1 m%	(+ 80 mL water)	5.9 ± 0.5 (-22%)	35.8 ± 1.4 (-47%)	2
Reference				
No SAP	/	8.6 ± 0.2	68.4 ± 1.1	1
No SAP	/	7.6 ± 1.1	67.3 ± 1.9	2
No SAP	/	7.6 ± 0.5	73.1 ± 1.6	3
No SAP	/	8.4 ± 0.4	63.2 ± 1.3	4

IV.3.7. Self-sealing and -healing of mortar samples by addition of SAPs

Self-sealing is related to the possibility of the SAPs to block the cracks and as such stop the entrance of particles dissolved in solution or gases which can attack the reinforcement. Self-healing is related to the strength regain after healing cracks. At first, a four-point-bending test was performed to induce multiple cracking when the samples were at the age of 28 days. The area between the point loads will contain the majority of the cracks and will be used to investigate the self-sealing potential. Multiple cracking occurs up to the point of critical damage where one crack starts to develop further and leads to total failure of the mortar sample. The test samples were thinner compared to the samples made for flexural and compressive tests (10 mm instead of 40 mm) to limit the needed amount of force to break the specimens [14]. On top of this, fibers have been used to create multiple cracking and limit the crack width. Several parameters of the mortar samples have been determined during this experiment (as described in Figure II.3, §II.3.15.): the first-cracking strength σ_{fc}, the regain in σ_{fc}, the peak strength σ_p and

the amount of multiple cracking MC. All tests have been performed at least in triplicate. For all SAP materials, 0.5 and 1 m% in function of the amount of cement has been added. For one material (p(alg(1)_AA_{100}(7))_L) it has been tested what the effect would be to add 0.7 and 1.3 m% SAP.

In order to investigate the crack sealing behavior of the used polymers, specimens have been studied which were loaded until a strain of approximately 1% or until complete failure. As such, the sealing of both small and larger cracks could be visualized. The large cracks are useful to identify where the crack width limitation is above which almost no crack sealing will be found. For that reason, these cracks have only been measured immediately after cracking and after 28 days of wet-dry cycles. For the samples loaded until 1% strain, the cracks have been investigated right after loading, and then after 3, 7, 14 and 28 days of wet-dry cycles. After 28 days, these samples were loaded again, now until complete failure. As such, the regain in first-cracking strength could be determined, which is the indicative parameter for the self-healing behavior of these samples.

The results visualized in Figures IV.16 (except top right) and IV.17 indicate the crack widths of samples loaded until a strain of 1%. In function of the crack width, (after cracking and after 3, 7, 14 and 28 days of wet-dry cycles) the closure of cracks is depicted by presenting the percentage of cracks smaller than a certain width w. Figure IV.16 (top right) and Figures IV.18 and IV.19 show similar graphs for samples which have been loaded till failure immediately. This provides an idea of the sealing potential of SAPs for larger cracks.
First, when comparing p(alg(1)_AA_{100}(7))_H with the reference for samples loaded until 1% strain, it was found that larger cracks were obtained for the former (90% of the cracks smaller than 65 and 52 µm for 0.5 and 1 m% SAP respectively as a function of the amount of cement) than for the latter (90% of the cracks smaller than 38 µm). Despite the larger cracks, addition of p(alg(1)_AA_{100}(7))_H resulted in an stronger self-sealing (72 and 68% cracks completely sealed after 28 days through addition of 0.5 and 1 m% respectively and 38 and 53% after 3 days) as the reference (51% of cracks were completely sealed after 28 days and 22% after 3 days). As can be seen no real difference was seen after 28 days between addition of 0.5 or 1 m% of SAP, but the sealing was reached faster for 1 m%. For 0.5 m% SAP, cracks up to 80 µm showed partial or complete sealing. For 1 m%, this increased to cracks up to 90 µm.

When investigating the different concentrations of p(alg(1)_AA_{100}(7))_L, it was found that an addition of 0.5 or 0.7 m% (Figures IV.16 bottom left and IV.17 top left respectively) led to similar trends regarding the crack width (90% of cracks smaller than 57 and 58 µm respectively) and self-sealing behavior (48% and 56% respectively completely sealed after 28 days and 22 and 29% after 3 days) with 0.7 m% performing slightly better than expected. Despite their larger cracks widths, both amounts sealed a similar amount of cracks as the reference, with the 0.7 m% mix performing slightly better than the reference. Addition of 1 or 1.3 m% led to a similar percentage of complete self-sealing as the lower concentration after 3 days (20 and 29 % respectively), but a superior closure after 28 days (75 and 71% respectively), which was especially promising for the larger cracks in the 1.3 m% SAP mix as 90% of the cracks had a size up to 73 µm (in comparison

to 40 µm for 1 m%). Self-sealing of cracks by addition of both 1 and 1.3 m% of SAP was superior compared to the reference.
Interestingly, when comparing the high and low DS, a stronger sealing was found in the case of 0.5 m% for the high DS and for 1 (and 1.3) m% for the low DS. However, for the low DS, the swelling capacity was up to 5 times higher, causing the self-sealing to be stronger upon adding a higher amount of SAP.

When comparing p(alg(1)_AA_{75}/AM_{25}(7))_H and p(alg(1)_AA_{75}/AM_{25}(7))_L with the reference (again samples loaded until 1% strain), it can be seen that p(alg(1)_AA_{75}/AM_{25}(7))_H showed generally larger cracks to start with (90% of the cracks were smaller than 35 and 85 µm for 0.5 and 1 m% of SAP, respectively) than p(alg(1)_AA_{75}/AM_{25}(7))_L (90% of the cracks smaller than 29 and 54 µm for 0.5 and 1 m% of SAP, respectively) and the reference (90% of the cracks smaller than 38 µm). For all the added amounts of SAPs, a stronger sealing could be observed than the reference where 51% of cracks were completely sealed after 28 days and 22% after 3 days. For p(alg(1)_AA_{75}/AM_{25}(7))_H, 86 – 80% of the cracks were completely sealed after 28 days for 0.5 and 1 m%, respectively. More than half of this sealing was already visible in the first 3 days (47 – 59% sealed, respectively). In the case of p(alg(1)_AA_{75}/AM_{25}(7))_L, 88 – 70% of the cracks were completely sealed after 4 weeks of wet-dry cycles for 0.5 and 1 m% of SAP. Again, after 3 days 60 – 37% of the cracks were sealed. A stronger sealing was observed for the samples with 0.5 m% SAP which could be explained by the smaller crack-size in general compared to the 1 m% samples. Interestingly, p(alg(1)_AA_{75}/AM_{25}(7))_H with 1 m% SAP showed a stronger sealing than his counterpart with a low DS, despite the larger cracks which indicated a faster efficiency of the sealing. When now comparing p(alg(1)_AA_{75}/AM_{25}(7))_H with p(alg(1)_AA_{100}(7))_H it can be seen that the former sealed better for both 0.5 and 1 m% addition of SAPs (86 – 80% vs. 72 – 68%, respectively). For 0.5 m%, the larger crack widths of the pure AA-based SAP (90% of the cracks smaller than 65 µm) could explain this difference. For 1 m% this was not the case and the AA/AM SAP had a superior sealing.

To assess the self-sealing capacity of larger cracks, the crack-widths of samples loaded until failure were investigated. The general boundary for partial self-sealing of cracks with SAPs was found to be around 150 µm and even 200 µm for p(alg(1)_AA_{100}(7))_L. This was more limited for the reference where only cracks smaller than 100 µm showed partial self-sealing. SAPs block the cracks in their swollen state, reducing the washout of healing products, thus ameliorating the healing conditions. The mortars with p(alg(1)_AA_{100}(7))_H performed better than p(alg(1)_AA_{75}/AM_{25}(7))_H. A similar trend was observed for addition of 1 m% of p(alg(1)_AA_{100}(7))_L and p(alg(1)_AA_{75}/AM_{25}(7))_L.

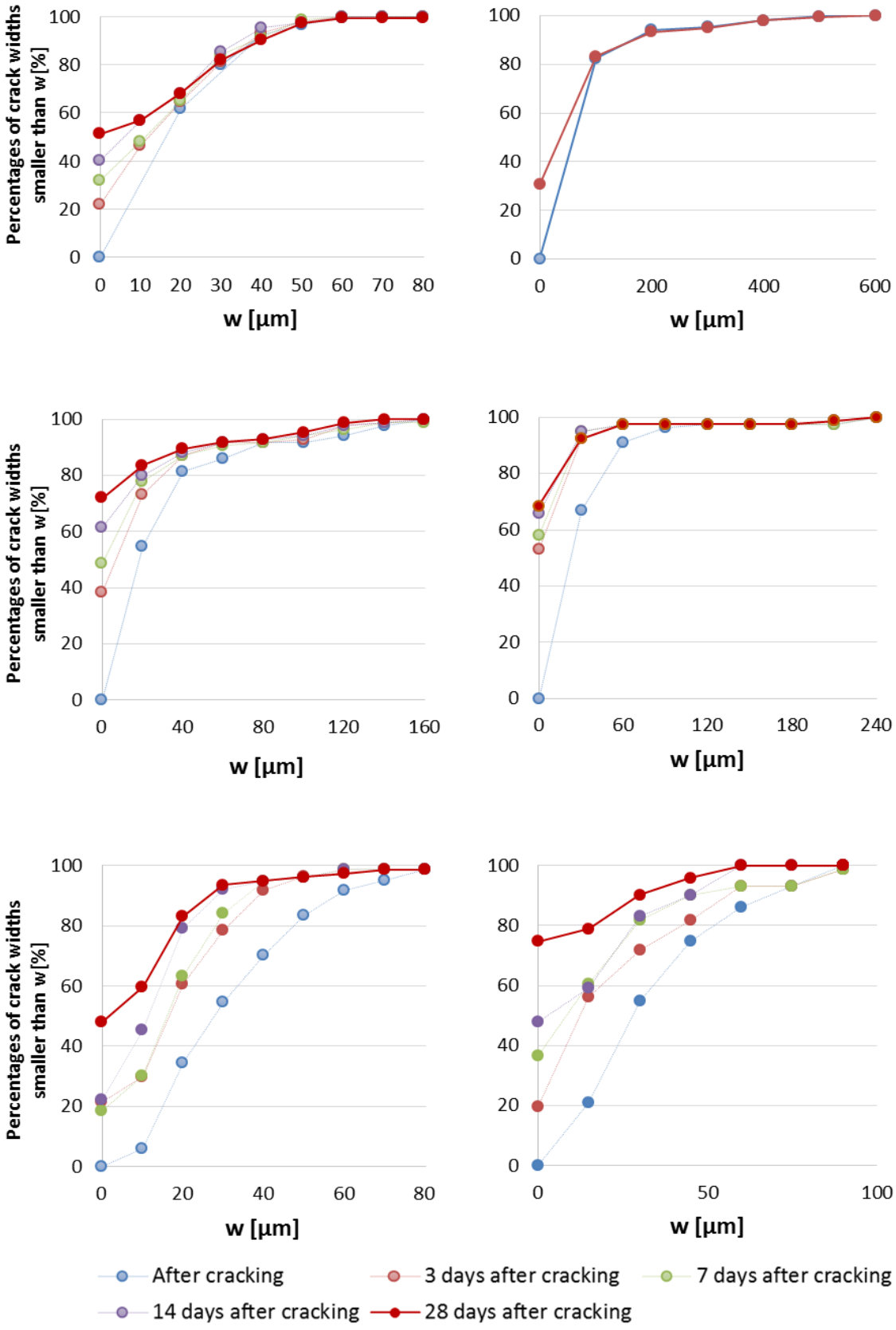

Figure IV.16: Crack closure of the wet-dry cycles for the reference mortar after loading until 1% strain (top left) and until failure (top right) and after loading until 1% strain for mortars containing p(alg(1)_AA_{100}(7))_H (0.5 m% SAP, center left and 1 m% SAP, center right) and p(alg(1)_AA_{100}(7))_L (0.5 m% SAP, bottom left and 1 m% SAP, bottom right).

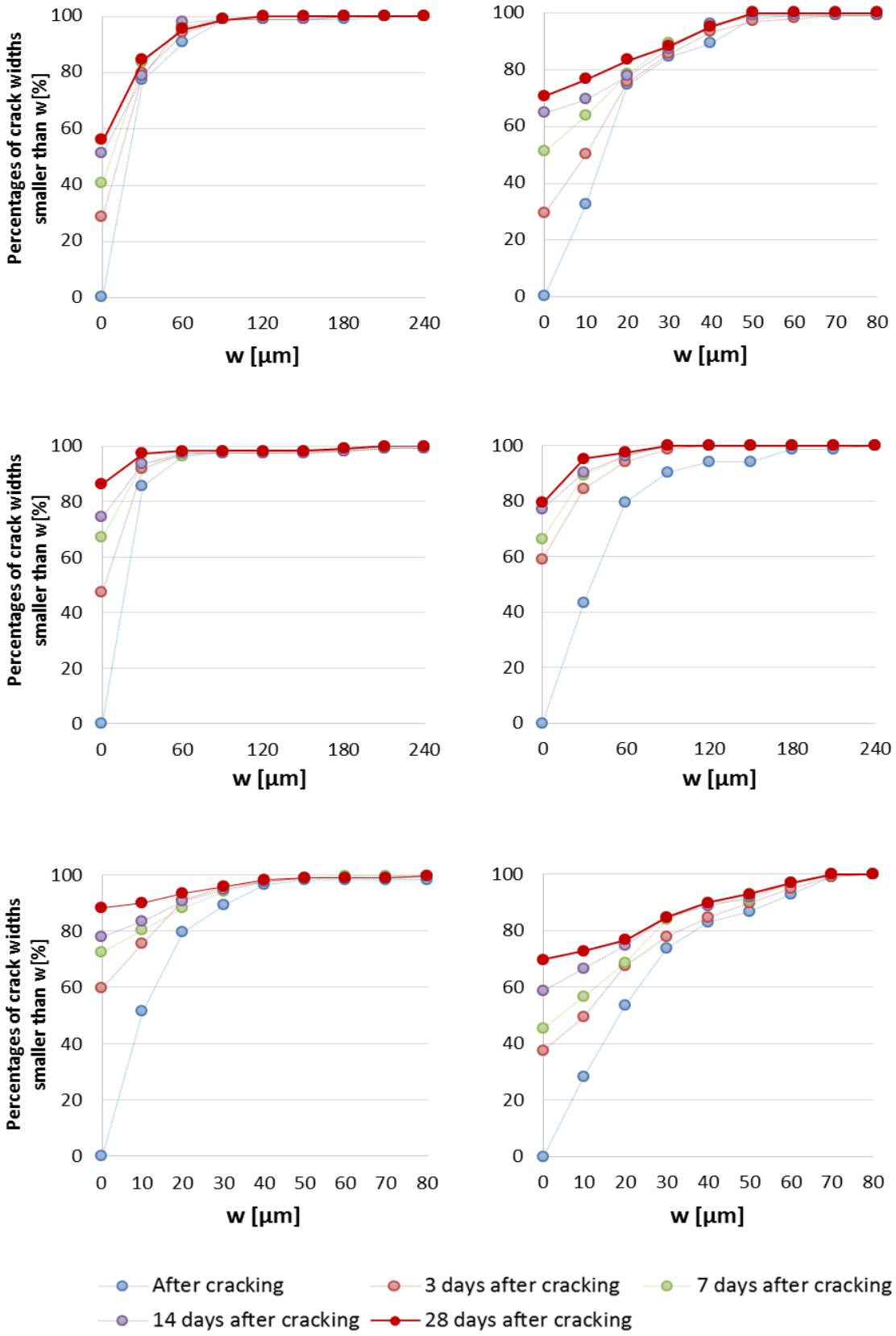

Figure IV.17: Crack closure of the wet-dry cycles after loading until 1% strain for mortars containing p(alg(1)_AA_{100}(7))_L (0.7 m% SAP, top left and 1.3 m% SAP, top right), p(alg(1)_$AA_{75}AM_{25}$(7))_H (0.5 m% SAP, center left and 1 m% SAP, center right) and p(alg(1)_$AA_{75}AM_{25}$(7))_L (0.5 m% SAP, bottom left and 1 m% SAP, bottom right).

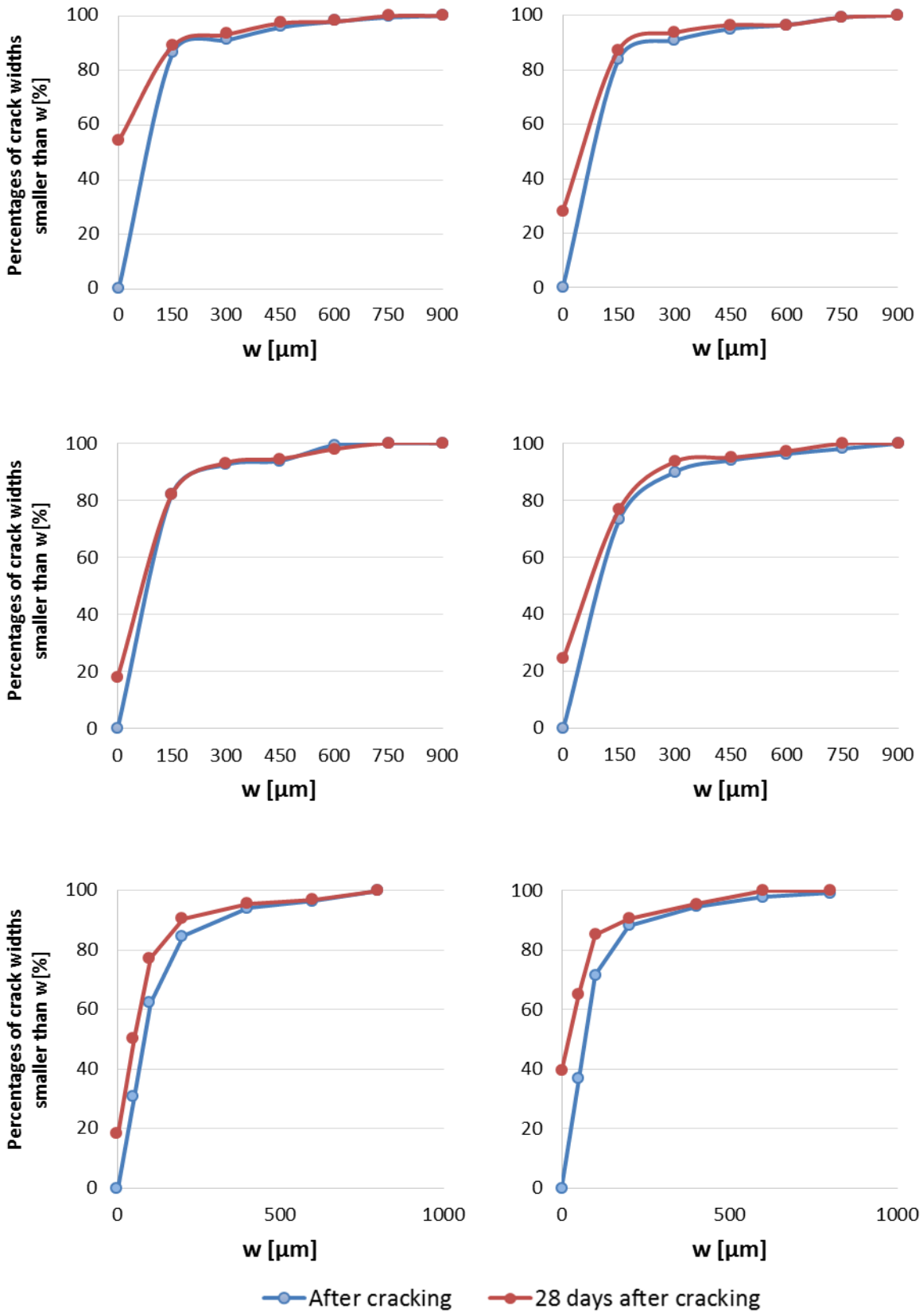

Figure IV.18: Crack closure of the wet-dry cycles after loading until failure for mortars containing p(alg(1)_AA_{100}(7))_H (0.5 m% SAP, top left and 1 m% SAP, top right), p(alg(1)_AA_{100}(7))_L (0.5 m% SAP, center left and 1 m% SAP, center right) and p(alg(1)_AA_{100}(7))_L (0.7 m% SAP, bottom left and 1.3 m% SAP, bottom right).

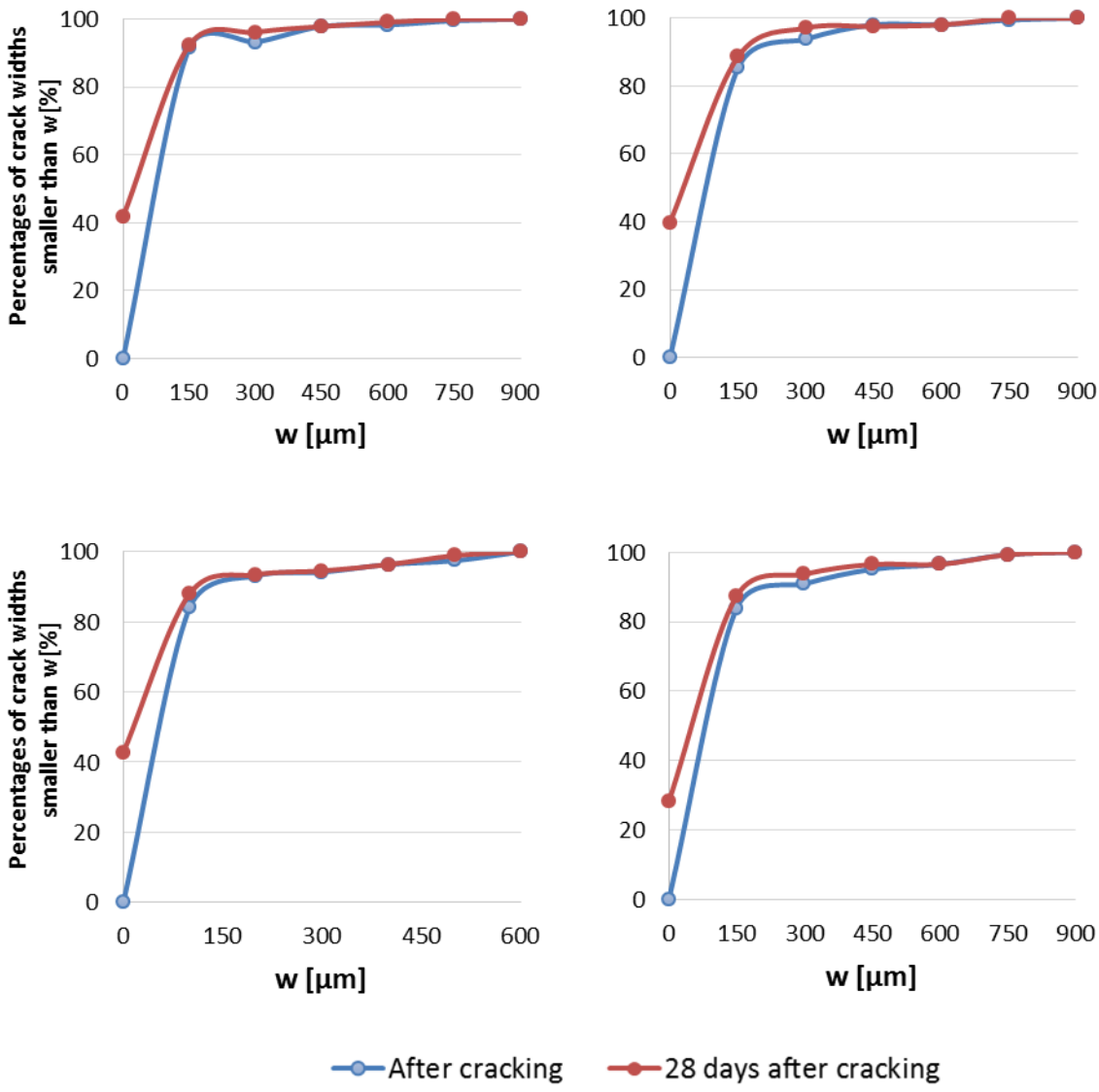

Figure IV.19: Crack closure of the wet-dry cycles after loading until failure for mortars containing p(alg(1)_$AA_{75}AM_{25}$(7))_H (0.5 m% SAP, top left and 1 m% SAP, top right) and p(alg(1)_$AA_{75}AM_{25}$(7))_L (0.5 m% SAP, bottom left and 1 m% SAP, bottom right).

Table IV.13 gives an overview of the mechanical parameters measured for the mortars to indicate the self-healing potential obtained by addition of SAPs. All measurements were done at least in triplicate, except for σ_p and MC of p(alg(1)_AA_{100} (7))_H (1m%) and p(alg(1)_AA_{75}/AM_{25} (7))_L (0.5 m%) where one of the samples had broken on first contact. When comparing the data it was found that the mean σ_{fc} was not significantly different from the reference for samples containing SAP with a low DS (both AA and AA/AM, except for addition of 1 m% p(alg(1)_AA_{100}(7))_L). The samples containing SAP with a high DS showed a significant decrease in the mean σ_{fc} (except for 0.5 m% p(alg(1)_AA_{100}(7))_L). SAPs may have 2 opposite effects on the strength. They could increase the strength upon further hydration of the matrix during the hardening phase by releasing mixing water (internal curing). However, due to the formation of macro-pores they could also decrease the strength [15, 16]. The reason why for a low DS no significant difference in strength was found, could be related to the fact that these combined

effects cancel each other. In the case of a high DS, the swelling might not be high enough for a strong internal curing, while still the high amount of SAPs added lead to more macro-pores.

Overall it was found that the regain in σ_{fc} for all mortars containing SAPs increased strongly compared to the reference mortar, albeit only significant for the samples with a high DS and 1 m% p(alg(1)_AA_{100}(7))_L. The values obtained for σ_{fc} (6.1 MPa) and regain in σ_{fc} (40%) from the reference were in compliance with Snoeck et al. [14]. The strongest healing was found for p(alg(1)_AA_{100}(7))_H (63 ± 4 % and 59 ± 7% for 0.5 and 1 m% respectively). Interestingly, this material also showed no effect on the flexural and compressive strength as described above (§IV.3.6.) which makes this material extremely interesting. The results obtained for p(alg(1)_AA_{75}/AM_{25}(7))_H were also promising (57.2 ± 4.2 % and 57.0 ± 6.8 % for 0.5 and 1 m% respectively) although they have a more pronounced effect on the compressive strength. Strange enough, no differences were found when higher amounts of p(alg(1)_AA_{100}(7))_L were added compared for both the σ_{fc} as well as the regain in σ_{fc}. A variation (addition of 0.7 m% and 1.3 m%) of such a low extent thus had no real influence on the self-healing parameters.

There was no significant difference for the multiple cracking MC in any of the samples, although the value of the reference (3.1 ± 0.9 %) was higher than what was found by Snoeck et al. (2%, [14]). Nonetheless, most of the values of MC were higher for the samples with SAP which could be related to an increase in the ductility of mortar by addition of SAPs. The polymers act as flaws, facilitating MC [17].

When comparing the results to data obtained by Snoeck et al. [14] for commercially available SAPs (i.e. for the addition of 0.5 m% SAP A (copolymer of acrylamide and sodium acrylate) and 0.5 and 1 m% SAP B (cross-linked potassium salt poly(acrylate)) [16]), no significant differences were found for the MC. Additionally, σ_{fc} was similar for the commercial and the synthesized SAPs, although it was significantly lower than for addition of 1 m% p(alg(1)_AA_{75}/AM_{25}(7))_L and 0.7 m% p(alg(1)_AA_{100}(7))_L. These latter 2 showed a rather high σ_{fc} with a large standard deviation. More interestingly, when comparing the regain in σ_{fc}, addition of 0.5 m% SAP A showed only a significant difference ($p < 0.05$) with 0.5 m% p(alg(1)_AA_{75}/AM_{25}(7))_H, 0.7 and 1.3 m% of p(alg(1)_AA_{100}(7))_L and 1 m% p(alg(1)_AA_{75}/AM_{25}(7))_L. The rest of the SAP additions led to no significant difference. Addition of 0.5 m% SAP B showed no significant difference ($p < 0.05$) with 0.5 m% p(alg(1)_AA_{75}/AM_{25}(7))_L (due to the large standard deviation of the latter) and 0.5 and 1 m% of p(alg(1)_AA_{100}(7))_H. To go even further in depth, there was no very significant difference ($p < 0.01$) with 0.5 and 1 m% addition of both p(alg(1)_AA_{100}(7))_L and p(alg(1)_AA_{75}/AM_{25}(7))_H. Finally, addition of 1 m% SAP B was very significantly better ($p < 0.01$) than all synthesized SAPs, except for the addition of 0.5 m% p(alg(1)_AA_{100}(7))_H.

Table IV.13: Mechanical properties indicating self-healing capacity of mortars by adding SAPs.

Sample	SAP conc. [w%]	σ_{fc} [MPa]	Regain in σ_{fc} [%]	Peak strength σ_p [MPa]	MC [%]
Reference	0.0	6.1 ± 0.9	40.2 ± 7.9	9.6 ± 1.3	3.1 ± 0.9
p(alg(1)_AA_{100}(7))_H	0.5	5.4 ± 0.9	62.7 ± 4.3	7.5 ± 0.8	2.3 ± 0.1
	1.0	4.7 ± 0.6	59.0 ± 6.7	6.3 ± 0.5	3.1 ± 0.0
p(alg(1)_AA_{100}(7))_L	0.5	5.2 ± 0.6	53.9 ± 8.6	6.9 ± 0.9	3.4 ± 0.2
	0.7	6.3 ± 1.0	46.4 ± 4.4	9.0 ± 1.7	3.1 ± 0.6
	1.0	4.9 ± 0.4	55.7 ± 6.6	7.3 ± 0.6	3.8 ± 0.4
	1.3	5.7 ± 0.3	49.2 ± 7.2	9.2 ± 1.8	4.1. ± 1.6
p(alg(1)_AA_{75}/AM_{25}(7))_H	0.5	5.1 ± 0.4	57.2 ± 4.2	7.5 ± 1.2	3.6 ± 0.8
	1.0	4.7 ± 0.7	57.0 ± 6.8	7.8 ± 2.9	3.3 ± 1.7
p(alg(1)_AA_{75}/AM_{25}(7))_L	0.5	5.6 ± 0.8	53.4 ± 10.9	10.8 ± 0.9	4.2 ± 0.7
	1.0	6.7 ± 1.3	38.2 ± 4.2	9.2 ± 0.8	2.8 ± 0.4

It can thus be concluded that all materials showed a superior regain in σ_{fc} over the reference albeit only significant for the samples with a high DS and 1 m% p(alg(1)_AA_{100}(7))_L (the latter due to a large standard deviation). The more extreme swelling capacity of the SAPs with a low DS was thus not always beneficial as this led to a strong macro-pore formation. Especially the addition of p(alg(1)_AA_{100}(7))_H to mortar was the most promising as it showed comparable self-healing properties as commercial SAPs and additionally induced only a very limited compressive strength reduction.

IV.3.8. Conclusions

Building further on the results obtained in §IV.2., alginate was methacrylated with a DS of 19% and 9% per OH-moiety to explore a variation in the substitution degree. The algMOD was combined on the one hand with AA and on the other hand a copolymer of AA and AM. The chemical structure was elucidated by ATR-IR spectroscopy and HR-MAS ^{1}H-NMR spectroscopy quantified the cross-linking efficiency. High gel fractions (> 85%) were obtained for all materials. The moisture uptake capacity was rather limited, though it still reached values up to 54% of the weight of the SAP at a RH of 95%. The effect of the varying DS was most pronounced on the swelling capacity, as the SAP with low DS showed in both cases (AA and AA/AM) a superior swelling over the complete pH-range and especially above the pKa of the carboxylic acid moieties. Maximal swelling capacities were reached up to 630 g_{water}/g_{SAP}. For all SAPs partial hydrolysis was found, especially in extreme alkaline aqueous solutions (pH 13). Interestingly, less degradation is found in cement filtrate (CF) solutions. This postponed hydrolysis in CF due to the presence of multivalent cations makes these SAPs still interesting to be used for the currently envisaged application. Incorporation in mortar to test the effect on bending and compressive strength led to the conclusion that especially p(alg(1)_AA_{100}(7))_H showed a negligible reduction in strength, even when 1 m%, compared to the added amount of cement, was incorporated.

P(alg(1)_AA_{100}(7))_L also did not cause any strength reduction when 0.5 m% was added, but induced a reduction of 18% with a higher amount of SAP (1 m%). The materials with AM showed a significant reduction of the compressive strength. Finally, the SAPs were incorporated in mortars with additional fibers and were tested in four-point-bending to identify the self-sealing and self-healing behavior. The results indicated that 85% of the cracks up to 40 µm could completely seal after 28 days (compared to 51% for the reference), with no distinct increase of sealing with an increase of the amount of SAP from 0.5 to 1 m%. Finally, the mechanical parameters proved that especially mortar with p(alg(1)_AA_{100}(7))_H showed the strongest regain in σ_{fc}, where addition of 0.5 m% could compete with addition of commercially available SAPs. This material also induced only a very limited mortar strength reduction, making it better than the commercial SAPs. In the next part of the chapter, basic monomers have been tested to induce pH-responsiveness. This is combined with varying the used polysaccharide to also induce an additional pH-sensitivity.

IV.3.9. References

[1] Mignon A, Graulus G-J, Snoeck D, Martins J, De Belie N, Dubruel P, et al. pH-sensitive superabsorbent polymers: a potential candidate material for self-healing concrete. J Mater Sci. 2014;50(2):970-9.
[2] Mignon A, Snoeck D, Schaubroeck D, Luickx N, Dubruel P, Van Vlierberghe S, et al. pH-responsive superabsorbent polymers: A pathway to self-healing of mortar. Reactive and Functional Polymers. 2015;93(0):68-76.
[3] Mignon A, Snoeck D, D'Halluin K, Balcaen L, Vanhaecke F, Dubruel P, et al. Alginate biopolymers: Counteracting the impact of superabsorbent polymers on mortar strength. Construction and Building Materials. 2016;110:169-74.
[4] Pourjavadi A, Jahromi PE, Seidi F, Salimi H. Synthesis and swelling behavior of acrylatedstarch-g-poly (acrylic acid) and acrylatedstarch-g-poly (acrylamide) hydrogels. Carbohydrate Polymers. 2010;79(4):933-40.
[5] Tomar RS, Gupta I, Singhal R, Nagpal AK. Synthesis of poly (acrylamide-co-acrylic acid) based superabsorbent hydrogels: Study of network parameters and swelling behaviour. Polymer-Plastics Technology and Engineering. 2007;46(5):481-8.
[6] Rabat NE, Hashim S, Majid RA. Effect of Different Monomers on Water Retention Properties of Slow Release Fertilizer Hydrogel. Procedia Engineering. 2016;148:201-7.
[7] Snoeck D, Schaubroeck D, Dubruel P, De Belie N. Effect of high amounts of superabsorbent polymers and additional water on the workability, microstructure and strength of mortars with a water-to-cement ratio of 0.50. Construction and Building Materials. 2014;72(0):148-57.
[8] Hancock RD, Martell AE. Ligand design for selective complexation of metal ions in aqueous solution. Chemical Reviews. 1989;89(8):1875-914.
[9] Omidian H, Hashemi SA, Sammes PG, Meldrum I. Modified acrylic-based superabsorbent polymers (dependence on particle size and salinity). Polymer. 1999;40(7):1753-61.
[10] Patricelli MP, Cravatt BF. Fatty Acid Amide Hydrolase Competitively Degrades Bioactive Amides and Esters through a Nonconventional Catalytic Mechanism. Biochemistry. 1999;38(43):14125-30.
[11] Fife TH, Squillacote VL. Metal ion effects on intramolecular nucleophilic carboxyl group participation in amide and ester hydrolysis. Hydrolysis of N-(8-quinolyl)phthalamic acid and 8-quinolyl hydrogen glutarate. Journal of the American Chemical Society. 1978;100(15):4787-93.
[12] Robinson BA, Tester JW. Kinetics of alkaline hydrolysis of organic esters and amides in neutrally-buffered solution. International Journal of Chemical Kinetics. 1990;22(5):431-48.
[13] Snoeck D, Dubruel P, De Belie N. How to seal and heal cracks in cementitious materials by using superabsorbent polymers. Application of Superabsorbent Polymers and Other New Admixtures in Concrete Construction: RILEM Publications; 2014. p. 375-84.
[14] Snoeck D, De Belie N. Repeated autogenous healing in strain-hardening cementitious composites by using superabsorbent polymers. Journal of Materials in Civil Engineering. 2015;28(1):04015086.
[15] Hasholt MT, Jensen OM, Kovler K, Zhutovsky S. Can superabsorbent polymers mitigate autogenous shrinkage of internally cured concrete without compromising the strength? Construction and Building Materials. 2012;31:226-30.
[16] Snoeck D. Self-healing and microstructure of cementitious materials with microfibres and superabsorbent polymers. PhD thesis: Ghent University; 2015.
[17] Mechtcherine V, Reinhardt H-W. Application of super absorbent polymers (SAP) in concrete construction: state-of-the-art report prepared by Technical Committee 225-SAP: Springer Science & Business Media; 2012.

IV.4 Creating varying polysaccharide-based SAPs with basic monomers

In the previous section (§IV.3.), alginate was used in combination with acrylic acid and/or acrylamide in varying molar fractions and in combination with two degrees of substitution (DS) for algMOD. These SAPs turned out to be promising materials as some of them not only exhibited a high swelling capacity, but also a limited effect on the bending and compressive strength of mortar samples. In addition, they showed a strong crack sealing capacity together with a first-cracking strength regain up to 63% as compared to the reference (only 43%). Although these materials are already quite promising, they showed a limited moisture uptake capacity, they were prone to partial degradation at extremely alkaline conditions and their self-healing capacity could still be further improved. §III.3. has described the incorporation of 2-(dimethylamino)ethyl methacrylate (DMAEMA) as a pH-responsive monomer in synthetic superabsorbent polymers (SAPs). In addition to DMAEMA, dimethylaminopropyl methacrylamide (DMAPMA) could also be of interest to become incorporated as pH-sensitive monomer in SAPs as amides (present in DMAPMA) are less prone to hydrolysis than esters (present in DMAEMA) [1-3]. Researchers have already reported on its use in combination with 2-hydroxyethyl methacrylate [4] or acrylic acid (AA) to develop 'smart' pH-responsive materials for biomedical applications [5]. It has also been applied in systems for recovering hydrocarbon fluids from subterranean reservoirs [6], in hairspray compositions [7] and for reactive dyeing of meta-aramid fabrics [8]. For concrete applications, it has already been applied in combination with other polymers to develop an antifouling coating on concrete [9, 10].

As was shown earlier in §IV.3., the use of alginate could, especially in alkaline aqueous and cement filtrate (CF) solutions, lead to a strong screening effect due to the presence of (multivalent) cations which had its effect on the swelling capacity. It can therefore be interesting to investigate the effect of polysaccharides which do not possess carboxylates in a pH-range relevant for concrete (e.g. agarose) or which show an opposite pH-sensitivity in alkali conditions (e.g. chitosan). Chitosan can be especially interesting as it will show a similar pH-responsiveness as the monomers used (albeit with a different pKa). Agarose has already been applied for numerous applications including tissue engineering [11-14], as bio-organic ligand, as support for the stabilization of palladium nanoparticles [15], etc. [16-18]. Furthermore, it has been used for creating a fiber humidity sensor to monitor the relative humidity in fresh concrete [19]. Chitosan has already been applied as pH-sensitive polymer for many biomedical applications such as wound dressings [20, 21], tissue engineering [22, 23], drug delivery [24, 25], etc. [26, 27]. Interestingly, it has been tested in combination with latex to improve the mechanical properties of concrete [28]. Based on previous results obtained for the methacrylation of alginate combined with its straightforward radical polymerization in the presence of acrylic monomers, a similar route has been pursued for agarose and chitosan.

In the current study, a variation of polysaccharides (alginate, agarose and chitosan) has been methacrylated and used as backbone to be combined subsequently with either DMAEMA or DMAPMA. First, the DS of the functionalized polysaccharides has been determined by proton nuclear magnetic resonance (^{1}H-NMR) spectroscopy. The chemical structure of the SAPs has been identified by attenuated total reflectance-infrared (ATR-IR) spectroscopy. High resolution magic-angle spinning (HR-MAS) ^{1}H-NMR spectroscopy combined with gel fraction experiments have been applied to determine the cross-linking efficiency. Dynamic vapor sorption measurements has been used to assess the moisture uptake capacity at varying relative humidities (RH). Furthermore, the pH-responsiveness has been evaluated by performing swelling tests in aqueous and CF solutions of varying pH followed by ATR-IR spectroscopy to identify potential degradation phenomena. After extensive physico-chemical characterization, the SAPs have been incorporated in mortar to determine their effect on the flexural and compressive strength of the mortar samples. Finally, their self-sealing and -healing capacity has been determined through a four-point-bending test. The results obtained have also been compared to commercial SAPs (SAP A, copolymer of acrylamide and sodium acrylate, with a particle size of 100.0 ± 21.5 µm and SAP B, a cross-linked potassium salt poly(acrylate), which has a particle size of 476.6 ± 52.9 µm [29]).

IV.4.1. Methacrylation of the polysaccharides alginate, agarose and chitosan

Three polysaccharides were modified with methacrylate moieties to incorporate double bonds enabling subsequent cross-linking as required for SAP development. The DS was determined by ^{1}H-NMR spectroscopy. AlgMOD with a high DS (i.e. 38% per repeating monosaccharide or 19% with respect to the hydroxyl moieties present) was developed and applied.

The integration of the characteristic peaks of the vinyl protons from the methacrylate backbone of agaMOD at 5.70 and 6.06 ppm were compared with the integration of the signal of the proton of the anhydrogalactose unit at 5.06 ppm. The DS could be calculated using equation (IV.3) [30].

$$DS\ (\%) = \frac{(H_a+H_b)/2}{H_1} * 100\ \% = \frac{\left(\frac{I_{5.70\ ppm}+I_{6.06\ ppm}}{2}\right)}{I_{5.06\ ppm}} * 100\ \% \qquad \text{(IV.3)}$$

The protons $H_{G\text{-}1}$, $H_{M\text{-}1}$, H_a and H_b are related to the integration of their characteristic peaks indicated in the NMR spectrum (see Figure IV.20).
A DS of 14% per repeating unit or 4% with respect to the hydroxyls present was obtained by addition of 0.09 equivalents MAAH with respect to the hydroxyl functionalities. The result is in compliance with data obtained before by De Paepe et al.[30]. They have plotted a methacrylation master curve showing the DS as a function of the added amount of methacrylic anhydride [30]. De Paepe et al. also found that at a DS higher than 26%, agaMOD turned into a water-insoluble polymer, which is undesirable for the further development. The difference in DS between algMOD and agaMOD is unwanted. However, it must be noticed that the ^{1}H-NMR measurements of algMOD were performed in cooperation with the group of Peter Adriaensens

and the results were only obtained when the agaMOD polymers had already been further developed.

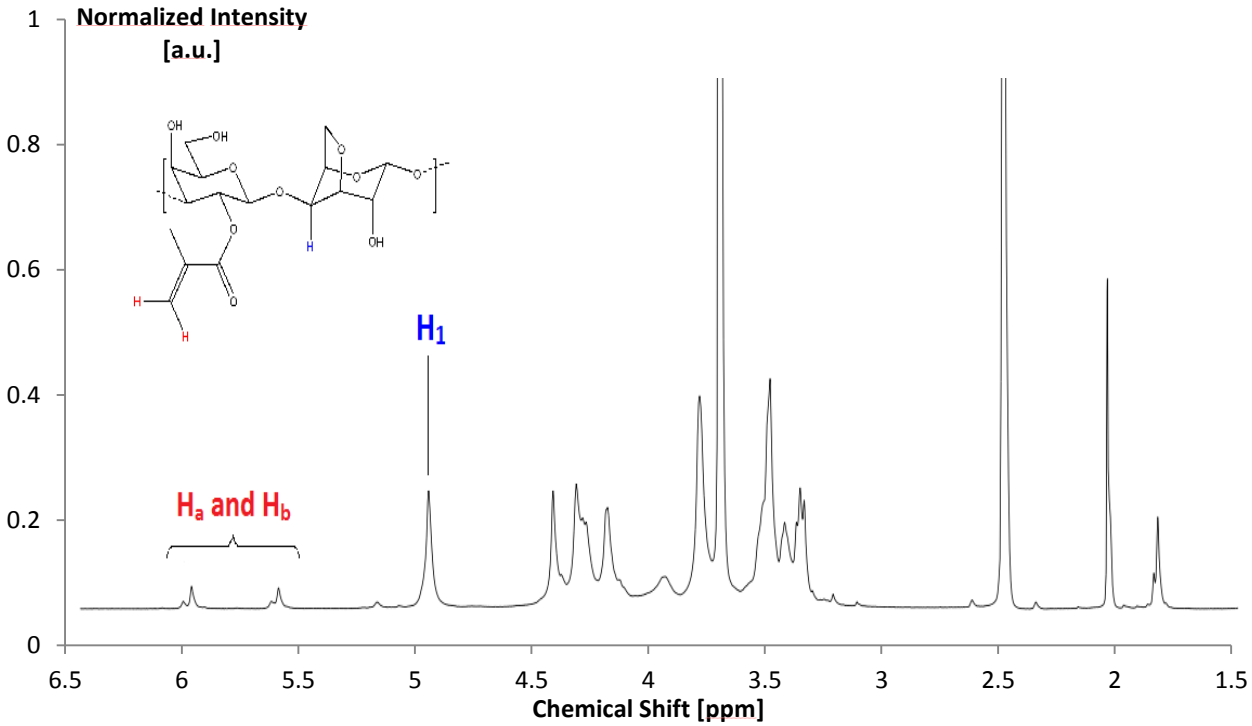

Figure IV.20: ^{1}H NMR spectrum of agaMOD with annotation of the relevant peaks required for the calculation of the DS.

The DS of ChiMOD was calculated using equation (IV.4). The peak of the methyl group on the methacrylate (H_{Me}) at 1.85 ppm was compared with the six $H_{2\text{-}6}$ peaks between 2.80 and 4.00 ppm. Correction factors of 1/3 and 1/6 were added to account for the amount of protons corresponding with the respective peaks of H_{Me} and $H_{2\text{-}6}$.

$$\mathrm{DS}(\%) = \left(\frac{1}{3}\mathrm{H}_{Me} / \frac{1}{6}\mathrm{H}_{2-6}\right) * 100\ \% \qquad \text{(IV.4)}$$

A DS of 6.59% with respect to the repeating monosaccharides was obtained for ChiMOD (Figure IV.21). Interestingly, the DS for agaMOD was obtained per repeating unit, which was a disaccharide, this makes the DS-values of agaMOD and chiMOD similar.

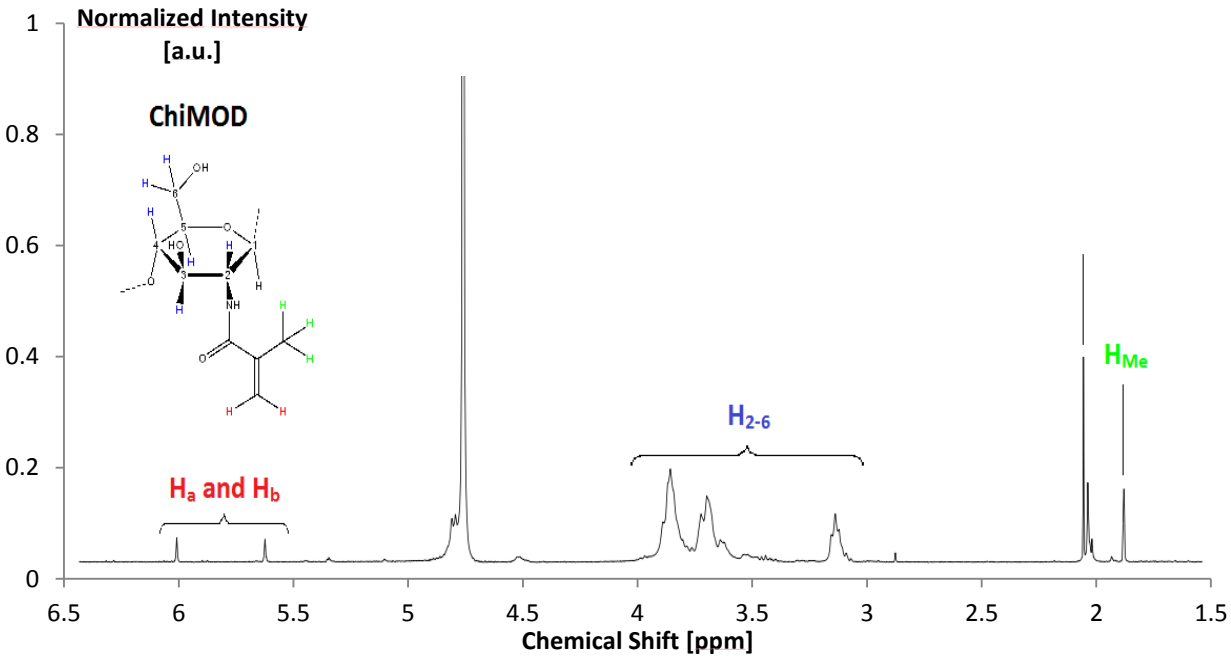

Figure IV.21: ^{1}H-NMR spectrum of chiMOD with annotation of the relevant peaks for the calculation of the DS. The glucosamine building block of chitosan is displayed in its methacrylated form together with its carbon atoms labelled according to the method of Lavertu et al. [31].

IV.4.2. Development of SAPs based on methacrylated polysaccharides and basic monomers

After modification, the methacrylated polysaccharides were combined with monomers showing pH-sensitivity in an alkaline environment. The composition of all materials developed is listed in Table IV.14. The main difference between both monomers is their pKa-value which is 8.4 and 8.9 for DMAEMA and DMAPMA, respectively [32, 33]. As a polysaccharide/monomer ratio of 1g versus 7g did not result in a polymer with gel-like properties a ratio of 1/3 was used for p(aga(1)_EMA(3)) and p(aga(1)_PMA(3)) giving rise to polymers with superabsorbent properties. A ratio of 1/3 could also be tested in the future for algMOD and chiMOD, however, as all other materials combined with alginate in this chapter (§IV.2 and §IV.3) were performed with this 1/7 ratio, this value was kept at 1/7 to enable proper comparison.

The gel fractions of the SAPs were determined (see Table IV.14) and generally, the materials constituting DMAPMA were characterized by lower gel fractions (only significant for p(alg(1)_PMA(7))). When comparing the various polysaccharides, agaMOD-based SAPs exhibited the highest gel fractions (i.e. 85 ± 2% upon incorporating DMAEMA and 82 ± 4% for DMAPMA), closely followed by algMOD (80 ± 0% and 65 ± 1% for DMAEMA and DMAPMA respectively) and chiMOD (65 ± 5% and 49 ± 1%). The difference in gel fraction is likely to be related to the presence or absence of charges on the methacrylated backbone during cross-linking. More specifically, methacrylated agarose only possesses alcohol moieties which show no pH-responsiveness around neutral pH (pKa of OH-moieties is 17 – 18). DMAEMA and DMAPMA, on

the other hand, possess a low concentration of positively charged amine functionalities which can easily approach the activated double bonds, incorporated during the modification. Modified alginate had a slightly lower gel fraction. As this anionic polysaccharide contains negatively charged carboxylate moieties, electrostatic interactions occur with the monomers, decreasing the movement of the chains and hindering the reaction between the algMOD and monomer [34]. ChiMOD is a cationic polysaccharide, positively charged during the cross-linking reaction in water, which can result in potential repulsion of the acrylic monomers. In principle, this effect should be limited due to the low concentration of charged amines. Nonetheless, a shielding effect might arise hindering the monomers to approach the methacrylates, which can result in a less efficient polymerization and thus a lower gel fraction for the obtained SAPs.

Table IV.14: Chemical composition of semi-synthetic SAPs (PS abbreviated for polysaccharide).

Sample	PS-type	$\frac{PS}{monomer}$ g/g	DMAEMA mol%	DMAPMA mol%	Gel fraction (%)
p(alg(1)_EMA(7))	Alginate	1/7	100	0	80 ± 0
p(alg(1)_PMA(7))	Alginate	1/7	0	100	65 ± 1
p(aga(1)_EMA(3))	Agarose	1/3	100	0	85 ± 2
p(aga(1)_PMA(3))	Agarose	1/3	0	100	82 ± 4
p(chi(1)_EMA(7))	Chitosan	1/7	100	0	65 ± 5
p(chi(1)_PMA(7))	Chitosan	1/7	0	100	49 ± 11

Care must be taken when comparing the gel fraction data for p(aga(1)_EMA(3)) and p(aga(1)_PMA(3)) with the other SAPs due to the varying polysaccharide – monomer ratio (1/3 for agarose and 1/7 for chitosan and alginate). However, due to the absence of charges in agaMOD, a different ratio would still lead to a high gel fraction as explained above.

Because of its effect on the moisture uptake and the swelling, the particle size distribution was determined for all SAPs developed (Table IV.15). The results showed that 10% of all particles had a diameter below 15 µm. However, no direct trends were found for d_{50} and d_{90} where especially larger particles were observed for p(alg(1)_PMA(7)) and p(aga(1)_EMA(3)). If any unexpected trends were found for the moisture or water uptake capacity, a link could be made with the particle sizes.

Table IV.15: Particle size distribution of semi-synthetic SAPs combined with acrylate monomers.

Sample	d_{10} [µm]	d_{50} [µm]	d_{90} [µm]
p(alg(1)_EMA(7))	13	58	133
p(alg(1)_PMA(7))	11	35	228
p(aga(1)_EMA(3))	12	86	191
p(aga(1)_PMA(3))	11	56	127
p(chi(1)_EMA(7))	11	18	119
p(chi(1)_PMA(7))	11	30	142

IV.4.3. Chemical structure elucidation and assessment of SAP cross-linking efficiency

ATR-IR spectroscopy was performed to identify both the methacrylated polysaccharides and the incorporated monomers. Figures IV.22 and IV.23 show the ATR-IR spectra of the methacrylated polysaccharides after polymerization in the presence of DMAEMA and DMAPMA respectively. Table S.3 (in supplementary info) indicates the relevant absorption signals corresponding with the chemical functionalities present in the SAPs. As observed in Figure IV.22, the carbon-oxygen double bond stretch vibration (ν(C=O)) at 1720 cm^{-1} was strongly present which could be correlated to the ester moieties from both the modified polysaccharide as well as DMAEMA. The nitrogen-carbon bond stretch vibrations (ν(N-C)) at 2775 and 2825 cm^{-1} corresponded with the tertiary amine from DMAEMA. The asymmetric carbon-oxygen bond stretch (ν_{as}(C-O)) was also clearly visible and could be attributed to the ester moieties from both the natural backbone as well as the incorporated monomers. Furthermore, a peak at 1620 cm^{-1} for p(alg(1)_EMA(7)) could be distinguished, which was related to the carbon-oxygen double bond stretch vibration (ν(C=O)) from the carboxylates of algMOD. The nitrogen-hydrogen stretch vibrations (ν(N-H)) associated with the amides and located around 3100-3500 cm^{-1} were less straightforward to be distinguished from the oxygen-hydrogen stretch (ν(O-H)) within the same wavenumber region. The combination of the above-mentioned signals confirmed the presence of the monomers within the synthesized SAPs.

Figure IV.23 shows distinct features which could be attributed to the secondary amide of DMAPMA. All spectra showed the nitrogen-hydrogen bending vibration (δ(N-H)) at 1520 cm^{-1}. Around 1700 cm^{-1}, three peaks became apparent including the weak signal related to ν(C=O) from the ester, ν(C=O) of the amide at 1645 cm^{-1} and ν(C=O) from the carboxylates which was only visible in the spectrum of p(alg(1)_PMA(7)). The peaks from the tertiary amine (ν(N-C)) from DMAPMA could be distinguished at 2775 and 2825 cm^{-1}. The spectra thus confirmed the incorporation of DMAPMA within the corresponding SAPs.

To quantify the cross-linking efficiency, high resolution magic-angle spinning (HR-MAS) ^{1}H NMR spectroscopy was performed. The characteristic alkene signals found by HR-MAS were positioned in the range of 5.5 – 6.5 ppm. As an example, the spectra of p(aga(1)_PMA(3)) and p(aga(1)_EMA(3)) were shown in Figure IV.24 and illustrated the absence of the peaks corresponding with the double bond protons after polymerization. What is more, they also shifted to a lower ppm range (1.5 – 2.5 ppm) since they became protons associated with alkyl moieties in the vicinity of electron-withdrawing functionalities. The other materials showed similar results (data not shown).

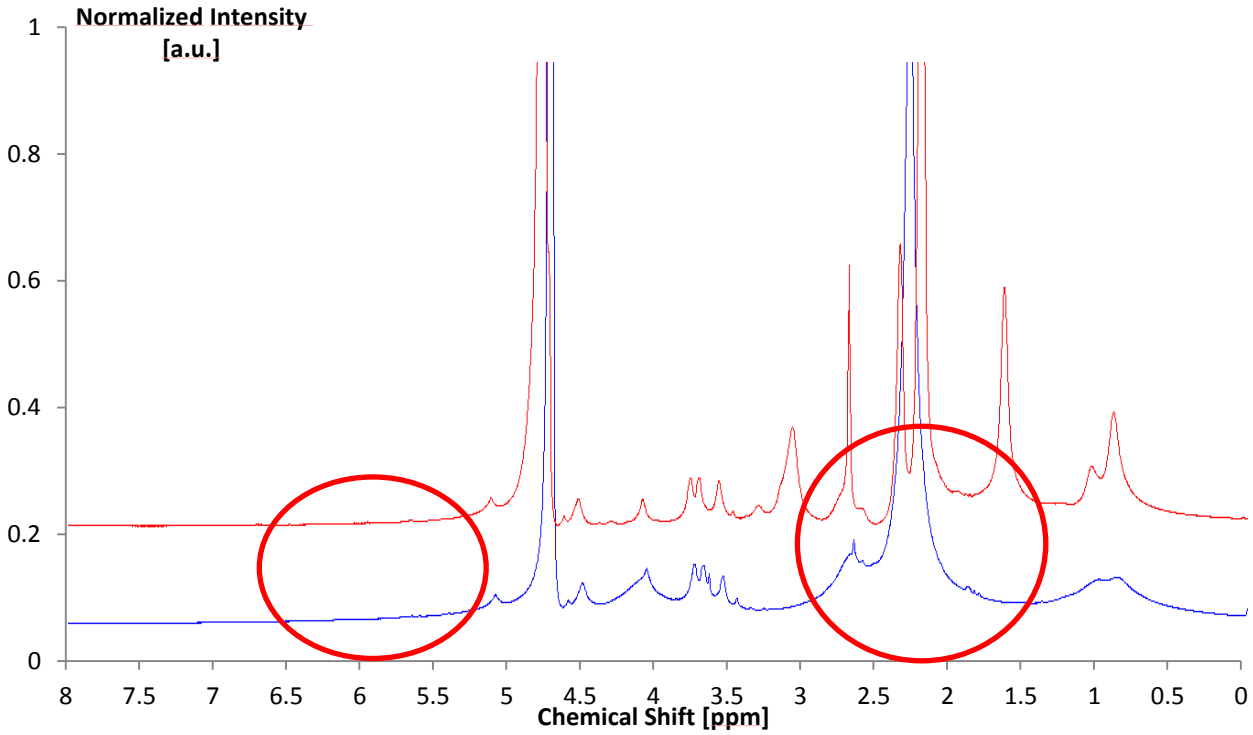

Figure IV.24: HR-MAS ^{1}H-NMR spectrum of p(aga(1)_PMA(3)) (red) and p(aga(1)_EMA(3)) (blue).

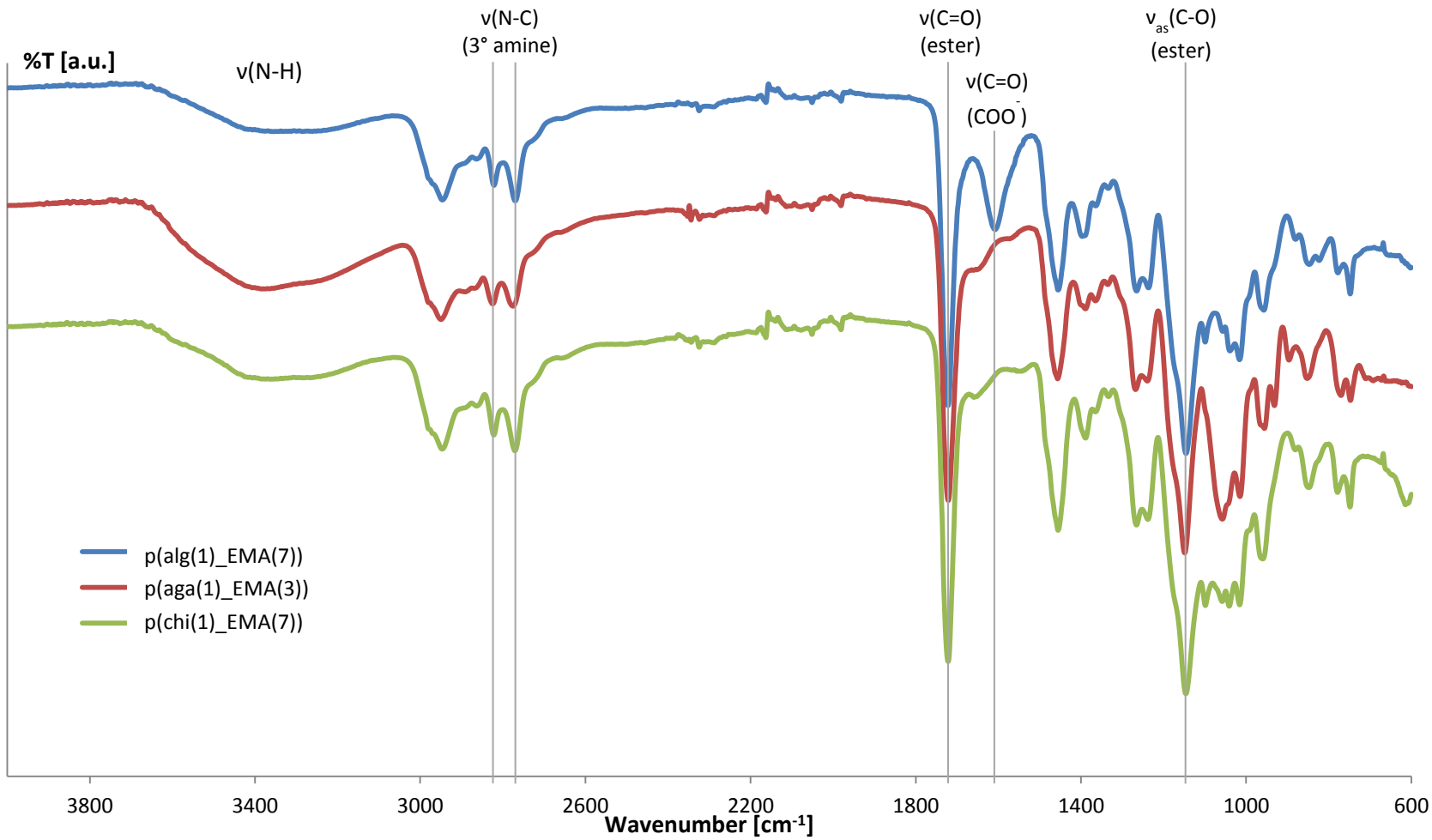

Figure IV.22: ATR-IR spectra of p(alg(1)_EMA(7)), p(aga(1)_EMA(3)) and p(chi(1)_EMA(7)) with designation of the relevant peaks and their functional bond vibration.

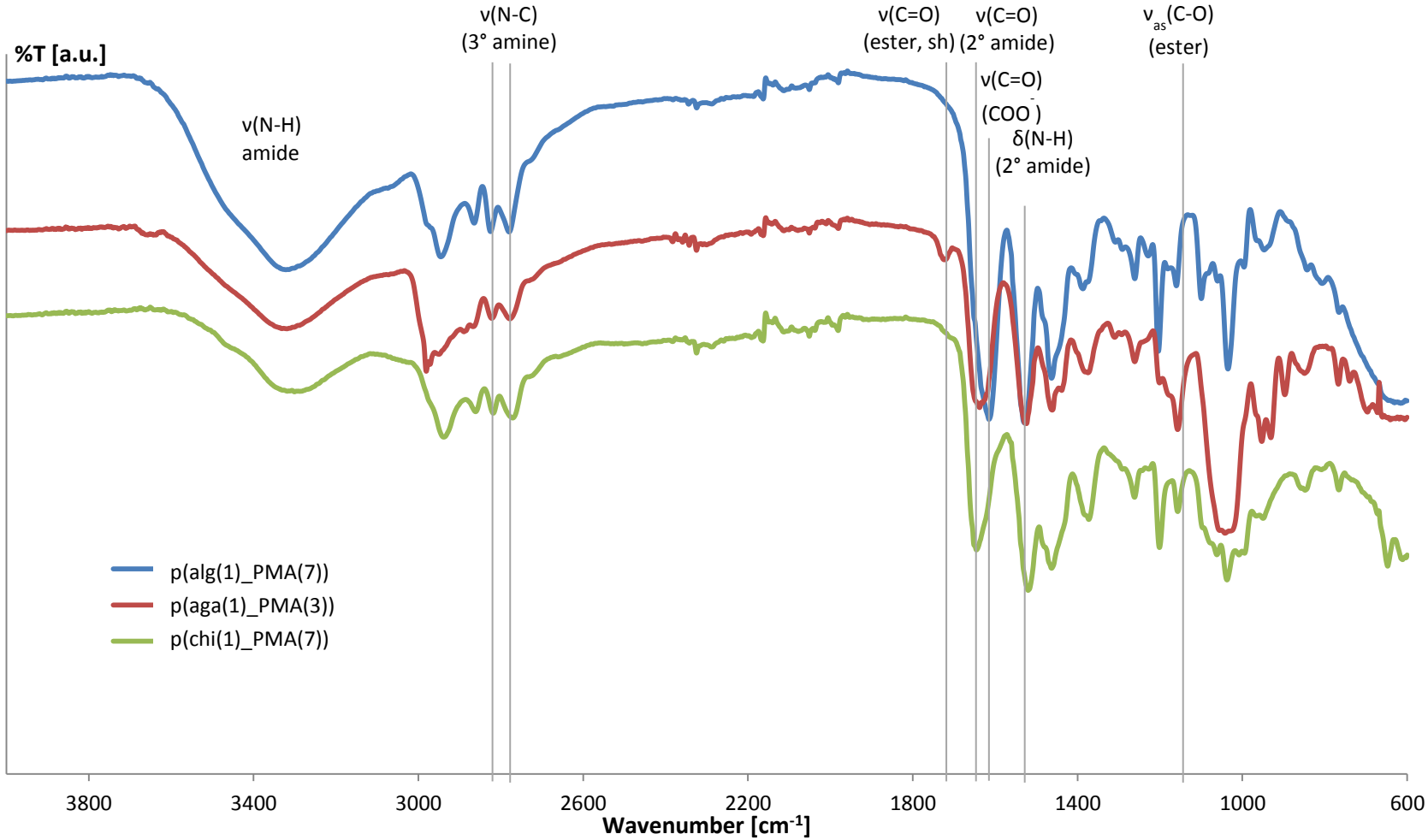

Figure IV.23: ATR-IR spectra of p(alg(1)_PMA(7)), p(aga(1)_PMA(3)) and p(chi(1)_PMA(7)) with designation of the relevant peaks and their functional bond vibration.

IV.4.4. Moisture uptake capacity assessment by dynamic vapor sorption measurements

The results obtained by DVS measurements performed on the synthesized SAPs are depicted in Table IV.16. The SAPs showed a moisture sorption ranging between 35 and 122% at a relative humidity (RH) of 95%. Materials constituting DMAPMA exhibited a higher moisture uptake compared to SAPs with DMAEMA, with the highest value being 121.6% for p(chi(1)_PMA(7)). This was expected as the acrylamide-based DMAPMA contains hydrophilic amide moieties, while the acrylate-based DMAEMA contains the slightly less hydrophilic esters [35, 36]. The materials based on chiMOD were concomitant with the highest moisture uptake capacity, followed by algMOD and agaMOD. The superior moisture uptake capacity of algMOD over agaMOD was related to the stronger hydrophilicity of the ionic presence in carboxylates and protonated amines over the alcohols [37, 38]. Alginate has a stronger swelling capacity than chitosan at neutral pH [39] due to their respectively pKa-values of 3.38 and 3.65 for mannuronic and guluronic acid and 6.3 for chitosan [40]. However, the combination of the methacrylated polysaccharides with the monomers led in the case of algMOD to a strong ionic interaction at neutral pH by the combination of the carboxylates and protonated amines, which shielded part of the carboxylates from the formation of H-bridges and thus led finally to a lower moisture uptake than for chiMOD. Additionally, the overall particle sizes of the chiMOD-based SAPs were smaller than algMOD, leading to a larger surface area and an increased moisture uptake capacity. Some materials (i.e. p(alg(1)_PMA(7)) and p(chi(1)_PMA(7))) absorbed more moisture at 90% in contrast with the previously developed synthetic SAPs at 95% RH, rendering them more promising for applications for which no direct contact between water and incorporated SAPs can occur. All materials showed a negligible (up to 1.8%) hysteresis. The SAPs can thus completely release all absorbed moisture back to its environment (cfr. the matrix of mortar or concrete) by a decrease in the RH. Interestingly, p(chi(1)_PMA(7)) even takes up a higher amount at 90% RH than commercial SAPs (83% and 84% respectively for SAP A and B as previously described in Table IV.1) and comparable amounts for 95% RH (130% and 119% for SAP A and B respectively).

Table IV.16: Overview of the sorption capacities (at 30-60-90-95% RH) of the synthesized semi-synthetic SAPs combined with basic monomers.

Sample	30% RH	60% RH	90% RH	95% RH
p(alg(1)_EMA(7))	4	12	45	62
p(alg(1)_PMA(7))	9	21	63	88
p(aga(1)_EMA(3))	4	9	25	35
p(aga(1)_PMA(3))	9	19	47	64
p(chi(1)_EMA(7))	4	13	47	65
p(chi(1)_PMA(7))	18	38	93	122

IV.4.5. Swelling potential of semi-synthetic SAPs

The SAP swelling capacity was measured in aqueous and cement filtrate (CF) solutions. First, the algMOD-based samples were measured in pH 3, 8 and 12. However, Figure IV.25 shows that the highest swelling occurred at pH 12 (36.2 ± 1.4 g_{water}/g_{SAP} and 47.4 ± 2.0 g_{water}/g_{SAP} for p(alg(1)_EMA(7)) and p(alg(1)_PMA(7)) respectively), which decreased to 11.5 ± 0.7 g_{water}/g_{SAP} and 11.4 ± 0.3 g_{water}/g_{SAP} respectively at pH 8 and increased again at pH 3 up to 22.4 ± 1.0 g_{water}/g_{SAP} and 13.2 ± 2.3 g_{water}/g_{SAP} respectively. This is the completely opposite trend compared to what is required for the intended application. Ideally, SAPs should not swell during mixing (pH > 12), yet extensively at neutral or slightly alkaline pH upon exposure to intruding water into concrete cracks. The observed trend could be explained by the pH-responsiveness. AlgMOD is an anionic polysaccharide consisting of carboxylic acid moieties which become negatively charged above their pKa (at pH 4) turning into carboxylates. Conversely, the basic monomers DMAEMA and DMAPMA showed an opposite effect as the concentration of positively charged amines increased below their pKa (8.4 and 8.9 respectively for both monomers). The combination of both charges around neutral pH led to electrostatic interactions and thus a decreased swelling capacity. As this is undesired, these materials were not selected further in the present study (i.e. for incorporation in mortar). The higher swelling capacity of p(alg(1)_EMA(7)) and p(alg(1)_PMA(7)) at pH 12 in comparison to pH 3 can also be explained by the concentration of charges. At pH 3, the concentration of positive charges is high while the concentration of negative charges is low, yet not to be neglected as pH 3 is close to the pKa of the carboxylic acids. At pH 12, on the other hand, the concentration of negative charges is extremely high, yet the concentration of positive charges can be neglected and will therefore not result in electrostatic interactions occurring between amines and carboxylates. In CF solutions, the swelling is reduced as anticipated due to the presence of multivalent cations in the solution [41, 42].

Subsequently, the swelling capacity of p(aga(1)_EMA(3)) and p(aga(1)_PMA(3)) was evaluated in aqueous solutions at pH 3, 6, 9, 12 and 13 (see Figure IV.26). As agaMOD only possesses alcohol functionalities with a pKa outside the relevant pH-range (pKa of 15-16), only the amine moieties from DMAEMA and DMAPMA became charged due to protonation upon decreasing the pH. Both materials showed an increased swelling (111.2 ± 2.2 g_{water}/g_{SAP} and 59.2 ± 3.3 g_{water}/g_{SAP} for p(aga(1)_EMA(3)) and p(aga(1)_PMA(3)) respectively at pH 3) upon decreasing the pH. Although swelling was rather limited, the trend was anticipated. Throughout the upcoming sections, the effect of these polymers on mortar strength as well as their self-healing capacity has been described. Swelling in CF solutions was higher compared to algMOD-based SAPs. This could be due to the strong attraction of the carboxylate moieties of algMOD to multivalent counter cations (mainly Ca^{2+} and Mg^{2+} in these solutions) compared to neutral alcohol moieties in agaMOD [42].

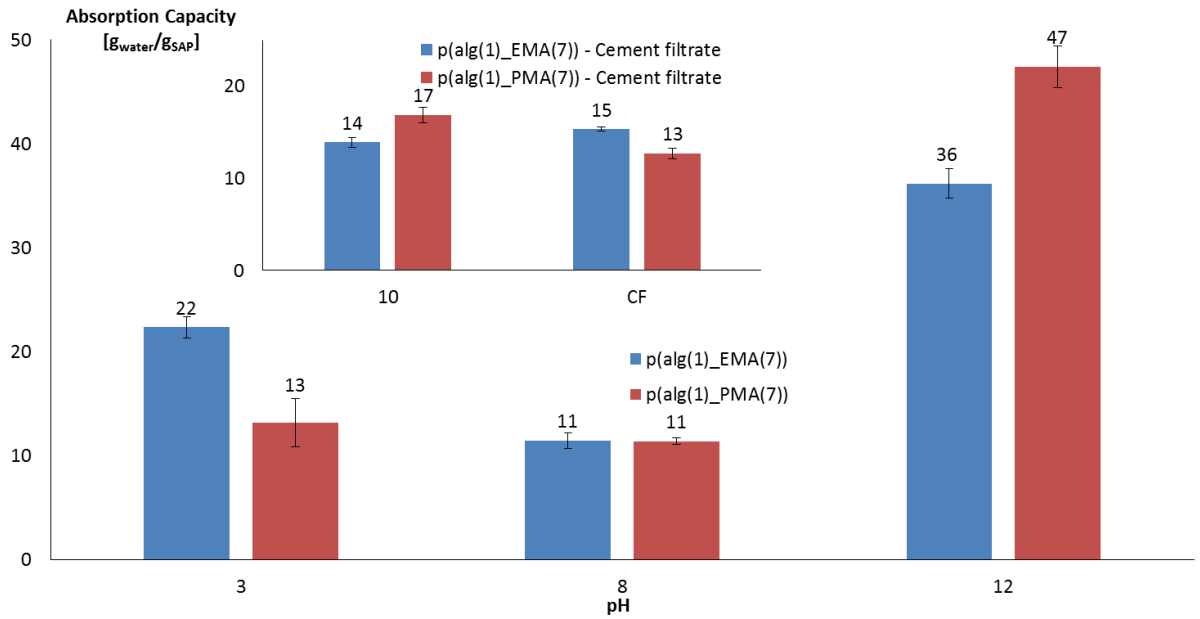

Figure IV.25: The swelling capacity in p(alg(1)_EMA(7)) and p(alg(1)_PMA(7)), both in aqueous solutions and (acidified/basified) cement filtrate solutions (inset).

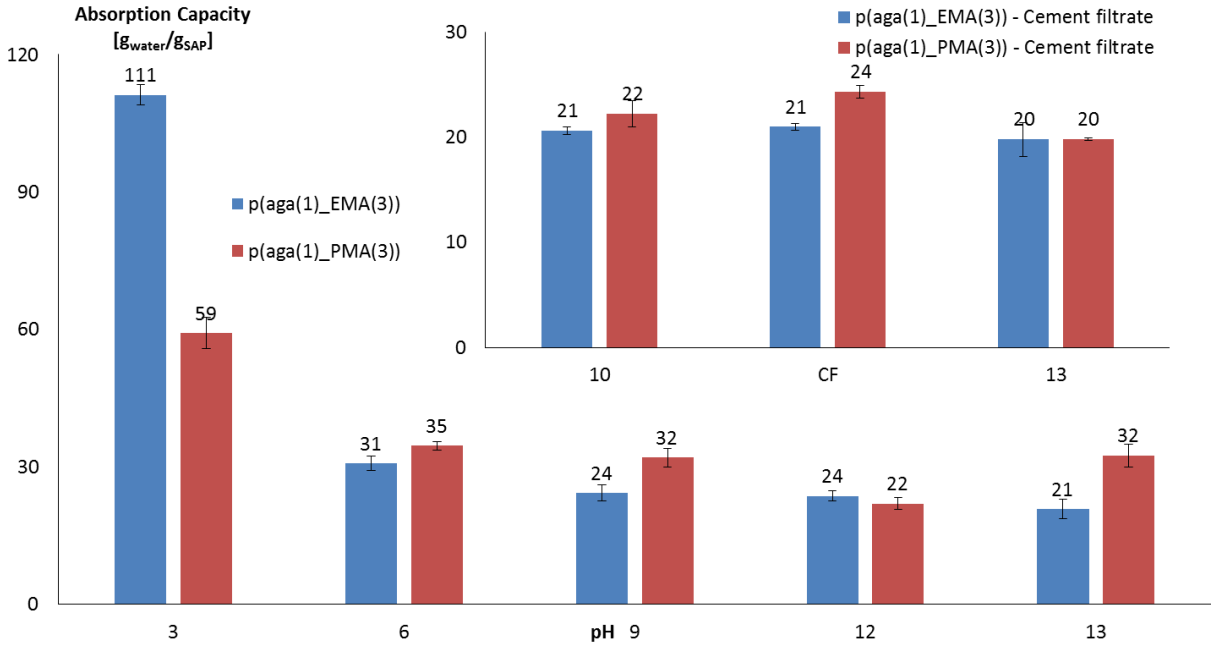

Figure IV.26: Swelling capacity of p(aga(1)_EMA(3)) and p(aga(1)_PMA(3)), both in aqueous solutions and in (acidified/basified) cement filtrate solutions (inset).

P(chi(1)_EMA(7)) and p(chi(1)_PMA(7)) showed a double pH-responsivity (Figure IV.27). The tertiary amine functionalities possess pKa-values of 8.4 and 8.9 for DMAEMA and DMAPMA respectively [43]. The primary amine moiety of chiMOD corresponds with a pKa of 6.5 [44]. The swelling at pH 13 only amounted 17 ± 1 g_{water}/g_{SAP} and 17 ± 2 g_{water}/g_{SAP} for p(chi(1)_EMA(7)) and p(chi(1)_PMA(7)) and increased up to 39 ± 3 g_{water}/g_{SAP} and 36 ± 3 g_{water}/g_{SAP} at pH 8 and to 47 ± 1 g_{water}/g_{SAP} and 75 ± 11 g_{water}/g_{SAP} at pH 3, with the latter being the only pH at which a significant difference in swelling was found for p(chi(1)_EMA(7)) and p(chi(1)_PMA(7)). At pH 3,

the difference in concentration of protonated amines was strongest. In CF solutions, similar swelling capacities were obtained compared to the other synthesized SAPs.

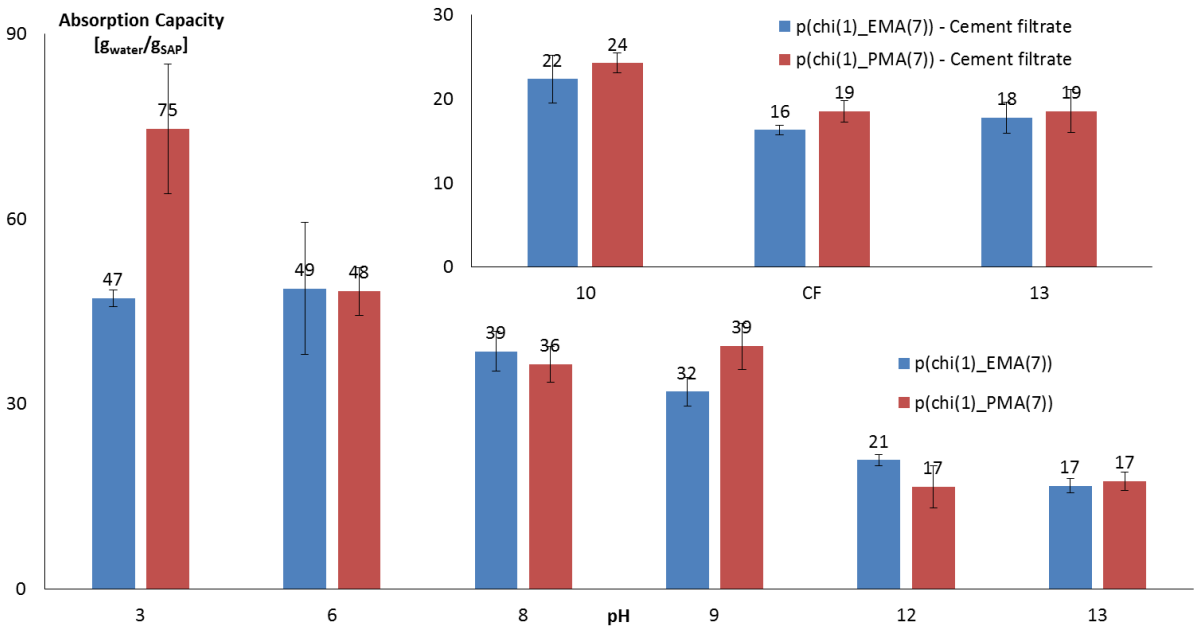

Figure IV.27: Swelling capacity of p(chi(1)_EMA(7)) and p(chi(1)_PMA(7)) both in aqueous solutions as well as (acidified/basified) cement filtrate solutions (inset).

After the swelling experiments, the polymers were dried and characterized by ATR-IR spectroscopy to identify potential degradation phenomena. Interestingly, for p(alg(1)_EMA(7)) and p(alg(1)_PMA(7)), no changes in the characteristic signals could be retrieved in any of the IR spectra. However, due to their swelling being opposite to the required one as described above, these materials have not been tested further for self-healing applications. On the other hand, these materials could be useful for internal curing for which less SAP is required (0.1 – 0.3 % with respect to the added amount of cement) where swelling is preferred during mixing of concrete (pH > 12).

The ATR-IR spectrum of p(aga(1)_EMA(3)) only showed a sudden increase of the intensity of the peak at 1400 cm^{-1} after incubation in basified CF solution, which could result from carbonate ions [45] present in the solution which were not filtered out completely. For p(aga(1)_PMA(3)), a strong increase of the symmetric carbon-oxygen stretch vibration (ν_s(C-O)) was observed at 1410 cm^{-1}, resulting in an overlap with the correlated asymmetric stretch (ν_{as}(C-O)), upon incubation in an aqueous solution at pH 13 and in basified CF solution. This was expected as extremely high amounts of NaOH were needed to reach these pH values. The postponed hydrolysis behavior in solutions with a high ion concentration was not observed in the latter case. However, care must be taken upon interpreting the results obtained for CF of pH 13, as CF acts as a buffer so a high amount of NaOH is required to increase the pH to 13, which obviously affects the incubated SAP. This measurement is not useful in a practical sense, but was taken into account to compare with the aqueous solutions at an equal pH.

In CF and any other aqueous solutions (at pH < 13), no form of degradation was observed with ATR-IR spectroscopy. As a conclusion, p(aga(1)_EMA(3)) did not show hydrolysis, which is in line with the results obtained in §IV.3.4. for p($DMAEMA_{100}$)_x. The stronger hydrolysis of the p(aga(1)_PMA(3)) compared to p(aga(1)_EMA(3)) could be related to the particle size, which was smaller for the former. This led to a larger surface area, more prone to degradation. For p(chi(1)_EMA(7)) and p(chi(1)_PMA(7)), similar trends were observed. The spectra of p(aga(1)_PMA(3)) before and after incubation (in aqueous and CF solution at pH 13) are presented in Figure IV.28 The obtained results could be considered very promising, as the materials did not show any degradation in CF solution nor in aqueous solution (pH < 13), which corresponds with the actual environments they are exposed to.

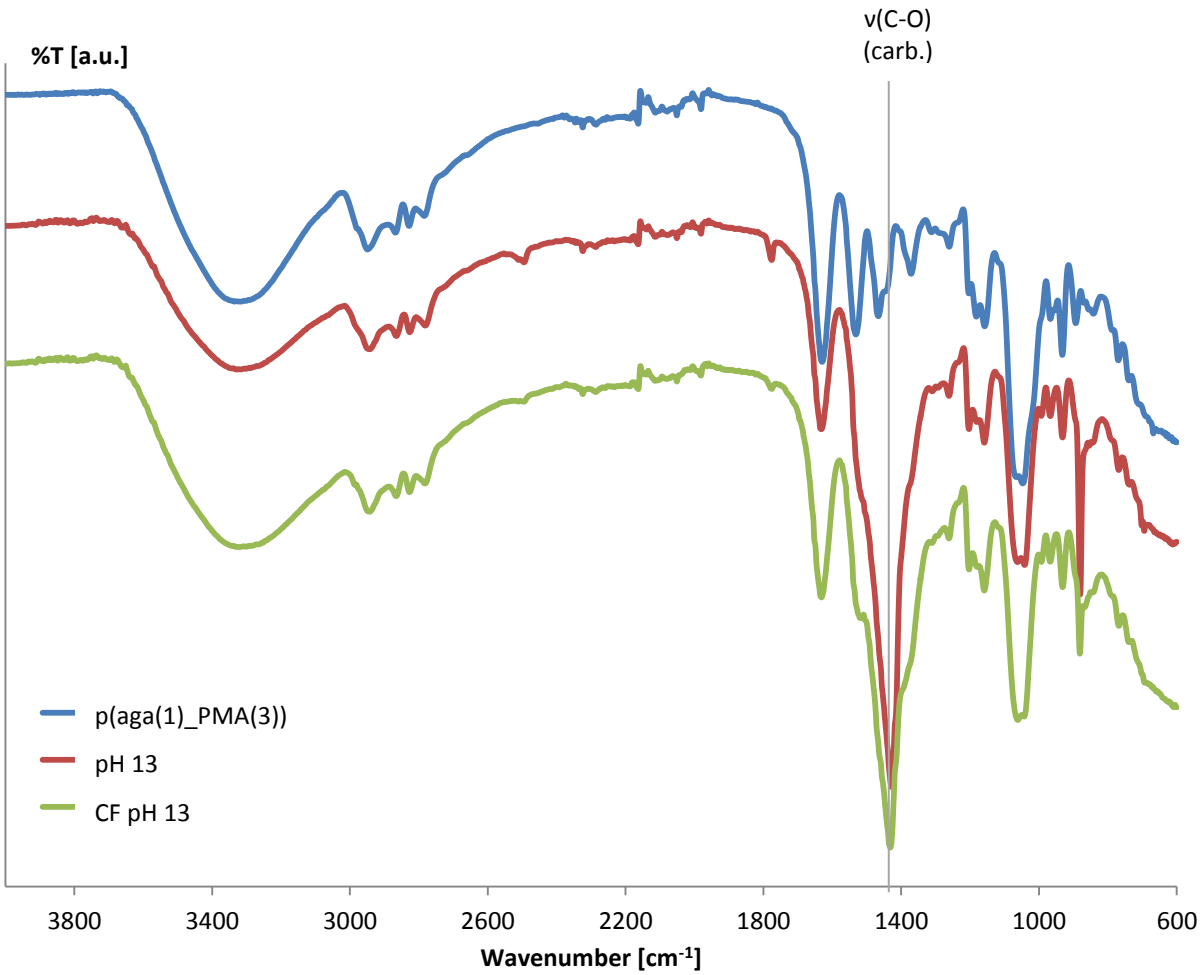

Figure IV.28: ATR-IR spectra showing dry p(aga(1)_PMA(3)) prior to and after immersion in aqueous and CF solution at pH 13.

Due to the swelling behavior, opposite to the requirements, which p(alg(1)_EMA(7)) and p(alg(1)_PMA(7)) showed, these materials were not used further throughout the current study. P(chi(1)_PMA(7)) had the highest moisture uptake capacity, even competing with commercial SAPs. P(aga(1)_PMA(3)) had a higher swelling capacity at neutral pH compared to p(aga(1)_EMA(3)). Despite their lower swelling capacities in aqueous solutions compared to

commercial SAPs (305 ± 3.7 and 283.2 ± 2.4 g_{water}/g_{SAP} respectively for SAP A and B) [29], p(chi(1)_PMA(7)) and p(aga(1)_PMA(3)) should be further investigated for incorporation into mortar to identify their effect on the strength as well as their potential to realize self-sealing and -healing of cracks.

IV.4.6. Evaluation of flexural and compressive strength after incorporation of SAPs in mortar

The selected SAPs were incorporated in mortar and the flexural and compressive strength were monitored after 28 days (Table IV.17). Interestingly, for addition of 0.5 m% p(aga(1)_PMA(3)) (with respect to the added amount of cement), a bending strength reduction of 13% and a compressive strength reduction of 18% were obtained. Upon increasing the SAP amount, the bending strength did not further decrease, yet the compressive strength was reduced with 31% (down to 43.6 ± 1.2 MPa). This reduction was more limited for p(chi(1)_PMA(7)) for which 15% and 24% compressive strength reduction were observed upon adding 0.5 and 1 m% respectively. The bending strength reduction associated with the use of 0.5 m% p(chi(1)_PMA(7)) was very limited. The more severe decrease associated with the use of p(aga(1)_PMA(3)) can be correlated with the higher amount of additional water required to create mortar with an equal workability compared to the reference sample.

The obtained results can be compared with strength tests performed upon incorporation of commercially available SAPs. The tests indicated that addition of SAP A led to a decrease of the compressive strength by 35% and 55% upon addition of 0.5 and 1 m%, respectively [46]. The synthesized SAPs thus exhibited a significantly lower effect on mortar strength. SAP B on the other hand resulted in a strength reduction of 20% upon introducing 0.5 and 1 m% SAP [46]. Interestingly, p(chi(1)_PMA(7)) resulted in a smaller reduction upon addition of 0.5 m% while a comparable strength reduction was found when introducing 1 m%. For p(aga(1)_PMA(3)), the strength for 0.5 m% SAP addition was similar compared to SAP B. However, when 1 m% SAP was added, the mortar strength decreased more significant than for commercial SAP B [46].

Table IV.17: Flexural and compressive strength of mortars upon addition of semi-synthetic SAPs.

p(aga(1)_PMA(3))		Bending strength [MPa]	Compressive Strength [MPa]	Batch
0.5 m%	(+ 40 mL water)	7.3 ± 0.3 (-13%)	51.6 ± 1.1 (-18%)	2
1 m%	(+ 70 mL water)	7.2 ± 0.1 (-14%)	43.6 ± 1.2 (-31%)	2
p(chi(1)_PMA(7))				
0.5 m%	(+ 30 mL water)	8.1 ± 0.1 (-6%)	58.1 ± 1.4 (-15%)	1
1 m%	(+ 40 mL water)	7.3 ± 0.4 (-15%)	51.8 ± 1.3 (-24%)	1
Reference				
No SAP	/	8.6 ± 0.2	68.4 ± 1.1	1
No SAP	/	8.4 ± 0.4	63.2 ± 1.3	2

IV.4.7. Self-sealing and -healing of mortar samples upon addition of SAPs

In order to assess the use for the intended application, a self-sealing and -healing study was performed using p(aga(1)_PMA(3)) and p(chi(1)_PMA(7)) as most promising SAPs of this study. For p(chi(1)_PMA(7)), 0.5 and 1 m% (calculated based on the total amount of cement present) were added to the mortar samples. However, as the swelling was lower for p(aga(1)_PMA(3)) in aqueous solutions around neutral pH (i.e. 34.5 ± 1.0 g_{water}/g_{SAP} for p(aga(1)_PMA(3)) vs. 48.3 ± 3.9 g_{water}/g_{SAP} for p(chi(1)_PMA(7)) at pH 6 respectively), a higher amount of SAP (i.e. 0.7 and 1.3 m%) was introduced to mortar to realize similar self-sealing and -healing. However, results of §IV. 3.7. indicated that a small variation of the amount of SAP (0.5 to 0.7 m% and 1 to 1.3 m%) did not lead to a significant variation in the mechanical parameters, which makes it possible to compare the results obtained for p(aga(1)_PMA(3)) and p(chi(1)_PMA(7)).

Figure IV.29 (except top right) represents the data from samples loaded until 1% strain. As a function of the crack width (after cracking and after 3, 7, 14 and 28 days of wet-dry cycles), the closure of cracks is depicted by presenting the percentage of cracks smaller than a certain width w. Figure IV.29 (top right) and Figure IV.30 show similar data obtained for the samples loaded immediately until failure, which gives a better idea on the sealing behavior of large cracks.

For the reference material, 90% of the crack widths were below 38 µm. After 28 days executing wet-dry cycles, 51% of the cracks were sealed, while only 22% were sealed after 3 days. Partial crack closure was limited to crack widths up to 30 µm. Upon addition of 0.7 m% p(aga(1)_PMA(3)), 90% of the initial cracks were lower than 31 µm. After healing, 93% of the cracks were sealed completely after 28 days and what is more, after 3 days already 79% was sealed. Interestingly, the strong crack sealing already occurring after 3 days was not observed when using other SAPs from this or the previous study, for which a more gradual increase was

observed over time. Cracks up to 40 µm showed partial to complete crack closure. Upon introducing 1.3 m% p(aga(1)_PMA(3)), with cracks being similar compared to the reference material (cfr. 90% below 39 µm in width), 89% of the cracks were fully sealed after 28 days, while 44% after 3 days. Cracks up to 50 µm showed crack closure to some extent. The results thus showed that any addition of p(aga(1)_PMA(3)) outperformed the reference by far. However, a higher amount of SAP addition resulted in some decreased self-sealing. This could be related to the presence of larger cracks upon adding 1.3 m%. What is more, crack closure even occurred slower for the higher SAP concentration. It could be anticipated that this high SAP amount could lead to more extensive macro-pore formation, which could result in a pathway for cracks to manifest internally rendering it more difficult for the SAPs to completely fill these openings.

When comparing the results obtained for p(chi(1)_PMA(7)) with the reference samples, the crack sizes of the latter (90% smaller than 38 µm) were ranging between the crack widths for mortar samples containing SAP (90% of the cracks smaller than 30 µm and 43 µm for 0.5 and 1 m% respectively). It could also be observed that the crack widths were comparable to mortars containing p(aga(1)_PMA(3)) (90% smaller than 31 µm and 39 µm for 0.7 and 1.3 m% respectively). The latter could be explained by the fact that both polymers show a similar grain size distribution which led to a similar degree of macro-pore formation after hardening. When applying 0.5 m% p(chi(1)_PMA(7)), 82% of the cracks were closed after 28 days while 54% after 3 days already. All cracks (up to 40 µm in width) showed partial self-sealing. Upon introduction of 1 m% p(chi(1)_PMA(7)), 79% and 46% of the cracks were completely sealed after respectively 28 days and 3 days of wet-dry cycles. Interestingly, all cracks (up to 60 µm in width) were partially or completely sealed. A gradual sealing process over the 28 days was found for both quantities. Interestingly, an increase with respect to the added SAP amount did not result in a further increase in the total degree of sealed cracks. Both additions outperformed the reference when comparing self-sealing behavior and crack closure. Upon comparing the algMOD and chiMOD series mutually, the addition of p(aga(1)_PMA(3)) would lead to a stronger and faster sealing for the lowest amount of SAP incorporated.

When looking at the samples loaded until failure (Figure IV.29 (right) and Figure IV.30), for the reference materials, only cracks up to 100 µm showed partial self-sealing (90% of the cracks were smaller than 150 µm). The results also showed that only 31% of the cracks were completely sealed. In case of p(aga(1)_PMA(3)), crack widths up to 150 µm were partially sealed whereby 60% of the cracks were sealed upon 0.7 m% addition and only 34% for 1.3 m% SAP. This could be related to the crack size as 90% of the cracks were smaller than 135 µm for the 0.7 m% concentration while 90% were smaller than 190 µm upon adding 1.3 m% p(aga(1)_PMA(3)). Thus despite the far larger cracks for mortars with 1.3 m% SAP, they still showed a somewhat higher sealing compared to the reference mortar specimens.

For p(chi(1)_PMA(7)), cracks up to 150 µm (0.5 m% SAP, 90% of the cracks below 100 µm in width) or even 200 µm (1 m% SAP, 90% of the cracks smaller than 155 µm) showed partial to full

self-sealing while in both series 44% of the cracks were completely sealed. Addition of p(chi(1)_PMA(7)) outperformed the reference.

Overall it could be concluded that, especially upon addition of a low amount of SAP, smaller crack widths were obtained compared to reference mortars. This could be related to multiple cracking behavior being enhanced by the inclusion of superabsorbent polymers [47]. Thus, an additional number of cracks will be formed, but with a decreased size, thereby facilitating crack closure. In case of introduction of higher SAP amounts, the latter phenomenon was not enhanced, probably due to a more extensive formation of macro-pores.

An increase of the SAP amount resulted in partial sealing of larger cracks when mortars were loaded until 1% strain. There was however no clear indication that an increase in the amount of SAP would lead to a stronger self-sealing behavior. By taking into account that more SAP led to a more severe strength reduction, combined with the results obtained regarding the self-sealing capacity, it could be concluded that any addition of SAP leads to a stronger sealing than the reference samples and an addition of a low amount of SAP (0.5 m% for p(chi(1)_PMA(7)) and 0.7 m% for p(aga(1)_PMA(3))) already showed a high sealing potential. However, an increase in the amount of SAP (1 m% for p(chi(1)_PMA(7)) and 1.3 m% for p(aga(1)_PMA(3))) did not lead to a further increased sealing, rather a small decrease, which could be related to the increased macro-pore formation which could lead to pathways for the cracks to manifest. This makes it more difficult for the SAPS to completely fill up the crevices.

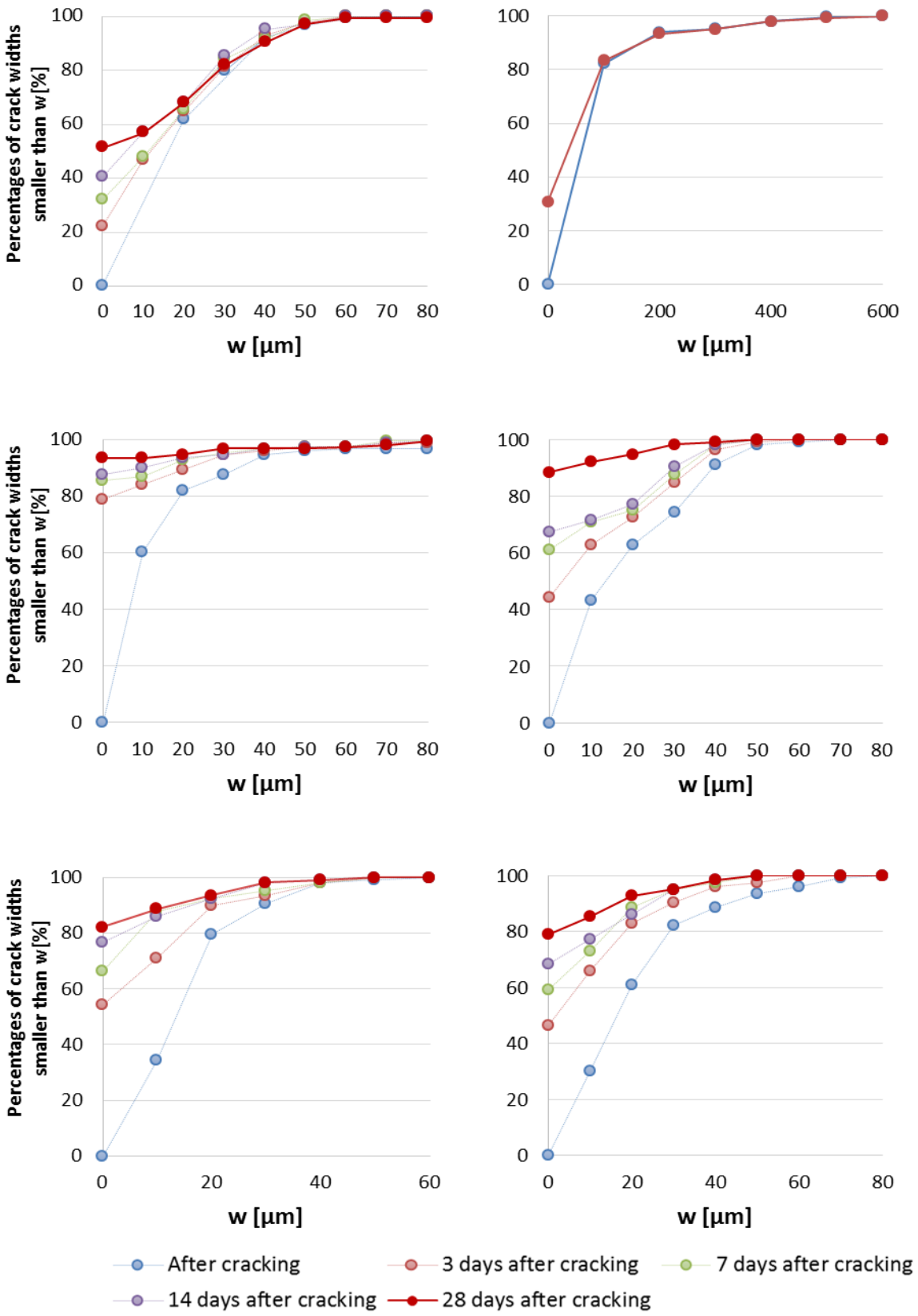

Figure IV.29: Crack closure of the wet-dry cycles for the reference mortar after loading until 1% strain (top left) and until failure (top right) and after loading until 1% strain for mortars containing p(aga(1)_PMA(3)) (0.5 m% SAP, center left and 1 m% SAP, center right) and p(chi(1)_PMA(3)) (0.5 m% SAP, bottom left and 1 m% SAP, bottom right).

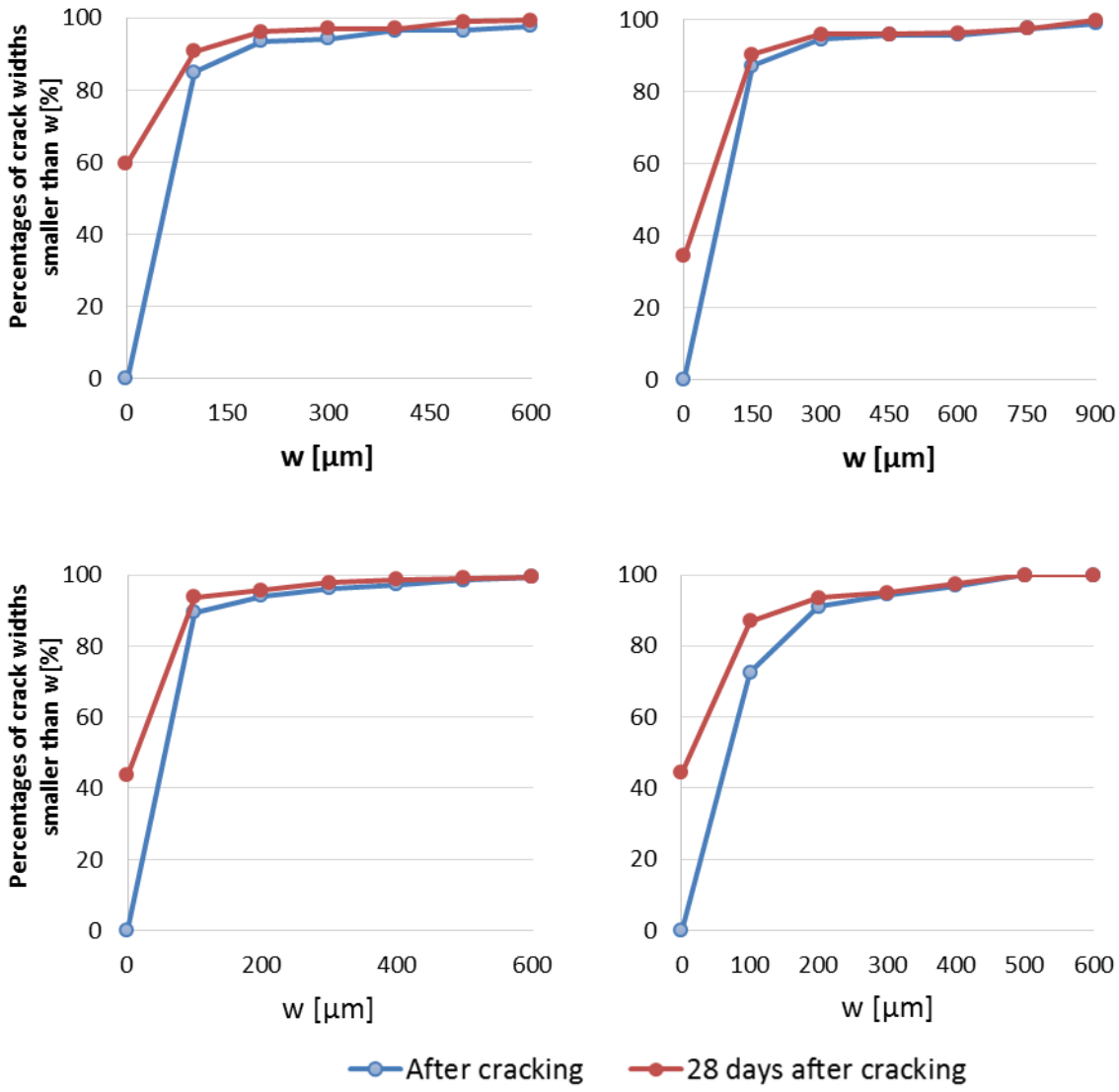

Figure IV.30: Crack closure of the wet-dry cycles after loading until failure for mortars containing p(aga(1)_PMA(3)) (0.5 m% SAP, top left and 1 m% SAP, top right) and p(chi(1)_PMA(3)) (0.5 m% SAP, bottom left and 1 m% SAP, bottom right).

To identify the self-healing behavior of the SAPs in mortar, several mechanical parameters were investigated. The parameters obtained as depicted in the stress-strain curves after loading included the stress at the point of first crack formation (strength at which the first drop in the stress-strain curve occurred due to an unstable extension of the matrix fiber tunnel), further defined as first-cracking-strength σ_{fc}, the regain in σ_{fc} after reloading, the peak stress σ_p and the increase in strain over the hardening part, also called multiple cracking MC. For σ_{fc} and the regain in σ_{fc}, measurements were done in triplicate. For σ_p and MC, measurements were also performed in triplicate except for 0.7 m% p(aga(1)_PMA(3)), for which one of the three samples was broken at first contact.

Table IV.18: Mechanical parameters defining self-healing capacity of mortars by adding SAPs.

Sample	SAP conc. [w%]	σ_{fc} [MPa]	Regain in σ_{fc} [%]	Peak strength σ_p [MPa]	MC [%]
Reference	0.0	6.1 ± 0.9	40.2 ± 7.9	9.6 ± 1.3	3.1 ± 0.9
p(aga(1)_PMA(3))	0.7	5.0 ± 0.6	50.8 ± 4.3	8.1 ± 1.4	3.1 ± 1.3
	1.3	4.4 ± 0.5	66.9 ± 5.8	7.8 ± 0.2	4.4 ± 2.1
p(chi(1)_PMA(7))	0.5	4.4 ± 0.4	64.5 ± 8.7	8.8 ± 3.1	4.5 ± 2.7
	1.0	4.8 ± 0.6	56.7 ± 7.8	7.6 ± 1.9	3.3. ± 1.6

Table IV.18 shows the different mechanical parameters measured for the mortars. The results showed that the mean σ_{fc} for samples containing polymers at the age of 28 days was lower compared to the reference. However, this difference was only significant ($p < 0.05$) upon addition of 0.5 m% p(chi(1)_PMA(7)) and 1.3 m% p(aga(1)_PMA(3)). This decrease was anticipated as the addition of SAPs to mortar results in a (significant) strength decrease. The mean values of σ_{fc} for mortars with SAPs did not differ significantly among each other.

When looking at the regain in σ_{fc}, both materials showed a larger regain in σ_{fc} compared to the reference, irrespective of the amount or type of SAP. Although, due to the large standard deviations, only the values for 1.3 m% p(aga(1)_PMA(3)) and 0.5 m% p(chi(1)_PMA(7)) were significantly different (66.9 ± 5.8 % and 64.5 ± 8.7 % respectively). Although the values of the mortars containing SAP showed a lower σ_p, none of these values were significantly different.
By using SAPs, the ductility of the mortar was increased. The SAPs could act as flaws which facilitated MC. Especially upon addition of 1.3 m% p(aga(1)_PMA(3)) and 0.5 m% of p(chi(1)_PMA(7)), an increase was observed for MC. These samples also showed a significant increase in their strength regain. However, due to variations in sample geometry, large standard deviations were obtained resulting in the MC differences being not significant. It should be mentioned that the MC for the reference was quite high as Snoeck et al. [47] obtained a value of only 2%. As no statistical differences were found for the peak strength nor for MC, no decisive conclusions could be drawn.
When comparing the results with the use of commercially available SAPs A and B (cfr. for the addition of 0.5 m% SAP A and 0.5 and 1 m% SAP B) [48], σ_{fc} and MC did not differ significantly ($p < 0.05$) from the values obtained for these novel, in-house developed SAPs. Moreover, when comparing the regain in σ_{fc}, the addition of 0.7 m% p(aga(1)_PMA(3)) resulted in a significantly lower strength regain. However, the strength regain upon introducing 1.3 m% was not significantly different from adding both 0.5 m% SAP A or B. It was significantly lower though compared to what was obtained upon addition of 1 m% SAP B, albeit not very significant ($p < 0.01$). A similar conclusion could be drawn for the addition of 0.5 m% p(chi(1)_PMA(7)). Finally, for the mortars containing 1 m% p(chi(1)_PMA(7)), the strength regain was not significantly different compared to samples containing 0.5 m% SAP A or 0.5 m% SAP B, yet significantly different for 1 m% SAP B.

It can be concluded that addition of both p(aga(1)_PMA(3)) and p(chi(1)_PMA(7)) led to a strong increase in the regain of first-cracking-strength. Significant differences (67% and 65%) with the reference (40%) were found upon addition of 1.3 m% p(aga(1)_PMA(3)) and 0.5 m% p(chi(1)_PMA(7)) which were comparable to the effect of commercially available SAPs.

IV.4.8. Conclusions and future perspectives

Alginate, agarose and chitosan were successfully methacrylated and a DS of 37.8%, 14.19% and 6.59% per repeating monosaccharide were obtained for algMOD, agaMOD and chiMOD respectively. The combination of ATR-IR spectroscopy and HR-MAS ^{1}H-NMR spectroscopy enabled to identify the SAP structures as well as their cross-linking efficiency. Gel fractions ranged between 49 and 85% with lower values being obtained for the SAPs containing DMAPMA. The gel fractions of the agarose-based SAPs were the highest, followed by alginate-containing SAPs. All SAPs showed a high moisture uptake capacity, especially for the SAPs containing DMAPMA with values up to 122% the original weight of the SAP for a RH of 95%. All materials exhibited a negligible hysteresis of the water vapor sorption isotherms (up to 1.8%). The SAPs showed a pH-responsive swelling capacity due to both the presence of the basic monomers and responsive polysaccharides (alginate and chitosan). For p(alg(1)_EMA(7)) and p(alg(1)_PMA(7)), the pH-sensitivity was in conflict with what was required for the envisaged application. They were therefore not further tested in mortar. P(aga(1)_EMA(3)) and p(aga(1)_PMA(3)) were more promising because of their increase in swelling capacity found upon decreasing the pH (up to 111 g_{water}/g_{SAP} at a pH of 3 for p(aga(1)_EMA(3))). The swelling in CF solution amounted to 21 and 24 g_{water}/g_{SAP} (for p(aga(1)_EMA(3)) and p(aga(1)_PMA(3)) respectively) with no significant difference upon varying the pH.

For p(chi(1)_EMA(7)) and p(chi(1)_PMA(7)), a double pH-sensitivity was observed. Upon decreasing the pH, a first increase in swelling was observed due to the presence of the monomers, followed by a second increase in swelling capacity due to the amines of the chitosan. Additionally, the chitosan is also composed of pH-responsive amine moieties which created a second increase of the swelling with a further decrease of the pH. Maximal swelling capacities up to 75 g_{water}/g_{SAP} were obtained. The swelling potential in CF solutions was 16 – 19 g_{water}/g_{SAP} for p(chi(1)_EMA(7)) and p(chi(1)_PMA(7)) with a small, but significant increase with a decreasing pH. After incubation in the different solutions, the samples were dried again and tested by ATR-IR spectroscopy for possible degradation. P(alg(1)_EMA(7)), p(alg(1)_PMA(7)) and p(aga(1)_EMA(3)) showed no hydrolysis whatsoever. Hydrolysis occurred in p(aga(1)_PMA(3)) in aqueous solutions at pH 13 and extremely basified CF solution (pH 13), where in the latter case a high amount of NaOH was needed to reach this pH, which influences the SAP. In CF, no form of degradation is yet observed, which is very promising. A similar trend is identified for p(chi(1)_EMA(7)) and p(chi(1)_EMA(7)). All these materials are thus interesting to be used in mortar.

After characterization, p(aga(1)_PMA(3)) and p(chi(1)_PMA(7)) were selected to test further in mortar. At first, the effect on the flexural and compressive strength was tested and it was observed that especially p(chi(1)_PMA(7)) showed a rather limited effect on the strength, comparable to (addition of 1 m%) or even better than (addition of 0.5 m%) commercially available SAP B from BASF. For p(aga(1)_PMA(3)), the strength at 0.5 m% addition was similar to SAP B and at 1 m% SAP, the strength decrease was more significant.

Finally, a four-point-bending test was performed to identify the self-sealing and -healing potential of the selected SAPs. It was found that addition of SAP would lead to a stronger self-sealing than the reference (up to 93% of cracks with widths up to 30 µm completely sealed for 0.7 m% p(aga(1)_PMA(3))). Larger cracks up to even 200 µm showed partial self-sealing, where in the case of the reference mortar this only happened for cracks up to 100 µm.

At last, self-healing measurements were performed by processing the mechanical properties. No significant differences could be observed for the MC and peak strength, although an increasing trend for MC was observed for 1.3 m% p(aga(1)_PMA(3)) and 0.5 m% p(chi(1)_PMA(7)). To identify the self-healing, the regain in σ_{fc} was measured. A significant increase was observed for 1.3 m% p(aga(1)_PMA(3)) and 0.5 m% p(chi(1)_PMA(7)) (67% and 65% respectively, compared to 40% for the reference mortar). These values were similar to self-healing obtained through addition of 0.5 m% commercial SAP B, however, they were significantly ($p < 0.05$) (although not very significant, $p < 0.01$) lower than for addition of 1 m% SAP B. It could be concluded based on the limited reduction of the mortar strength and high regain in σ_{fc} that these SAPs are very promising for the intended application.

IV.4.9. References

[1] Patricelli MP, Cravatt BF. Fatty Acid Amide Hydrolase Competitively Degrades Bioactive Amides and Esters through a Nonconventional Catalytic Mechanism. Biochemistry. 1999;38(43):14125-30.
[2] Fife TH, Squillacote VL. Metal ion effects on intramolecular nucleophilic carboxyl group participation in amide and ester hydrolysis. Hydrolysis of N-(8-quinolyl)phthalamic acid and 8-quinolyl hydrogen glutarate. Journal of the American Chemical Society. 1978;100(15):4787-93.
[3] Robinson BA, Tester JW. Kinetics of alkaline hydrolysis of organic esters and amides in neutrally-buffered solution. International Journal of Chemical Kinetics. 1990;22(5):431-48.
[4] Mishra RK, Ramasamy K, Majeed ABA. pH-responsive poly (DMAPMA-co-HEMA)-based hydrogels for prolonged release of 5-fluorouracil. Journal of Applied Polymer Science. 2012;126(S2).
[5] Das A, Ghosh S, Ray AR. Unveiling the self-assembly behavior of copolymers of AAc and DMAPMA in situ to form smart hydrogels displaying nanogels-within-macrogel hierarchical morphology. Polymer. 2011;52(17):3800-10.
[6] Chang K-T, Frampton H, Morgan JC. Composition and method for recovering hydrocarbon fluids from a subterranean reservoir. Google Patents; 2002.
[7] Liu K-C, Rocafort CM, Anderson LR, Reuven Y. Low VOC hair spray compositions containing terpolymers of vinyl pyrrolidone, vinyl caprolactam and 3-(N-dimethylaminopropyl) methacrylamide. Google Patents; 1997.
[8] Kim E-M, Min BG, Jang J. Reactive dyeing of meta-aramid fabrics photografted with dimethylaminopropyl methacrylamide. Fibers and Polymers. 2011;12(5):580-6.
[9] Dotzauer B, Wistuba E, Schwartz M, Petri R, Bechert B, Denu H-J. Polymer-coated precast concrete. Google Patents; 1993.
[10] Finnie AA, Price C, Ramsden RM. Polymer with salt groups and antifouling coating composition comprising said polymer. Google Patents; 2015.
[11] Mercey E, Obeïd P, Glaise D, Calvo-Muñoz M-L, Guguen-Guillouzo C, Fouqué B. The application of 3D micropatterning of agarose substrate for cell culture and in situ comet assays. Biomaterials. 2010;31(12):3156-65.
[12] Chung BG, Lee K-H, Khademhosseini A, Lee S-H. Microfluidic fabrication of microengineered hydrogels and their application in tissue engineering. Lab on a Chip. 2012;12(1):45-59.
[13] Li X, Valadez AV, Zuo P, Nie Z. Microfluidic 3D cell culture: potential application for tissue-based bioassays. Bioanalysis. 2012;4(12):1509-25.
[14] Miguel SP, Ribeiro MP, Brancal H, Coutinho P, Correia IJ. Thermoresponsive chitosan–agarose hydrogel for skin regeneration. Carbohydrate Polymers. 2014;111:366-73.
[15] Firouzabadi H, Iranpoor N, Gholinejad M, Kazemi F. Agarose hydrogel as an effective bioorganic ligand and support for the stabilization of palladium nanoparticles. Application as a recyclable catalyst for Suzuki–Miyaura reaction in aqueous media. RSC Advances. 2011;1(6):1013-9.
[16] Armisén R. Agar and agarose biotechnological applications. Hydrobiologia. 1991;221(1):157-66.
[17] Boyde TRC. Swelling and contraction of polyacrylamide gel slabs in aqueous solutions. Journal of Chromatography A. 1976;124(2):219-30.
[18] de Koning HWM, Chamuleau RAFM, Bantjes A. Crosslinked agarose encapsulated sorbents resistant to steam sterilization. Preparation and mechanical properties. Journal of Biomedical Materials Research. 1984;18(1):1-13.
[19] Zhang X, Deng Z, Xu H. Calibrating an optical fiber humidity sensor and applying it in real-time monitoring of relative humidity in fresh concrete. Chinese Optics Letters. 2013;11(9):090604.
[20] Paul W, Sharma CP. Chitosan and alginate wound dressings: a short review. Trends Biomater Artif Organs. 2004;18(1):18-23.
[21] Jayakumar R, Prabaharan M, Kumar PTS, Nair SV, Tamura H. Biomaterials based on chitin and chitosan in wound dressing applications. Biotechnology advances. 2011;29(3):322-37.

[22] Crompton KE, Goud JD, Bellamkonda RV, Gengenbach TR, Finkelstein DI, Horne MK, et al. Polylysine-functionalised thermoresponsive chitosan hydrogel for neural tissue engineering. Biomaterials. 2007;28(3):441-9.
[23] Croisier F, Jérôme C. Chitosan-based biomaterials for tissue engineering. European Polymer Journal. 2013;49(4):780-92.
[24] Bernkop-Schnürch A, Dünnhaupt S. Chitosan-based drug delivery systems. European Journal of Pharmaceutics and Biopharmaceutics. 2012;81(3):463-9.
[25] Fang YE, Cheng Q, Lu XB. Kinetics of in vitro drug release from chitosan/gelatin hybrid membranes. Journal of Applied Polymer Science. 1998;68(11):1751-8.
[26] Dash M, Chiellini F, Ottenbrite RM, Chiellini E. Chitosan—A versatile semi-synthetic polymer in biomedical applications. Progress in polymer science. 2011;36(8):981-1014.
[27] Giri TK, Thakur A, Alexander A, Badwaik H, Tripathi DK. Modified chitosan hydrogels as drug delivery and tissue engineering systems: present status and applications. Acta Pharmaceutica Sinica B. 2012;2(5):439-49.
[28] Bezerra UT, Ferreira RM, Castro-Gomes JP. The effect of latex and chitosan biopolymer on concrete properties and performance. Key Engineering Materials: Trans Tech Publ; 2011. p. 37-46.
[29] Snoeck D, Van Tittelboom K, Steuperaert S, Dubruel P, De Belie N. Self-healing cementitious materials by the combination of microfibres and superabsorbent polymers. Journal of Intelligent Material Systems and Structures. 2014;25(1):13-24.
[30] Paepe ID, Declercq H, Cornelissen M, Schacht E. Novel hydrogels based on methacrylate-modified agarose. Polymer International. 2002;51(10):867-70.
[31] Lavertu M, Xia Z, Serreqi AN, Berrada M, Rodrigues A, Wang D, et al. A validated 1 H NMR method for the determination of the degree of deacetylation of chitosan. Journal of Pharmaceutical and Biomedical Analysis. 2003;32(6):1149-58.
[32] Nurmi L, Peng H, Seppälä J, Haddleton DM, Blakey I, Whittaker AK. Synthesis and evaluation of partly fluorinated polyelectrolytes as components in 19F MRI-detectable nanoparticles. Polymer Chemistry. 2010;1(7):1039-47.
[33] Creutz S, Jérôme R. Effectiveness of block copolymers as stabilizers for aqueous titanium dioxide dispersions of a high solid content. Progress in Organic Coatings. 2000;40(1–4):21-9.
[34] Ilavský M. Effect of electrostatic interactions on phase transition in the swollen polymeric network. Polymer. 1981;22(12):1687-91.
[35] Campbell D, Tighe BJ. Zwitterionic and Charge-Balanced Polyampholyte Copolymer Hydrogels. Advanced Materials Research: Trans Tech Publ; 2008. p. 729-32.
[36] Barlow RB, Bremner JB, Soh KS. The effects of replacing ester by amide on the biological properties of compounds related to acetylcholine. British journal of pharmacology. 1978;62(1):39-50.
[37] Pirinen S, Karvinen J, Tiitu V, Suvanto M, Pakkanen TT. Control of swelling properties of polyvinyl alcohol/hyaluronic acid hydrogels for the encapsulation of chondrocyte cells. Journal of Applied Polymer Science. 2015;132(28):n/a-n/a.
[38] Lee YM, Kim SH, Cho CS. Synthesis and swelling characteristics of pH and thermoresponsive interpenetrating polymer network hydrogel composed of poly (vinyl alcohol) and poly (acrylic acid). Journal of Applied Polymer Science. 1996;62(2):301-11.
[39] Dima C, Pătraşcu L, Cantaragiu A, Alexe P, Dima Ş. The kinetics of the swelling process and the release mechanisms of Coriandrum sativum L. essential oil from chitosan/alginate/inulin microcapsules. Food chemistry. 2016;195:39-48.
[40] Meng X, Tian F, Yang J, He C-N, Xing N, Li F. Chitosan and alginate polyelectrolyte complex membranes and their properties for wound dressing application. Journal of Materials Science: Materials in Medicine. 2010;21(5):1751-9.
[41] Snoeck D, Schaubroeck D, Dubruel P, De Belie N. Effect of high amounts of superabsorbent polymers and additional water on the workability, microstructure and strength of mortars with a water-to-cement ratio of 0.50. Construction and Building Materials. 2014;72(0):148-57.
[42] Hancock RD, Martell AE. Ligand design for selective complexation of metal ions in aqueous solution. Chemical Reviews. 1989;89(8):1875-914.

[43] Van de Wetering P, Zuidam NJ, Van Steenbergen MJ, Van der Houwen O, Underberg WJM, Hennink WE. A mechanistic study of the hydrolytic stability of poly (2-(dimethylamino) ethyl methacrylate). Macromolecules. 1998;31(23):8063-8.
[44] LogithKumar R, KeshavNarayan A, Dhivya S, Chawla A, Saravanan S, Selvamurugan N. A review of chitosan and its derivatives in bone tissue engineering. Carbohydrate Polymers. 2016;151:172-88.
[45] Andersen FA, Brecevic L. Infrared spectra of amorphous and crystalline calcium carbonate. Acta Chem Scand. 1991;45:1018-24.
[46] Snoeck D, Dubruel P, De Belie N. How to seal and heal cracks in cementitious materials by using superabsorbent polymers. Application of Superabsorbent Polymers and Other New Admixtures in Concrete Construction: RILEM Publications; 2014. p. 375-84.
[47] Snoeck D, De Belie N. Repeated autogenous healing in strain-hardening cementitious composites by using superabsorbent polymers. Journal of Materials in Civil Engineering. 2015;28(1):04015086.
[48] Snoeck D. Self-healing and microstructure of cementitious materials with microfibres and superabsorbent polymers. PhD thesis: Ghent University; 2015.

IV.5 Identifying the potential of sulfated polysaccharides

Previously (see §IV.2), it was shown that the combination of 2-acrylamido-2-methylpropanesulfonic acid (AMPS) with methacrylated alginate led to a strong moisture uptake capacity of 110% at a relative humidity (RH) of 95%. What is more, these materials swelled up to 246 times their own weight in ultrapure (highest level of purity) water. However, the effect on the strength upon incorporation in mortar was too severe for practical use. Nevertheless, the effect of different sulfated materials was subsequently investigated given their high swelling and moisture uptake potential. Carrageenan is a family of sulfated polysaccharides consisting of D-galactose and 3,6-anhydro-D-galactose repeating units which is extracted from certain red seaweeds of the Rhodophyceae class. It has found its use in the food industry as thickening agent [1], gelling agent in combination with gelatin [2], protein suspending agent [3] and in dairy applications [4]. Carrageenan is also known to induce inflammation in rats [5, 6], an immune response [7, 8] and anti-oxidant activity [9, 10]. It can also be used for controlled delivery (of e.g. platelet derived growth factor) in bone tissue engineering [11, 12]. Of all types, κ-carrageenan is the most abundant and contains one sulfate group per disaccharide. It has already been tested recently in a construction-related application to improve a fly ash-based geopolymer [13]. Interestingly, this polysaccharide has already been methacrylated using methacrylic anhydride for tissue engineering applications [14]. Based on the above-mentioned literature data, it was thus considered useful to investigate its potential for applications associated with mortar and concrete. As methacrylated alginate also showed interesting characteristics in mortar, it could be interesting to evaluate the potential of sulfation of methacrylated alginate. Alginate has proven its use based on data described in the previous chapters either by physical cross-linking with Ca^{2+} (§IV.1) or by methacrylation and combination with a carboxylic or sulfonic acid (§IV.2). Subsequently, it was combined with acrylic acid and acrylamide and the effect of changing the degree of substitution was investigated (§IV.3.). To assess the effect of the presence of sulfate moieties on the moisture and swelling capacity, irrespective of the polysaccharide structure, the methacrylated polysaccharide was sulfated in collaboration with 'L'Institut Français de Recherche pour l'Exploitation de la Mer' (iFremer, Dr. Sylvia Colliec-Jouault) according to a previously established procedure [15-18].

First, κ-carrageenan has been methacrylated (carMOD) in a similar way compared to the other polysaccharides. The degree of substitution has been determined using ^{1}H-NMR spectroscopy. Subsequently, the methacrylated κ-carrageenan has been cross-linked using a UV-induced polymerization. Next, cross-linked carMOD has been characterized by attenuated total reflectance infrared (ATR-IR) spectroscopy to identify its chemical structure and dynamic vapor sorption (DVS) measurements to determine the moisture uptake capacity at different RH. The obtained results were compared with the previously synthesized methacrylated alginate in combination with AMPS. Swelling tests have also been performed in ultrapure water and cement filtrate. Additionally, methacrylated alginate (algMOD) has been sulfated by iFremer. Using ^{1}H-NMR spectroscopy, the effect of the sulfation methodology on the DS has been investigated.

An attempt has been made to photo-polymerize the sulfated algMOD. All techniques have also been used for sulfated algMOD and compared with regular algMOD.

IV.5.1. Modification of polysaccharides using methacrylic anhydride followed by photo-polymerization

In a first step, κ-carrageenan was methacrylated (11 equivalents of methacrylic anhydride). The degree of substitution (DS) was determined by ^{1}H NMR spectroscopy (Figure IV.31).

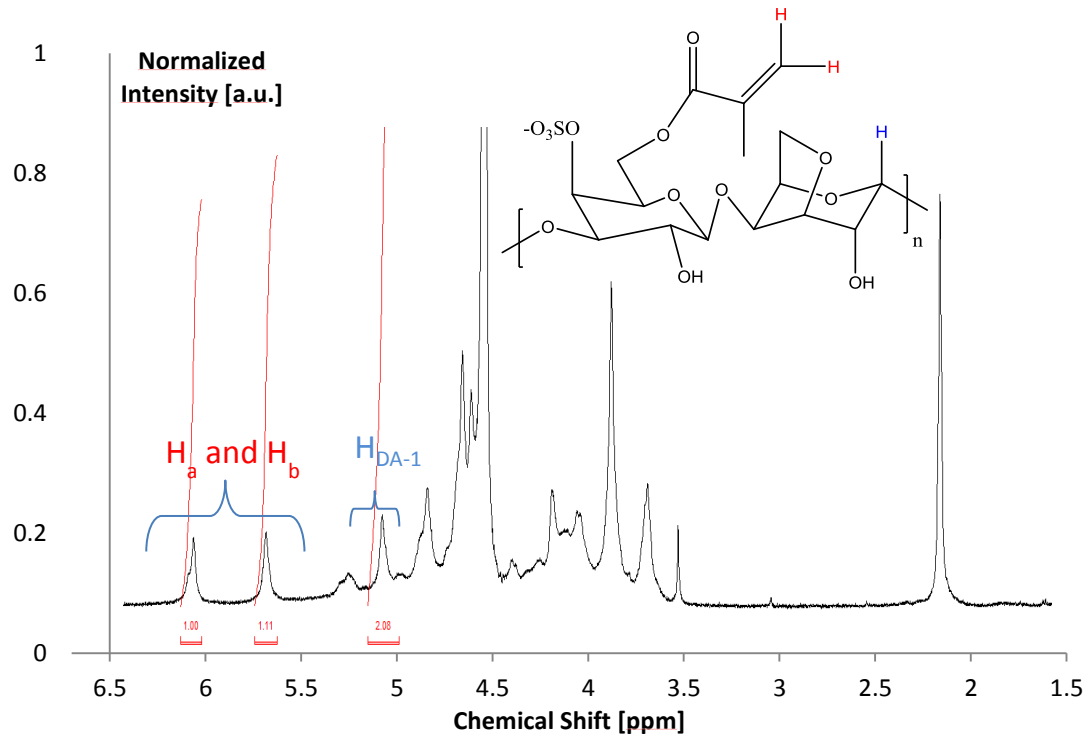

Figure IV.31: ^{1}H NMR spectrum of carMOD with annotation of the relevant peaks for the calculation of the DS.

The obtained spectra were analyzed by comparing the characteristic peaks of the methacrylate group corresponding to the vinyl protons at 5.95 and 6.36 ppm with a reference peak from the κ-carrageenan backbone at 5.29 ppm. As this latter peak corresponds with the α-anomeric proton of the 4-linked 3,6-anhydro-α-D-galactopyranose (DA) [19-21], the ratio of the average integration of the peaks from the methacrylates and the integration of the characteristic signal from the anomeric proton resulted in the degree of substitution (DS) per repeating unit by applying equation (IV.5). To obtain the DS per hydroxyl moiety, this value had to be divided by three as the considered repeating unit (3-linked-β-D-glactopyranose 4-sulfate (G4S) and DA) possessed in total three hydroxyl groups. A DS of 51% was obtained per repeating unit, or 17% as a function of the total amount of hydroxyl functionalities present.

$$DS\ [\%] = \frac{\frac{H_a + H_b}{2}}{H_{DA-1}} = \frac{\frac{I_{5.95ppm} + I_{6.36ppm}}{2}}{I_{5.29ppm}} \qquad \text{(IV.5)}$$

The DS of the used algMOD before sulfation was 6% as a function of the total amount of alcohol moieties. After sulfation, the DS values were again measured to determine the effect of the sulfation procedure on the DS (Figure IV.32). Two degrees of sulfation including 6 wt%S (algMOD_6S) and 9 wt%S (algMOD_9S) were obtained as determined by high-performance anion-exchange chromatography (HPAEC) (iFremer). Unfortunately, the DS values decreased down to 5 and 3%. The sulfation process thus negatively influenced the methacrylation. Future work could include the sulfation of pure sodium alginate followed by methacrylation. However, as the sulfation process is very time-consuming to synthesize even small amounts (up to 1 – 1.5 g), it was not possible to further test this within the timeframe of the current PhD.

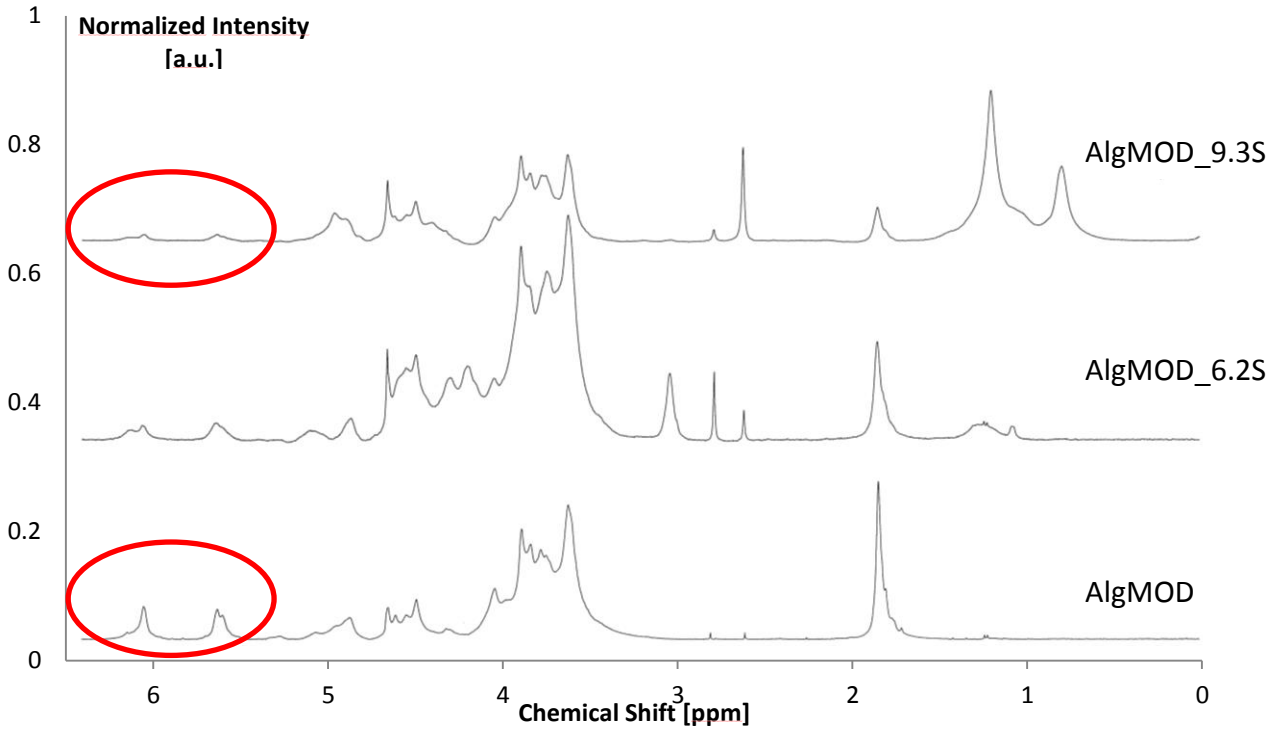

Figure IV.32: Determination of the degree of substitution of algMOD (bottom) and sulfated algMOD (6% S center, 9%S top).

Subsequently, an attempt was made to photo-polymerize the modified polysaccharides. CarMOD was successfully cross-linked ($\lambda_{operating}$ = 300 – 400 nm, intensity of 9 – 10 mW/cm² per unit) using Irgacure® 2959 as photo-initiator. Flexible, but strong sheets with gel-like properties were obtained which could be further used for material characterization. However, for sulfated algMOD, no gel could be obtained by photo-cross-linking. The DS thus became low (down to 3%), which was apparently insufficient to ensure the formation of the alginate-based gel. A solution would be to perform the sulfation before methacrylation.

IV.5.2. Chemical structure elucidation of sulfated polymers by attenuated total reflectance infrared spectroscopy

ATR-IR spectroscopy was performed on the sulfated materials (Figure IV.33) to elucidate the chemical structure. AlgMOD has been included to enable comparison with sulfated algMOD. As anticipated, carMOD and both algMOD_6S and algMOD_9S showed the weak presence of the carbon-sulfur bond stretch ν(C-S) around 725 cm^{-1} and a strong peak related to the symmetric sulfur-oxygen double bond stretch ν_s(S=O) at 1235 cm^{-1}. At 1410 cm^{-1}, both the symmetric carbon-oxygen bond stretch ν_s(C-O) of alginate and the asymmetric sulfur-oxygen double bond stretch ν_s(S=O) were located, which explains the stronger presence of the peak for sulfated algMOD. However, this peak was only weakly visible in the carMOD spectrum due to the absence of the ν_s(C-O). Finally, the carbon-oxygen double bond stretch vibration ν(C=O) from the esters was visible at 1720 cm^{-1} while additional qualitative confirmation for the decrease of the DS by sulfation of algMOD was obtained. Indeed, the peak almost completely disappeared in the shoulder of the adjacent peak upon increasing the sulfation.

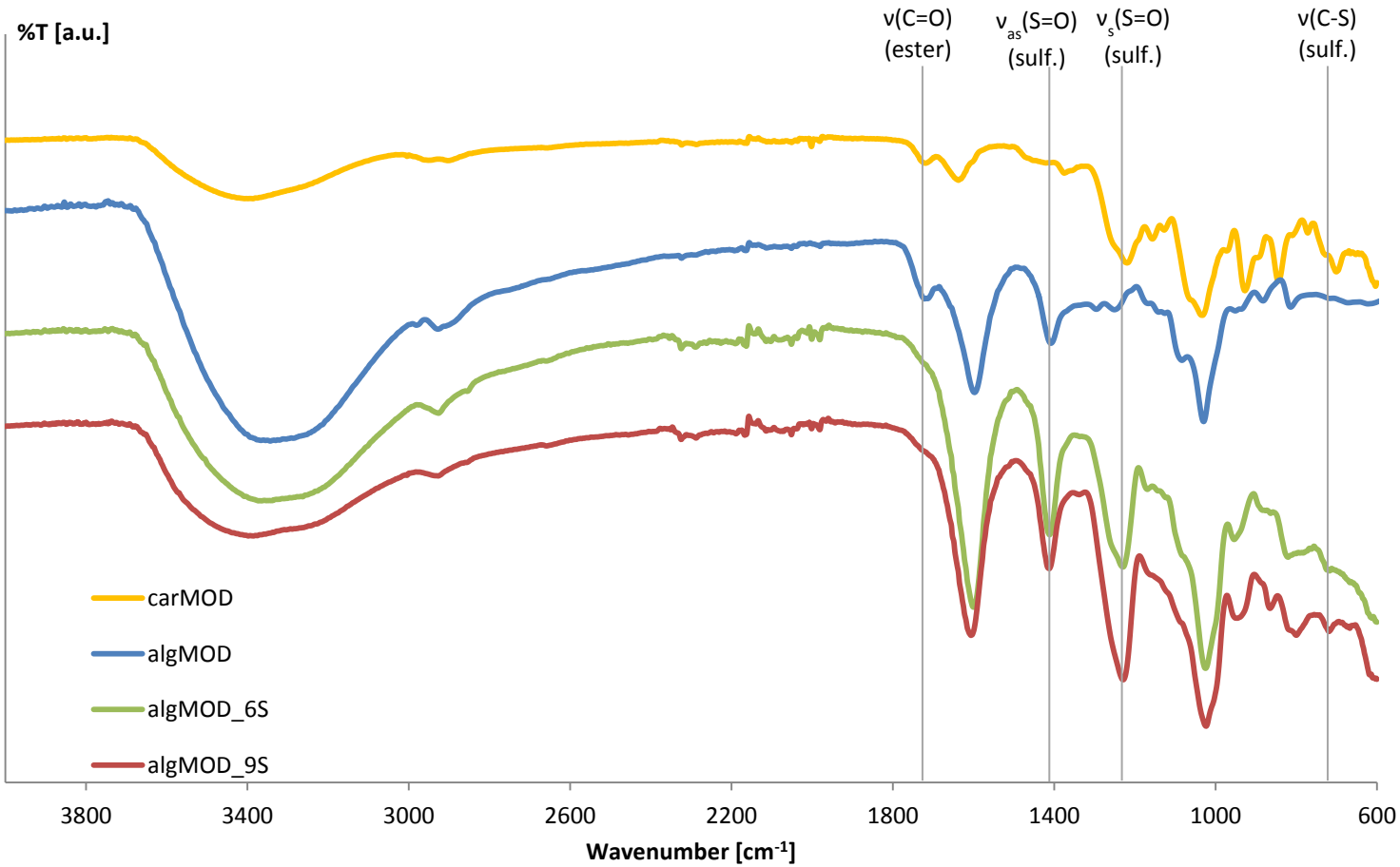

Figure IV.33: ATR-IR spectra of methacrylated κ-carrageenan (carMOD, yellow), methacrylated alginate (algMOD, blue) and sulfated algMOD (6-7 wt%S, green and 9 wt%S, red) with designation of the relevant peaks and their functional bond vibration.

IV.5.3. Moisture uptake capacity of methacrylated and sulfated polysaccharides

The SAPs were tested for their moisture uptake capacity with dynamic vapor sorption measurements. Next to carMOD and sulfated algMOD (algMOD_6S and algMOD_9S), p(alg(1)_AA_0/$AMPS_{100}$(7)) (described in §IV.2.) was included and non-sulfated algMOD was included as reference. As shown in Table IV.19, the samples exhibited significant moisture uptake capacities due to the presence of the negatively charged sulfate moieties. The stronger uptake for sulfated SAPs compared to algMOD (possessing carboxylate moieties) could be related on the one hand to the higher polarity of the sulfonic acid compared to the carboxylic acid [22-24]. On the other hand, the increase could also be related to the higher amount of sulfonic acid groups being ionized at the same pH (pKa sulfonic acid < pKa carboxylic acid). Interestingly, they all showed a negligible hysteresis, with a maximum of 3% making them useful as moisture reservoir similar as the other SAPs synthesized in this PhD. CarMOD had a lower moisture uptake capacity of less than half (up to 54% of its weight at 95% RH) what was found for p(alg(1)_AA_0/$AMPS_{100}$(7)) (122% at 95% RH). This could be related to the high percentage of AMPS monomers built-in in the SAP (1/7 algMOD/AMPS mass ratio), leading to a high amount of sulfate groups. As shown in §IV.2., a high amount of sulfate functionalities compared to carboxylate moieties led to a higher swelling and moisture uptake capacity.
By comparing the moisture uptake capacity of sulfated algMOD with conventional algMOD, it was noticed that the moisture uptake capacity increased significantly upon sulfation, especially at higher RH. Surprisingly, algMOD_6S showed a higher moisture uptake than algMOD_9S. This difference could possibly be related to the dialysis procedure used to isolate sulfated algMOD. Indeed, it can be anticipated that the dialysis time periods were insufficiently long implemented, resulting in remaining 1-butyl-3-methylimidazolium chloride [25] and a decrease in the moisture uptake capacity of algMOD_9S, irrespective of the S content.

Table IV.19: Overview of the sorption capacities of the sulfated polymers (algMOD as reference).

Moisture uptake capacity [%]	algMOD	algMOD_6S	algMOD_9S	carMOD	p(alg(1)_AA_0/$AMPS_{100}$(7))
20% RH	8.8	/*	9.2	/	8.0
30% RH	/	13.5	/	10.9	/
40% RH	13.8	/	14.1	/	12.9
60% RH	19.7	23.4	20.1	18.7	17.6
70% RH	23.9	/	/	/	/
80% RH	29.6	41.4	31.1	28.2	37.7
90% RH	39.3	66.2	45.4	40.3	93.0
95% RH	55.5	94.4	61.4	54.4	121.6

* the '/' indicates that for this sample the mentioned RH has not been measured.

IV.5.4. Swelling capacity of sulfated and modified polysaccharides

The swelling capacity of algMOD_6S and algMOD_9S could not be determined as it was not possible to cross-link them by photo-polymerization. The swelling capacity of algMOD in ultrapure water was 112.4 ± 1.4 g_{water}/g_{SAP}. The swelling ratio of carMOD, however, was substantially lower as it amounted 7.3 ± 2.8 g_{water}/g_{SAP}. The extremely low swelling was related to the high DS (50.7% per repeating unit). Unfortunately, upon testing this material in cement filtrate (CF) solution, complete material degradation occurred. CarMOD was thus not useful for the application targeted herein. However, this carMOD system could potentially lead to polymer networks for biomedical applications including drug delivery or wound treatment. To date, κ-carrageenan is mainly used after ion-induced complexation [26, 27] which could be compared to a stronger covalently cross-linked network. Finally, the swelling of p(alg(1)_AA_0/$AMPS_{100}$(7)) in ultrapure water was 246 g_{water}/g_{SAP}, which outperforms algMOD due to the presence of sulfate moieties which have a higher polarity than the carboxylate moieties.

IV.5.5. Conclusions

A comparative study has been made for polysaccharides containing sulfate moieties either directly linked to their backbone (carMOD), sulfated after methacrylation (algMOD_6S and algMOD_9S) or by incorporation of sulfonic monomers (p(alg(1)_AA_0/$AMPS_{100}$(7))). The results showed that by sulfation, the DS of algMOD decreased substantially, down to the point that photo-polymerization did not lead to a gel. Interestingly, carMOD was successfully cross-linked. ATR-IR spectroscopy was performed to elucidate the characteristic bands of the functionalities of all polymers developed. DVS indicated that especially p(alg(1)_AA_0/$AMPS_{100}$(7)) and algMOD_6S were characterized by extremely high moisture uptake capacities with the former reaching values comparable to commercial SAPs (Table IV.1 in §IV.1). As anticipated, sulfating the material led to an increase of the moisture uptake capacity. The reason of the decreased uptake for 9%S could be related to insufficient purification. Unfortunately, carMOD completely dissolved in CF solution, rendering it not useful for the envisaged application.

IV.5.6. References

[1] Imeson AP. Thickening and gelling agents for food: Springer Science & Business Media; 2012.
[2] Jianlong W, Yi Q. Microbial degradation of 4-chlorophenol by microorganisms entrapped in carrageenan-chitosan gels. Chemosphere. 1999;38(13):3109-17.
[3] Campo VL, Kawano DF, Silva Jr DBd, Carvalho I. Carrageenans: Biological properties, chemical modifications and structural analysis – A review. Carbohydrate Polymers. 2009;77(2):167-80.
[4] Bixler HJ, Johndro K, Falshaw R. Kappa-2 carrageenan: structure and performance of commercial extracts: II. Performance in two simulated dairy applications. Food Hydrocolloids. 2001;15(4–6):619-30.
[5] Ji G-C, Zhang Y-Q, Ma F, Wu G-C. Increase of nociceptive threshold induced by intrathecal injection of interleukin-1β in normal and carrageenan inflammatory rat. Cytokine. 2002;19(1):31-6.
[6] Morikawa K, Nonaka M, Narahara M, Torii I, Kawaguchi K, Yoshikawa T, et al. Inhibitory effect of quercetin on carrageenan-induced inflammation in rats. Life Sciences. 2003;74(6):709-21.
[7] Bhattacharyya S, Liu H, Zhang Z, Jam M, Dudeja PK, Michel G, et al. Carrageenan-induced innate immune response is modified by enzymes that hydrolyze distinct galactosidic bonds. The Journal of nutritional biochemistry. 2010;21(10):906-13.
[8] Yuan H, Song J, Li X, Li N, Dai J. Immunomodulation and antitumor activity of κ-carrageenan oligosaccharides. Cancer letters. 2006;243(2):228-34.
[9] Yuan H, Zhang W, Li X, Lü X, Li N, Gao X, et al. Preparation and in vitro antioxidant activity of κ-carrageenan oligosaccharides and their oversulfated, acetylated, and phosphorylated derivatives. Carbohydrate Research. 2005;340(4):685-92.
[10] Yuan H, Song J, Zhang W, Li X, Li N, Gao X. Antioxidant activity and cytoprotective effect of κ-carrageenan oligosaccharides and their different derivatives. Bioorganic & medicinal chemistry letters. 2006;16(5):1329-34.
[11] Santo VtEr, Frias AM, Carida M, Cancedda R, Gomes ME, Mano JF, et al. Carrageenan-based hydrogels for the controlled delivery of PDGF-BB in bone tissue engineering applications. Biomacromolecules. 2009;10(6):1392-401.
[12] Popa EG, Gomes ME, Reis RL. Cell delivery systems using alginate–carrageenan hydrogel beads and fibers for regenerative medicine applications. Biomacromolecules. 2011;12(11):3952-61.
[13] Li Z, Zhang L. Fly ash-based geopolymer with kappa-carrageenan biopolymer. Biopolymers and Biotech Admixtures for Eco-Efficient Construction Materials. 2016:173.
[14] Mihaila SM, Gaharwar AK, Reis RL, Marques AP, Gomes ME, Khademhosseini A. Photocrosslinkable Kappa-Carrageenan Hydrogels for Tissue Engineering Applications. Advanced healthcare materials. 2013;2(6):895-907.
[15] Chopin N, Sinquin C, Ratiskol J, Zykwinska A, Weiss P, Cérantola S, et al. A Direct Sulfation Process of a Marine Polysaccharide in Ionic Liquid. BioMed research international. 2015;2015.
[16] Senni K, Gueniche F, Foucault-Bertaud A, Igondjo-Tchen S, Fioretti F, Colliec-Jouault S, et al. Fucoidan a sulfated polysaccharide from brown algae is a potent modulator of connective tissue proteolysis. Archives of biochemistry and biophysics. 2006;445(1):56-64.
[17] Bouhlal R, Haslin C, Chermann J-C, Colliec-Jouault S, Sinquin C, Simon G, et al. Antiviral activities of sulfated polysaccharides isolated from Sphaerococcus coronopifolius (Rhodophytha, Gigartinales) and Boergeseniella thuyoides (Rhodophyta, Ceramiales). Marine drugs. 2011;9(7):1187-209.
[18] Matou S, Colliec-Jouault S, Galy-Fauroux I, Ratiskol J, Sinquin C, Guezennec J, et al. Effect of an oversulfated exopolysaccharide on angiogenesis induced by fibroblast growth factor-2 or vascular endothelial growth factor in vitro. Biochemical pharmacology. 2005;69(5):751-9.
[19] Campo VL, Kawano DF, da Silva DB, Carvalho I. Carrageenans: Biological properties, chemical modifications and structural analysis–A review. Carbohydrate Polymers. 2009;77(2):167-80.
[20] Van de Velde F, Knutsen SH, Usov AI, Rollema HS, Cerezo AS. 1 H and 13 C high resolution NMR spectroscopy of carrageenans: application in research and industry. Trends in Food Science & Technology. 2002;13(3):73-92.

[21] Tojo E, Prado J. A simple 1 H NMR method for the quantification of carrageenans in blends. Carbohydrate Polymers. 2003;53(3):325-9.
[22] Lundberg RD, Makowski HS. A comparison of sulfonate and carboxylate ionomers. Ions in Polymers. 1980:21-36.
[23] Twardowski Z, Yeager HL, O'Dell B. A Comparison of Perfluorinated Carboxylate and Sulfonate Ion Exchange Polymers II. Sorption and Transport Properties in Concentrated Solution Environments. Journal of The Electrochemical Society. 1982;129(2):328-32.
[24] Hensley JE, Way JD. Synthesis and characterization of perfluorinated carboxylate/sulfonate ionomer membranes for separation and solid electrolyte applications. Chemistry of Materials. 2007;19(18):4576-84.
[25] MatthewáReichert W. Solvation of 1-butyl-3-methylimidazolium hexafluorophosphate in aqueous ethanol–a green solution for dissolving 'hydrophobic'ionic liquids. Chemical Communications. 2001(20):2070-1.
[26] Grenha A, Gomes ME, Rodrigues M, Santo VE, Mano JF, Neves NM, et al. Development of new chitosan/carrageenan nanoparticles for drug delivery applications. Journal of Biomedical Materials Research Part A. 2010;92(4):1265-72.
[27] Şen M, Avcı EN. Radiation synthesis of poly (N-vinyl-2-pyrrolidone)–κ-carrageenan hydrogels and their use in wound dressing applications. I. Preliminary laboratory tests. Journal of Biomedical Materials Research Part A. 2005;74(2):187-96.

IV.6 Comparative study covering superabsorbent polymers

The previous chapters gave an overview of the synthesis and in-depth characterization of semi-synthetic superabsorbent polymers (SAPs). In a first part (§ IV.1), sodium and calcium alginate (NaAlg and CaAlg respectively) were evaluated and compared with commercial SAPs to provide an indication of the applicability of biopolymers in the field of self-sealing and -healing concrete. Subsequently (§ IV.2), alginate was modified with methacrylic anhydride to create methacrylate moieties to enable subsequent covalent cross-linking of the polysaccharides. The methacrylate functionalities incorporated possess a double bond which can be used to perform a free radical polymerization in the presence of acrylic monomers. In that study, the development and characterization of SAPs based on methacrylated alginate (algMOD) combined with a varying molar fraction of acrylic acid (AA) and/or 2-acrylamido-2-methylpropanesulfonic acid (AMPS) was reported. The results showed that algMOD combined with AA was the most promising material for the targeted application because of its limited effect on the compressive mortar strength. As described in § IV.3, the latter material was compared with algMOD in combination with AA and acrylamide (AM) in a 75/25 molar ratio to enable proper comparison with the synthetic SAPs which were based on the same monomers. Furthermore, these materials were also synthesized using algMOD with a lower degree of substitution (DS) as starting material. In addition to a full characterization and investigation of the bending and compressive strength of mortars with SAP incorporation, the SAP-containing mortars were also tested for their self-sealing and -healing potential using a four-point-bending test. Finally, the potential of using a different polysaccharide backbone was explored by methacrylation of agarose and chitosan, as these biopolymers exhibit different pH-sensitivity compared to methacrylated alginate. Furthermore, the basic monomers 2-(dimethylamino)ethyl methacrylate (DMAEMA) or dimethylaminopropyl methacrylamide (DMAPMA) were also combined with these methacrylated polysaccharides followed by cross-linking, to explore their pH-sensitivity.

The chemical structure of the SAPs has been elucidated by attenuated total-reflectance infrared (ATR-IR) spectroscopy. Additionally, high resolution magic-angle spinning (HR-MAS) ^{1}H-NMR spectroscopy has been used to determine the consumption of double bonds. All materials showed efficient polymerization, with in some cases still a small amount of C=C remaining.
Finally, a cost analysis has been made and the cost of the SAP-based healing strategy has been compared with other self-healing techniques. All characteristics have been compared with data obtained for commercial SAP A (copolymer of acrylamide and sodium acrylate) and SAP B (cross-linked potassium salt poly(acrylate)) [1].

IV.6.1. Moisture uptake capacity study

First, dynamic vapor sorption measurements were used to investigate the moisture uptake capacity of all SAPs. Interestingly, all polymers showed a negligible percentage of hysteresis with a maximum of 3%. The SAPs can thus be used as moisture reservoirs and desorb the absorbed moisture with a decrease in the relative humidity (RH). It is important to compare the moisture

uptake capacity at 60, 90 and 95% RH as described earlier in §III.4. As shown in Table IV.20, all materials showed a rather limited moisture uptake at 60% RH, except for p(chi(1)_PMA(7)) and CaAlg which took up 38% and 67% of their own weight. Interestingly, compared to the synthetic SAPs in Table III.9 (maximal moisture uptake capacity of 46% the weight of the SAP at 95% RH for p($DMAEMA_{100}$)_4), the semi-synthetic SAPs exhibited a superior moisture uptake capacity, even to the point that they outperformed the commercial SAPs (Table III.9, [1]), even at 90% RH (absorbing up to 169% the weight of the SAP). However, at 90% RH, p(alg(1)_AA_{50}/$AMPS_{50}$(7)) and p(alg(1)_AA_0/$AMPS_{100}$(7)) also showed a high moisture uptake capacity exceeding 70% which was only slightly lower than for the commercial SAPs. When increasing the RH from 60 to 90%, the water uptake capacity increased with a factor ranging between 2 and 4. At 95% RH, some of these materials even took up more than their own weight and CaAlg even took up more than twice its weight. P(chi(1)_PMA(7)), on the other hand, had a similar moisture uptake capacity than SAP B and only CaAlg outperformed all SAPs. Interestingly, for all materials, the increase in moisture uptake going from 90 to 95% RH was exactly 1.4. To understand the effect of the polysaccharides, the corresponding synthetic SAPs should be compared with their semi-synthetic counterparts.

Both p(alg(1)_AA_{100}(7))_H and p(alg(1)_AA_{100}(7))_L outperformed p(AA_{100})_0.2 with a factor 1.2 – 1.4 at 90 – 95% RH respectively. P(alg(1)_AA_{75}/AM_{25}(7))_H and p(alg(1)_AA_{75}/AM_{25}(7))_L had a slightly higher moisture uptake (factor 1.1 and 1.3 respectively) than p(AA_{75}/AM_{25})_0.2 both for 90 and 95% RH. Finally, the materials consisting of DMAEMA were also compared. The results showed that all materials with DMAPMA had a higher moisture uptake capacity than their DMAEMA counterparts as the acrylamide-based DMAPMA contains hydrophilic amide moieties, while the acrylate-based DMAEMA contains the slightly less hydrophilic esters [2, 3]. P(alg(1)_EMA(7)) and p(chi(1)_EMA(7)) were performing better than p($DMAEMA_{100}$)_2 and p($DMAEMA_{100}$)_4 (factor 1.4 – 1.5 at RH ≥ 90%). However, p(aga(1)_EMA(3)) only showed 80% of the moisture uptake capacity of both p($DMAEMA_{100}$)_2 and p($DMAEMA_{100}$)_4. This could be related to the lower molar concentration of DMAEMA compared to the other semi-synthetic SAPs and the stronger hydrophilicity of the amides in the synthetic cross-linker compared to the alcohols in modified agarose [4, 5]. Overall it can be concluded that most of the polysaccharide-based SAPs outperformed the synthetic SAPs due to the more hydrophilic carboxylates and protonated amines present in alginate and chitosan respectively compared to the neutral internal amide in N,N'-methylene bisacrylamide (MBA) [6-8]. CaAlg and p(chi(1)_PMA(7)) even outperformed the commercial SAPs which makes them especially interesting.

Table IV.20: Comparative study of the moisture uptake capacity of the semi-synthetic SAPs at 60, 90 and 95% relative humidity (RH).

Moisture uptake capacity [%]	60% RH	90% RH	95% RH
NaAlg	22	46	63
CaAlg	67	169	227
p(alg(1)_AA_{50}/$AMPS_{50}$(7))	22	70	101
p(alg(1)_AA_0/$AMPS_{100}$(7))	21	77	110
p(alg(1)_AA_{100}(7))_H	11	39	54
p(alg(1)_AA_{100}(7))_L	10	35	48
p(alg(1)_AA_{75}/AM_{25}(7))_H	8	25	35
p(alg(1)_AA_{75}/AM_{25}(7))_L	12	29	40
p(alg(1)_EMA(7))	12	45	62
p(alg(1)_PMA(7))	21	63	88
p(aga(1)_EMA(3))	9	25	35
p(aga(1)_PMA(3))	19	47	64
p(chi(1)_EMA(7))	13	47	65
p(chi(1)_PMA(7))	38	93	122
SAP A	26	83	129
SAP B	28	84	120

IV.6.2. Comparative study of the swelling capacity

The swelling potential in demineralized water and cement filtrate solutions of the SAPs tested in §IV.1 and §IV.2 (NaAlg and CaAlg on the one hand and p(alg(1)_AA_x/$AMPS_{100-x}$(7)) on the other hand) was compared. For the SAPs tested in §IV.3 and §IV.4, a pH-responsive study was performed. As indicated in Table IV.21, the swelling capacity of CaAlg was lower than for p(alg(1)_AA_x/$AMPS_{100-x}$(7)) SAPs with the highest swelling being obtained for p(alg(1)_AA_0/$AMPS_{100}$(7)). Interestingly, these swelling ratios were significantly higher compared to all synthetic SAPs at neutral pH, except for p(AA_{50}/AM_{50})_0.2, which has a swelling of 115 g_{water}/g_{SAP}, comparable to p(alg(1)_AA_{50}/$AMPS_{50}$(7)). The superior swelling capacity of p(AA_{50}/AM_{50}) _0.2 could again be related to the presence of cations in demineralized water creating a shielding effect towards the anions present in AA, alginate and AMPS [9-11], which is

not the case for the neutral amides in AM. On the other hand, this effect is limited, as the p(alg(1)_AA_0/$AMPS_{100}$(7)) still showed a superior swelling capacity due to the higher polarity of sulfonic acid compared to the carboxylic acid [12]. The swelling in CF for CaAlg and p(alg(1)_AA_{100}(7))_H was comparable to the synthetic ones (values between 12 and 17 g_{water}/g_{SAP}) due to the presence of carboxylates which were shielded by the presence of divalent cations (Ca^{2+} and Mg^{2+}). However, this shielding effect increased substantially with an increase of the sulfonic acids (AMPS) due to its higher polarity. On the other hand, as NaAlg became insoluble due to the presence of multivalent cations in CF, this polymer started to swell to a similar extent as CaAlg did in demineralized water.

Table IV.21: Comparative study of the swelling capacity of the semi-synthetic SAPs in both demineralized water and cement filtrate solution (CF).

Swelling capacity [g_{water}/g_{SAP}]	Demineralized water	Cement filtrate solution
NaAlg	/	67.0 ± 2.3
CaAlg	72.0 ± 2.5	12.0 ± 2.3
p(alg(1)_AA_{100}(7))_H	81.4 ± 3.3	17.8 ± 2.0
p(alg(1)_AA_{50}/$AMPS_{50}$(7))	122.5 ± 9.3	30.8 ± 2.0
p(alg(1)_AA_0/$AMPS_{100}$(7))	195.2 ± 7.8	34.1 ± 0.9

When comparing the data for the SAPs tested in §IV.3 and §IV.4 in Table IV.22, the first sample series (algMOD combined with AA and AA/AM) showed a maximum swelling capacity at pH 12, similar to their synthetic counterparts (values of 393 g_{water}/g_{SAP} and 434 g_{water}/g_{SAP} obtained for p(AA_{100})_0.2 and p(AA_{75}/AM_{25})_0.2 respectively) with the highest swelling being obtained for those with the lowest DS (371 and 630 g_{water}/g_{SAP} for p(alg(1)_AA_{75}/AM_{25}(7))_L and p(alg(1)_AA_{100}(7))_L respectively). This is evident as a decrease in the DS is related to a decrease in the density of the network. A more open network has a stronger potential to absorb water [13, 14].

P(alg(1)_AA_{100}(7))_L had a superior swelling capacity over p(AA_{100})_0.2, which was up to 7.5 times higher at neutral pH (pH 6 – 10). The denser p(alg(1)_AA_{100}(7))_H had a similar swelling capacity as p(AA_{100})_0.2 at neutral pH. Interestingly, its maximal swelling capacity in aqueous solutions at pH 12 was 4 times lower, which would lead to smaller macro-pores arising during the mixing process in mortar which is anticipated to have an influence on the strength. The swelling in CF was comparable, although for p(alg(1)_AA_{100}(7))_L this was somewhat higher. The latter could again be related to the presence of divalent cations in CF.

P(alg(1)_AA_{75}/AM_{25}(7))_H was compared to p(AA_{75}/AM_{25})_0.2. The swelling capacity of the former was similar at pH 6 and 8, after which a substantial swelling increase occurred at pH 10

and above. This could be related to the Na^+ cations arising from NaOH, which start to interact with alginate thereby creating less possibility for repelling charges and thus decreased swelling. P(alg(1)_AA_{75}/AM_{25}(7))_L, on the other hand, swelled more extensive than p(AA_{75}/AM_{25}) _0.2 at pH 6 – 10. At pH 12, the swelling of the latter was still higher though (shielding effect of carboxylates in alginate). In CF solution, no significant differences could be found between p(alg(1)_AA_{75}/AM_{25}(7))_H, p(alg(1)_AA_{75}/AM_{25}(7))_L and p(AA_{75}/AM_{25})_0.2.

It was proven that p(alg(1)_EMA(7)) and p(alg(1)_PMA(7)) showed a complete opposite pH-responsive trend as targeted, so these will not be taken into account in the further comparative study. The last four materials in Table IV.22 showed a more interesting pH-sensitivity with the higher swelling for the DMAPMA-based SAPs upon decreasing the pH. For a better comparison, p(aga(1)_PMA(7)) was used further, next to p(chi(1)_PMA(7)). When comparing the data of these last four materials from Table IV.22 (based on agarose and chitosan) with p($DMAEMA_{100}$)_2 and p($DMAEMA_{100}$)_4, the former showed an overall higher swelling than p(aga(1)_EMA(3)) and p(aga(1)_PMA(3)), except for p(aga(1)_EMA(7)) at pH 3. This effect was the result of the higher polarity of the amides in MBA compared to the alcohols in agarose.

P($DMAEMA_{100}$)_2 also exhibited a similar swelling capacity as p(chi(1)_EMA(7)) and p(chi(1)_PMA(7)). All semi-synthetic SAPs outperformed p($DMAEMA_{100}$)_4. The swelling in CF for these polymers was also higher than for p($DMAEMA_{100}$)_2 and p($DMAEMA_{100}$)_4 (13 g_{water}/g_{SAP} and 14 g_{water}/g_{SAP} respectively). It could be concluded that only for the materials with a low degree of substitution the swelling was higher than for their synthetic counterparts, while the swelling of all other materials was comparable or (in the case of the materials based on AA and AA/AM in Table IV.22 at pH 12) lower than the synthetic SAPs (p(AA_{75}/AM_{25}) _0.2 reaching a maximal swelling of 434 g_{water}/g_{SAP}).

Comparing the swelling capacity of the semi-synthetic SAPs with the commercially available SAP A and B is not evident as for example a different pH-responsiveness (amine vs. carboxylic acid) leads to a completely different behavior on the mortar strength. When comparing the data obtained with the DVS results, a few trends could be noticed. First, a decrease in the network density did not lead to an increase in the moisture uptake capacity as already described earlier (Table III.3, §III.2.3.), while it did result in an increase of the swelling capacity, as anticipated. On the other hand, due to the more hydrophilic acrylamide-based DMAPMA compared to the slightly less hydrophilic esters of the acrylate-based DMAEMA [2, 3], not only the moisture uptake capacity, but also the swelling capacity was higher for DMAPMA-containing SAPs. The different polarity explains the variations observed for the sulfonic acids versus the carboxylic acids in both DVS and swelling tests. The swelling of CaAlg was far below that of their covalent counterparts, because CaAlg is prone to disintegration in the presence of monovalent cations [15]. Covalent links generally lead to mechanically superior SAPs [16]. The effect of the monovalent cations is obviously ruled out during DVS measurements. CaAlg therefore showed a higher moisture uptake. This higher moisture uptake is also proven as the methacrylation is performed using the alcohol moieties, rendering algMOD somewhat less hydrophilic.

A final comparison can be made with respect to potential hydrolysis of the SAPs in alkaline conditions. This test was especially performed on the last materials based on algMOD with AA and AA/AM and the combination of basic monomers combined with varying polysaccharides (§IV.3. and §IV.4.) after swelling in both aqueous and CF solutions. The results showed that the DMAEMA-based semi-synthetic SAPs showed no clear form of degradation in CF, similar to their synthetic counterparts. For the AA and AA/AM-based SAPs, hydrolysis was observed to a greater extent compared to the synthetic SAPs, due to the stronger alkaline hydrolysis of the esters present as a result of the modification (cfr. methacrylate moieties) compared to the amides of the synthetic cross-linker [17-19].

Table IV.22: Comparative study of the swelling capacity of the semi-synthetic SAPs in both aqueous solutions (with a varying pH) and cement filtrate solution (CF). The underlined values for each SAP are the maximal swelling capacities.

Swelling capacity [g_{water}/g_{SAP}]	pH 2	pH 3	pH 4	pH 6	pH 8	pH 10	pH 12	pH 13	CF
p(alg(1)_AA_{100}(7))_H	20 ± 2	/	46 ± 3	49 ± 1	48 ± 3	52 ± 3	99 ± 5	63 ± 6	12 ± 1
p(alg(1)_AA_{100}(7))_L	21 ± 3	/	/	261 ± 13	/	263 ± 20	630 ± 31	/	18 ± 3
p(alg(1)_AA_{75}/AM_{25}(7))_H	14 ± 2	/	37 ± 5	60 ± 4	62 ± 10	73 ± 19	132 ± 14	56 ± 6	11 ± 1
p(alg(1)_AA_{75}/AM_{25}(7))_L	13 ± 1	/	/	136 ± 10	/	138 ± 18	371 ± 17	/	12 ± 2
p(alg(1)_EMA(7))	/	22 ± 1	/	/	12 ± 1	/	36 ± 1	/	15 ± 0
p(alg(1)_PMA(7))	/	13 ± 2	/	/	11 ± 0	/	47 ± 2	/	13 ± 1
p(aga(1)_EMA(3))	/	111 ± 2	/	31 ± 2	/	24 ± 2	24 ± 1	21 ± 2	21 ± 0
p(aga(1)_PMA(3))	/	59 ± 3	/	35 ± 1	/	32 ± 2	22 ± 1	32 ± 3	24 ± 1
p(chi(1)_EMA(7))	/	47 ± 1	/	49 ± 11	39 ± 3	32 ± 2	21 ± 1	17 ± 1	16 ± 1
p(chi(1)_PMA(7))	/	75 ± 11	/	48 ± 4	36 ± 3	39 ± 4	17 ± 4	18 ± 2	19 ± 1

IV.6.3. Comparison of the bending and compressive strength of SAPs incorporated in mortar

First, it should be mentioned that strength tests were performed in five different batches using an identical procedure. For every batch, a reference was measured as this typically shows different properties depending on e.g. the age of the used cement. For each of the SAPs, the percentage of strength reduction was assessed with respect to the reference of the concerned batch.

The result in Table IV.23 showed that most materials only had a limited effect on the bending strength, except for the materials with a high amount of AMPS (> 50 mol%). Interestingly, when looking at the compressive strength, especially p(alg(1)_AA_{100}(7))_H performed excellent upon addition of even 1 m% with respect to cement mass, followed by p(alg(1)_AA_{100}(7))_L and CaAlg. However, p(alg(1)_AA_{75}/AM_{25}(7))_L, p(alg(1)_AA_{50}/$AMPS_{50}$(7)) and p(alg(1)_AA_0/$AMPS_{100}$(7)) induced a significant impact on the compressive strength. This severe effect could for the AA/AMPS-based SAPs be related to the strong swelling capacity of the sulfonic acid, which led to a high needed amount of additional mixing water and a large macro pore formation.

When comparing with the synthetic SAPs, both p(alg(1)_AA_{100}(7))_H and p(alg(1)_AA_{100}(7))_H showed a smaller decrease in compressive strength than p(AA_{100})_0.2 (decrease of 22% upon addition of 1 m% SAP to mortar). Addition of p(alg(1)_AA_{75}/AM_{25}(7))_H showed a similar effect on the strength compared to p(AA_{75}/AM_{25})_0.2 (19% and 31% reduction for 0.5 and 1 m% SAP addition respectively). However, p(alg(1)_AA_{75}/AM_{25}(7))_L induced a more severe effect on the strength due to its stronger swelling capacity.

No DMAEMA-based semi-synthetic SAPs were selected in further studies. Next, the pH-responsive SAPs based on DMAPMA were compared with synthetic p($DMAEMA_{100}$)_x. P(aga(1)_PMA(3)) had a more severe effect on the compressive strength than both p($DMAEMA_{100}$)_2 and p($DMAEMA_{100}$)_4 (reductions up to 24% for 1 m% addition of p($DMAEMA_{100}$)_2), which is related to the higher amount of additional water required. P(chi(1)_PMA(7)) on the other hand performed similar as p($DMAEMA_{100}$)_2 and slightly worse than p($DMAEMA_{100}$)_4.

Interestingly, all materials outperformed commercial SAP A [1], except for the materials containing a high amount of AMPS (> 50 mol%). CaAlg, p(alg(1)_AA_{100}(7))_H and p(alg(1)_AA_{100}(7))_L performed superior than SAP B (for additions up to 1 m% SAP) while NaAlg, p(alg(1)_AA_{75}/AM_{25}(7))_H, p(aga(1)_PMA(3)) and p(chi(1)_PMA(7)) performed better when 0.5 m% was incorporated. As high amounts up to 1 m% are required for the envisaged application of self-sealing and -healing of cracks, it is particularly interesting to investigate those SAPs that have a low impact on the mortar strength.

Table IV.23: Comparative study of the bending and compressive strength of mortar samples with SAP addition. The colors indicate the percentage reduction: (x < 10%), (10% < x < 20%), (20% < x < 30%) and (x > 30%). The strength reduction with respect to the used reference has been assessed.

Sample	SAP conc. [m%]	Extra water [ml]	Bending strength [MPa]	Compressive Strength [MPa]	Batch
Reference	0.0	0	7.7 ± 0.4 8.6 ± 0.2 7.6 ± 1.1 7.6 ± 0.5 8.4 ± 0.4	65.4 ± 3.2 68.4 ± 1.1 67.3 ± 1.9 73.1 ± 1.6 63.2 ± 1.3	1 2 3 4 5
NaAlg	0.5 1.0	30 65	6.8 ± 0.3 (-12%) 7.2 ± 0.3 (-6%)	58.9 ± 0.4 (-10%) 47.2 ± 1.0 (-28%)	1 1
CaAlg	0.5 1.0	10 15	7.3 ± 0.4 (-5%) 6.6 ± 0.2 (-14%)	65.8 ± 2.0 (/) 55.8 ± 2.3 (-15%)	1 1
p(alg(1)_AA_{50}/$AMPS_{50}$(7))	0.5 1	80 150	6.3 ± 0.4 (-17%) 5.1 ± 0.6 (-33%)	42.1 ± 1.4 (-42%) 26.9 ± 0.2 (-63%)	4 4
p(alg(1)_AA_0/$AMPS_{100}$(7))	0.5	100	5.9 ± 0.3 (-22%)	36.6 ± 0.9 (-50%)	4
p(alg(1)_AA_{100}(7))_H	0.5 1.0	15 30	6.8 ± 0.4 (-11%) 7.6 ± 0.3 (/)	68.9 ± 1.6 (-6%) 68.3 ± 0.6 (-7%)	4 4
p(alg(1)_AA_{100}(7))_L	0.5 1.0	25 60	8.2 ± 0.1 (-2%) 8.0 ± 0.4 (/)	64.2 ± 1.9 (/) 55.0 ± 1.2 (-18%)	5 3
p(alg(1)_AA_{75}/AM_{25}(7))_H	0.5 1.0	25 40	8.3 ± 0.3 (-2%) 7.5 ± 0.3 (-13%)	56.9 ± 1.4 (-17%) 49.3 ± 2.0 (-28%)	2 2
p(alg(1)_AA_{75}/AM_{25}(7))_L	0.5 1.0	33 80	7.1 ± 0.7 (-7%) 5.9 ± 0.5 (-22%)	49.1 ± 0.9 (-27%) 35.8 ± 1.4 (-47%)	3 3
p(aga(1)_PMA(3))	0.5 1.0	40 70	7.3 ± 0.3 (-13%) 7.2 ± 0.1 (-14%)	51.6 ± 1.1 (-18%) 43.6 ± 1.2 (-31%)	5 5
p(chi(1)_PMA(7))	0.5 1.0	30 40	8.1 ± 0.1 (-6%) 7.3 ± 0.4 (-15%)	58.1 ± 1.4 (-15%) 51.8 ± 1.3 (-24%)	2 2

IV.6.4. Self-sealing and self-healing of mortar containing SAPs

It is difficult to compare the data obtained by self-sealing with data described earlier in literature or with commercially available SAPs as different techniques were used to study these properties while the crack width variation among sample series is generally rather high [20, 21]. It can,

however, be concluded that they all had a stronger sealing capacity than the reference as indicated by fully closed cracks up to 80 µm and partially sealed cracks up to 200 µm crack width. The mechanical parameters obtained with respect to self-healing are compared in Table IV.24.

First, the first-cracking strength σ_{fc} was decreased for most SAPs, albeit not significant for all samples except the ones with a high DS (p(alg(1)_AA_{100}(7))_H and p(alg(1)_AA_{75}/AM_{25}(7))_H). This significant decrease could be explained by a combination of two effects. During hardening of the mortar matrix, the SAPs can release mixing water and through internal curing increase the strength. However, addition of a large amount of SAP leads to a strong macro-pore formation which decreases the strength [20, 22]. No significant decrease was found upon addition of the commercial SAPs [20]. Additionally, when investigating the multiple cracking (MC), the value of the reference was higher than what was obtained by Snoeck et al. (i.e. 2%) [20]. The obtained values for any addition of SAP to mortar led to an increase of the MC, albeit not significant. This trend was similar as for the commercial SAPs and could be related to an increase in the ductility of mortar due to the addition of SAPs. The polymers induces flaws which facilitates MC [23].

The most important parameter is the regain in σ_{fc}, which is a value indicating the self-healing potential of the SAP. P(alg(1)_AA_{100}(7))_H showed the strongest self-healing potential of the algMOD-based SAPs with values up to 63% (compared to 40% for the reference). There was no significant difference ($p < 0.05$) observed upon addition of 0.5 m% SAP B and interestingly, no very significant difference ($p < 0.01$) when 1 m% SAP B was added. Noteworthy is that other materials involved in this study (0.5 m% of p(alg(1)_AA_{75}/AM_{25}(7))_H, 1 m% of p(alg(1)_AA_{75}/AM_{25}(7))_H and p(alg(1)_AA_{100}(7))_L) reached a regain in σ_{fc} up to 55%. These values were, however, significantly lower than upon addition of SAP B. They were not significantly different from the samples containing 0.5 m% SAP A. The semi-synthetic SAPs containing basic monomers (p(aga(1)_PMA(3)) and p(chi(1)_PMA(7))) showed strength regains up to 67 and 65% respectively. These values were also not very significantly ($p < 0.01$) different from mortar samples containing 1 m% SAP B and were similar to the values obtained for p(alg(1)_AA_{100}(7))_H, p(alg(1)_AA_{75}/AM_{25}(7))_H and 1 m% p(alg(1)_AA_{100}(7))_L. These values were in the same order of magnitude as what was obtained for tubular capsules with poly(urethane) immobilized bacteria [24, 25]. Despite not having a significantly stronger regain in σ_{fc}, the developed SAPs are more cost-effective compared to commercial SAPs and other self-healing systems, as discussed in the upcoming section.

Table IV.24: Comparative study of the mechanical properties measured to indicate the self-healing capacity of mortars upon addition of SAPs.

Sample	SAP conc. [w%]	σ_{fc} [MPa]	Regain in σ_{fc} [%]	Peak strength σ_p [MPa]	MC [%]
Reference	0.0	6.1 ± 0.9	40.2 ± 7.9	9.6 ± 1.3	3.1 ± 0.9
p(alg(1)_AA_{100}(7))_H	0.5	5.4 ± 0.9	62.7 ± 4.3	7.5 ± 0.8	2.3 ± 0.1
	1.0	4.7 ± 0.6	59.0 ± 6.7	6.3 ± 0.5	3.1 ± 0.0
p(alg(1)_AA_{100}(7))_L	0.5	5.2 ± 0.6	53.9 ± 8.6	6.9 ± 0.9	3.4 ± 0.2
	0.7	6.3 ± 1.0	46.4 ± 4.4	9.0 ± 1.7	3.1 ± 0.6
	1.0	4.9 ± 0.4	55.7 ± 6.6	7.3 ± 0.6	3.8 ± 0.4
	1.3	5.7 ± 0.3	49.2 ± 7.2	9.2 ± 1.8	4.1. ± 1.6
p(alg(1)_AA_{75}/AM_{25}(7))_H	0.5	5.1 ± 0.4	57.2 ± 4.2	7.5 ± 1.2	3.6 ± 0.8
	1.0	4.7 ± 0.7	57.0 ± 6.8	7.8 ± 2.9	3.3 ± 1.7
p(alg(1)_AA_{75}/AM_{25}(7))_L	0.5	5.6 ± 0.8	53.4 ± 10.9	10.8 ± 0.9	4.2 ± 0.7
	1.0	6.7 ± 1.3	38.2 ± 4.2	9.2 ± 0.8	2.8 ± 0.4
p(aga(1)_PMA(3))	0.7	5.0 ± 0.6	50.8 ± 4.3	8.1 ± 1.4	3.1 ± 1.3
	1.3	4.4 ± 0.5	66.9 ± 5.8	7.8 ± 0.2	4.4 ± 2.1
p(chi(1)_PMA(7))	0.5	4.4 ± 0.4	64.5 ± 8.7	8.8 ± 3.1	4.5 ± 2.7
	1.0	4.8 ± 0.6	56.7 ± 7.8	7.6 ± 1.9	3.3. ± 1.6
SAP A	0.5	4.9 ± 1.5	64.5 ± 1.9	/	3.5 ± 0.4
SAP B	0.5	5.1 ± 1.1	68.6 ± 3.0	/	3.5 ± 0.3
	1	4.9 ± 0.9	86.2 ± 8.3	/	3.8 ± 0.4

IV.6.5. Evaluation of the valorization opportunities of semi-synthetic SAPs

As mentioned in §III.4., the additional cost associated with the incorporation of SAP in concrete is an important factor for industry and application feasibility. The estimation was executed by taking into account the bulk manufacturer prices for the polysaccharides, the monomers and the required amount of methacrylic anhydride. As indicated in Table IV.25, except for a few, almost all materials showed a price between € 5 and € 10 / m³ concrete (3 kg SAP / m³ concrete). NaAlg was more expensive than CaAlg as the $CaCl_2$ solution is cheaper in the latter case and thus led after mixing to a decrease in the general price. It can be commented that Ca^{2+}-ions are also present in mortar, however, $CaCl_2$ is necessary to have a more controlled CaAlg network. Despite their good overall performance, p(aga(1)_PMA(3)) and p(chi(1)_PMA(7)) were very expensive. The reason could be found in the high bulk prices of chitosan and agarose. If it would be possible to decrease this price, they would become very interesting materials.

Table IV.25: Estimated cost calculations of SAPs per kg and per m³ of concrete.

Sample	Price €/kg	Price €/m³ concrete
NaAlg	6.3	18.8
CaAlg	3.0	9.1
p(alg(1)_AA_{50}/$AMPS_{50}$(7))	2.4	7.3
p(alg(1)_AA_{0}/$AMPS_{100}$(7))	2.6	7.8
p(alg(1)_AA_{100}(7))_H	2.0	5.9
p(alg(1)_AA_{100}(7))_L	1.9	5.6
p(alg(1)_AA_{75}/AM_{25}(7))_H	2.0	6.1
p(alg(1)_AA_{75}/AM_{25}(7))_L	2.0	5.9
p(aga(1)_PMA(3))	60.5	181.5
p(chi(1)_PMA(7))	45.4	136.2
SAP B	3	9

When taking into account a profit and production margin of respectively 20% and 50% of the bulk price (cfr. see also §III.4.5), the prices of the SAPs (upon excluding the 3 most expensive ones) would range between € 9.5 and 15.5 / m³ concrete. The prices of p(alg(1)_AA_{100}(7))_H, p(alg(1)_AA_{100}(7))_L, p(alg(1)_AA_{75}/AM_{25}(7))_H and p(alg(1)_AA_{75}/AM_{25}(7))_L are similar as those of commercial SAP B. The others were up to 1.5 times more expensive. The use of NaAlg would correspond with € 32 / m³ concrete and the DMAPMA-based SAPs were even going up to € 309 and € 232 / m³ concrete. When comparing the prices to other self-healing systems (as described in §III.4.5.), the prices of the two most expensive SAPs are close to the costs applicable for using microcapsules [26]. The prices of the other synthesized SAPs are in the same range as the commercial SAPs while normal concrete has a price of approximately € 65 /m³ concrete. This means that the price would go up with 15 – 24 %. This is an acceptable surplus as manual injection of one crack per m³ concrete in a tunnel would cost € 120 – 140 /m³, which is far more expensive than using the self-healing alternatives [20].

IV.6.6. Conclusions

Despite having a limited moisture uptake capacity, p(alg(1)_AA_{100}(7))_H exhibited a strong swelling capacity, a very limited effect on the compressive strength of mortar and a strong self-sealing and -healing capacity, comparable to other self-healing systems such as tubular capsules with poly(urethane) immobilized bacteria and not very significantly different from tested commercial SAPs. The price of p(alg(1)_AA_{100}(7))_H was also similar to commercial SAPs, making it a strategy able to compete with commercial SAPs, as these show a more severe effect on the compressive strength. The SAPs with a fraction of AMPS (> 50%) had a large swelling capacity

and moisture uptake capacity. However, they showed a very severe effect on the mortar strength, making them unsuitable to be used. When comparing NaAlg and CaAlg, especially CaAlg showed a very strong moisture uptake capacity and a very limited mortar strength decrease. However, they had a limited swelling degree in demineralized water compared to some of the other covalently cross-linked semi-synthetic SAPs and were not tested for their self-healing potential. P(alg(1)_AA_{100}(7))_L had despite its limited moisture uptake capacity the strongest swelling potential. Nonetheless, it induced only a small effect on the compressive mortar strength and led to strong healing capacities. Its price was again similar to commercial SAPs, making it another very promising material in addition to p(alg(1)_AA_{100}(7))_H. P(alg(1)_AA_{75}/AM_{25}(7))_H and p(alg(1)_AA_{75}/AM_{25}(7))_L exhibited a low moisture uptake capacity, but the low DS type showed a strong swelling capacity. This, however, was also associated with a severe decrease in the mortar strength, which was more acceptable for the high DS. Next to having a low price, similar as p(alg(1)_AA_{100}(7)), p(alg(1)_AA_{75}/AM_{25}(7))_H resulted in a strong regain in σ_{fc}, albeit significantly lower than SAP B. As it showed a comparable effect on the mortar strength, it cannot yet compete with the commercial SAPs. The possible degradation occurring for the above-mentioned SAPs was comparable to their synthetic counterparts for which MBA was used as a cross-linker and was less in CF solutions than in alkaline aqueous solutions due to a shielding effect caused by the divalent cations. Finally, the pH-responsive SAPs with DMAPMA had stronger moisture uptake capacities going up to 122% their original weight which is comparable to the commercial SAPs. Despite their pH-responsiveness, they showed a limited swelling capacity at neutral pH and more strongly at pH 3, which makes them more interesting towards the ingress of acid rain. However, they induced a slightly more severe effect on the mortar strength than SAP B, but had a self-healing capacity going up to 67% and 65% for p(aga(1)_PMA(3)) and p(chi(1)_PMA(7)) respectively, which comes close to the strength regain of SAP B. Unfortunately, due to the high bulk prices of agarose and chitosan, these SAPs are too expensive and could only be useful if those bulk prices can decrease significantly.

Finally, the materials performing superior and able to compete with commercial SAPs were p(alg(1)_AA_{100}(7))_H and p(alg(1)_AA_{100}(7))_L, closely followed by p(alg(1)_AA_{75}/AM_{25}(7))_H. It would, however, in future work be interesting to revisit and optimize the synthetic SAPs based on DMAEMA, as they showed only a slightly lower swelling capacity than the semi-synthetic DMAPMA SAPs and induced less effect on the mortar strength. As p(chi(1)_PMA(7)) showed very promising self-healing potential, synthetic SAPs with DMAEMA (or even with DMAPMA) could perhaps reach the same regain with a price which is more comparable to commercial SAPs.

IV.6.7. References

[1] Snoeck D, Dubruel P, De Belie N. How to seal and heal cracks in cementitious materials by using superabsorbent polymers. Application of Superabsorbent Polymers and Other New Admixtures in Concrete Construction: RILEM Publications; 2014. p. 375-84.
[2] Campbell D, Tighe BJ. Zwitterionic and Charge-Balanced Polyampholyte Copolymer Hydrogels. Advanced Materials Research: Trans Tech Publ; 2008. p. 729-32.
[3] Barlow RB, Bremner JB, Soh KS. The effects of replacing ester by amide on the biological properties of compounds related to acetylcholine. British journal of pharmacology. 1978;62(1):39-50.
[4] Jahanshahi M, Rahimpour A, Peyravi M. Developing thin film composite poly (piperazine-amide) and poly (vinyl-alcohol) nanofiltration membranes. Desalination. 2010;257(1):129-36.
[5] Masuyama A, Shindoh A, Ono D, Okahara M. Preparation and surface active properties of terminal amide type of alcohol ethoxylates. Journal of the American Oil Chemists Society. 1989;66(6):834-7.
[6] Konkolewicz D, Poon CK, Gray-Weale A, Perrier S. Hyperbranched alternating block copolymers using thiol–yne chemistry: materials with tuneable properties. Chemical Communications. 2011;47(1):239-41.
[7] Remko M, Scheiner S. Ab initio investigation of interactions between models of local anesthetics and receptor: Complexes involving amine, phosphate, amide, Na+, K+, Ca2+, and Cl–. Journal of pharmaceutical sciences. 1988;77(4):304-8.
[8] Remko M, Scheiner S. Ab initio investigation of interactions between models of membrane-active compounds and polar groups of membranes: Complexes involving amine, ether, amide, phosphate, and carboxylate. Journal of pharmaceutical sciences. 1991;80(4):328-32.
[9] Snoeck D, Schaubroeck D, Dubruel P, De Belie N. Effect of high amounts of superabsorbent polymers and additional water on the workability, microstructure and strength of mortars with a water-to-cement ratio of 0.50. Construction and Building Materials. 2014;72(0):148-57.
[10] Hancock RD, Martell AE. Ligand design for selective complexation of metal ions in aqueous solution. Chemical Reviews. 1989;89(8):1875-914.
[11] Li A, Wang A, Chen J. Studies on poly (acrylic acid)/attapulgite superabsorbent composites. II. Swelling behaviors of superabsorbent composites in saline solutions and hydrophilic solvent–water mixtures. Journal of Applied Polymer Science. 2004;94(5):1869-76.
[12] Pretsch E, Bühlmann P, Affolter C, Pretsch E, Bhuhlmann P, Affolter C. Structure determination of organic compounds: Springer; 2009.
[13] Lee KY, Rowley JA, Eiselt P, Moy EM, Bouhadir KH, Mooney DJ. Controlling mechanical and swelling properties of alginate hydrogels independently by cross-linker type and cross-linking density. Macromolecules. 2000;33(11):4291-4.
[14] Okay O, Durmaz S, Erman B. Solution cross-linked poly (isobutylene) gels: synthesis and swelling behavior. Macromolecules. 2000;33(13):4822-7.
[15] Bajpai SK, Sharma S. Investigation of swelling/degradation behaviour of alginate beads crosslinked with Ca2+ and Ba2+ ions. Reactive and Functional Polymers. 2004;59(2):129-40.
[16] Povh B, Rosina M. Scattering and structures: essentials and analogies in quantum physics: Springer Science & Business Media; 2005.
[17] Patricelli MP, Cravatt BF. Fatty Acid Amide Hydrolase Competitively Degrades Bioactive Amides and Esters through a Nonconventional Catalytic Mechanism. Biochemistry. 1999;38(43):14125-30.
[18] Fife TH, Squillacote VL. Metal ion effects on intramolecular nucleophilic carboxyl group participation in amide and ester hydrolysis. Hydrolysis of N-(8-quinolyl)phthalamic acid and 8-quinolyl hydrogen glutarate. Journal of the American Chemical Society. 1978;100(15):4787-93.
[19] Robinson BA, Tester JW. Kinetics of alkaline hydrolysis of organic esters and amides in neutrally-buffered solution. International Journal of Chemical Kinetics. 1990;22(5):431-48.

[20] Snoeck D. Self-healing and microstructure of cementitious materials with microfibres and superabsorbent polymers. PhD thesis: Ghent University; 2015.
[21] Snoeck D, Van Tittelboom K, Steuperaert S, Dubruel P, De Belie N. Self-healing cementitious materials by the combination of microfibres and superabsorbent polymers. Journal of Intelligent Material Systems and Structures. 2014;25(1):13-24.
[22] Hasholt MT, Jensen OM, Kovler K, Zhutovsky S. Can superabsorbent polymers mitigate autogenous shrinkage of internally cured concrete without compromising the strength? Construction and Building Materials. 2012;31:226-30.
[23] Mechtcherine V, Reinhardt H-W. Application of super absorbent polymers (SAP) in concrete construction: state-of-the-art report prepared by Technical Committee 225-SAP: Springer Science & Business Media; 2012.
[24] Wang J, Van Tittelboom K, De Belie N, Verstraete W. Use of silica gel or polyurethane immobilized bacteria for self-healing concrete. Construction and Building Materials. 2012;26(1):532-40.
[25] Van Tittelboom K, De Belie N, Van Loo D, Jacobs P. Self-healing efficiency of cementitious materials containing tubular capsules filled with healing agent. Cement and Concrete Composites. 2011;33(4):497-505.
[26] Wang J. Self-healing concrete by means of immobilized carbonate precipitating bacteria. PhD thesis: Ghent University; 2013.

V. General conclusions and future perspectives

The general objective of this PhD was to synthesize a superabsorbent polymer (SAP) able to be used for self-sealing and -healing cracks in mortar and concrete. These SAPs should exhibit a strong moisture and water uptake capacity to completely block the cracks and should not degrade upon incubation in mortar. Additionally, they should only induce a negligible decrease in bending and compressive mortar strength and should induce a strong sealing capacity and strength regain after crack formation. In addition, they should be cost-effective to increase their valorization opportunity. A lot of aspects thus need to be covered in order to obtain the most performing solution. It was therefore important to investigate a whole range of different types of SAPs to explore for each their strengths and weaknesses.

The performed work has been subdivided into two parts, with the first dealing with fully synthetic SAPs and the second part introducing polysaccharides to create semi-synthetic SAPs. The terminology used to abbreviate all samples has been highlighted throughout the manuscript and overviewed in the general table.

First, SAPs containing N,N'-methylene bisacrylamide (MBA) as synthetic cross-linker were studied. The SAP based on acrylic acid (AA) (i.e. p(AA_{100})_0.2) showed a high swelling capacity, although this was obtained at a pH of 12 which is undesired. It was also prone to hydrolysis at alkaline conditions and had a limited moisture uptake capacity rendering the SAP inappropriate. Introducing acrylamide (AM) as a second monomer resulted in SAPs (p(AA_{50}/AM_{50})_0.2 and p(AA_{75}/AM_{25})_0.2) with a superior swelling capacity in demineralized water compared to the other synthetic SAPs (up to 456 g_{water}/g_{SAP}). This, however, was associated with a significant decrease in the compressive strength of mortar, especially for p(AA_{50}/AM_{50})_0.2. Interestingly, they showed a strong form of hydrolysis in alkaline aqueous solutions, which they did not exhibit in cement filtrate (CF). Due to an internal shielding effect by the presence of dissolved cations in the solution, a pH-delayed hydrolysis was observed. When incorporated in mortar, the SAPs were tested for their sealing potential by water permeability tests and the results showed that upon incorporation of 1 m% with respect to the cement mass, they showed a strong self-sealing capacity with permeability factors close to uncracked samples. Finally, a pH-sensitive methacrylate was incorporated (p($DMAEMA_{100}$)_2 and p($DMAEMA_{100}$)_4) with a varying ratio of MBA. As anticipated, a lower cross-linking density led to a stronger swelling capacity. Both SAPs did not show any form of hydrolysis and induced a similar, yet limited, decrease in compressive strength. Due to its greater swelling and lower cost, p($DMAEMA_{100}$)_2 was more promising compared to p($DMAEMA_{100}$)_4. Unfortunately, the moisture uptake capacity of all synthetic SAPs was limited, more specifically below 50% of the weight of the dry SAP, which is inferior to commercially available SAPs. P(AA_{100})_0.2, p(AA_{50}/AM_{50})_0.2 and p(AA_{75}/AM_{25})_0.2 showed superior swelling capacities, albeit at pH 12, the point at which they were already prone to partial hydrolysis. The estimated cost for all synthetic SAPs was lower than for any other self-healing system while p(AA_{50}/AM_{50})_0.2 and p(AA_{75}/AM_{25})_0.2 were even less expensive than the commercial SAPs.

To improve the obtained properties, polysaccharides including alginate, were introduced in a second part of the current PhD research. These bio-based polymers show great swelling capacities, rendering them interesting to become introduced in the SAPs. The ionic network of CaAlg led to moisture uptake capacities more than twice the original weight of the SAP at a

relative humidity of 95% and a negligible mortar strength reduction. However, it exhibited a limited swelling capacity in demineralized water and was therefore not tested further. In a next step, alginate was modified using methacrylic anhydride to incorporate methacrylate moieties which can react with other monomers to create covalently cross-linked networks. By comparing the effect of incorporating carboxylic acid versus sulfonic acid monomers, it was noticed that the addition of sulfonic acid amounts exceeding 50% resulted in a strong moisture and water uptake capacity, but also in a severe decrease of the mortar strength, rendering them unsuitable for the intended application. P(alg(1)_AA_{100}(7))_H, on the other hand, exhibited an acceptable swelling capacity of 80 g_{water}/g_{SAP}, a limited degree of hydrolysis and a negligible effect on the compressive strength, even upon addition of 1 m% with respect to the cement mass. This specific SAP was further studied and compared with a network consisting of AA and AM which was characterized by a different cross-linking density by decreasing the degree of substitution (DS). P(alg(1)_AA_{100}(7))_L exhibited an extremely great swelling up to 630 g_{water}/g_{SAP}, while it only induced a limited effect on the mortar strength. A four-point-bending test showed that p(alg(1)_AA_{100}(7))_H and p(alg(1)_AA_{100}(7))_L both resulted in a strong sealing capacity of cracks up to 50 µm completely and up to 200 µm partially in addition to strength regains up to 63% (versus a reference strength regain of 40%). The latter are comparable values as obtained for alternative self-healing systems such as tubular capsules with poly(urethane) immobilized bacteria albeit more cost-effective with prices ranging around € 6 / m³ concrete. In addition, no significant difference was found with the best performing commercial SAPs.

P(alg(1)_AA_{75}/AM_{25}(7))_H exhibited a low moisture uptake capacity and a limited swelling capacity compared to p(alg(1)_AA_{75}/AM_{25}(7))_L, but resulted in a less severe decrease in strength. Both materials also showed comparable hydrolysis as their synthetic counterparts with a limited degradation in CF due to the shielding effect of the cations present. Their cost was also acceptably low (€ 6 / m³ concrete) and they showed a strong self-healing capacity with a regain in strength up to 57%. Finally, pH-responsive, basic monomers were combined with different polysaccharides and the results showed that SAPs with dimethylaminopropyl methacrylamide (DMAPMA) exhibited a strong moisture uptake capacity (up to 122%) comparable to values obtained for commercial SAPs. Due to their pH-sensitivity, they especially showed more extensive swelling at low pH, rendering them more promising in case of ingress of acid rain. Interestingly, they did not show a significant degree of hydrolysis in CF and resulted in high strength regain of cracks up to 67% for p(aga(1)_PMA(3)) and 65% for p(chi(1)_PMA(7)). However, the bulk prices of agarose and chitosan are high, which renders these SAPs quite expensive for practical use. In a final part, different sulfated polymers were synthesized. A sulfation technique presented in literature was used to sulfate methacrylated alginate. This led to a strong decrease in the degree of substitution and no cross-linking of the sulfated polymers was possible. Interestingly, it did show an increased moisture uptake capacity compared to non-sulfated algMOD. A sulfate-containing polysaccharide, κ-carrageenan was also methacrylated and cross-linked by photo-polymerization. Unfortunately, it was completely hydrolyzed in CF, rendering it impossible to be used for the targeted application. It can thus finally be concluded that especially p(alg(1)_AA_{100}(7))_H and p(alg(1)_AA_{100}(7))_L perform best. They show a self-healing capacity comparable to commercially used SAPs and interestingly induce only a very

limited compressive mortar strength reduction, making them better than the commercial SAPs, while p(alg(1)_AA_{75}/AM_{25}(7))_H also is a very promising material (strength regains up to 57%).

Future work can be performed to further improve a few aspects. For example, the use of a different synthetic cross-linker to further reduce the hydrolysis behavior at the extreme alkaline conditions of CF solutions could be explored. It could also be interesting to revisit and optimize the synthetic SAPs based on DMAEMA, as they only showed a slightly lower swelling capacity than the semi-synthetic DMAPMA SAPs and induced a reduced effect on the mortar strength. Moreover, synthetic SAPs containing DMAPMA instead of DMAEMA could be explored. In addition, if the bulk price for agarose and chitosan can be reduced, p(chi(1)_PMA(7)) and p(aga(1)_PMA(7)) could become extremely promising SAPs. Another aspect could be to increase the swelling capacity of the pH-sensitive synthetic SAPs by decreasing their cross-link density. What is more, the strategy to create sulfated algMOD should be modified by first sulfating alginate, followed by methacrylation instead of the other way around. The potential of carMOD can also be explored in other application fields. Finally, the most promising materials such as p(alg(1)_AA_{100}(7))_H, p(alg(1)_AA_{100}(7))_L and p(alg(1)_AA_{75}/AM_{25}(7))_H should be developed in high bulk quantities followed by large scale tests.

S. Supplementary info

Table S.1 : ATR-IR spectroscopy results obtained for dried SAPs after incubation of p(alg(1)_AA_{100}(7))_L in different solutions.

Frequency [cm^{-1}]	Assignment	Reference	pH 10	pH 12	CF (pH 12.6)	CF pH 13.0
1170	ν_{as}(C-O) ester	s	s	w	w	w
1220	ν_{s}(C-O) ester	s	s	sh	/	/
1410	ν_{s}(C-O) carboxylate	w	w	s	s	s
1550	ν_{as}(C-O) carboxylate	sh	sh	vs	vs	vs
1700	ν(C=O) ester	vs	vs	m,sh	/	/

w: weak, m: medium, s: strong, vs: very strong, sh: shoulder, shp: sharp, br: broad

Table S.2: ATR-IR spectroscopy results obtained for dried SAPs after incubation of p(alg(1)_AA_{75}/AM_{25}(7))_L in different solutions.

Frequency [cm^{-1}]	Assignment	Reference	pH 10	pH 12	CF (pH 12.5)	CF pH 13.0
794	γ(N-H) amide (1°/2°)*	m, br	m, br	sh	/	/
1170	ν_{as}(C-O) ester	s	s	w	w	w
1220	ν_{s}(C-O) ester	s	s	sh	/	/
1410	ν_{s}(C-O) carboxylate	w	w	s	vs	vs
1550	ν_{as}(C-O) carboxylate	sh	sh	vs	vs	vs
1675	ν(C=O) amide	vs	vs	s	m	m
1700	ν(C=O) ester	vs	vs	/	/	/

w: weak, m: medium, s: strong, vs: very strong, sh: shoulder, shp: sharp, br: broad
* 1° and 2° represent primary and secondary amide respectively

Tabel S.3: Characteristic absorption signals in the ATR-IR spectra of methacrylated alginate, agarose and chitosan as well as the monomers DMAEMA and DMAPMA.

Wavenumber (cm^{-1}) AlgMOD	Vibration	Width	Functionality
1150	ν_{as}(C-O)	Sharp	Ester
1620	ν(C=O)	Broad	Carboxylate
1720	ν(C=O)	Sharp	Ester
2400-3400	ν(O-H)	Broad	Alcohol/carboxylic acid
AgaMOD			
1150	ν_{as}(C-O)	Sharp	Ester
1720	ν(C=O)	Sharp	Ester
2400-3400	ν(O-H)	Broad	Alcohol/carboxylic acid
ChiMOD			
1150	ν_{as}(C-O)	Sharp	Ester
1720	ν(C=O)	Sharp	Ester
2400-3400	ν(O-H)	Broad	Alcohol/carboxylic acid
3100-3500	ν(N-H)	Broad	Amide
DMAEMA			
1145	ν_{s}(C-O)	Sharp	Ester
1175	ν_{as}(C-O)	Sharp	Ester
1720	ν(C=O)	Sharp	Ester
2775	ν(N-C)	Sharp	Tertiary amine
2825	ν(N-C)	Sharp	Tertiary amine
2945	ν_{as}(C-H)	Broad	Alkane
DMAPMA			
1520	δ(N-H)	Sharp	Secondary amide
1645	ν(C=O)	Sharp	Secondary amide
2775	ν(N-C)	Sharp	Tertiary amine

2825	ν(N-C)	Sharp	Tertiary amine
2945	ν_{as}(C-H)	Broad	Alkane
3100-3500	ν(N-H)	Broad	Secondary amide

Curriculum vitae

Personal information

Name	Arn Mignon
Date of birth	August 5th 1989
Nationality	Belgium
Address	Zavelstraat 112, 9500 Geraardsbergen
E-mail	Arn.Mignon@UGent.be

Education

2012-2016 Doctor in de Ingenieurswetenschappen, University Ghent
Effect of pH-responsive superabsorbent polymers for self-sealing and -healing of cracks in mortar and concrete

2010-2012 Master in de Ingenieurswetenschappen: Chemische Technologie, University Ghent
Thesis: *Development and computational modelling study of polymer-coated stents*

2007-2010 Bachelor in de Ingenieurswetenschappen: Chemische Technologie, University Ghent

Experience

2013-2016 Seminars + practical courses Organic Chemistry

2012 Student job 2012: ERGO Insurance
Responsible classification system

2008-2011 Federal Office 'Wetenschapsbeleid'
Responsible classification files Airbus 380
Electronical processing research data Science Connection

2005-2007 Postal service Colruyt Halle

+ *Increasing teaching skills*
Learning to work as employee
Expand social skills
Maintain the French language

Extracurricular activities

Course *Effective Scientific Communication*
Course *Project Management*
Winter School Advanced Materials for Biomedical Applications (AMBA)
Summer school Concrete Microscopy Course (TU delft)
Course *Gevorderderde polymeerchemie (Advanced Polymer Chemistry)*
Course *Betontechnologie (Concrete Technology)*

Prizes

Best oral presentation (soft matter) on ICSHM conference 2015: “Smart superabsorbent polymers for self-sealing and -healing of mortar”
Poster award FEA Research symposium 2015
Poster award CMaC meeting
https://www.linkedin.com/profile/view?id=153790112
https://www.researchgate.net/profile/Arn_Mignon

Software/Equipment knowledge

Knowledge of Abaqus , Fluent, Gambit (Course “Computational Fluid Dynamics”), Aspen, Maple
Knowledge to work with Infra-Red, Dynamic Vapour Sorption, Static Contact Angle, Scanning Electron Microscopy, High-Resolution Magic Angle Spinning Nuclear Magnetic Resonance, Rheology, Thermogravimetric Analysis, Differential Scanning Calorimetry and Gel Permeation Chromatography

Articles

A1 (articles viewable in one of the ISI Web of Science databases: 'Science Citation Index', 'Social Science Citation Index' or 'Arts and Humanities Citation Index'):

A. Mignon, D. Devisscher, G.-J. Graulus, B. Stubbe, J. Martins, P. Dubruel, N. De Belie and S. Van Vlierberghe, Combinatory approach of methacrylated alginate and acid monomers for concrete applications, Carbohydrate polymers, 155 (2017), 448-455
A. Mignon, D. Snoeck, K. D’Halluin, Lieve Balcaen, Frank Vanhaecke, S. Van Vlierberghe, P. Dubruel, N. De Belie, Alginate biopolymers: Counteracting the impact of superabsorbent polymers on mortar strength, Construction and Building Materials, 110 (2016) 169-174.
A. Mignon, D. Snoeck, D. Schaubroeck, N. Luickx, P. Dubruel, S. Van Vlierberghe, N. De Belie, pH-responsive superabsorbent polymers: a pathway to self-healing of mortar, Reactive and Functional Polymers, 93 (2015) 68-76.
A. Mignon, G.-J. Graulus, D. Snoeck, J. Martins, P. Dubruel, N. De Belie, S. Van Vlierberghe, pH-sensitive superabsorbent polymers: a potential candidate material for self-healing concrete, J Mater Sci, 50 (2014) 970-979.
J. Wang, A. Mignon, D. Snoeck, V. Wiktor, N. Boon, N. De Belie, Application of modified-alginate encapsulated carbonate producing bacteria in concrete: a promising strategy for crack self-healing, Frontiers in Microbiology, 6 (2015) 1088.
G.-J. Graulus, A. Mignon, S. Van Vlierberghe, H. Declercq, K. Fehér, M. Cornelissen, J.C. Martins, P. Dubruel, Cross-linkable alginate-graft-gelatin copolymers for Tissue Engineering Applications, European Polymer Journal, 72 (2015) 494-506.
J. Lewandowska-Łańcucka, K. Mystek, A. Mignon, S. Van Vlierberghe, A. Łatkiewicz, M. Nowakowska, Alginate- and gelatin-based bioactive photocross-linkable hybrid materials for bone tissue engineering, Carbohydrate Polymers, in press (2016).
http://dx.doi.org/10.1016/j.carbpol.2016.11.051
L. F. Velasco, D. Snoeck, A. Mignon, L. Misseeuw, C. O. Ania, S. Van Vlierberghe, P. Dubruel, N. De Belie, P. Lodewyckx, Role of the surface chemistry of the adsorbent on the initialization step of the water sorption process, Carbon, 106(2016) 284-288

D. Snoeck, L.F. Velasco, A. Mignon, S. Van Vlierberghe, P. Dubruel, P. Lodewyckx, N. De Belie, The effects of superabsorbent polymers on the microstructure of cementitious materials studied by means of sorption experiments, Cement and Concrete Research, 77 (2015) 26-35.
D. Snoeck, L.F. Velasco, A. Mignon, S. Van Vlierberghe, P. Dubruel, P. Lodewyckx, N. De Belie, The influence of different drying techniques on the water sorption properties of cement-based materials, Cement and Concrete Research, 64 (2014) 54-62.

A1 submitted:

A. Mignon, M. Vagenende, J. Martins, P. Dubruel, S. Van Vlierberghe and N. De Belie, Development of amine-based pH-responsive superabsorbent polymers for mortar applications, Construction and Building Materials, **revised manuscript under review**
A. Mignon, D. Snoeck, P. Dubruel, S. Van Vlierberghe, N. De Belie, Crack mitigation in concrete: review of superabsorbent polymers as key to success, Cement and Concrete Research, **under review**
A. Mignon, D. Devisscher, J. Vermeulen, M. Vagenende, J. martins, P. Dubruel, N. De Belie and S. Van Vlierberghe, Characterization of methacrylated polysaccharides in combination with amine-based monomers for application in mortar, Carbohydrate polymers, **under review**
A. Mignon, J. Vermeulen, G.-J. Graulus, J. Martins, P. Dubruel, N. De Belie and S. Van Vlierberghe, Characterization of methacrylated alginate and acrylic monomers for self-healing applications in mortar, Carbohydrate polymers, **under review**
N. Alderete, Y. Villagrán Zaccardi, A. Mignon, D. Snoeck, N. De Belie, Pore structure description of mortars containing ground granulated blast-furnace slag by mercury intrusion porosimetry and dynamic vapour sorption, Construction and Building Materials, **revised manuscript under review**

C1 (articles published in proceedings of scientific conferences):

A. Mignon, D. Devisscher, J. Vermeulen, P. Dubruel, S. Van Vlierberghe, N. De Belie, Bio-based pH-responsive superabsorbent polymers for self-healing cracks in concrete, International RILEM Conference on Materials, Systems and Structures in Civil Engineering; Conference segment on Service Life of Cement-Based Materials and Structures, August 22-24 2016, Lyngby, Denmark (2016)
A. Mignon, D. Snoeck, L. Balcaen, F. Vanhaecke, P. Dubruel , S. Van Vlierberghe, N. De Belie, Biopolymers for self-sealing and -healing of mortar, IMRC conference: XXIV international materials research congress, August 16-20, 2015, Cancún, México (2015)
A. Mignon, D. Snoeck, L. Velasco, P. Lodewyckx, P. Dubruel, S. Van Vlierberghe, N. De Belie, Smart superabsorbent polymers for self-sealing and -healing of mortar, ICSHM conference, June 21-24, 2015, Durham, North Carolina (2015)
A. Mignon, D. Snoeck, S. Van Vlierberghe, P. Dubruel, N. De Belie, Comparing pH-sensitive with commercial superabsorbent polymers in cementitious material, Application of Superabsorbent Polymers and Other New Admixtures in Concrete Construction, RILEM Proceedings (2014)
D. Snoeck, L.F. Velasco, A. Mignon, S. Van Vlierberghe, P. Dubruel, P. Lodewyckx, N. De Belie, Effect of the drying technique on the sorption properties in cementitious materials Water transport in cementitious materials : TRANSCEND conference, November 3-6, 2013, Guilford, UK (2013)

C3 (conference abstracts):

G.-J. Graulus, A. Mignon, S. Van Vlierberghe and P. Dubruel, Alginate-graft-gelatin copolymers for tissue engineering applications, IMRC 2015 : XXIV international materials research congress, August 16 – 20, 2015, Cancún, Mexico (2015)
A. Mignon, G.-J. Graulus, J. Martins, P. Dubruel, S. Van Vlierberghe, N. De Belie, Utility of pH-sensitive superabsorbent polymers in concrete repair, ChemCYS book of abstracts (2014)
A. Mignon, J. Wang, K. D'Halluin, D. Snoeck, S. Van Vlierberghe, P. Dubruel, N. De Belie, Photo-Induced Polymerization of Bacteria-Encapsulated Superabsorbent Polymers, NB-Photonics annual meeting, Gent, Belgium (2014)
A. Mignon, D. Snoeck, S. Van Vlierberghe, P. Dubruel, N. De Belie, Application of pH sensitive hydrogels for concrete applications, Water transport in cementitious materials : TRANSCEND conference, November 3-6, 2013, Guilford, UK (2013)
L.F. Velasco, D. Snoeck, A. Mignon, S. Van Vlierberghe, P. Dubruel, N. De Belie and P. Lodewyckx, Influence of the surface oxygen content of the material on the specific interactions taking place at the first stages of water sorption Carbon Materials for Ubiquitous and Sustainable Life., Jeju, June 29 - July 4, 2014, 2 p POT7-23 (2014)
L.F. Velasco, D. Snoeck, A. Mignon, S. Van Vlierberghe, P. Dubruel, N. De Belie and P. Lodewyckx, Correlating the water adsorption mechanism at low relative pressures of activated carbons with cements, 10th International Symposium on the Characterization of Porous Solids (COPS-X), May 11-14, Granada, p 242 (2014)
L.F. Velasco, D. Snoeck, A. Mignon, S. Van Vlierberghe, P. Dubruel, N. De Belie, P. Lodewyckx, Broadening the water vapour absorption modeling of activated carbons towards cementitious materials, Carbon for Energy Storage/Conversion and Environment Protection, 5th International conference, Abstracts (2013)